

AN INVESTIGATION OF SQUISH GENERATED TURBULENCE IN. I.C. ENGINES

By

CECILIA DIANNE CAMERON

B.A.Sc., The University of British Columbia, 1981

B.Sc., The University of British Columbia, 1977

A THESIS SUBMITTED IN PARTIAL FULFILLMENT OF
THE REQUIREMENTS FOR THE DEGREE OF
MASTER OF APPLIED SCIENCE

in

THE FACULTY OF GRADUATE STUDIES
Department of Mechanical Engineering

We accept this thesis as conforming
to the required standard

THE UNIVERSITY OF BRITISH COLUMBIA

October 1985

© CECILIA DIANNE CAMERON, 1985

In presenting this thesis in partial fulfilment of the requirements for an advanced degree at the University of British Columbia, I agree that the Library shall make it freely available for reference and study. I further agree that permission for extensive copying of this thesis for scholarly purposes may be granted by the head of my department or by his or her representatives. It is understood that copying or publication of this thesis for financial gain shall not be allowed without my written permission.

Department of Mechanical Engineering

The University of British Columbia
1956 Main Mall
Vancouver, Canada
V6T 1Y3

Date OCTOBER 11, 1985

ABSTRACT

Experiments were performed with a single cylinder C.F.R. engine to provide data for the evaluation of the squish designs. Several reference squish chambers were manufactured for the C.F.R. engine. Flow field data was obtained via hot wire anemometer measurements taken in the cylinder during motored operation of the engine. Pressure data recorded while the engine was operated on natural gas yielded mass burn rate information.

Mass burn rate analysis of cylinder pressure data shows the squish design to have greatest impact on the main combustion period (2% to 85% mass burned). A comparison of the reference squish design in these experiments to the disc chamber shows a 32% reduction in the combustion duration and a 30% increase in peak pressure occurring 5 crank angle degrees earlier. The squish-jet design provided the additional effect of a reduction in the ignition delay time (spark to 2% mass burned). The squish-jet design resulted in a reduction of the ignition delay time by 3 crank angle degrees and in a 4% increase in peak pressure occurring 3 crank angle degrees earlier compared to the reference squish chamber. The total combustion duration was 5% less with the squish-jet design.

TABLE OF CONTENTS

	<u>Page</u>
ABSTRACT	ii
LIST OF TABLES	vi
LIST OF FIGURES	vii
NOMENCLATURE	x
ACKNOWLEDGEMENT	xii
1. INTRODUCTION	1
1.1 General Discussion	1
1.2 The Turbulent Flow Field in an Engine	2
1.3 Objectives and Scope of Work	6
2. LITERATURE REVIEW	7
2.1 Introduction	7
2.2 Turbulence Measurements in Engines	7
2.3 Combustion Experiments in Engines	11
3. THE SQUISH COMBUSTION CHAMBER	13
3.1 Introduction	13
3.2 Squish Velocity Calculations	13
3.3 The Squish Chamber Experiments	16
4. APPARATUS AND INSTRUMENTATION	17
4.1 Introduction	17
4.2 Engine and Test Bed	17
4.3 Squish Piston Inserts	18
4.4 Air Supply	19
4.5 Gas Supply	19
4.6 Instrumentation	19
4.7 Data Acquisition System	21
5. EXPERIMENTAL METHOD	23
5.1 Introduction	23
5.2 Motored Engine Tests	23
5.2.1 Hot Wire Preparation	24
5.2.2 Routine Experimental Procedure	25
5.2.3 Flow Measurement Locations	26
5.3 Combustion Tests	26
6. DATA ANALYSIS	27
6.1 Introduction	27
6.2 Pressure Signal Processing	27
6.3 Anemometer Signal Processing	27
6.4 Flow Field Data	32

TABLE OF CONTENTS (Continued)

	<u>Page</u>
6.4.1 Ensemble Averaged Mean Velocity and Turbulence Intensity	33
6.4.2 Cycle by Cycle Time Averaged Means and RMS Velocity	35
6.4.3 Time Scale Analysis	38
6.5 Combustion Data	39
7. DISCUSSION OF RESULTS	40
7.1 Introduction	40
7.2 Flow Field Results	40
7.2.1 Ensemble Averaging vs. Time Averaging	40
7.2.2 Standard Squish Piston (Piston A) Results	42
7.2.3 Squish-Jet Piston (Piston B) Results	44
7.2.4 Comparison of Geometries	46
7.3 Combustion Results	48
8. CONCLUSIONS AND RECOMMENDATIONS	51
BIBLIOGRAPHY	53
APPENDIX A - CALIBRATION CURVES	56
APPENDIX B - HOT WIRE ANEMOMETER CALIBRATION	59
1. Welding and Preparation	59
2. Calibration	59
3. Analytical Procedure for Correlation	60
4. Hot Wire Calibration Computer Program HWCAL	62
APPENDIX C - DATA ACQUISITION PROGRAMS	67
1. Data Acquisition from C.F.R. (CDAQ)	67
2. Transfer of Digital Data to MTS (BYTRD)	72
APPENDIX D - HOT WIRE ANEMOMETER DATA PROCESSING PROGRAMS	75
1. Instantaneous Velocity Evaluation and Ensemble Averaging (ANEM)	75
2. Cycle by Cycle Time Averaged Mean and RMS Velocity (TRAP)	83
3. Nonstationary Analysis (NOTIME)	91
4. Time Scale Analysis (PEAK)	97
APPENDIX E - COMBUSTION DATA PROCESSING	104
1. Pressure Evaluation and Ensemble Averaging from Digital Data (PENH)	104
2. Geometric Analysis of Spherical Flame Front (DFLAME)	108
3. Burning Rate Analysis (MASBRN)	120
APPENDIX F - PROPERTIES OF B.C. NATURAL GAS	150

LIST OF TABLES

Page

I. Engine Specifications	153
II. Hot Wire Probe and Anemometer Specifications	154

LIST OF FIGURES

	<u>Page</u>
1.1 The squish combustion chamber	155
3.1 The standard squish chamber	156
3.2 The squish-jet chamber	157
3.3 The effect of clearance height on squish velocity	158
3.4 The effect of the squish-jet design on squish velocity	159
4.1 Schematic of experimental setup and instrumentation	160
4.2 The C.F.R. engine	161
4.3 The squish piston inserts	162
4.4 Photograph of squish piston inserts	163
4.5 Top and side view of C.F.R. combustion chamber	164
4.6 Fitting for hot wire probe	165
4.7 Schematic of data acquisition	166
4.8 Photograph of data acquisition system	167
4.9 Photograph of optical trigger system	168
5.1 Hot wire probe locations	169
5.2 Hot wire probe orientation	170
7.1 Three consecutive instantaneous velocity records	171
7.2 Comparison of time averaged and ensemble averaged mean velocity	172
7.3 Cyclic variation of the mean velocity	173
7.4 Comparison of time and ensemble averaging techniques for the evaluation of turbulence intensity	174
7.5 Turbulence intensity evaluated with Lancaster's nonstationary technique	175

LIST OF FIGURES (Continued)

	<u>Page</u>
7.6 Mean velocity and turbulence intensity for Piston A; $h_c = 3.5$ mm; probe at cup edge	176
7.7 Mean velocity and turbulence intensity for Piston A; $h_c = 1.5$ mm; probe at cup edge	177
7.8 Mean velocity and turbulence intensity for Piston A; $h_c = 1.5$ mm; probe at chamber center	178
7.9 Mean velocity and turbulence intensity for Piston A; $h_c = 1.5$ mm; probe at cup edge; $\theta = 90^\circ$	179
7.10 Mean velocity and turbulence intensity for Piston A; $h_c = 1.5$ mm; probe at chamber center; $\theta = 90^\circ$	180
7.11 Comparison of mean velocity traces for Piston A; $h_c = 3.5$ and 1.5 mm; probe at cup edge	181
7.12 Comparison of relative turbulence intensities for Piston A; $h_c = 3.5$ and 1.5 mm; probe at cup edge	182
7.13 Mean velocity and turbulence intensity for Piston B; $h_c = 3.5$ mm; probe at cup edge	183
7.14 Mean velocity and turbulence intensity for Piston B; $h_c = 1.5$ mm; probe at cup edge	184
7.15 Mean velocity and turbulence intensity for Piston B; $h_c = 1.5$ mm; probe at chamber center	185
7.16 Mean velocity and turbulence intensity for Piston B; $h_c = 1.5$ mm; probe inside cup	186
7.17 Comparison of relative turbulence intensities for Piston B; $h_c = 3.5$ and 1.5 mm; probe at cup edge	187
7.18 Comparison of mean velocity traces for Pistons A and B; $h_c = 1.5$ mm; probe at cup edge	188
7.19 Comparison of relative turbulence intensities for Pistons A and B; $h_c = 1.5$ mm; probe at cup edge	189
7.20 Comparison of the relative probability distributions of small scale turbulence structure for Piston A at the chamber center and at the cup edge	190
7.21 Comparison of relative probability distributions of small scale turbulence structure at the chamber center for Piston A and the flat piston	191

LIST OF FIGURES (Continued)

	<u>Page</u>
7.22 Comparison of relative probability distributions of small scale turbulence structure at the cup edge for Pistons A and B	192
7.23 Comparison of relative probability distributions of small scale turbulence structure at the chamber center for Pistons A and B	193
7.24 Comparison of pressure history for Pistons A and B and the flat piston for a spark timing of 30° BTDC	194
7.25 Comparison of mass fraction burn curves for the flat piston and for Piston A at a spark timing of 30° BTDC	195
7.26 Comparison of mass friction burn curves for Pistons A and B at a spark timing of 30° BTDC	196
7.27 Comparison of mass fraction burn curves for all three pistons at a spark timing of 30° BTDC	197
7.28 Comparison of mass fraction burn curves for Pistons A and B at a spark timing of 25° BTDC	198
A.1 Calibration curve for laminar flow element	57
A.2 Calibration curve for orifice metre	58
E.1 Flame geometry for a section through a flame above piston bowl (flame section 1)	109
E.2 Flame geometry for a section through a flame in a piston bowl (flame section 2)	110

NOMENCLATURE

A	area, m^2
a,b	calibration constants for hot wire correlation
C_p	constant pressure specific heat, $J/kg \text{ } ^\circ K$
D	engine bore, m
d	wire diameter, m
H	depth of bowl in squish piston, m
h	heat transfer coefficient, $W/m^2 \text{ } ^\circ K$
h_c	clearance height, m
I	electric current, amps
k	thermal conductivity, $W/m \text{ } ^\circ K$
L_t	integral time scale, s
l	wire length, m
N	number of engine cycles
Nu	Nusselt number
P	pressure, Pa
R	resistance, ohms
R_{op}	resistance of wire at operating condition, ohms
R_τ	autocorrelation coefficient
S	distance of piston from TDC, m
T	temperature, K
U	velocity, m/s
$U(i,\theta)$	instantaneous velocity at crank angle θ in cycle i , m/s
\bar{U}	mean velocity with respect to time, m/s
$\bar{U}(\theta)$	true ensemble averaged mean velocity, m/s

$\bar{U}_\theta(i)$	average (time) velocity in window θ for record i , m/s
\bar{U}_θ	$U(i)$ ensemble averaged over N cycles, m/s
U_{rms}	cyclic variation in mean velocity, m/s
$u'(\theta)$	true ensemble averaged turbulence intensity, m/s
$u'_\theta(i)$	time averaged turbulence intensity in cycle i , m/s
u'_θ	$u(i)$ ensemble averaged over N cycles
V	volume, m^3
α	temperature coefficient of resistance, ohms/ $^{\circ}C$
β	orientation angle
γ	specific heat ratio
λ_t	micro time scale, s
θ	crank angle
τ	correlation time, s
μ	viscosity, N.s/ m^2

subscripts

O	reference condition
B	squish piston bowl
g	gas
P	piston
Ref	reference condition
SA	squish piston A
SB	squish piston B
SC	squish piston B channel
t	time, s
w	wire
x	length, m

ACKNOWLEDGEMENTS

The author would like to acknowledge the guidance and support of Professor Evans during the course of the thesis work. Professors Hill and Hauptmann are also acknowledged for numerous enlightening discussions and contributions. Special thanks go to Mr. Allan Jones for the development and construction of the data acquisition system. John Hoar, John Wiebe, and Bruce Hansen machined the parts required for the experimental apparatus. Phillip Hurren and John Richards helped in the design of the data acquisition system.

1. INTRODUCTION

1.1 General Discussion

The combustion rate in an internal combustion (I.C.) engine plays a key role in engine performance. Fast burning in engines produces a greater resistance to knock which allows operation at higher compression ratios and thus leads to increased engine efficiency. Fast burning also permits the use of leaner air-fuel mixtures [1]. Furthermore, fast combustion rates have been shown to reduce NO_x emissions and the cyclic variation of engine performance [1,2]. Combustion rate is thought to depend primarily upon flame front area, turbulence and the chemical kinetics of the mixture. To increase the combustion rate in engines engineers must address two questions; how to increase the flame front area, and how to increase the propagation rate of the flame front into the unburned region. Combustion chamber geometry and turbulence enhancement during the combustion period are the major design variables investigators have focussed on to answer these questions.

The effects of chamber geometry and the flow field are directly linked since chamber configuration does affect turbulence generation. Modern combustion chambers are designed with a large volume to surface area ratio (compact chambers) minimizing contact between the flame and the cylinder walls. With central ignition in these chambers designers achieve a large flame front area and a reduction in heat transfer (due to minimal contact between flame and walls). Both are factors which contribute to an increase in burn rate.

The turbulent flow field in an engine is the more dominant factor in determining the combustion rate. The mechanism responsible for increased

burn rate is still a subject of debate among researchers. The two most widely accepted theories of turbulent combustion in engines are the wrinkled flame front and turbulent entrainment theories.

The wrinkled flame front model, first proposed by Damkohler [3], states that the turbulence distorts (wrinkles) the flame front thereby increasing the area available for molecular transport. Entrainment models have been developed by Tabaczynski [4] and Blizzard and Keck [5]. These models propose that a turbulent entrainment process is responsible for increased flame propagation. It is assumed that laminar burning takes place in cells of size characterized by the Taylor micro-scale and rapid burning takes place along vortex tubes of size characterized by the Kolmogorov scale. The entrainment velocity is assumed to be proportional to the turbulence intensity.

Irrespective of these theories, the link between increased flame speed and turbulence has been firmly established through experiment. The work of Andrews et al. [6] demonstrates that turbulence can be used to increase flame speeds.

1.2 The Turbulent Flow Field in an Engine

The flow field in an engine is primarily governed by the valve events and the piston motion. The shear flow past the intake valve is a major source of turbulence generation prior to the combustion period. After the intake valve closes this turbulence decays rapidly during the compression stroke. In conventional disc chambers very little additional turbulence is generated during the compression stroke as a result of the piston movement. This is the critical period for the combustion process.

Designers have taken two approaches towards the enhancement of

turbulence during compression. Modifications to the inlet port which produce high swirl in the intake jet have proven to increase turbulence levels prior to the combustion period. Also the combustion chamber can be designed so that turbulence is generated on the compression stroke as a result of the piston motion. This type of design is called a squish chamber.

A bowl in piston type of squish chamber design is shown schematically in Figure 1.1. As the piston approaches TDC on the compression stroke a pressure differential between the outside annular area (squish area) and the inner area drives a radial jet inward. Thus an additional source of turbulence is generated by the strong shear flow in the jet motion during the latter phase of compression.

The flow field quantities of interest in an engine are the mean velocity, turbulence intensity, and the macro and micro scales of turbulence. The mean velocity characterizes the gas motion due to the valve events and the piston travel. The mean velocity is defined to be the time average over a specific interval of the instantaneous velocity. The mean velocity \bar{U} , is:

$$\bar{U} = \frac{1}{T} \int_0^T U \, dt \quad (1.1)$$

where U is the instantaneous velocity and T is the time interval. In an engine where the mean velocity is periodic this type of definition can cause problems since the calculated mean will be dependent upon the time interval chosen. This problem is discussed in detail in the data analysis chapter.

The turbulence intensity, u' , is the root mean square of the velocity

fluctuations about the mean. If the instantaneous velocity is written as:

$$U = \bar{U} + u \quad (1.2)$$

where u represents the fluctuation from the mean, then the turbulence intensity u' , may be expressed as:

$$u' = \left\{ \frac{1}{T} \int_0^T [U - \bar{U}]^2 dt \right\}^{1/2} \quad (1.3)$$

The scales of length and time describe the structure of the flow field. Length scale measurements are very difficult to obtain since they require measurements at two points simultaneously and correlation of vast amounts of data. Because of this, in engine research time scales are used to characterize the eddy size distribution. The integral scale L_t , is evaluated from the integral of the autocorrelation coefficient of the fluctuating velocity at a single point. The autocorrelation coefficient R_τ , is expressed by:

$$R_\tau = \frac{1}{T} \int_0^T \frac{u(\tau)u(t+\tau)}{\bar{u}^2} d\tau \quad (1.4)$$

where τ is the correlation time. The integral time scale is then given as:

$$L_t = \int_0^T R_\tau d\tau \quad (1.5)$$

The integral scale characterizes the larger eddies of the flow field and

can be thought of as the mixing time scale.

The Taylor micro scale is also obtained from the autocorrelation coefficient. For small values of the correlation time τ the Taylor series expansion of the autocorrelation function describes a parabola. The microscale is defined to be the point at which this parabola intersects the time correlation (τ) axis: intersects the time correlation axis (τ axis):

$$\lambda_t^2 = -2 (\partial^2 R_\tau / \partial \tau^2) |_{\tau=0} \quad (1.6)$$

The micro scale describes the small scale structure of the flow. In the model proposed by Tennekes [7] in which a turbulence structure can be thought of as consisting of tangled vortex tubes (much like spaghetti) the micro scale can be viewed as the typical time between vortex tubes as they are convected past a stationary observer.

The turbulence intensity is thought to be primarily responsible for the increased flame speed observed for turbulent conditions. This view is supported by the results of Andrews et al. [6] in which a strong correlation between the intensity and turbulent burning velocity is demonstrated. The role of turbulence scale is thought to be important only in the initial stages of combustion. There is little evidence that scale affects the flame speed in a fully developed turbulent flame, although there is some indication that the micro scales are important to the ignition delay process. The ignition delay time is arbitrarily defined here to be the time required to burn two percent of the charge mass. Variation in the ignition delay time is usually considered to be responsible for the cyclic variation observed in cylinder pressure [5].

1.3 Objectives and Scope of Work

The objective of this thesis was to investigate the effects of the squish chamber design on the flow field and combustion process in an I.C. engine. The specific focus of the investigation was the comparison of a reference squish chamber design to a new squish-jet chamber design proposed by Evans [8]. The squish-jet is intended to be an improvement over the conventional design by providing enhanced turbulence production and mixing in the combustion region. It was the purpose of this study to provide experimental data for an initial evaluation of the basic squish-jet design.

A comparison of mass burn rate, combustion duration and pressure history was made for the two chamber designs; as well as flow field characteristics mean velocity and turbulence intensity.

A series of experiments were designed to meet the objectives of the investigation. Several variations of the two squish designs were manufactured for a single cylinder C.F.R. engine. For each design flow field data were obtained with a hot wire anemometer for motored conditions, and pressure data was recorded while the engine was operated on natural gas. The experiments were also conducted for the standard C.F.R. disc chamber design as a basis of comparison.

The data were processed to yield mass burn rate, combustion duration and the turbulence parameters of interest. The designs were then analyzed on a comparative basis.

2. LITERATURE REVIEW

2.1 Introduction

This chapter reviews the literature in two areas relevant to the investigation. The first section reviews fundamental turbulence measurements in engines. The second section is concerned with combustion experiments made in engines of different types of geometry, and the correlation of combustion data with turbulence data.

2.2 Turbulence Measurements in Engines

Semenov [9] was one of the pioneers in engine turbulence studies. He investigated the intake and compression process in a C.F.R. engine with a shrouded intake valve and disc combustion chamber. By traversing a hot wire probe across the bore of the chamber he obtained spatial velocity gradients as well as the mean velocity and turbulence intensity. Evidence of large velocity gradients during the intake process confirmed the jet nature of the incoming flow. In comparison velocity gradients near TDC on the compression stroke were insignificant. He also found very little spatial variation of the turbulence intensity near TDC.

Semenov observed a strong correlation between the turbulence intensity during compression and the velocity gradient during intake. From this he concluded the shear flow through the intake valve was the primary source for turbulence during the compression stroke. Increased engine speed resulted in increased mean velocity and turbulence intensity; however, compression ratio increases yielded relatively small decreases in the two quantities.

Dent and Salama [10] were among the first investigators to measure turbulent time scales in engines. A fast Fourier Transform analyzer was used to obtain the correlation coefficient and spectral density function. The macro and micro time scales were computed from the correlation coefficient.

The measurements were performed in two engines of different geometry; a disc chamber design, and a wedge (squish) design. In the disc chamber they found a general decrease in the mean velocity and turbulence intensity during the compression stroke. In the squish chamber however, they found an increase in the mean velocity during compression, although a corresponding increase in the turbulence intensity was not observed.

The micro time scale was found to be virtually independent of geometry and the mean velocity during compression. Calculated values of the micro length scale ranged from 0.2 to 0.6 mm. The macro length scales were three to four times larger than this.

Lancaster [11] studied the effects of engine speed, volumetric efficiency, and compression ratio on the flow field of an engine. The tests were performed in a C.F.R. engine with a disc chamber and two intake configurations; shrouded valve (swirl), and a standard valve. A hot wire anemometer probe was used to obtain measurements of mean velocity, turbulence intensity, and turbulence time scales.

Regardless of intake configuration, Lancaster found increased engine speed resulted in increased mean velocity and turbulence intensity. Throttling or decreased volumetric efficiency yielded similar trends. However, the values near TDC attained with the standard valve were approximately half of those achieved with the shrouded valve. This was attributed to the high swirl velocity generated by the shrouded valve. The micro

time scale decreased with increased engine speed but was otherwise independent of operating conditions. The micro-time scale ranged from 0.05 to 0.25 milliseconds. Compression ratio had a relatively insignificant effect on mean velocity and turbulence intensity. The spectral distribution of the turbulent energy near TDC was also studied for the shrouded valve configuration. Most of the energy was contained in frequencies below 1 kHz.

Lancaster used single point measurements with a triaxial probe. Close agreement between the intensities measured by the three sensors near TDC led him to conclude that the turbulence was isotropic.

Witze [12] did a similar set of measurements in an engine with a squish combustion chamber. His major conclusions were that the mean velocity and turbulence intensity are proportional to engine speed, and that the time scale is inversely proportional to the engine speed. He also measured the spatial variation of the turbulence intensity near TDC and concluded the structure was not homogeneous.

Witze's results for the mean velocity and turbulence intensity show an increase of both quantities during the compression stroke. The increase can be attributed to the bulk gas motion caused by the squish chamber. However, Witze argued that this is not the production of new turbulence; but simply a magnification of the intake turbulence due to compression.

James and Lucas [13] studied flow conditions within several frequency ranges. They used both a squish chamber and a disc chamber in their investigation. They found most of the turbulence energy was in the frequency range below 700 Hz. They reported that the major effect of the squish chamber was the enhancement of the magnitude of the fluctuating velocities in the frequency range below 1600 Hz. Higher frequency

fluctuations appeared to be unaffected by combustion chamber geometry. They also found that the effectiveness of the squish chamber was a strong inverse function of the squish or clearance height.

Haghgoole et al. [14] took a somewhat different approach than other investigators by using uncalibrated hot wire signals to determine micro time scales in an engine. Their work was based on the assumption that there is a definable small scale structure of the turbulence in an engine similar to that postulated by Tennekes [7]. They analyzed the anemometer data to obtain the statistical distribution of the peak to peak time separation. They then interpreted the most probable time of this distribution as the characteristic time of the small scale structure. This time scale was in the range of 0.1 to 0.25 milliseconds. They reported a shift to higher frequencies as engine speed increased.

In summary then, fundamental turbulence measurements in engines established the following:

- i) shear flow past the intake valve is a major source of turbulence,
- ii) turbulence intensity and mean velocity are proportional to engine speed,
- iii) turbulence length and time scales are inversely proportional to engine speed,
- iv) turbulence micro time scales are on the order of tenths of milliseconds,
- v) turbulence micro length scales are on the order of tenths of millimeters,
- vi) turbulence is isotropic near TDC compression however it is not homogeneous, and
- vii) turbulence energy is concentrated in the low frequencies, below 1000 Hz.

2.3 Combustion Experiments in Engines

Studies in which turbulence and combustion data are correlated for engines of different geometry are rare. Lancaster et al. [15] correlated turbulence and combustion data for a disc chamber with and without "swirl". A modified Kreiger-Borman [16] heat release model was used to obtain the turbulent flame speed from cylinder pressure history. To separate thermal effects from those of turbulence the turbulent flame speed was normalized by the laminar flame speed. Operating conditions were identical to those for which turbulence measurements were obtained [11]. Turbulence intensity was varied by using shrouded and standard intake valves, as well as by changing engine speed.

Lancaster et al. concluded that the normalized flame speed was a linear function of turbulence intensity. The effect of turbulence scale on flame speed was found to be insignificant. However these tests were conducted for a limited range of turbulent micro scale, 1 to 2 mm.

Nagayama et al. [17] examined the effect of swirl and squish geometries on combustion duration. No flow measurements were taken in these experiments. They had four chamber configurations; disc, swirl, squish, and squish plus swirl. They found that squish and swirl both reduced combustion duration and that furthermore, they had distinctly separate effects on the combustion interval. Swirl was effective in the initial stage of combustion; whereas, squish was most effective during the main stage of combustion. The two effects were additive and thus the combination squish plus swirl chamber yielded the best results.

More recently investigators have used engine simulation models to predict the effect of chamber geometry on combustion duration [18-21]. In general these models predict that squish type chambers give better

performance than disc chambers. In addition, the importance of central spark plug location is established by these models.

Although there is an abundance of engine performance data for a variety of chamber designs available in the literature [2,15,18,19,21-25], very few attempts have been made to isolate the effects which result in one design's superiority over another. Thus progress towards defining the criteria for optimal chamber design has been slow.

3. THE SQUISH COMBUSTION CHAMBER

3.1 Introduction

An illustration of the conventional bowl in piston squish design is shown in Figure 1.1. Although the chamber shown is in the piston it is also possible to achieve the same effect with a flat piston and a recessed chamber in the head.

The squish design is intended to provide an additional source of turbulence on the compression stroke. In Figure 3.1 a schematic of the squish process is shown. As the piston approaches TDC (compression) the relative compression in volume V_1 in the figure is higher than that in volume V_2 . Thus, there is a 'squish' velocity, U_{SA} , as air moves from V across the boundary A_3 into V_2 .

In this investigation a variation of the squish design, the squish-jet design proposed by Evans [8] will be studied as well. A schematic of this design is illustrated in Figure 3.2. The concept here is similar to that discussed above except that the channels (see Figure 3.2) provide an additional route for the squished air. The desired results are an increase in the relative turbulence intensity and enhanced mixture turbulence at the center of the chamber where the jets collide. Several embodiments of this design have been described by Evans [8].

In Figure 3.1 the conventional squish design is labelled Piston A and the squish-jet design in Figure 3.2 is labelled Piston B. This convention will be used throughout the thesis.

3.2 Squish Velocity Calculations

In this section a very simplified model will be used to predict the squish velocity during the final stage of the compression stroke for each of the two designs.

To predict the squish velocity for the conventional design the basic assumption is that the density is uniform throughout the chamber. The squish velocity is calculated for the piston movement over one crank angle degree. From mass conservation the following equation can be written,

$$\frac{U_P A_2}{V_2} + \frac{U_{SA} A_3}{V_2} = \frac{U_P A_1}{V_1} - \frac{U_{SA} A_3}{V_1} \quad (3.1)$$

The quantities U_P , U_{SA} , A_1 , A_2 , A_3 , V_1 , and V_2 are defined in Figure 3.1. Equation (3.1) can then be solved for the squish velocity U_{SA} ,

$$U_{SA} = \frac{U_P}{A_3} \{ (A_1 V_2 - A_2 V_1) / (V_1 + V_2) \} \quad (3.2)$$

From Equation (3.2) it can be seen that squish velocity is proportional to the piston speed (or engine speed) and that it is inversely proportional to area A_3 . The area A_3 is a function of the bowl diameter D_B , the clearance height h_c , and the distance of the piston from TDC, S .

The prediction of the squish velocity for the squish-jet design is similar to that above except that now there is an additional route for the gas. The design is Piston B in Figure 3.2. Equation (3.1) is rewritten as:

$$\frac{U_P A_2}{V_2} + \frac{U_{SB} A_3}{V_2} + \frac{U_{SC} A_4}{V_2} = \frac{U_P A_1}{V_1} - \frac{U_{SB} A_3}{V_1} - \frac{U_{SC} A_4}{V_1} \quad (3.3)$$

In this equation U_{SB} is the squish velocity normal to the area A_3 and U_{SC} is the squish velocity (hereafter called squish-jet velocity) normal to A_4 . The other terms in the equation are defined in Figure 3.2. An additional equation is required to solve for the new velocity term U_{SC} . This

is obtained by treating the problem with a parallel pipe flow method. The assumption is that the pressure drop of the flow across the boundary A_3 is equal to that of the flow through the channels and across the boundary A_4 . The pressure drop will be a function of the hydraulic radius and the velocity head. Simultaneous solution of the equations for conservation of mass and head loss yields expressions for the squish velocity U_{SB} , and the squish-jet velocity U_{SC} . The squish velocity U_{SB} is:

$$U_{SB} = \frac{U_P \{A_2 - (A_1 + A_2)[A_2(h_c + S)]/(V_1 + V_2)\}}{A_3 + [2D_B(S + h_c)/(D_H(D_B + S + h_c))]^{1/2}} \quad (3.4)$$

and the squish-jet velocity U_{SC} is:

$$U_{SC} = \frac{U_{SB}}{\{2D_B(S + h_c)/D_H(D_B + S + h_c)\}^{1/2}} \quad (3.5)$$

It can be seen from both Equations (3.2) and (3.4) that the squish velocity across the piston face (U_{SA} and U_{SB}) will be a strong function of the clearance height. In Figure 3.3, the squish velocity calculated from Equation (3.2) is shown for two clearance heights, 3.5 and 1.5 mm. The geometric parameters for the C.F.R. engine were used in the calculations. From the graph it can be seen that the squish velocity reaches a maximum at approximately 10° BTDC and decays rapidly to zero at TDC. It is clear from this figure that clearance height is very important. The peak mean velocity calculated for a clearance height of 1.5 mm is almost twice that for a clearance height of 3.5 mm. In Figure 3.4 the effect of adding the squish-jet channels is shown. The squish velocity across the face of the

piston is reduced by about 30%. The squish-jet velocity is consistently lower than U_{SB} except near the peak which occurs at approximately 10° BTDC.

3.3 The Squish Chamber Experiments

The method of predicting squish velocities outlined above was very simplified and not intended to yield quantitative results. Rather it was employed as an aid in designing the experiments.

As a result of the calculations it was decided to vary the clearance height and observe the effect. Three heights were selected 1.5, 2.5, and 3.5 mm. Both chamber designs were tested at these heights. The clearance height of 1.5 mm was the minimum that could be attained due to the clearance between the valves and the piston.

The piston wall thickness and the placement of the channels for Piston B were the constraints governing the selection of bowl diameter. A bowl diameter of 1.5 inches resulted in a 78% squish area expressed here as a percent and is defined to be the ratio of the area A_1 (see Figure 3.1) to the total area ($A_1 + A_2$).

Because it was desirable to compare both flow and combustion data from case to case the compression ratio was kept constant. The bowl depth was varied to accommodate the various clearance heights.

Hot wire anemometer measurements were made at the edge of the bowl and at the center of the chamber for each configuration. In addition, for Piston B a measurement was made with the probe inside the bowl opposite a channel at TDC.

In summary, the experiments were designed to observe the effects of clearance height, and squish-jet channels on the flow field and combustion process. Tests were also conducted with a disc chamber operating at the same compression ratio as a standard for comparison.

4. APPARATUS AND INSTRUMENTATION

4.1 Introduction

This investigation required test results operating with several combustion chamber designs. To facilitate changes of configuration for each test, a C.F.R. engine with a flat head was used in conjunction with a squish piston design. Thus a change in combustion geometry required only a change of pistons. The engine was then instrumented to obtain pressure and flow field information. The instrumentation and engine are described in detail in the following sections.

4.2 Engine and Test Bed

A schematic of the experimental apparatus is shown in Figure 4.1. The engine used for the tests was a single cylinder C.F.R. coupled to a synchronous reluctance type motor by twin v-belts. Specifications for the engine are presented in Table I. The C.F.R. cylinder and head is cast in one piece which has an adjustable height above the TDC position of the piston to allow for variable compression ratio.

For these experiments the following changes were necessary to the basic C.F.R. configuration:

- i) the pulley set was replaced to obtain a higher operating speed than the standard 900 RPM. The speed achieved was 1140 RPM,
- ii) the shrouded intake valve was replaced by a standard intake valve to reduce the effects of inlet swirl,
- iii) the gasoline carburetor was removed and replaced with a venturi element so that the engine could be operated with natural gas, and

iv) the C.F.R. ignition system was replaced with a capacitive discharge ignition circuit.

The synchronous motor was used to start the engine, to maintain constant speed, and to absorb the power developed by the engine when fired. The engine and motor are shown in Figure 4.2.

4.3 Squish Piston Inserts

Seven pistons were required for the tests. Rather than manufacture a piston for each test, the original C.F.R. piston was bored through the crown and the inside wall threaded. Threaded inserts were then manufactured for each experiment.

The piston material was cast iron so steel was used in the production of the inserts. Three basic designs were manufactured; the basic squish design (Piston A), the squish-jet design (Piston B), and the flat disc chamber design. The design drawings of these piston inserts are in Figure 4.3 and a photograph is in Figure 4.4. In Figure 4.3 case 1 corresponds to a clearance height of 1.5 mm; case 2 corresponds to a clearance height 3.5 mm.

The two squish designs were altered to accommodate the three clearance heights used. The bowl diameter was held constant at 1.5 inches. Because the bottom of the insert had to clear the top of the oil ring the maximum depth of the bowl that could be achieved was 1.4 inches. This maximum depth was used for the test of minimum clearance height (1.5 mm). The bowl depth was decreased for the other tests so that a constant compression ratio was maintained throughout the experiments. The center line of the access port for the hot wire anemometer probe was 9 mm below the head. Because of this and the small clearance heights used a slot was milled in the inserts to accommodate the probe.

4.4 Air Supply

The intake air for the engine was drawn into a 2.5 inch pipe through an orifice plate and into a surge tank. The air was then filtered as it left the surge tank and passed into the venturi. The intake air was not throttled at anytime.

4.5 Gas Supply

The natural gas used as fuel was supplied from the building mains at a pressure of 5 psig to a pressure regulator where the pressure was reduced to 3 inches of water above atmospheric pressure. From the regulator the gas flowed first through a laminar flow element then through a control valve which was used to adjust the air/fuel ratio. From the control valve the gas flowed through 1/2 inch tubing to the venturi.

4.6 Instrumentation

A schematic of the instrumentation layout is shown in Figure 4.1.

Pressure measurements were made for combustion and motored operation. The location of the transducer for each of the operational modes is shown in Figure 4.5. The pressure transducer installed in the cylinder was a Kistler 609C piezo electric transducer mounted in a steel sleeve. The transducer was recessed 2 mm to eliminate thermal shock effects as recommended by Benson [26]. The transducer signal was transmitted via low noise cable to a Kistler 5004 charge amplifier. The amplified signal was sent to an analogue to digital converter which was interfaced to an I.B.M. personal computer. The digitized pressure signals for 120 engine cycles were then stored on floppy discs.

The air flowrate was monitored with an orifice plate mounted on top of

the surge tank. The pressure drop across the plate was measured on an inclined manometer. Volumetric flowrate was calculated from the calibration curve for the orifice plate. The orifice plate was calibrated against a Meriam Laminar Flow Element Model 50MW-1.5. The calibration curves for both instruments are in Appendix A.

The natural gas flowrate was metered with a Meriam Laminar Flow Element Model 50MW-1.5 positioned in the gas line between the pressure regulator and control valve. The pressure drop was recorded on an inclined manometer. Volumetric flowrate was determined from the calibration supplied by the manufacturer with appropriate correction factors applied for the effects of natural gas viscosity (see Appendix F).

Air movement within the cylinder during motored operation was measured with a hot wire anemometer probe. The probe used was a TSI Model 1226 which is designed for high temperature environments. The sensor, Platinum-Iridium wire of 6.3 micrometer diameter, was mounted on the support needles by spot welding. The probe was installed in the side port of the cylinder through an airtight fitting. The fitting is shown in Figure 4.6. The access port for the probe is shown in Figure 4.5. A Disa Model 50D anemometer bridge unit, operated in the constant temperature mode, was used in conjunction with the probe. The specifications for the probe and the anemometer are listed in Table II.

The anemometer voltage signal was sent to a Hewlett Packard Model 3968A tape recorder where it was recorded on analogue tape. This was necessary because high resolution was required for the hot wire data. A sample rate of every 0.2 crank angle degrees was selected. However the data acquisition system could not perform analogue to digital conversions this fast, so the anemometer signal was first recorded on tape and then

played back to the data acquisition system at a slower speed. This procedure is described in more detail in the following section. The anemometer signal was recorded on two channels; one with a passband of 70 to 64,000 Hz, and the other with a passband of DC to 5,000 Hz. The data stored on the channel with the broad passband was processed to obtain frequency distribution information. The data recorded in the narrow band was used to obtain mean velocity and turbulence intensity information.

4.7 Data Acquisition System

The basic data acquisition system consisted of an optical crank angle trigger, a trigger and clock circuit, an analogue to digital converter, and an I.B.M. PC. In addition, for turbulence measurements a Hewlett Packard Model 3968A tape recorder was used for data acquisition. A schematic of the system is shown in Figure 4.7. A photograph of the system is shown in Figure 4.8.

Optical pickups mounted on a slotted wheel coupled to the engine crankshaft provided pulses every two crank angle degrees and at BDC. The optical pickup system is shown in Figure 4.9. These pulses were fed to the trigger and clock circuit simultaneously with the pressure and the signal being sampled. The two degree signal was passed through a phase lock loop which multiplied the frequency by ten. The BDC input pulse and pressure signal were used to start the A/D process. The analogue pressure signal was input to a comparator whose output was sent to a flip flop. The output of the flip flop and the BDC pulse were fed to a NOR gate. The flip flop went low when a preset pressure threshold was reached at the start of compression and thus when the next BDC pulse arrived at the NOR gate a trigger pulse was sent out. This pulse served two functions; it signaled the computer to initiate data acquisition, and it enabled an AND gate which

allowed the 0.2 degree pulses to flow to a counter. If a slower sample rate was desired (0.4, 1.0, and 2.0 degrees), this could be set at the counter and the frequency of the pulses reduced by 2, 5, or 10. The output of this counter was then fed to a clock counter where pulses were counted until 16,000 pulses had been detected. After this threshold was reached the clock counter shut off the pulses until the whole process was started again. For each pulse leaving the clock counter the signal of interest was sampled and an analogue to digital conversion performed. When 16,000 points were collected the data was transferred to a floppy disc for further processing off-line.

The analogue-to-digital converter had an upper frequency limit of 27 kHz. The pressure signal from combustion experiments was sampled every degree and posed no problem. High resolution was required, however, for the hot wire data and hence a sample rate of every 0.2 degrees was selected. At a speed of 1140 rpm the 0.2 degree pulses arrive at the clock counter at a frequency of 34.2 kHz. To overcome this problem a tape recorder was used to record the two degree and BDC pulses, pressure, and anemometer signals at a tape speed of 15 inches per second. The signals were then played back to the trigger and clock circuit at a speed of 7.5 inches per second. Thus the clock counter saw pulses with a frequency of 17.1 kHz but because the anemometer signal was "stretched" the same amount as the original 2 degree pulses the effective sample rate was 34.2 kHz as desired.

Data acquisition was performed with the aid of the program CDAQ which was loaded into the I.B.M. microcomputer. This program was interactive and allowed the user to issue commands to the analogue-to-digital conversion system. This program is described in Appendix C.

5. EXPERIMENTAL METHOD

5.1 Introduction

The goal of the experiments was to provide combustion and turbulence data for the combustion chambers under study. For each combustion chamber geometry two types of experiments were performed; combustion tests in which the pressure trace was recorded, and motored tests in which the air movements were monitored.

All of the tests were conducted at a constant engine speed of 1140 rpm, a compression ratio of 11.3, and with a wide open throttle. The combustion tests were performed with a stoichiometric air-fuel ratio.

5.2 Motored Engine Tests

These tests yielded flow field data for each of the configurations. The quantities of primary interest were the mean velocity and turbulence intensity for several locations in the chamber: at the edge of the bowl (i.e. a measurement of squish velocity as it left the squish region); at the center of the chamber. For configurations with channels (Piston B) the probe was positioned so that it would be directly opposite a channel exit at TDC in an attempt to measure the jet entering the bowl via the channels. These positions are shown schematically in Figure 5.1.

The majority of these tests were performed with the wire axis oriented perpendicular to the cylinder axis (parallel to the piston face). This position is shown in Figure 5.2 as $\alpha = 0$. This orientation was selected since the radial (or squish) velocity was of primary interest. However, in one set of tests the sensor was rotated 90° (see Figure 5.2) to obtain an indication of the tangential velocity.

5.2.1 Hot Wire Preparation

Wire breakage was a frequent occurrence during the course of the experiments and thus it became necessary to establish a routine procedure for repair and calibration. Sensors were repaired by spot welding Platinum-Iridium wire onto the support needles. The welding was done with the aid of a microscope and a Disa welding unit. Each wire was inspected to ensure that the weld was of acceptable quality and that the wire was free of any dirt or defects.

The sensor was calibrated in a wind tunnel against a pitot tube. The operating temperature of the wire was 600°C. The probe was calibrated for air speeds of 0.5 to 20 meters per second. From the velocity obtained from the pitot tube a Reynolds number was formed based on the wire diameter and the ambient conditions. From the corresponding anemometer voltage a Nusselt number was calculated based on the free stream gas properties. The method used to determine the Nusselt number from the anemometer voltage is that proposed by Witze [27]. This involves solving the one-dimensional heat balance equation for the hot wire (neglecting radiation) to obtain an expression for the mean wire temperature in which the heat transfer coefficient is the only unknown. The heat transfer coefficient is determined through iteration and the Nusselt number formed. This technique is discussed more fully in the following chapter and in Appendix B. From the calibration data set a correlation of the form

$$Nu = a + b Re^n \quad (5.1)$$

was found using a non-linear curve fitting procedure [27].

After calibration the probe was placed into the three-piece fitting shown in Figure 4.6. This assembly was then positioned in a measurement test rig. There the probe orientation was set (0° or 90°) with spirit levels and by lining up sight lines on the probe and test rig. In addition the length of the probe to extend into the chamber was set. The pressure fitting was then tightened to secure the probe position within the fitting.

5.2.2 Routine Experimental Procedure

At the start of each experiment the one-piece cylinder head and cylinder were lifted off the engine block and the appropriate piston inserted. After careful cleaning of all parts the head was replaced. To adjust the clearance height the flywheel was rotated until the piston was at TDC. A plug gauge was inserted between the head and the piston crown in the top access port shown in Figure 4.5 and the cylinder was cranked up (via a worm gear) to the proper position. A dial micrometer mounted between the stationary crankcase and the cylinder was set to a reference point. The cylinder was then clamped into position, the flywheel rotated beyond TDC and the plug gauge removed. The pressure transducer was then installed.

Next the valve rocker arm linkage was lifted over the cylinder and the pushrods removed to allow for insertion of the probe. The threaded portion of the probe fitting assembly (part A in Figure 4.6) was first tightened into the side access port. The remainder of the assembly with probe tightened into position was pressed into the threaded sleeve. The fitting was then rotated in the sleeve until the probe was properly oriented. This was done by lining up sight lines on the fitting and on the engine. Finally a nut was threaded onto the sleeve to secure the entire assembly.

The pushrods were replaced, the rocker arm linkage brought down into position, tightened, and the valve clearances set. The engine was started and allowed to come to speed before data acquisition was initiated.

5.2.3 Flow Measurement Locations

For each of the squish chambers tested the probe was positioned 10 mm from the bowl edge for one set of measurements, and then at the chamber center for another set. In addition, measurements were taken in the bowl for the squish-jet chamber. For the disc chamber one measurement was made at the center of the chamber. These positions are shown in Figure 5.1 and labelled R1, R2 and R3, respectively.

For each of the clearance heights tested the probe was positioned so that the sensor was 2 mm below the chamber head. These positions are also shown in Figure 5.1 and labelled Z1, Z2, and Z3, respectively.

5.3 Combustion Tests

These combustion tests provided the pressure history of the combustion process for each of the configurations. Combustion tests were performed after the motored tests as the configuration was already in place. For these tests the hot wire probe was removed from the side port and the pressure transducer mounted. The spark plug was installed in the top access port. These positions are shown in Figure 4.5. After the instrumentation was in place the valve clearance and TDC clearance height were checked.

The engine was started with the motor. Once speed was achieved the ignition was switched on and the gas flow started. The air-fuel mixture was maintained at the stoichiometric point by adjusting the gas control valve. Spark timing was varied from 20 to 40 degrees BTDC in 5 degree increments. For each setting 120 cycles of data was collected.

6. DATA ANALYSIS

6.1 Introduction

The techniques employed for data reduction and analysis are described in this chapter. Two types of signals were processed, hot-wire anemometer and pressure data. The first part of this chapter briefly describes the method of processing the analogue signals to obtain meaningful data. The second part describes in detail the methods used to interpret this data.

6.2 Pressure Signal Processing

The raw digital data was first ensemble-averaged over 120 engine cycles. The digital data was then transformed to pressures with the appropriate conversion factor. This conversion factor was a function of the system gain and the charge amplifier setting. The pressures obtained from this conversion were relative pressures and had to be shifted by the appropriate value to obtain the absolute cylinder pressure. The method of Lancaster et al. [29] was used to determine the reference condition. This involves assuming that the pressure in the cylinder at BDC after intake is equal to the average intake manifold pressure. The intake manifold pressure was estimated by subtracting the measured losses through the intake system from the ambient pressure. After the absolute cylinder pressures were evaluated the pressure trace was smoothed using cubic spline interpolation.

6.3 Anemometer Signal Processing

The hot wire anemometer registers the change in resistance (electrical) which results from the heat transfer from the sensor due to the

cooling effect of the flow. Because the heat transfer process is a function of the driving temperature differential and fluid properties such as viscosity, density, and conductivity the sensor response is highly sensitive to changes in temperature and pressure in the flow. Ideally a probe should be calibrated over the range of temperatures and pressures encountered in the engine cylinder. However, this time-consuming procedure is not practical in light of the frequent occurrence of wire breakage. Thus it becomes necessary to rely on analytical models to correct for variations from the calibrated conditions.

The two most widely used models of heat transfer from a hot-wire are those of Collis and Williams [30] and Davies and Fisher [31]. Both models are modifications to the theory developed by King [32], known as King's Law which gives the Nusselt number as a function of the Reynolds number:

$$Nu = a + b Re^{1/2} \quad (6.1)$$

where a and b are determined by calibration. Collis and Williams [30] developed a heat transfer correlation in which convection was the only significant form of heat transfer considered. They were able to justify this by using wires with a length to diameter ratio greater than 2000. In the work of Davies and Fisher conduction to the wire supports was considered to be significant. Their theory involves solving the one dimensional heat balance equation along the wire to obtain an expression for the mean wire temperature in which the heat transfer coefficient is the only unknown. The heat transfer coefficient is determined through iteration.

In this study neither of these universal correlations was used; however, an approach similar to that of Davies and Fisher as proposed by Witze [27] was taken. In this method the one-dimensional energy equation for the wire is solved to obtain an expression for the temperature distribution along the wire. This temperature distribution is integrated along the wire to yield a mean wire temperature:

$$T_M = \frac{2(T_p - C_1)}{\sqrt{C_2} \ell} \tanh [\sqrt{C_2} \ell/2] + C_1 \quad (6.2)$$

where

$$C_1 = \frac{hT_g + I^2 R_0 (1 - \alpha_0 T_0)/(\pi d \ell)}{h - I^2 R_0 \alpha_0/(\pi d \ell)} \quad (6.3)$$

and

$$C_2 = 4[h - I^2 R_0 \alpha_0/(\pi d \ell)]/k_w d \quad (6.4)$$

where h is the heat transfer coefficient, T_p is the sensor support temperature, T_g is the gas temperature, k_w is the mean thermal conductivity of the wire, R_0 is the resistance of the wire at the reference temperature T_0 , α_0 is the temperature coefficient of resistance for the wire, and I is the current through the wire.

The mean wire temperature can be calculated from the probe resistance and the wire temperature coefficient of resistance. All other quantities except the heat transfer coefficient h are known. The heat transfer coefficient is determined from iteration. Thus for a given flow condition the heat transfer coefficient can be determined from the measured probe current, and a Nusselt number formed. Then a Reynolds number may be found from Equation (5.1). The fluid velocity is then determined from the Reynolds number.

There are several important points to make about this procedure. First in the correlation both the Reynolds number and the Nusselt number are based on the free stream gas temperature. In an extensive study in which hot wire anemometer results were compared to LDV results Witze [27] found that this choice of reference temperature gave the best agreement between the two results.

The support temperature T_p in Equation (6.2) was taken as room temperature and invariant. The support needles are much larger than the wire and are not appreciably heated by the electric current. Their temperature can be assumed to follow the instantaneous gas temperature somewhat. However, unless a direct measurement of the needle temperature is made, as Lancaster [10] did, there is no straight forward method to estimate the temperature. Again using LDV results as a standard for comparison Witze found that the choice of invariant room temperature for the supports gave adequate results.

Determination of the gas temperature in the cylinder is very important to the results. In this study the air temperature was calculated from:

$$(T_g)_i = (T_g)_{i-1} (P_i/P_{i-1})^{\frac{\gamma-1}{\gamma}} \quad (6.5)$$

where γ is the temperature dependent specific heat ratio evaluated at

$$(T_g)_{i-1}.$$

The initial reference condition was taken at the point of intake valve closing, where the pressure and temperature were taken as ambient conditions. The temperature dependent specific heat ratio was calculated by assuming the air was 21% O_2 and 79% N_2 . The constant pressure specific heats of N_2 and O_2 were evaluated from expressions given in Van Wylen and Sontag [33]:

$$(C_p)_{N_2} = 39.060 - 512.79\theta^{-1.5} + 1072.7\theta^{-2} - 820.40\theta^{-3} \quad (6.6)$$

and

$$(C_p)_{O_2} = 37.432 + 0.020102\theta^{1.5} - 178.57\theta^{-1.5} + 236.88\theta^{-2} \quad (6.6)$$

where $\theta = T(\text{kelvin})/100$. Witze [27] compared mean velocities obtained using measured and calculated temperatures. His results show that the adiabatic computation gives good results during the compression process but tends to perform poorly beyond approximately 50 degrees after TDC. Since the region of interest in this study was the combustion period (from 60 degrees before TDC to 40 degrees after TDC) the adiabatic calculation was deemed adequate for temperature evaluation.

The thermal conductivity and viscosity of the air were calculated from the expressions used by Collis and Williams [30]:

$$\frac{K_g}{K_{Ref}} = \left(\frac{T_g}{T_{Ref}}\right)^{0.80} \quad (6.8)$$

and

$$\frac{\mu_g}{\mu_{Ref}} = \left(\frac{T_g}{T_{Ref}}\right)^{0.76} \quad (6.9)$$

Details of the calculation procedure for the determination of the instantaneous velocity from the anemometer are presented in Appendix B.

From the foregoing discussion it can be seen that there are many sources for uncertainties in the evaluation of the instantaneous velocity from the anemometer signal. The main uncertainties are: wire physical properties such as uniformity of diameter, sensing length, and temperature coefficient of resistance; imperfections of the weld at the supports; and fouling of the wire during measurement. Uncertainty in the experimental

value of pressure, the reference temperature, the computed gas temperature, and the selected sensor support temperature lead to uncertainty in the heat transfer coefficient and thus the computed velocity. For these experiments the uncertainty in the reference temperature is estimated to be 5% and in the reference pressure 5%. Sensitivity analysis shows this leads to uncertainty on the order of 35% in the calculated instantaneous velocity. In addition to uncertainty arising from the analytical procedure the effects of probe interference and the probe's insensitivity to flow direction also contribute to error in the interpreted results. In light of the high uncertainty associated with hot wire measurements caution should be exercised when they are interpreted, especially when absolute magnitudes of mean velocity or turbulence intensity are to be applied to empirical models. However, hot wire measurements do provide a qualitative indication of the flow field in an engine and are valuable in studies such as this one where evaluation is based on a relative comparison rather than the absolute magnitudes of the flow field characteristics.

6.4 Flow Field Data

Interpretation of hot wire measurements in engines poses several dilemmas. Because of the complex nature of the flow field generated by the valve events and piston motion the directional characteristics are difficult to determine since the sensor cannot distinguish between forward and reverse flow conditions. Although analytical models can be used to predict the sensor response to conditions different from the calibration, there are many assumptions and variables involved in the computation of the instantaneous velocity, and thus many sources of error exist.

The major obstacle to data interpretation and processing arises from the periodic and thus nonstationary nature of the flow field in the engine. Because of this, most investigators have resorted to ensemble averaging techniques. There are two problems with this approach. The first is that

the fundamental equations which define turbulence characteristics use time averages. For most stationary processes time averages of the statistical properties are equal to ensemble averages. These are called ergodic processes. Since many turbulent flows may be considered as stationary and ergodic the substitution of ensemble averages for time averages poses no problem. However the flow field in an engine is unsteady and non-stationary. This means that the time averaged mean will be dependent upon the length of the averaging interval and furthermore ensemble averages will not equal time averages. The second objection to ensemble averaging is that not only is the "mean" velocity periodic but there is also a cycle to cycle variation in the mean velocity itself. This cyclic variation in the mean velocity is included in the computed turbulence intensity when ensemble averaging is used.

Time averaging methods also present difficulties. The main problem arises in the selection of a window size for averaging. The calculated mean velocity will be highly dependent upon the length of the averaging interval. Ideally the window size should be as small as possible since the mean velocity can change quite rapidly. If the window size is made too large then information is lost. The same problem arises in calculation of the turbulence intensity; if the window size is too small then low frequency turbulence data is lost. Thus a compromise must be made.

In this investigation both techniques (time and ensemble averaging) were employed to interpret the data and the results were compared.

6.4.1 Ensemble Averaged Mean and RMS Velocity

An ensemble average is performed on a series of records each consisting of a sequence of equally spaced samples in time. If the instantaneous

velocity is written as $U(i, \theta)$ where i denotes the engine cycle (record) and θ the crank position (time) within the cycle then the ensemble averaged mean velocity for the position θ obtained from an ensemble of N cycles is:

$$\bar{U}(\theta) = \frac{1}{N} \sum_{i=1}^N U(i, \theta) \quad (6.10)$$

The turbulence intensity is defined as the rms of the velocity fluctuations about the mean and is:

$$u'(\theta) = \left\{ \frac{1}{N} \sum_{i=1}^N (U(i, \theta) - \bar{U}(\theta))^2 \right\}^{1/2} \quad (6.11)$$

There are several variations on this method. Rask [34] compared two methods; a window ensemble and a smoothed ensemble. In the window ensemble a crank angle interval was selected and data points within averaged to obtain a single point. The window averages were then ensembled as described above. In the smoothed ensemble a curve was fitted to the window averages for each cycle using cubic spline interpolation. The smoothed curves were then ensembled to obtain mean and rms velocities. He also performed a cycle by cycle analysis on the smoothed mean velocity curves. This involved evaluating the rms velocity from the smoothed curves for each cycle. The respective mean and rms velocity curves were then ensembled. He found that the turbulence intensity obtained by a cycle by cycle analysis was lower than that obtained from the other methods. This confirmed the fact that conventional ensemble averaging includes the cyclic variation of the mean flow in computed intensity.

In this study conventional ensemble averaging was compared to a cycle by cycle time averaging technique. The ensemble averaging was taken over 100 engine cycles. Each cycle consisted of samples for every $1/5$ of a

crank angle degree. The mean velocity was obtained from Equation (6.10) and the turbulence intensity in Equation (6.11) was obtained by:

$$u'(\theta) = \left\{ \frac{1}{N} \sum_{i=1}^N U^2(i, \theta) - \bar{U}^2(\theta) \right\}^{1/2} \quad (6.12)$$

Details of the calculation and the computer program used are in Appendix D.

6.4.2 Cycle by Cycle Time Averaged Mean and RMS Velocity

Two approaches for evaluating the mean and rms velocities on a cycle by cycle time averaged basis were studied. The majority of data was processed with a method similar to that of Catania and Mittica [35]. This technique is similar to the cycle-by-cycle smoothed ensemble proposed by Rask [34] except that time averages were performed in the windows rather than arithmetic averages. In their study Catania and Mittica evaluated a mean velocity curve for each cycle. This was done by finding the time average of the instantaneous velocity for specific time intervals (crank angles) within the engine cycle. The average values, taken at the center of the window, were then used with cubic spline interpolation to generate a smoothed mean velocity curve. The turbulence intensity was then obtained in a similar fashion from the instantaneous velocity and smoothed mean velocity for each cycle. The mean and rms velocity curves for each cycle were then ensembled.

They investigated the effect of different averaging intervals on computed mean and rms velocities. They found that window sizes ranging from 4 to 12 crank angle degrees had no significant effect on the mean velocity. For turbulence intensity calculations they varied the windows

from 1 to 20 crank angle degrees. They found that for intervals less than 8° the intensity values decreased. Between 8° and 20° however, there was relatively little difference. This interval (8° to 20°) corresponded to a time interval of between 0.83 and 2.08 milliseconds which corresponds to the range of macro time scales that can be expected in an engine. The fact that the turbulence intensity decreased for averaging intervals less than 8° indicates that low frequency turbulence information was being lost.

In the present study the same type of technique was employed. The mean velocity within specified time intervals for each cycle i was calculated by:

$$\bar{U}_{\theta}(i) = \frac{1}{\Delta} \int_0^{\Delta} U(i, \theta) d\theta \quad (6.13)$$

Window sizes ranging from 2 to 8 crank angle degrees were examined. Since these window sizes had relatively little effect on the resulting mean velocity curve a 4 degree window was selected for computational ease. Mean velocity curves were then obtained using cubic spline interpolation [28] between the evaluated points for each cycle. The turbulence was then computed for each cycle by:

$$u'_{\theta}(i) = \frac{1}{\Delta} \int_0^{\Delta} \{ [U(i, \theta) - \bar{U}_{\theta}(i)]^2 d\theta \}^{1/2} \quad (6.14)$$

where the averaging window θ was 12 crank angle degrees. Window sizes ranging from 2 to 14 degrees were studied. There was a decrease in the turbulence intensity for windows smaller than 6 crank angle degrees, however there was relatively little difference for windows larger than this. Based on these results, an averaging interval of 12° was used throughout for evaluating the turbulence intensity from Equation (6.14).

The mean velocity and turbulence intensity curves were then ensembled over 40 cycles to obtain one representative curve for each of the two properties, the ensemble averaged mean velocity:

$$\bar{U}_\theta = \frac{1}{40} \sum_{i=1}^{40} \bar{U}_\theta(i) \quad (6.15)$$

and the ensemble averaged turbulence intensity without the cyclic variation of the mean velocity:

$$u'_\theta = \left\{ \frac{1}{40} \sum_{i=1}^{40} \left[\frac{1}{\Delta} \int_0^\Delta (U(i,\theta) - \bar{U}_\theta(i))^2 d\theta \right] \right\}^{1/2} \quad (6.16)$$

The cyclic dispersion of the mean velocity was determined from the difference between the ensembled mean velocity of Equation (6.15) and the individual mean velocity curves for each cycle:

$$U_{\text{RMS}} = \left\{ \frac{1}{40} \sum_{i=1}^{40} [\bar{U}_\theta(i) - \bar{U}_\theta]^2 \right\}^{1/2} \quad (6.17)$$

Also the nonstationary analysis proposed by Lancaster [10] was studied for comparative purposes. Lancaster redefined the instantaneous velocity to be the sum of a stationary mean velocity $\bar{U}(i)$, a time varying mean velocity $\bar{U}(\theta)$, and a turbulent fluctuation $u(i,\theta)$:

$$U(i,\theta) = \bar{U}(i) + \bar{U}(\theta) + u(i,\theta) \quad (6.18)$$

In the present study the mean velocity obtained from ensemble averaging was first evaluated. Then the stationary mean velocity $\bar{U}(i)$ was calculated from:

$$\bar{U}(i) = \frac{1}{\Delta} \int_0^\Delta [U(i,\theta) - \bar{U}(\theta)] d\theta \quad (6.19)$$

for each engine cycle (record). The window size θ was varied from 40 to 100 crank angle degrees about TDC. The intensity was then computed from:

$$u'(i) = \left\{ \frac{1}{\Delta} \int_0^{\Delta} [U(i, \theta) - \bar{U}(\theta) - \bar{U}(i)]^2 d\theta \right\}^{1/2} \quad (6.20)$$

The intensity records were then ensembled.

Details of the calculation and the computer program used are in Appendix D.

6.4.3 Time Scale Analysis

An analysis similar to that of Haghgoole et al. [13] was performed on uncalibrated hot wire anemometer signals to obtain relative probability distributions of the peak-to-peak time separation. This analysis depends on the assumption of a definable small scale structure of turbulence in an engine similar to that proposed by Tennekes [7].

The technique involves the determination of an amplitude threshold for peak discrimination. This is obtained by operating the probe in quiescent ambient air. The problem with this technique is that the "noise" level sampled in quiescent air will be a turbulence signal resulting from natural convection. This "noise" will be insignificant in forced convection flow. Thus by setting a discrimination level for peak identification some of the high frequency turbulence information is lost. After the amplitude threshold is set the signal is sampled and a relative probability distribution is formed for the peak-to-peak time separation. Haghgoole et al. [13] concluded that the most probable frequency obtained in this fashion appears to be related to the small scale structure of the turbulence.

Based on the assumption that there is a definable small scale structure of turbulence in an engine similar to that proposed by Tennekes and that the method of Haghgoole et al. can be used to detect differences in the turbulent frequency distribution in engines a peak-to-peak time separation analysis was performed on the anemometer data obtained for the chambers studied. The noise amplitude threshold was obtained by evaluating the probability distribution from data collected while operating the probe

in quiescent ambient air. The relative distribution of the peak-to-peak time separation was then formed. It was found that this distribution was relatively insensitive to variations of up to 30% in the amplitude threshold. This could mean that high frequency turbulence data was lost. A window of 60° around TDC compression was used in the evaluation of the relative probability distribution. Details of the procedure and a listing of the computer program are in Appendix D.

6.5 Combustion Data

The pressure recorded during combustion tests was processed to yield mass burn rate curves for the configurations under study. The raw digital data was processed as detailed earlier in the chapter. The computer program used to process the data was developed by Jones [36]. The thermodynamic model in the program is based on the two zone approach and is similar to that of Keck [37] and Lavoie et al. [38]. The basic assumptions are that a thin spherical flame front separates the charge into two zones; the unburned region containing the reactants, and the burned region containing the products. Properties are assumed to be spatially uniform throughout each region. Furthermore both products and reactants have varying specific heats and obey the equation of state for an ideal gas. The unburned gas is assumed to be isentropically compressed due to the expansion of the burned region. The heat transfer is calculated using the Annand [39] equation. Six dissociation reactions are accounted for.

With the assumptions above and the application of the first law and conservation of mass an iterative procedure is followed from which the mass fraction burned is obtained at each crank angle degree. Minor changes to the program were necessary to accommodate the C.F.R. combustion chamber geometries. A complete discussion of these changes and a program listing is in Appendix E. A detailed discussion of the calculation procedure is given in [36].

7. DISCUSSION OF RESULTS

7.1 Introduction

In this chapter the results obtained from the experiments conducted on the C.F.R. engine are presented and discussed. In the first section results from flow field measurements are presented, while in the second section results from the combustion tests are presented and discussed.

7.2 Flow Field Results

This section is divided into four parts. In part one the different methods of processing the data (discussed in Chapter 6) are examined and compared. In part two results obtained for the standard squish chamber, Piston A, are presented. In the following section results for Piston B the squish chamber with channels are given. The final section deals with a comparison of the geometries investigated.

In the following sections flow velocities are presented plotted against crank angle degrees. The convention used is that 0° is BDC and 180° is TDC compression. Most of the plots are shown from 60° to 220° degrees. This is the portion of the engine cycle important to the combustion process. At 60° the intake generated flow has decayed and in a disc chamber would continue to decrease through TDC. The combustion period ranges from 30° BTDC to approximately 30° ATDC. At 220° the combustion period is finished.

7.2.1 Ensemble Averaging vs. Time Averaging

In this section the averaging techniques discussed in the previous chapter are compared. The results shown in this section were obtained with

the standard squish chamber (Piston A) at a clearance height of 1.5 mm. Three consecutive instantaneous velocity traces are shown in Figure 7.1. The basic mean velocity trend is evident and repeatable although there is considerable variation in the individual traces from cycle to cycle.

In Figure 7.2 the mean velocity trace obtained from conventional ensemble averaging techniques (Equation (6.10)) is shown with the mean velocity evaluated from Equation (6.15) using a window of 4 crank angle degrees as the time averaging window. From the figure it is clear that the two techniques yield almost indistinguishable results for the mean velocity trace. The cyclic variation of the mean velocity is shown in Figure 7.3. This curve was formulated from Equation (6.17). The cyclic variation can be seen to be fairly consistent throughout the compression stroke with a slight increase near TDC.

In Figure 7.4 the turbulence intensities obtained from conventional ensemble averaging using Equation (6.12) and from the time averaged window, cycle-by-cycle analysis of Equation (6.16) are shown. The window size used in Equation (6.16) was 12 degrees for the reasons discussed in the previous chapter. It is evident that the ensembled intensity has included in it some of the cyclic variation of the mean velocity. This is shown even more by comparing Figures 7.3 and 7.4.

The turbulence intensity obtained from Equation (6.11) using the non-stationary analysis proposed by Lancaster [10] is shown in Figure 7.5 for averaging windows of 40, 60, 80, and 100 degrees around TDC. Comparison of Figures 7.4 and 7.5 shows that the computed values lie between the ensembled and time averaged results. The problem with this formulation is the assumption that the difference between the ensembled mean and the instantaneous mean is constant during an individual cycle; that is, that

the curves are in phase and simply shifted up or down with respect to one another. However inspection of Figures 7.1 and 7.3 shows that this is not the case.

In the following sections the mean velocity was evaluated using the method described in Chapter 6 from Equation (6.15). A four degree window was used for the averaging interval. Turbulence intensities were computed from Equation (6.16) with an averaging interval of 12 crank angle degrees. The basis for the selection of these windows was discussed in Chapter 6.

7.2.2 Standard Squish Piston (Piston A) Results

In Figure 7.6 the mean velocity and turbulence intensity traces for a clearance height of 3.5 mm are shown. This data was taken at the edge of the bowl. The mean velocity decays steadily as TDC is approached. At approximately 10° BTDC there is a slightly increase in the mean velocity. After the small peak the mean velocity decreases until 10° ATDC. Another peak is then reached at 20° ATDC. A comparison of these results with the calculations in Chapter 3 (see Figure 3.2) shows that although the magnitude of the velocities do not agree the timing of the velocity peaks in Figure 7.6 corresponds to the trend predicted for the squish velocity. The turbulence intensity remains relatively constant throughout.

The effect of squish for a clearance height of 1.5 mm is clearly evident in Figure 7.7. The mean velocity is steady throughout the compression stroke until about 20° BTDC where there is a sharp increase which comes to a peak near TDC and then decays.

The interesting effect here is that the previous case ($h_c = 3.5$ mm) showed the effect of squish on both sides of TDC (as the model presented in Chapter 3 predicts); however, in this case ($h_c = 1.5$ mm) only one peak

centered approximately around TDC is shown. The results of James [25] showed a similar trend to the previous case ($h_c = 3.5$ mm); that is, squish effects before TDC and reverse squish on the expansion stroke. However he used large clearance heights and did not achieve pronounced squish effects. The results of both Witze [12] and Dent and Salama [10] show only one velocity peak near TDC similar to the trend exhibited in the data for $h_c = 1.5$ mm. The calculations in Chapter 3 predict the trend of two velocity peaks as shown in the data for $h_c = 3.5$ mm. However this model was very simplified and did not account for effects such as momentum and viscosity. It is possible that there is another flow regime at work (such as a piston generated vortex) with the squish; however, without flow visualization it is difficult to determine exactly what is happening.

At 10° BTDC a comparison of Figures 7.6 and 7.7 shows that the mean velocity achieved for a clearance height of 1.5 mm is approximately four times that for the lower clearance height. This is in agreement with the trend predicted by the calculations in Chapter 3 and demonstrates the critical effect of clearance height.

In Figure 7.8 the velocity trace obtained with the probe positioned at the center of the chamber ($h_c = 1.5$ mm) is shown. Again there is a large velocity peak at TDC. However careful examination of the figure shows that the point at which the mean velocity starts to increase comes approximately 5° later than it did for the measurement taken at the cup edge. This trend is to be expected since the arrival time of the squish-jet should be later as the probe is moved away from the cup edge.

To get an indication of how much swirling motion was present the probe was rotated 90° (see Figure 5.4) so that the probe axis was perpendicular to the piston face. Results obtained at the cup edge and at the chamber

center are shown in Figures 7.9 and 7.10. Both mean velocity and turbulence intensity are slightly higher indicating the presence of a tangential velocity component. However because only single sensor measurements were made it was not possible to resolve this component. The later arrival time of the squish-jet to the center can be seen more clearly from these two figures.

In Figure 7.11 the mean velocity curves obtain at clearance heights of 3.5 and 1.5 mm are compared. Although the two curves are similar in the early part of the compression stroke the effect of the squish can be seen as they begin to deviate from one another at approximately 30° BTDC. Measurements were also made for the clearance height of 2.5 mm. The resulting velocity traces were not that different from the 3.5 mm case and are not presented. From these results it can be seen that the clearance height is important in the observed squish effect as predicted by the calculations in Chapter 3.

A comparison of the relative turbulence intensities for the two heights is shown in Figure 7.12. It is evident that although the magnitudes of the velocity traces vary considerably, the relative quantities show only a maximum increase of about 25% for the clearance height of 1.5 mm during the squish period.

7.2.3 Squish-Jet Combustion Chamber (Piston B) Results

Measurements were made at the same locations and conditions as for Piston A. The mean velocity and turbulence intensity profiles for a clearance height of 3.5 mm are shown in Figure 7.13. In this case it is difficult to detect any effect of squish at all prior to TDC and only a small peak occurs after TDC. However from calculations in Chapter 3 this trend

could be expected if the gas is now using the additional routes provided by the channels.

At the smaller clearance height shown in Figure 7.14 the squish effect can be seen again. In this case the peak effect at TDC is not as pronounced as it was for Piston A although the same general trend for both mean velocity and turbulence intensity is exhibited. Examination of the figure shows that the mean velocity trace is consistently lower for Piston B. The most probable explanation for this is that there was leakage past the piston rings for the previous measurements. All hot wire measurements except those for Piston B at a clearance height of 1.5 mm were obtained before a failure in the C.F.R. engine required that the cylinder be honed out and the piston rings replaced. If there was considerable blow-by past the piston rings then the velocity measurements would be artificially inflated. This could explain the observed differences in the velocity traces before the squish could start affecting the flow.

In Figure 7.15 the mean velocity trace and turbulence intensity traces are shown for Piston B at the center of the chamber ($h_c = 1.5$ mm). The interesting effect here is the character of the mean velocity trace after top dead center. After the peak starts to decay the velocity is relatively flat for a few degrees and then there is a small peak. This could be the separate effects of squish, and another flow regime.

In Figure 7.16 the velocity and intensity traces for the measurement taken inside the cup are shown. This was an attempt to get an idea of the jet velocity leaving the channel as it entered the bowl. Unfortunately geometric constraints would only permit the probe to be aligned with the channel centerline right at TDC. Although calculations in Chapter 3 indicate the velocity of the channel jet should be zero at TDC it was hoped

that the probe would detect the final part of the jet as the top of the channel passed the probe. As can be seen from Figure 7.15 the jet was not detected at all. However this is most probably due to the inability to position the probe properly rather than the lack of a jet velocity.

In Figure 7.17 the relative turbulence intensities for the clearance heights of 3.5 and 1.5 mm are shown. The maximum difference between the two is approximately 10 percentage points, on the same order as the difference between relative intensities for Piston A at the same height.

7.2.4 Comparison of Geometries

In this section a comparison between the two geometries is made. The two mean velocity traces ($h_c = 1.5$ mm) are compared in Figure 7.18. As was mentioned earlier it is believed that the mean velocity trace of Piston A is artificially inflated due to leakage past the piston rings. There is no other explanation for the difference between the two curves between 60 and 140 degrees. The points to notice from this figure are that the trends are basically similar; the mean velocity begins to increase about 20° BTDC, the peak occurs near TDC, and about 20° ATDC there is a slight secondary peak. In Figure 7.19 the relative intensities are compared for the probe located at the cup edge ($h_c = 1.5$ mm). The relative intensity of Piston B is consistently higher than for Piston A. The maximum difference between the two is 11 percentage points; that is, Piston B shows a 29% improvement. However it is difficult to say how much of this is due to increased turbulence generation by Piston B design. This is because although flow induced by leakage past the rings would create a higher mean velocity it might not generate new turbulence. Thus the relative intensity for Piston A might be artificially low. However a comparison of Figures 7.12 and 7.17 shows that even at the clearance height of 3.5 mm the relative turbulence

intensity was higher from Piston design B. In this case the relative turbulence intensities of the two designs were approximately equal until 30° BTDC through 20° ATDC. In this region the maximum difference between the two curves was approximately 6 percentage points. This trend indicates that the squish-jet piston design is more effective at generating turbulence during the compression stroke (or squish period). This would be important to combustion since it is the level of turbulence and not the mean velocity that enhances combustion.

The relative probability distributions of the peak-to-peak time separation are shown in Figures 7.20 to 7.23. These measurements were performed for the clearance heights of 1.5 mm and for the disc chamber for comparison. The distributions presented are for a crank angle window of 60° around TDC. The distributions were obtained using the peak to peak time separation technique described in Chapter 6.

In Figure 7.20 the distributions for Piston A at the bowl edge and at the chamber center are shown. From the graph it can be seen that there is a slight broadening of the distribution towards the center of the chamber. In Figure 7.21 the distribution for the flat piston is compared to that of Piston A at the center of the chamber. From this graph it is evident that there is some clustering of frequency bands for the flat piston chamber. In general the relative probability for Piston A is higher in the high frequency range than it is for the flat piston; however the differences are minor.

In Figure 7.22 the distributions of Pistons A and B are compared for the probe position at the cup edge. Although the most probable frequency for the two designs is the same, approximately 1 millisecond, the distribution for B shows less skew to the left (higher frequencies) than that of

Piston A. In Figure 7.23 the distributions for the two designs are shown for the center probe location. Here there has been a definite shift in Piston B's distribution to the right and lower frequencies; whereas for Piston A, although there has been some broadening of the distribution, the most probable time has not changed.

Although there are differences in the distributions they are minor and the results indicate that the squish chamber has a small effect on the turbulent frequency distribution in the chamber. However in view of the limitations of the analytical method the results are somewhat inconclusive since it is possible that high frequency information was lost.

7.3 Combustion Results

In this section results from the combustion tests are presented. The pressure traces for each of the pistons A and B as well as the flat piston were analyzed for mass fraction burned history. The final mass fraction burned for the tests was about 93%. There are a number of reasons 100% burned was not achieved; blow by could not be adequately accounted for in the calculations, combustion may have been incomplete, and there could have been an error in the heat transfer calculations. The uncertainty in the initial reference pressure is estimated to be 5%. However this gives an insignificant percentage error ($< .1\%$) in peak pressure. The major source of uncertainty in the mass burn rate analysis arises in the evaluation of the initial energy of the charge in the cylinder. The uncertainty in the initial energy is a function of uncertainty in pressure, temperature, and charge mass. The uncertainty in the charge mass arises from measurement of air and fuel rates, and estimation of the residual fraction. The total uncertainty in the mass is estimated to be 5%. This leads to an uncertainty of 15% in the mass fraction burned.

In Figure 7.24 the pressure histories for Pistons A and B ($h_c = 1.5$ mm) and the flat piston are shown for a spark timing of 30° BTDC. The maximum cylinder pressure of 63.3 Bar was achieved with Piston B at 8° ATDC. The maximum pressure obtained with Piston A was 61.1 Bar at a crank position of 11° ATDC. The flat piston yielded the poorest results with a maximum pressure of 46.0 Bar occurring 16° ATDC. In Figure 7.25 the mass fraction burned curves for the flat piston and Piston A are shown (spark timing 30° BTDC). It can be seen that the basic squish design appears to have very little effect on the ignition delay time. The ignition delay time here is defined to be the time taken to burn 2% of the charge mass. The effect of squish is seen in the main stage of combustion, defined here to be the period for 2 to 85% mass burned. The burn time for the flat piston was 38 crank angle degrees whereas for Piston A this time was reduced by 26% to 28 crank angle degrees. These results are in agreement with Nagayama et al. [17] who found that squish increased burning rate in the main combustion stage and resulted in higher maximum pressures. In Figure 7.26 the mass fraction burned curves are compared for Pistons A and B. The spark timing was again in both cases 30° BTDC. It can be seen from this figure that the main effect of the squish jet channels is a reduction in the ignition delay time. The ignition delay time is 3° less for Piston B; a 17% reduction. However the main stage of combustion does not appear to have been affected. The burn time for both designs is approximately 28 crank angle degrees. In Figure 7.27 the three curves are plotted together and the separate effects of faster burn rate during the main combustion period due to the squish, and reduced ignition delay due to the channels can be clearly seen. The total combustion duration is defined here to be the time from spark to 85% mass burned. The total combustion durations for

the flat piston and Pistons A and B were 58, 44 and 42 crank angle degrees respectively.

In Figure 7.28 the mass fraction burned curves for the two squish designs are compared for a spark timing of 25° BTDC. Again the only real effect appears to be a reduction in ignition delay time in the case of Piston B. However the effect is not as pronounced in this case. This is to be expected since ignition delay effects will be enhanced for earlier spark timing (as in the 30° BTDC case) since the initial pressure and temperature of the mixture is lower. In this case (25° BTDC) there is only 2° difference in the ignition delay period for the two designs.

8. CONCLUSIONS AND RECOMMENDATIONS

The objective of this thesis was to investigate the effects of the squish chamber design on the combustion process and flow field of an I.C. engine and particularly to compare the reference squish design to the squish-jet design [8]. A number of conclusions may be drawn on the basis of the experimental data.

Cylinder pressure data shows the squish design to be effective in increasing the mass burn rate during the main combustion period. For a spark timing of 30° BTDC the combustion duration for the disc chamber was 58° compared to 45° for Piston A at $h_c = 1.5$ mm. The peak pressure achieved with Piston A was 30% higher and occurred 5° earlier.

Comparisons of cylinder pressure data for Pistons A and B show the squish-jet chamber design to give superior performance. For a spark timing of 30° BTDC the maximum pressure attained with Piston B was 4% higher and occurred 3° earlier. The major effect of the squish-jet chamber design was the reduction in ignition delay time by 3° for a 17% improvement. The main stage of combustion does not appear to have been affected. The combustion duration for Piston B was 42° ; 3° less than for Piston A.

Although the uncertainty in the computed flow field parameters is high, because the experiments were performed from case to case with conditions as identical as possible some of the uncertainty is systematic. From the flow field data it appears that the clearance height has a significant effect on the mean velocity. The mean velocity computed for Piston B was less than that for Piston A for identical clearance heights. The peak-to-peak time separation analysis results indicated no significant difference in the turbulence frequency distributions for the two designs.

Further work is recommended for the combustion experiments in this study it was not possible to vary the operating conditions nor to obtain adequate performance data. Pressure history was the only obtainable data. Therefore, it is recommended that extensive performance tests be carried out with the two squish chamber designs. Also in this study the engine used had a side point ignition. It is recommended that further experiments be performed in an engine with a central ignition to study the full benefit of the mixing in the combustion chamber due to the squish-jet channels.

Further flow field experiments are also recommended. Flow visualization would be valuable. Measurement of length scales in the squish-jet chamber could provide valuable insight into the link between ignition delay and small scale turbulence structure.

BIBLIOGRAPHY

1. MATTAVI, J.N., "The Attributes of Fast Burning Rates in Engines", SAE 800920, 1980.
2. MAYO, J., "The Effect of Engine Design Parameters on Combustion Rate in Spark-Ignited Engines", SAE 750355, 1975.
3. DAMKOHLER, G., "The Effects of Turbulence on the Flame Velocities in Gas Mixtures", NACA TM 1112, 1947.
4. TABACZYNSKI, R.J., FERGUSON, C.R. and RADNAKRISHNAN, K., "A Turbulent Entrainment Model for Spark Ignition Engine Combustion", SAE 770 , 1975.
5. BLIZARD, N.C. and KECK, J.C., "Experimental and Theoretical Investigation of Turbulent Burning Model for Internal Combustion Engines", SAE 740191, 1974.
6. ANDREWS, G.E., BRADLEY, D. and LWAKABAMBA, S.B., "Turbulence and Turbulent Flame Propagation - A Critical Appraisal", Combustion and Flame, Vol. 24, pp. 285-304, 1975.
7. TENNEKES, H., "Simple Model for the Small-Scale Structure of Turbulence", Physics of Fluids, Vol. 11, No. 3, 1968.
8. EVANS, R.L., Patent Applications.
9. SEMENOV, E.S., "Studies of Turbulent Gas Flow in Piston Engines", Otdelenie Technicheskikh Navk, No. 8, 1958 (English Translation: NASA Technical Translation, F97).
10. DENT, J.C. and SALAMA, N.S., "The Measurement of the Turbulence Characteristics in an Internal Combustion Engine Cylinder", SAE 750886, 1975.
11. LANCASTER, D.R., "Effects of Engine Variables on Turbulence in a Spark-Ignition Engine", SAE 760159, 1975.
12. WITZE, P.O., "Measurements of the Spatial Distribution and Engine Speed Dependence of Turbulent Air Motion in an I.C. Engine", SAE 770220, 1977.
13. JAMES, E.H. and LUCAS, G.G., "Turbulent Flow in Spark Ignition Engine Combustion Chambers", SAE 750885, 1975.
14. HAGHGOOIE, M., KENT, J.C. and TABACZYNSKI, R.J., "Turbulent Time Scale Measurements in a Spark-Ignition Engine Using Hot Wire Anemometry and Fast Response Ion Probes", Symposium on Flows in I.C. Engines, ASME WAM, 1982.

15. LANCASTER, D.R., KRIEGER, R.B., SORENSON, S.C. and HULL, W.L., "Effects of Turbulence on Spark-Ignition Engine Combustion", SAE 760160, 1976.
16. KRIEGER, R.B. and BORMAN, G.L., "The Computation of Apparent Heat Release for Internal Combustion Engines", ASCE 66-WA/DGP-4, 1966.
17. NAGAYAMA, I., ARAKI, Y. and IOKA, Y., "Effects of Swirl and Squish on S.I. Engine Combustion and Emission", SAE 770217, 1977.
18. LUCAS, G.G. and BRUNT, M.F., "The Effect of Combustion Chamber Shape on the Rate of Combustion in a Spark Ignition Engine", SAE 820165, 1982.
19. DAVIS, G.C., TABACZYNSKI, R.J. and BELAIRE, R.C., "The Effect of Intake Valve Lift on Turbulence Intensity and Burnrate in S.I. Engines-Model Versus Experiment", SAE 240030, 1984.
20. POULOS, S.G. and HEYWOOD, J.B., "The Effect of Geometry on Spark-Ignition Engine Combustion", SAE 830334, 1983.
21. WITZE, P.O., MARTIN, J.K. and BORGNAKKE, C., "Measurements and Predictions of the Precombustion Fluid Motion and Combustion Rates in a Spark Ignition Engine", SAE 831697, 1983.
22. GROFF, E.G. and MATEKUNAS, F.A., "The Nature of Turbulent Flame Propagation in a Homogeneous Spark-Ignited Engine", SAE 800133, 1980.
23. BRANDL, F., REVERENCIC, I., CARTELLIERI, W. and DERT, J.C., "Turbulent Air Flow in the Combustion Bowl of a D.I. Diesel Engine and its Effect on Engine Performance", SAE 790040, 1979.
24. CHARBONGSAI, S., KADOTA, T. and HENEIN, N.A., "The Burning Velocity in a C.F.R. Engine with Different Turbulent Flow Fields Generated by Intake Valve", SAE 800860, 1980.
25. JAMES, E.H., "Investigations of Combustion in 'Squish' Chamber Spark Ignition Engines", ASME 84-DGP-10, 1984.
26. BENSON, R.S. and PICK, R., "Recent Advances in Internal Combustion Instrumentation with Particular Reference to High Speed Data Acquisition and Automated Test Bed", SAE 740695, 1974.
27. WITZE, P.O., "A Critical Comparison of Hot-Wire Anemometry and Laser Doppler Velocimetry for I.C. Engine Applications", SAE 800132, 1980.
28. MOORE, C., "UBC Curve, Curve Fitting Routines", Computing Centre, University of British Columbia, 1984.
29. LANCASTER, D.R., KRIEGER, R.B. and LIENESCH, J.H., "Measurement and Analysis of Engine Pressure Data", SAE 750026, 1975.

30. COLLIS, D.C. and WILLIAMS, M.J., "Two Dimensional Convection From Heated Wires at Low Reynold's Numbers", Journal of Fluid Mechanics, Vol. 6, 1959, pp. 357-384.
31. DAVIES, P.O.A.L. and FISHER, M.J., "Heat Transfer From Electrically Heated Cylinders", Proc. Roy. Soc. A., Vol. 280, 1964, pp. .
32. KING, L.V., "On Convection of Heat From Small Cylinders in a Stream of Fluid in Determination of the Convective Constants of Small Platinum Wires with Application to Hot Wire Anemometry", Proc. Roy. Soc., Vol. 214A, No. 14, 1974.
33. VAN WYLEN, G.J. and SONNTAG, R.E., "Fundamentals of Classical Thermodynamics", John Wiley & Sons, 1978.
34. RASK, R.B., "Comparison of Window, Smoothed-Ensemble, and Cycle-by-Cycle Data Reduction Techniques for Laser Doppler Anemometer Measurements of In-Cylinder Velocity", Symposium on Fluid Mechanics of Combustion Systems, ASME FED, Spring Meeting, 1981.
35. CATANIA, A.E. and MITTICA, A., "A Contribution to the Definition and Measurement of Turbulence in a Reciprocating I.C. Engine", ASME 85-DGP-12, 1985.
36. JONES, A.L., "The Performance of a Turbocharged Spark-Ignition Engine Fuelled with Natural Gas and Gasoline", M.A.Sc. Thesis, University of British Columbia, 1985.
37. KECK, J.C., "Turbulent Flame Structure and Speed in Spark Ignition Engines", Nineteenth Symposium {International} on Combustion, The Combustion Institute, 1982, p. 1451-1466.
38. LAVOIE, G., HEYWOOD, J.B. and KECK, J.C., "Experimental and Theoretical Study of Nitric Oxide Formation in Internal Combustion Engines", Combustion, Science & Technology 1, 313, 1970.
39. ANNAND, W.J.D., "Heat Transfer in the Cylinders of Reciprocating Internal Combustion Engines", Proc. I. Mech. E., Vol. 177, No. 36, 1963.
40. VINES, R.F., "The Platinum Metals and Their Alloys", The International Nickel Company, Inc., New York, New York, 1941.
41. NICOL, T., "Integration (Quadrature) Routines", Computing Centre, University of British Columbia, 1982.

APPENDIX A - CALIBRATION CURVES

In this appendix the calibration curves for the Meriam laminar flow element, used to monitor natural gas flow, and the orifice plate used to monitor air intake flow to the C.F.R., are presented. The calibration for the laminar flow element was supplied by the manufacturer. The laminar flow element was used to calibrate the orifice plate.

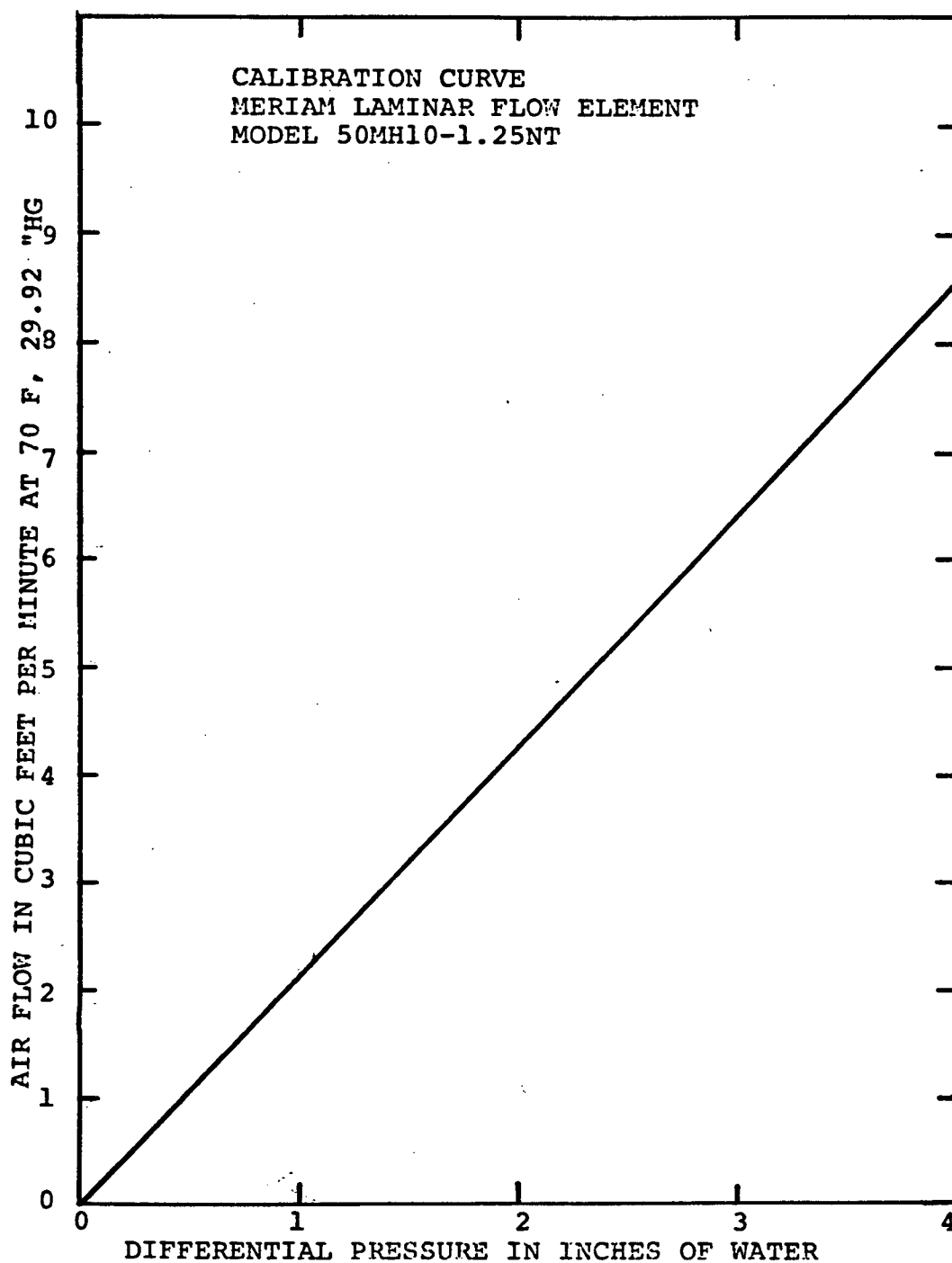


Figure A.1. Calibration curve for laminar flow element.

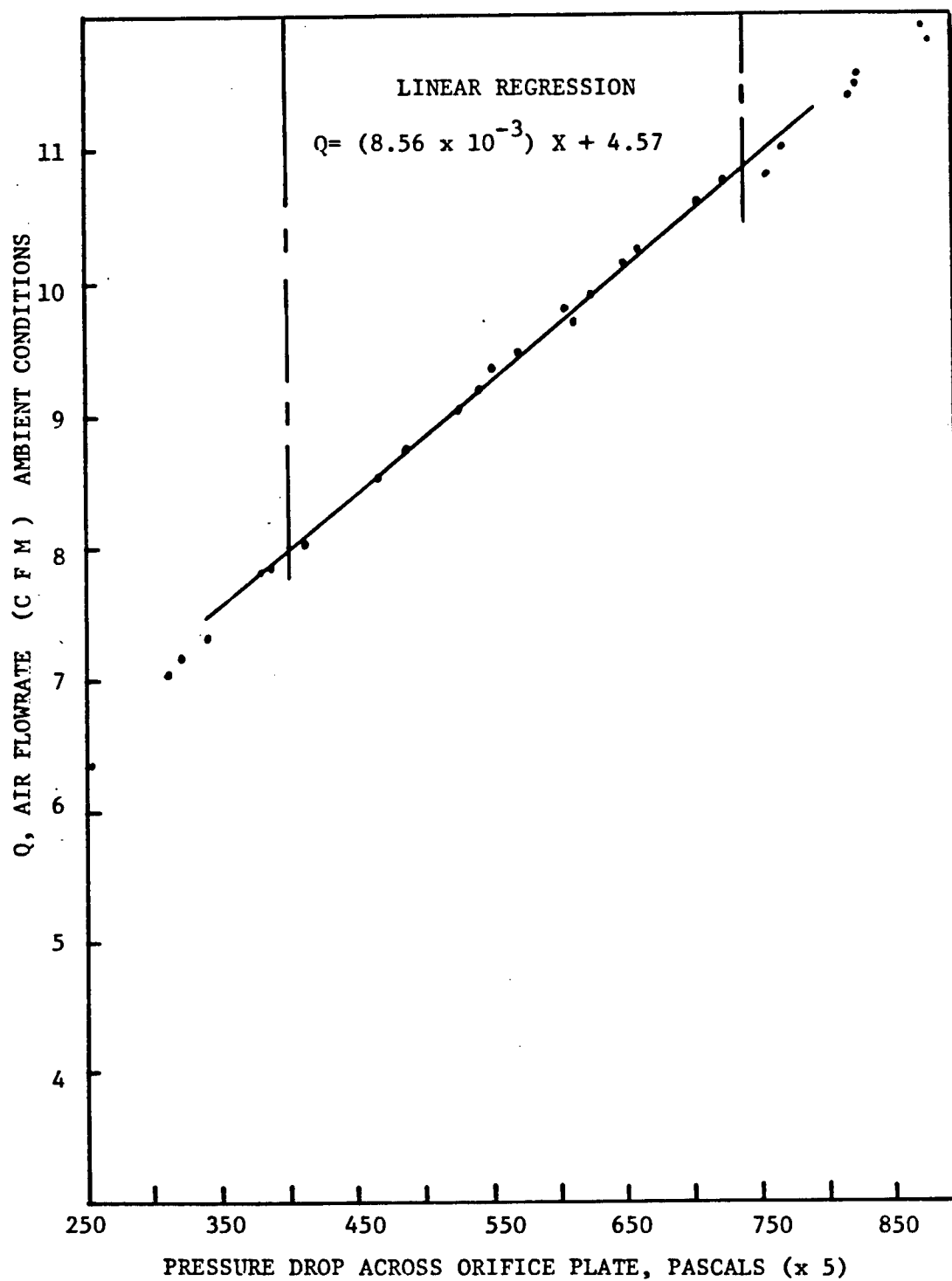


Figure A.2. Calibration curve for orificic metre.

APPENDIX B - HOT WIRE CALIBRATION PROCEDURE

In this appendix the preparation and calibration of hot wire probes for measurement of air movement within the C.F.R. cylinder are described.

1. Welding and Preparation

Wire breakage was a frequent occurrence during the course of experiments and thus it became necessary to establish a routine repair procedure.

Platinum Iridium wire (diameter = 6.3 micrometers) obtained from TSI Incorporated was spot welded onto the support needles. The welding was performed with the aid of a microscope and a Disa welding unit model 55A12. Each welded wire was inspected visually for any defects or contamination after welding.

The resistance of the sensor was measured by placing it into the anemometer bridge circuit and adjusting the variable load resistance until bridge balance was achieved. The resistance of the cable and the internal resistance of the probe were accounted for in this procedure. The internal resistance of the probe varied from weld to weld but was generally between 0.58 and 0.80 ohms. Some sensors were found to have a high weld resistance after repair. These wires were maintained at a high overheat ratio until the resistance dropped and stabilized. If the weld resistance remained high the wires were discarded.

2. Calibration

The probes were calibrated in an open wind tunnel with a pitot tube at ambient conditions for air speeds ranging from 0.5 to 20 m/s. The wire was operated at a temperature of 600°C. The operating temperature of 600°C was

selected because Vines [40] has reported that above this temperature platinum-iridium wire undergoes a phase transformation and thus its resistance characteristics are altered. The operating resistance of the wire was determined from:

$$R_{OP} = R_0 + R_0 \alpha_0 (T_{OP} - T_0) \quad (A.1)$$

where α_0 , R_0 , T_0 were supplied by the manufacturer.

From the pitot tube data a Reynolds number was formed based on the wire diameter and the ambient air conditions. From the corresponding anemometer voltage a Nusselt number was calculated again based on the air conditions. From the calibration data a correlation was formed. The analytical method is described in the next section.

3. Analytical Procedure for Correlation

The hot wire anemometer registers the change in resistance (electrical) which results from the heat transfer from the sensor. Heat is transferred by radiation, buoyant convection, forced convection by the flow, and conduction along the wire to the supports. The radiation portion is small and can be neglected. Also for all applications except those involving very small velocities buoyancy may be neglected. Thus forced convection induced by the flow and conduction to the supports are the main modes of heat transfer.

Because the convection heat transfer process is a function of the driving temperature differential and fluid properties such as viscosity, density, and conductivity the sensor response is sensitive to changes in temperature and pressure in the flow. Ideally a probe should be calibrated

over the range of temperatures and pressures encountered in the engine cylinder. However this is not a practical solution in light of the frequent occurrence of wire breakage. Thus it becomes necessary to rely on analytical models to correct for variations from the calibrated conditions.

Most of the universal calibrations developed are modifications to the theory of King [32] and express the Nusselt number as a function of the Reynolds number in the form:

$$Nu = a + b Re^h \quad (A.2)$$

where a , b , and n are determined from calibration. The Nusselt number is also a function of the Prandtl number; however, since the Prandtl number is almost constant in air (about 0.7) it is not considered explicitly in the correlation.

In this study an approach similar to that of Davies and Fisher as proposed by Witze [27] was taken. In this method the one dimensional energy equation for the wire is solved to obtain an expression for the temperature distribution along the wire. This temperature distribution is integrated along the wire to yield a mean wire temperature:

$$T_M = \frac{2(T_P - C_1)}{\sqrt{C_2} \ell} \tanh [\sqrt{C_2} \ell / 2] + C_1 \quad (A.3)$$

where

$$C_1 = \frac{hT_g + I^2 R_0 (1 - \alpha_0 T_0) / (\pi d \ell)}{h - I^2 R_0 \alpha_0 / (\pi d \ell)} \quad (A.4)$$

and

$$C_2 = 4[h - I^2 R_0 \alpha_0 / (\pi d \ell)] / k_w d \quad (A.5)$$

where h is the heat transfer coefficient, T_p is the sensor support temperature, T_g is the gas temperature, k_w is the mean thermal conductivity of the wire, R_0 is the resistance of the wire at the reference temperature T_0 , α_0 is the temperature coefficient of resistance for the wire, and I is the current through the wire. Since the mean wire temperature is fixed at 600°C , the only unknown in the above equations is h , the heat transfer coefficient. Iteration can be used to find h . The Nusselt number is then formed.

4. Hot Wire Calibration Computer Program HWCAL

This program uses the data obtained to fit a correlation of the form of Equation (A.2). The program uses a nonlinear least squares method [28] to fit the data.

Inputs to the program are the ambient conditions temperature and pressure, operating resistance of the wire, and the calibration data pressure differential and anemometer bridge voltage.

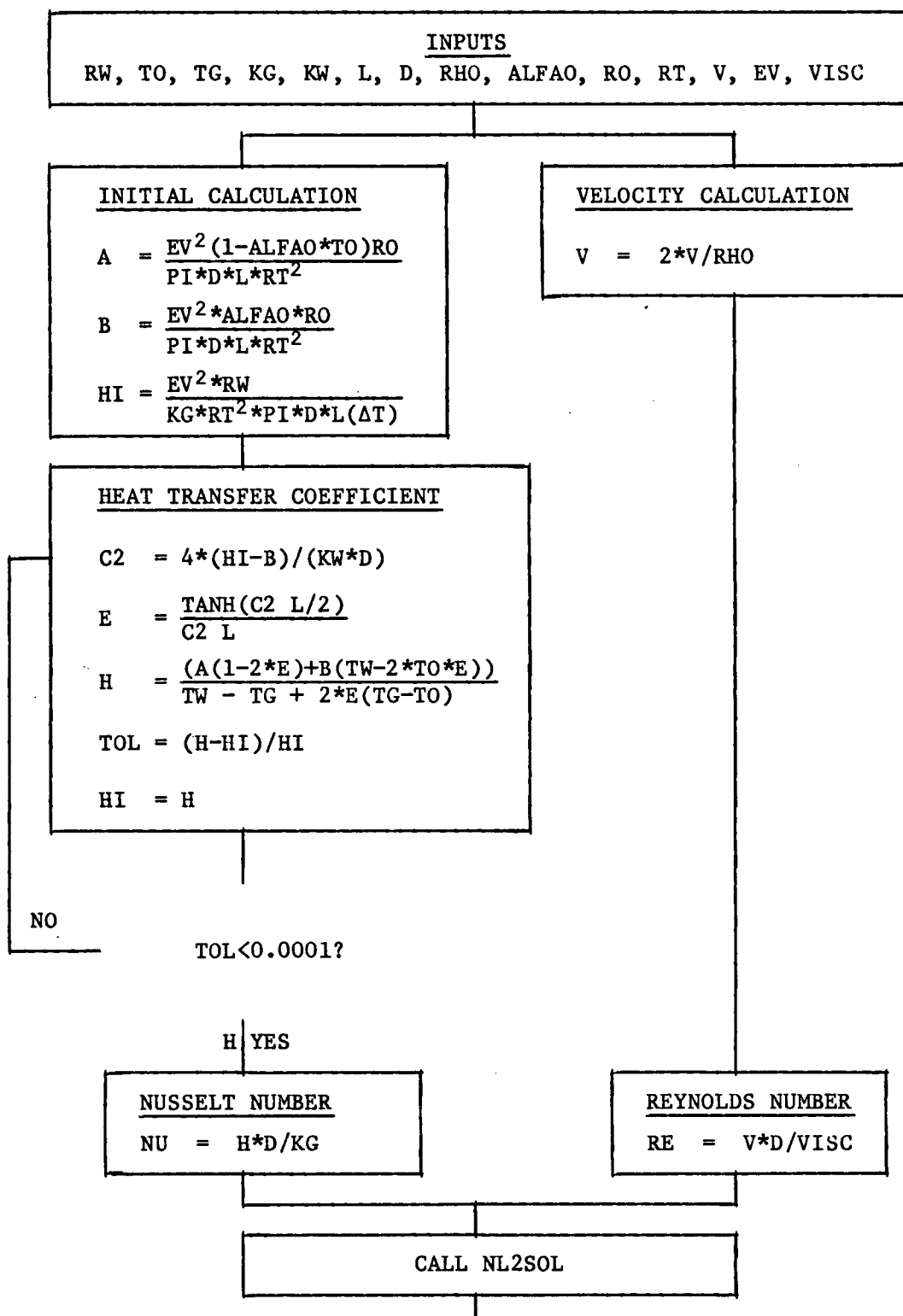
The data is processed within the subroutine ANEM to obtain Nusselt number, as described in the previous section, and Reynolds numbers from the pitot tube data. The arrays of Reynold and Nusselt numbers are then passed to the curve fitting program NL2SOL from the U.B.C. curve fitting library [20]. The outputs of the program are the calibration constants a, b, n and the residuals.

A program listing and flow chart follows.

DEFINITION OF PROGRAM SYMBOLS

A	Constant
ALFAO	Temperature coefficient of wire resistance
B	Constant
C2	Constant C2 in Equation A.5
D	Diameter of wire
EV	Anemometer bridge voltage corresponding to flow measurement
H	Heat transfer coefficient
IV	Working array of curve fit routine
KG	Thermal conductivity of gas
KW	Thermal conductivity of wire
L	Length of wire
NV	Nusselt number
P	Coefficient array
RE	Reynolds number
RHO	Density of gas
RO	Ice point resistance of wire
RW	Operating resistance of wire
V	Pressure differential corresponding to pitot tube measurement
VISC	Kinematic viscosity of gas

HWCAL FLOWCHART
CALL SUBROUTINE ANEM



HWCAL at 10:25:13 on JUN 27, 1985 for CCId=CILL Page 1

```

1      IMPLICIT REAL*8 (A-H,O-Z)
2      DIMENSION P(3),IV(65),V(350)
3      EXTERNAL CALCR,CALCJ
3.5    COMMON X(20),Y(20)
4      M=3
5      CALL ANEM(N)
8      P(1)=0.25DO
9      P(2)=0.25DO
10     P(3)=0.45DO
10.5   FIND (7'1000)
11     DO 88 JJ=1,N
11.5   READ(7,89) X(JJ),Y(JJ)
11.7   89  FORMAT(2F20.2)
11.8   88  CONTINUE
12     IV(1)=0
17     CALL NL2SOL(N,M,P,CALCR,CALCJ,IV,V,IPARM,RPARM,FPARM)
18     WRITE(6,300) IV(1)
19     300  FORMAT(' RETURN CODE = ',I2)
20     WRITE(6,301) (P(I),I=1,3),V(10)
21     301  FORMAT(' SOLUTION: ',1P3G16.8/
22           ' SUM OF SQUARES/2 = ',1PG16.8)
31     STOP
32     END
33     SUBROUTINE CALCR(N,M,P,NF,R,IPARM,RPARM,FPARM)
34     IMPLICIT REAL*8(A-H,O-Z)
35     DIMENSION P(M),R(N)
36     COMMON X(20),Y(20)
37     DO 100 I=1,N
38     R(I)= P(1) + P(2)*X(I)**P(3) - Y(I)
40     100  CONTINUE
43     RETURN
44     END
45     SUBROUTINE CALCJ(N,M,P,NF,D,IPARM,RPARM,FPARM)
46     IMPLICIT REAL*8(A-H,O-Z)
47     DIMENSION P(M),D(N,M)
47.2   COMMON X(20),Y(20)
47.7   DO 100 I=1,N
47.8   D(I,1)=1.DO
47.9   D(I,2)=X(I)**P(3)
47.95  D(I,3)=P(2)*(X(I)**P(3))*DLOG(X(I))
47.97  100  CONTINUE
48     RETURN
49     END
50     SUBROUTINE ANEM(NDAT)
51     REAL*8 KW,KG,L,D,RO,ALFAO,TO,TG,RW,TW,A,B,HI,C2,E,H
52     REAL*8 RE(18),NU(18),EV(18),V(18),VO
53     KW=18.DO
54     KG=0.0251DO
55     L=1.5E-03
56     D=6.30E-06
57     ALFAO=0.0009
58     TO=293.15
59     WRITE(6,1)
60     1    FORMAT(' AMBIENT TEMPERATURE = ?')
61     CALL FREAD('GUSER','R:',TO)
62     WRITE(6,2)
63     2    FORMAT(' GAS TEMPERATURE = ?')
64     CALL FREAD('GUSER','R:',TG)

```

HWCAL at 10:25:13 on JUN 27, 1985 for CCId=CILL Page 2

```

65      WRITE(6,3)
66      3      FORMAT(' AMBIENT RESISTENCE OF WIRE = ?')
67      CALL FREAD('GUSER','R:',RAMB)
68      WRITE(6,4)
69      4      FORMAT(' OPERATING RESISTENCE OF WIRE = ?')
70      CALL FREAD('GUSER','R:',RW)
71      WRITE(6,5)
72      5      FORMAT(' NUMBER OF DATA POINTS = ?')
73      CALL FREAD('GUSER','I:',NDAT)
74      DO 999 J=1,NDAT
75      WRITE(6,6)
76      6      FORMAT(' PRESSURE DIFFERENTIAL = ?')
77      CALL FREAD('GUSER','R:',V(J))
78      WRITE(6,7)
79      7      FORMAT(' ANEMOMETER VOLTAGE = ?')
80      CALL FREAD('GUSER','R:',EV(J))
81      999    CONTINUE
82      WRITE(6,8)
83      8      FORMAT(' ICE POINT RESISTANCE OF WIRE ? ')
84      CALL FREAD('GUSER','R:',RO)
85      TW=(RW-RO)/(ALFAO*RO)
86      TG=TG+273.15
86.5    RA=RAMB
87      TO=TO+273.15
87.5    TL=TO-273.15
88      RT=RW+50.214
89      TW=TW+273.15
90      ALFAO=0.0009
91      DO 10 J=1,NDAT
92      NCOUNT=0
93      V(J)=DSQRT(2.0*V(J)/1.144)
94      A=EV(J)**2*(1.-ALFAO*(273.15))/(3.141593*D*L*RT**2)*RC
95      B=EV(J)**2*ALFAO/(3.141593*D*L*RT**2)*RO
96      HI=EV(J)**2/(KG*(RT**2)*3.141593*D*L*(TW-TG))*RW
97      22    C2=4*(HI-B)/(KW*D)
98      NCOUNT=NCOUNT+1
99      IF (NCOUNT .GT. 100) GO TO 100
100     E=DTANH(DSQRT(C2)*L/2)/(DSQRT(C2)*L)
101     H=(A*(1.-2*E)+ B*(TW-2*TO*E))/(TW-TG+2*(TG-TO)*E)
102     TOL= DABS((H-HI)/HI)
103     HI=H
104     IF (TOL .GT. 0.001) GO TO 22
105     NU(J)=H*D/KG
106     RE(J)= V(J)*D/15.7E-06
111     10    CONTINUE
111.2    DO 102 J=1,NDAT
111.5    WRITE(7,101) RE(J),NU(J)
111.7    101  FORMAT(2F20.2)
111.8    102  CONTINUE
112      GO TO 98
113      100  WRITE(6,99)
114      99   FORMAT(' ', 'ERROR, TOO MANY ITERATIONS N=100!')
115      98   CONTINUE
116      RETURN
117      END

```

APPENDIX C - DATA ACQUISITION PROGRAMS

In this appendix the computer programs used for data acquisition are presented. The first program CDAQ, was used to collect data directly from the experiments. The second program BYTRD was used to transfer the digital data from floppy discs to the MTS system.

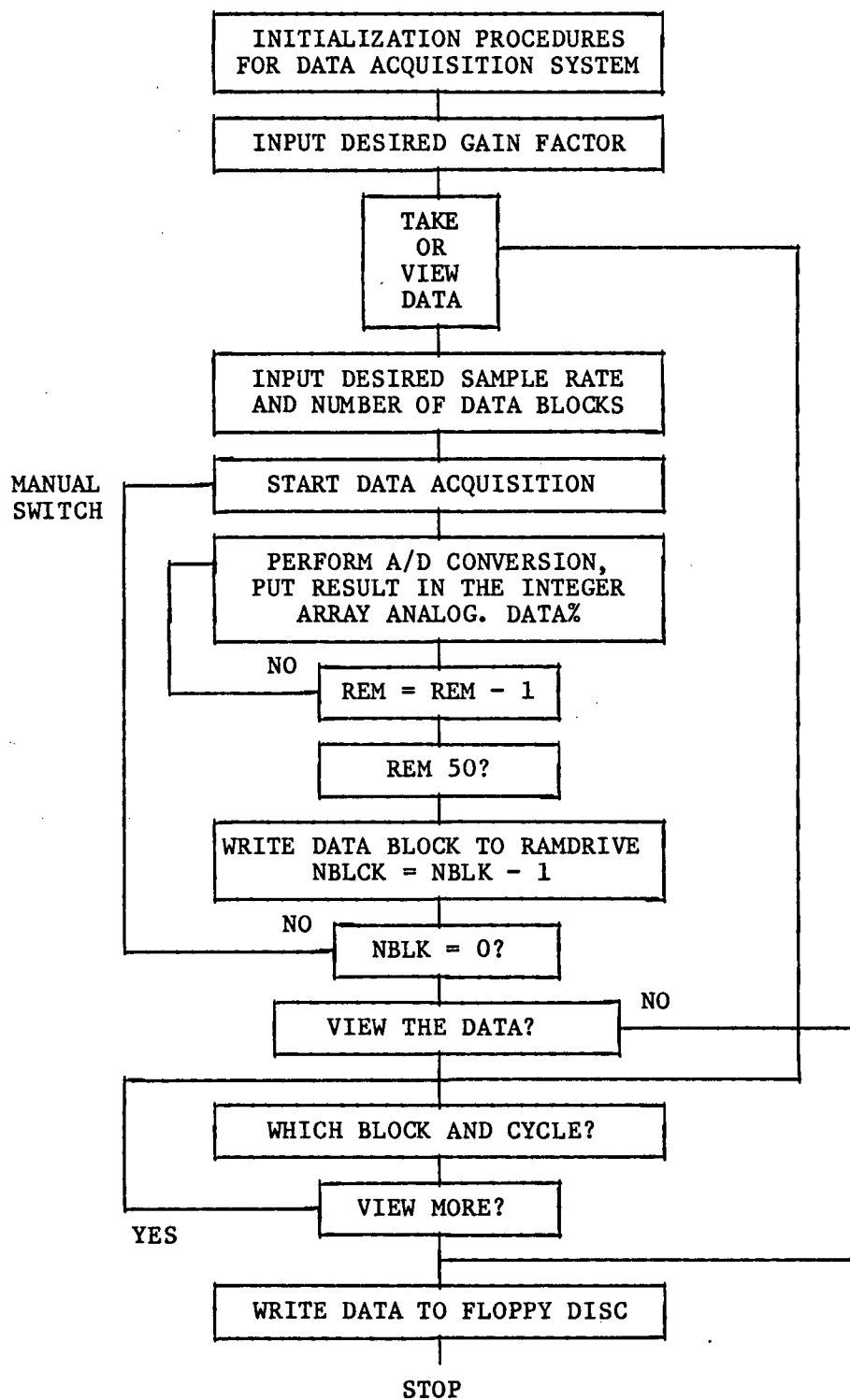
1. Data Acquisition from C.F.R. CDAQ

This program was used to acquire pressure and anemometer data from the C.F.R. engine. The program CDAQ was loaded into the I.B.M. microcomputer which was interfaced with an analogue to digital conversion board. The program CDAQ was linked with PCLAB software [41] so that commands for analogue to digital conversions could be issued from the terminal.

CDAQ is an interactive program which allows the user to select sample rate, gain, and amount of data to be taken. The user may also view stored data digitally or graphically.

CDAQ acquires data in blocks of 32K bytes. Each analogue data point is converted to a half word (2 byte) integer. Thus each block contains 16K data points. Once data acquisition is initiated CDAQ allows 16K analogue to digital conversions to occur. Each data point is stored in a 16K array. Once a block is complete CDAQ transfers the block to a file on a diskette. If more than one block was requested CDAQ then goes back for more.

A flow chart and the program listing follows.

CDAQ FLOWCHART

```

10  CFRDAO.BAS   This program acquires pressure or anemometer data from
20  =====   the C.F.R. engine.
30
40  PRINT "THIS PROGRAM ACQUIRES CYLINDER PRESSURE OR HOT WIRE ANEMOMETER"
50  PRINT "DATA FROM THE CFR ENGINE AND STORES THE VALUES ON DISK."
60  PRINT
70
80  TIMEOUT% = 20
90  CALL SET.TIMEOUT(TIMEOUT%)
100
110  PORT.SELECT% = 2
120  CALL ENABLE.FOR.OUTPUT(PORT.SELECT%) 'Enable both output ports
130
140  NCHAN% = 0
148  PRINT
149  INPUT; "INPUT DESIRED GAIN (1,2,4, OR 8)"; GAIN%
150  TIMING.SOURCE% = 3
190  START.CHAN% = NCHAN%
200  END.CHAN% = NCHAN%
210
220  CALL SETUP.ADD(TIMING.SOURCE%, START.CHAN%, END.CHAN%, GAIN%)
230
240  DEFINT V,X,Y,N,I,M,Z
250  DIM DUMMY%(14000),ANALOG.DATA%(16100)
260  INC% = 0
270  PRINT
280  INPUT; "TAKE NEW DATA (1) OR VIEW DATA IN RAMDRIVE (2) "; Q%
290  RATE = 1
300  IF Q% = 1 GOTO 320
310  IF Q% = 2 GOTO 1110
320  PRINT
330  PRINT "TO SET THE SAMPLE RATE, ADJUST THE THUMBWHEEL SWITCHES ON THE FRONT"
340  PRINT "OF THE CIRCUIT BDX TO: 01, 02, 05, OR 10, CORRESPONDING TO SAMPLING"
350  PRINT "AT EVERY 0.2, 0.4, 1, OR 2 DEGREES CRANK ANGLE RESPECTIVELY, ALSO,"
360  PRINT "INPUT THE RATE SELECTED (0.2, 0.4, 1.0 OR 2.0)"
370  INPUT; RATE
380  PRINT
390  INPUT; "HOW MANY BLOCKS OF DATA DO YOU WANT (MAX. 10) "; NBLOCK
400  PRINT
410  PRINT
420  N = 16000 'Sets the number data points taken in each block
430  K% = RATE * 4300 'Sets the delay time for data acquisition
440  NUMBER.OF.ELEMENTS% = N
450  M = N * 2 'Sets the number of bytes of memory for data
460
470  INPUT; "PRESS RETURN KEY TO START "; A$
480  PRINT
490  PRINT "DATA BEING ACQUIRED..... "
500  PRINT
510  INC% = INC% + 1 'Counts number of blocks of data acquired
520
525  PRINT "FLIP TOGGLE ON"
526  PRINT
530  'The following section sends the number of data points to be taken per
540  'block to the circuit boards. Only this number of clock pulses will be
550  'allowed through to the data acquisition board.
560
570  D.MASK% = &HB000 'Mask all the lines except 15 (load line)
580  D.VALUE% = &H0 'Set load line low
590  CALL OUTPUT.DIGITAL.VALUE(PORT.SELECT%, D.MASK%, D.VALUE%)
600
610  D.MASK% = &H7FFF 'Mask line number 15
620  D.VALUE% = N + 2 'Set the other lines to the number of samples

```

```

630 CALL OUTPUT.DIGITAL.VALUE(PORT.SELECT%, D.MASK%, D.VALUE%)
640 '
650 FOR I = 1 TO 80 'Delay for sufficient load time
660 NEXT I
670 '
680 D.MASK% = &H8000 'Mask every line except 15
690 D.VALUE% = &H8000 'Set line 15 high (load line)
700 CALL OUTPUT.DIGITAL.VALUE(PORT.SELECT%, D.MASK%, D.VALUE%)
710 '
720 'Start data acquisition....
730 '
740 CALL CONTINUOUS.ADC.DMA(NUMBER.OF.ELEMENTS%, ANALOG.DATA%(1))
750 CALL TEST.ADC.DMA(COUNT.REM%)
760 IF COUNT.REM% > 50 GOTO 750
770 '
780 '
790 CALL STOP.ADC.DMA
800 PRINT "COUNT.REM = ", COUNT.REM%
810 NEG% = -INC%
820 A$ = STR$(NEG%)
830 B$ = "C:DATA." + A$
840 '
850 Z = 0
860 Z = VARPTR(ANALOG.DATA%(1)) 'Finds the memory location of start of array
870 BSAVE B$, Z, M 'Saves the 16k data block to Ramdrive C:
880 '
885 PRINT
886 PRINT "FLIP TOGGLE OFF"
900 IF INC% < NBLOCK GOTO 510
910 PRINT
920 PRINT "<<<<<<< DATA ACQUISITION COMPLETE >>>>>>>"
930 PRINT
940 INPUT; "DO YOU WANT TO VIEW THE DATA (Y/N) "; ANS$
950 IF ANS$ = "Y" THEN 1110
960 IF ANS$ = "Y" THEN 1110
970 PRINT
980 PRINT "DATA RESIDES IN RAMDRIVE C: AND CAN NOW BE TRANSFERED TO DISK B:"
990 PRINT
1000 INPUT; "DO YOU WANT TO STORE THE DATA "; ANS$
1010 IF ANS$ = "Y" GOTO 1070
1020 IF ANS$ = "Y" GOTO 1070
1030 PRINT
1040 INPUT; "DO YOU WISH TO TAKE MORE DATA? "; ANS$
1050 IF ANS$ = "Y" GOTO 260
1060 IF ANS$ = "Y" GOTO 260
1070 END
1080 '
1090 '
1100 '
1110 PRINT
1120 INPUT; "WHICH DATA BLOCK DO YOU WISH TO VIEW "; NVIEW%
1130 PRINT
1140 INPUT; "INPUT N TO VIEW CYCLES 1,1+N,1+2N ETC"; V%
1150 PRINT
1160 '
1170 S% = 1
1180 NEG% = -NVIEW%
1190 A$ = STR$(NEG%)
1200 B$ = "C:DATA." + A$
1210 PRINT B$
1220 Z = VARPTR(ANALOG.DATA%(1))
1230 BLOAD B$, Z
1235 S% = S% - 1
1240 INPUT; "DO YOU WISH TO LIST THE DATA "; ANS$
1250 IF ANS$ = "N" GOTO 1340
1260 IF ANS$ = "N" GOTO 1340

```

```

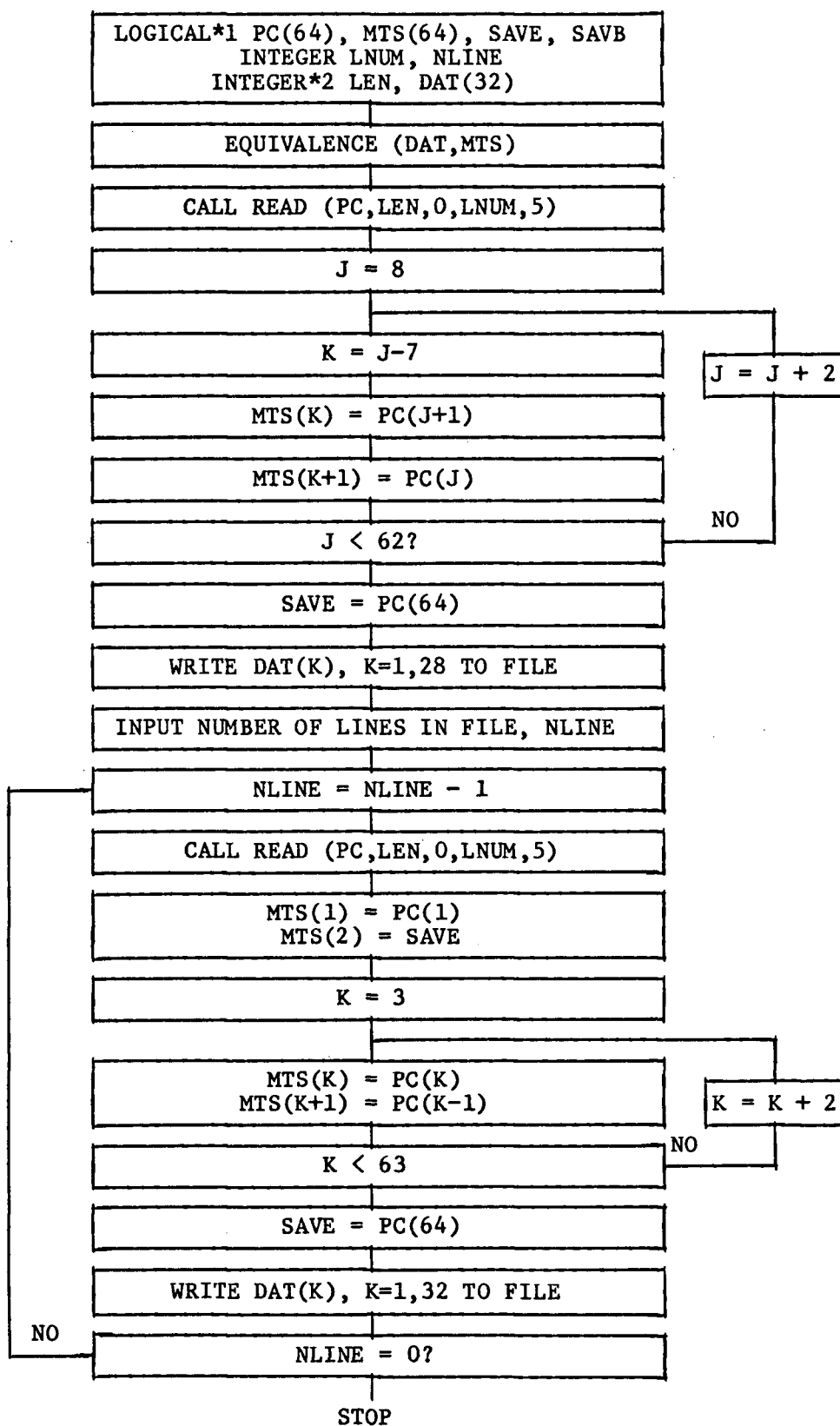
1270 L1=540/RATE-50
1280 L2=540/RATE+50
1290 PPC%=720/RATE
1300 FOR I = L1 TO L2
1310 PRINT I,ANALOG.DATA%(I+S%*PPC%)
1320 NEXT I
1330 INPUT; U%
1340 KEY OFF
1350 SCREEN 2,,0,0
1360 LINE (100,90)-(460,90)
1370 LINE (100,1)-(460,1)
1380 LINE (100,180)-(460,180)
1390 LINE (100,1)-(100,180)
1400 LINE (460,1)-(460,180)
1410 LINE (100,45)-(105,45)
1420 LINE (460,45)-(455,45)
1430 LINE (460,135)-(455,135)
1440 LINE (100,135)-(105,135)
1450 LINE (280,180)-(280,176)
1460 LOCATE 12,7,0 :PRINT "0.00";
1470 LOCATE 1,7,0 :PRINT "10.0";
1480 LOCATE 6,7,0 :PRINT " 5.0";
1490 LOCATE 23,6,0 :PRINT "-10.0";
1500 LOCATE 18,7,0 :PRINT "-5.0";
1510 LOCATE 25,40,0 :PRINT "DEGREES C.A.";
1520 LOCATE 9,1,0 :PRINT "VOLTS";
1530 LOCATE 1,20,0 :PRINT " ENGINE PRESSURE TRACE ";
1540 LOCATE 24,13,0 :PRINT "0";
1550 LOCATE 24,35,0 :PRINT "360";
1560 LOCATE 24,57,0 :PRINT "720";
1570 LOCATE 1,1,0
1580 FOR X = 100 TO 460
1590 Y = 180 - ANALOG.DATA%(((X-99)*2/RATE)+(S%*PPC%))/23
1600 PSET(X,Y)
1609 NEXT X
1610 INPUT; ST$
1611 SCREEN 0
1612 S%=S%+V%+1
1615 IF S%<=(22*RATE) GOTO 1235
1640
1650 INPUT; "DO YOU WANT TO VIEW ANOTHER BLOCK? "; ANS$
1660 IF ANS$="Y" GOTO 1110
1670 IF ANS$="Y" THEN 1110 ELSE 960
1680
1690 PROGRAM END.

```

2. Conversion of Digital Data to MTS (BYTRD)

This program was used to convert integer data from CDAQ into a form which could be read by the MTS system. This was necessary because the IBM microcomputer stored half word integers with the low order byte first, high order byte second and MTS uses the opposite order. The program reads the integer data as logical variables, in array form. The array indexes are interchanged and then the logical array is read into an integer array. BYTRD also strips off the seven byte label placed before each block of data by CDAQ.

A flow chart and program listing follow.

BYTRD FLOWCHART

Listing of BYTRD at 17:46:06 on JUN 26, 1985 for CCId=CILL Page 1

```

1          LOGICAL*1 PC(64),MTS(64),SAVB,SAVE
2          INTEGER LNUM,NLINE
3          INTEGER*2 LEN,DAT(32)
4          EQUIVALENCE(DAT,MTS)
5          LEN=2
5.5        JJ=1
6          CALL READ(PC,LEN,O,LNUM,5)
7          10 DO 1 J=8,62,2
8            K=J-7
9            MTS(K)=PC(J+1)
10           MTS(K+1)=PC(J)
11           1 CONTINUE
11.5        NFLG=1
12          SAVE=PC(64)
13          WRITE(7,99) (DAT(K),K=1,28)
13.5        IF (JJ.GT. 1 ) GO TO 11
14          WRITE(6,100)
15          100 FORMAT(' ','HOW MANY LINES ARE IN YOUR FILE ?')
16          CALL FREAD('GUSER','I:',NLINE)
18          11 JJ=JJ+1
19          NREC=JJ*1000
20          FIND(7,NREC)
21          CALL READ(PC,LEN,O,LNUM,5)
21.5        NFLG=NFLG + 1
21.7        IF (NFLG .EQ. 503) GO TO 10
22          MTS(1)=PC(1)
23          MTS(2)=SAVE
24          DO 2 K=3,63,2
25            MTS(K)=PC(K)
26            MTS(K+1)=PC(K-1)
27          2 CONTINUE
28          SAVE=PC(64)
29          WRITE(7,99) (DAT(K),K=1,32)
29.5        99 FORMAT(' ',32I5)
30          IF (JJ .LE. NLINE) GO TO 11
31          STOP
32          END

```

APPENDIX D - HOT WIRE ANEMOMETER DATA PROCESSING PROGRAMS1. Instantaneous Velocity Evaluation and Ensemble Averaging (ANEM)

In this section the program used to process the digitized anemometer signal to obtain an instantaneous velocity is described. All anemometer data for which velocity was required was processed with this program. Included in this program is the ensemble technique described in Chapter 6.4.1. The outputs of this program are the instantaneous velocity every $1/5$ of a crank angle degree for 40 or more engine cycles, the ensemble averaged mean velocity, and the ensemble averaged turbulence intensity.

The inputs to this program are the digitized anemometer voltage; the calibration constants a, b , and n for the hot wire correlation (Equation (5.1)), and the ensemble averaged pressure trace. The pressure trace contains data points for every crank angle degree in the engine cycle. At each point the temperature of the cylinder air is calculated assuming an adiabatic process (Equation (6.5)); the thermal conductivity is calculated from Equation (6.8), and the kinematic viscosity is calculated from Equation (6.9). The reference condition was taken at the point of intake valve closing, where the pressure and temperature were taken as the ambient condition.

The anemometer data is first converted back to a voltage using the appropriate system gain and offset. Then the heat transfer coefficient from Equations 6.2, 6.3, and 6.4 is solved for using the iteration technique described in Appendix B. Once the heat transfer coefficient has been determined the Nusselt number may be formed and from the correlation (Equation (5.12)) the velocity may be solved for.

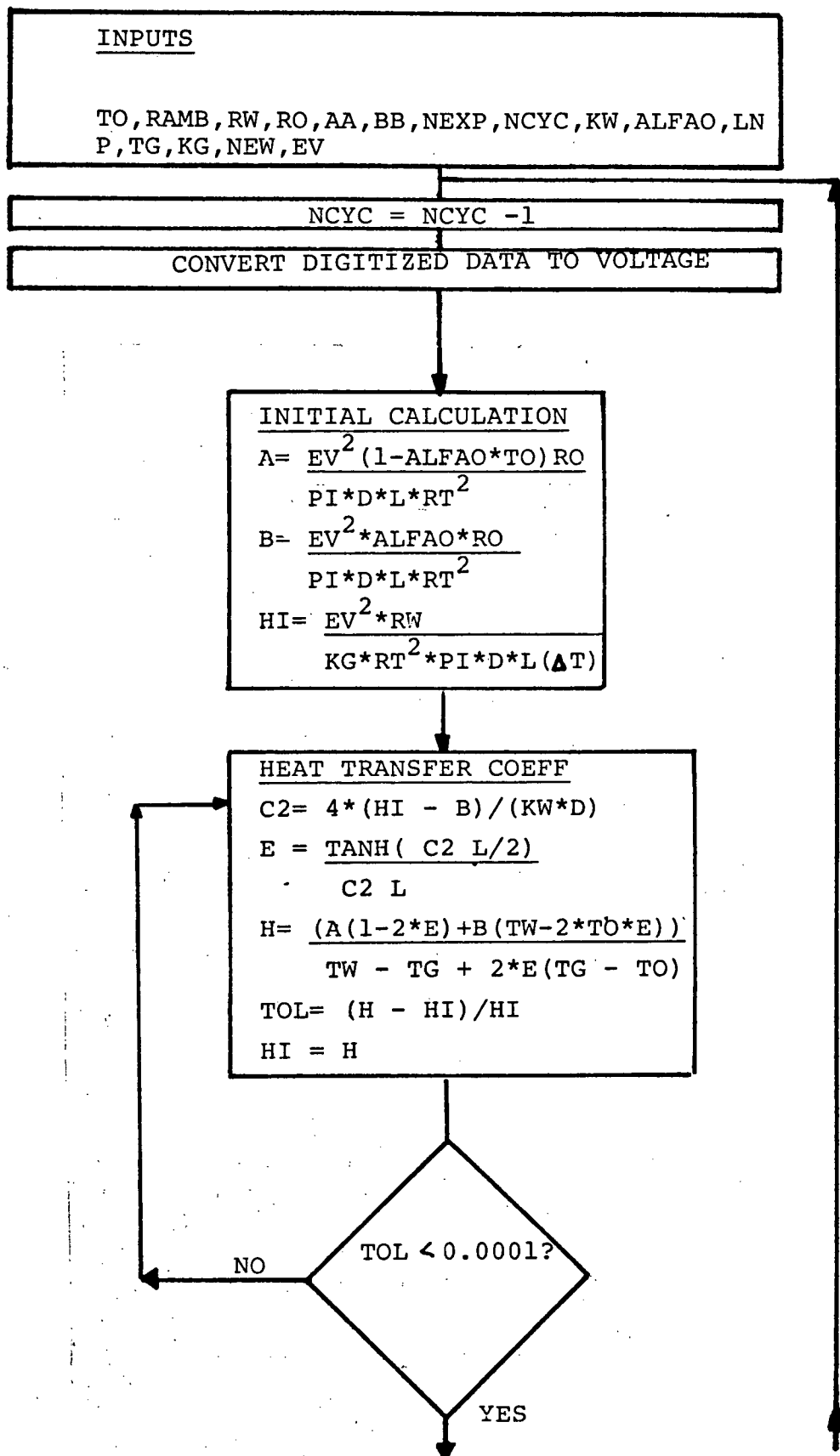
The instantaneous velocity obtained for each point is stored for later

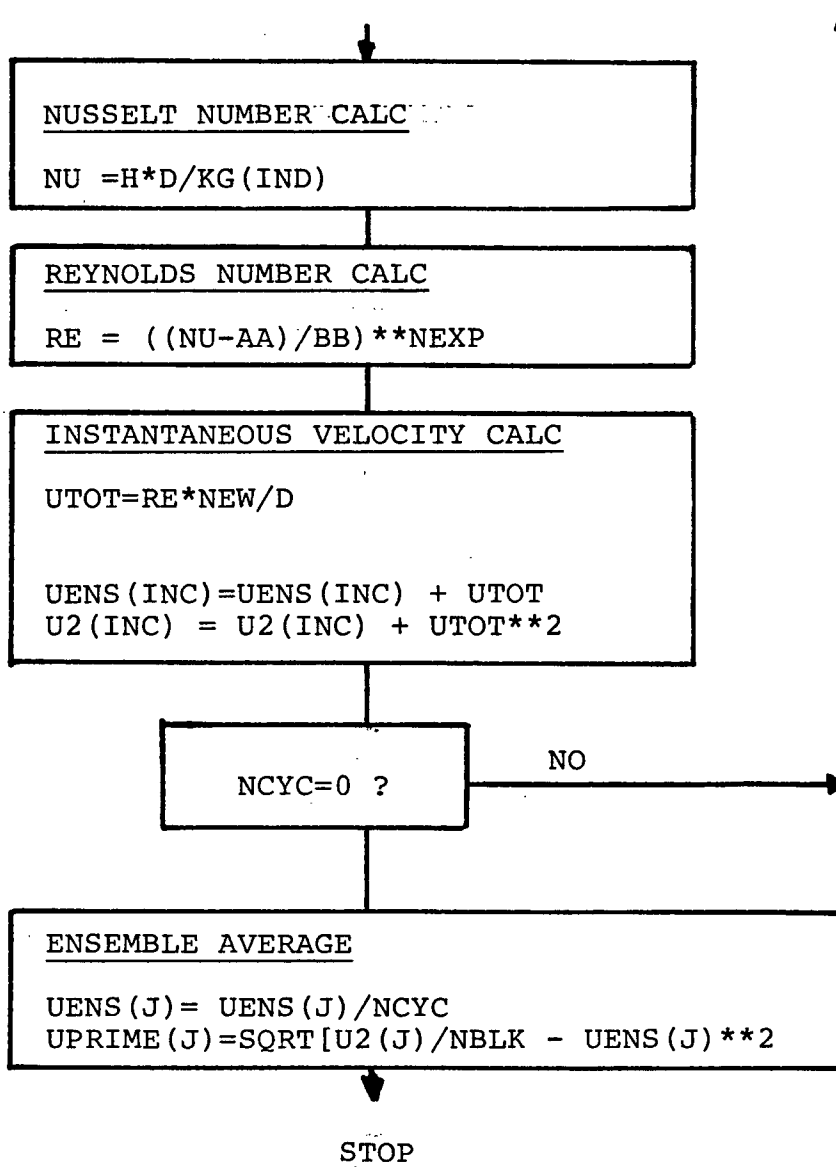
processing by other programs. In addition as the program runs through the data a cumulative sum of the instantaneous velocity as well as the square of the instantaneous velocity is kept. After all the data has been processed the ensemble average mean velocity and turbulence intensity is obtained from Equation 6.10 and 6.12 respectively.

A flow chart and a program listing follow.

Definition of Program Symbols (ANEM)

AA	Intercept for Nu-Re Correlation
ALFAO	Temperature Coefficient of Resistance for Wire
BB	Slope for Nu-Re Correlation
CEV	Anemometer Voltage Obtained from Digital Data
D	Wire Diameter
EV	Digitized Anemometer Voltage
H	Heat Transfer Coefficient
KG	Thermal Conductivity of Gas
KW	Thermal Conductivity of Wire
LN	Wire Length
NBLK	Number of 32K Byte Data Blocks
NEW	Kinematic Viscosity of Gas
NEXP	Exponent for Nu-Re Correlation
NU	Nusselt Number
P	Pressure
PPC	Data Points Per Engine Cycle
RAMB	Ambient Resistance of Wire
RATE	Data Acquisition Rate
RE	Reynolds Number
RO	Ice Point Resistance of Wire
RW	Operating Resistance of Wire
TG	Temperature of Gas
TO	Ambient Temperature
VENS	Ensemble Averaged Mean Velocity
UPRIME	Ensemble Averaged RMS Velocity
UTOT	Instantaneous Velocity





ANEM at 10:53:37 on JUN 27, 1985 for CCId=CILL Page 1

```

1      REAL    KW, LN, D, RO, ALFAO, TO, TG(720), RW, TW, A, B, HI, C2, E, H
2      REAL    RE, NU, P(720), KG(720), NEW(720), NEXP, AA, BB, RATE, TEMP
2.5    REAL    X(1801), Y1(1801), Y2(1801)
3      REAL    UTOT(3600), UENS(1801), VO, NEV, CEV, U2(1801), UPRIME(1801)
4      INTEGER EV(22, 3600), PPC, NCYC, NBLK, ULIM, NREC, IND, DD(3600)
5      KW=18.
7      LN=1.5E-03
8      D=6.3E-06
9      ALFAO=9.0E-04
10     DO 11 J=1, 1801
10.5    UENS(J)=0.
10.7    UTOT(J)=0.
10.75   U2(J)=0.
10.77   UPRIME(J)=0.
10.8    11     CONTINUE
11     WRITE(6,1)
12     1       FORMAT(' AMBIENT TEMPERATURE = ?')
13     CALL FREAD('GUSER', 'R:', TO)
14     WRITE(6,2)
15     2       FORMAT(' AMBIENT RESISTANCE OF WIRE = ?')
16     CALL FREAD('GUSER', 'R:', RAMB)
17     WRITE(6,3)
18     3       FORMAT(' OPERATING RESISTANCE OF WIRE = ?')
19     CALL FREAD('GUSER', 'R:', RW)
20     WRITE(6,4)
21     4       FORMAT(' ICE POINT RESISTANCE OF WIRE = ?')
22     CALL FREAD('GUSER', 'R:', RO)
23     WRITE(6,5)
24     5       FORMAT(' INTERCEPT FOR NU-RE CORRELATION = ?')
25     CALL FREAD('GUSER', 'R:', AA)
26     WRITE(6,6)
27     6       FORMAT(' SLOPE FOR NU-RE CORRELATION = ?')
28     CALL FREAD('GUSER', 'R:', BB)
29     WRITE(6,7)
30     7       FORMAT(' EXPONENT FOR NU-RE CORRELATION = ?')
31     CALL FREAD('GUSER', 'R:', NEXP)
32     WRITE(6,8)
33     8       FORMAT(' WHAT WAS THE DATA ACQUISITION RATE ?')
34     CALL FREAD('GUSER', 'R:', RATE)
35     WRITE(6,9)
36     9       FORMAT(' HOW MANY BLOCKS OF DATA WERE TAKEN ?')
37     CALL FREAD('GUSER', 'I:', NBLK)
38     DO 10 J=1, 720
39     READ(4, 100) Z, P(J), TG(J), KG(J), NEW(J)
40     CONTINUE
41     100     FORMAT(' ', F8.2, 2X, F12.2, 2X, F12.2, 2X, F12.8, 2X, F14.10)
42     PPC=720/RATE
43     NCYC=22*RATE
44     ULIM=713/RATE
47     TW=600. + 273.15
48     TO=TO+273.15
48.5    C READ IN THE DIGITIZED HOT WIRE DATA
49     DO 50 J=1, NBLK
49.5    WRITE(6, 987) J
49.7    987   FORMAT(' ', I4)
50     NREC=(502*(J-1)+1)*1000
51     FIND(5, NREC)
52     READ(5, 200) (EV(1, N), N=35, PPC), ((EV(M, N), N=1, PPC), M=2, NCYC),

```

ANEM at 10:53:37 on JUN 27, 1985 for CCId=CILL Page 2

```

52.2      1 (EV(1,N),N=1,34)
53      200      FORMAT(' ',32I5)
53.8      RT=RW+50.214
53.95     NCT=0
54      DO 40 K=1,NCYC
55      DO 30 L=1800,PPC
56      IND=L*RATE
56.7      NCT=NCT+1
57      NCOUNT=0
57.5     C CONVERT THE DIGITIZED DATA TO A VOLTAGE
58      CEV=0.004883*EV(K,L) - 10.
59      NEV=CEV
59.5     C BEGIN ITERATION FOR HEAT TRANSFER COEFFICIENT
60      A=NEV**2*(1.-ALFAO*(273.15))/(3.141593*D*LN*RT**2)*RO
61      B=NEV**2*ALFAO/(3.141593*D*LN*RT**2)*RO
62      HI=NEV**2/(KG(IND)*3.141593*D*LN*(TW-TG(IND))*RT**2)*RW
63      20      C2=4*(HI-B)/(KW*D)
64      NCOUNT=NCOUNT+1
65      IF (NCOUNT .GT. 100) GO TO 70
66      E=TANH(SQRT(C2)*LN/2)/(SQRT(C2)*LN)
67      H=(A*(1.-2*E)+B*(TW-2*TO*E))/(TW-TG(IND)+(TG(IND)-TO)*2*E)
68      TOL= ABS((H-HI)/HI)
69      HI=H
70      IF (TOL .GT. .001) GO TO 20
70.5     C ITERATION COMPLETE EVALUATE NUSSELT NUMBER
71      NU=H*D/KG(IND)
71.5     IF (NU-AA .LT. 0.) GO TO 21
72      RE=((NU-AA)/BB)**(1/NEXP)
72.5     C CALCULATE INSTANTANEOUS VELOCITY
73      22      UTOT(L)=RE*NEW(IND)/D
73.5     INC=L-1799
74      UENS(INC)=UENS(INC)+UTOT(L)
74.5     U2(INC)=U2(INC)+UTOT(L)**2
75      30      CONTINUE
76      WRITE(7,31) (UTOT(M),M=1800,3600)
77      31      FORMAT(' ',10F7.2)
78      40      CONTINUE
79      50      CONTINUE
79.5     C DO ENSEMBLE AVERAGING
80      DO 60 J=1,1801
81      UENS(J)=UENS(J)/(NCYC*NBLK)
81.5     U2(J)=U2(J)/(NCYC*NBLK)
82      60      CONTINUE
83      GO TO 80
84      70      WRITE(6,400)
85      400     FORMAT(' ','ERROR, TOO MANY ITERATIONS N=100!')
86      80      CONTINUE
86.2     WRITE(8,500)
86.3     C CALCULATE ENSEMBLED INTENSITY
86.5     DO 90 K=1,1801
86.7     UPRIME(K)=SQRT(U2(K)-UENS(K)**2)
86.77     CA=359.8+ K*RATE
86.8     WRITE(8,600)CA,UENS(K),UPRIME(K)
86.9     500     FORMAT(' ','CA ',5X,'UBAR',3X,'UPRIME')
86.95     600     FORMAT(' ',F5.1,3X,F6.2,3X,F6.2)
86.955   C PLOT OUT THE RESULTS
86.96     X(K)=K/1801. *20.
86.965     Y1(K)= UENS(K)/5. *2.

```

ANEM at 10:53:37 on JUN 27, 1985 for CCid=CILL Page 3

```
36.967      Y2(K)=UPRIME(K)/5. *2.  
86.968      IF (Y1(K) .GT. 20.)Y1(K)=20.  
86.969      IF (Y2(K) .GT. 20.)Y2(K)=20.  
86.97 90    CONTINUE  
86.98      CALL AXPLLOT('CA DEGREES;',0.,20.,0.,1.)  
86.99      CALL AXPLLOT('ENSEMBLES;',90.,20.,0.,1.)  
86.995      CALL LINE(X,Y1,1801,1)  
86.997      CALL LINE(X,Y2,1801,1)  
86.998      CALL PLOTND  
87         STOP  
88         END
```

2. Cycle by Cycle Time Averaged Mean and RMS Velocity (TRAP)

This program was used to obtain the mean velocity and turbulence intensity from the instantaneous velocity records processed with program ANEM.

The program begins by reading in the instantaneous velocity $U(i,v)$ obtained every $1/5$ of a crank angle degree over 40 engine cycles. For each velocity $U(i,v)$, the area under the curve, $A(i,v)$, is calculated for a grid size of $1/5$ of a crank angle degree using the trapezoidal approximation:

$$A(i,v) = U(i,v) + U(i,v+1)/2/5 \quad (D.1)$$

The mean velocity is calculated by constructing a 4 degree averaging interval. This is accomplished by summing the individual areas calculated above in blocks of 20 and averaging:

$$\bar{U}_{\theta}(i) = \frac{\sum_{v=-10}^{v+10} A(i,v)}{4} \quad (D.2)$$

The average is taken as the mid-point of each interval. The resulting curve is the mean velocity $\bar{U}_{\theta}(i)$ for the engine cycle being processed.

Next the turbulence intensity is computed. First cubic spline interpolation is used to generate points along the mean velocity record at every crank angle degree. The velocity fluctuation u_{θ} is then calculated as the difference between the mean velocity and the instantaneous velocity at each point:

$$u_{\theta} = U(i, \theta) - \bar{U}_{\theta}(i) \quad (D.3)$$

The average of u_{θ}^2 was then calculated using a 12 degree averaging window in the same manner as described for the mean velocity evaluation.

This procedure was performed for each of the 40 engine cycles evaluated. The ensemble averaged mean velocity was then obtained from:

$$\bar{U}_{\theta} = \frac{1}{40} \sum_{i=1}^{40} \bar{U}_{\theta}(i) \quad (D.4)$$

and the ensemble averaged turbulence intensity from:

$$u'_{\theta} = \left\{ \frac{1}{40} \sum_{i=1}^{40} \left[\frac{1}{\theta} \int_0^{\theta} (U(i, \theta) - \bar{U}_{\theta}(i))^2 d\theta \right] \right\}^{1/2} \quad (D.5)$$

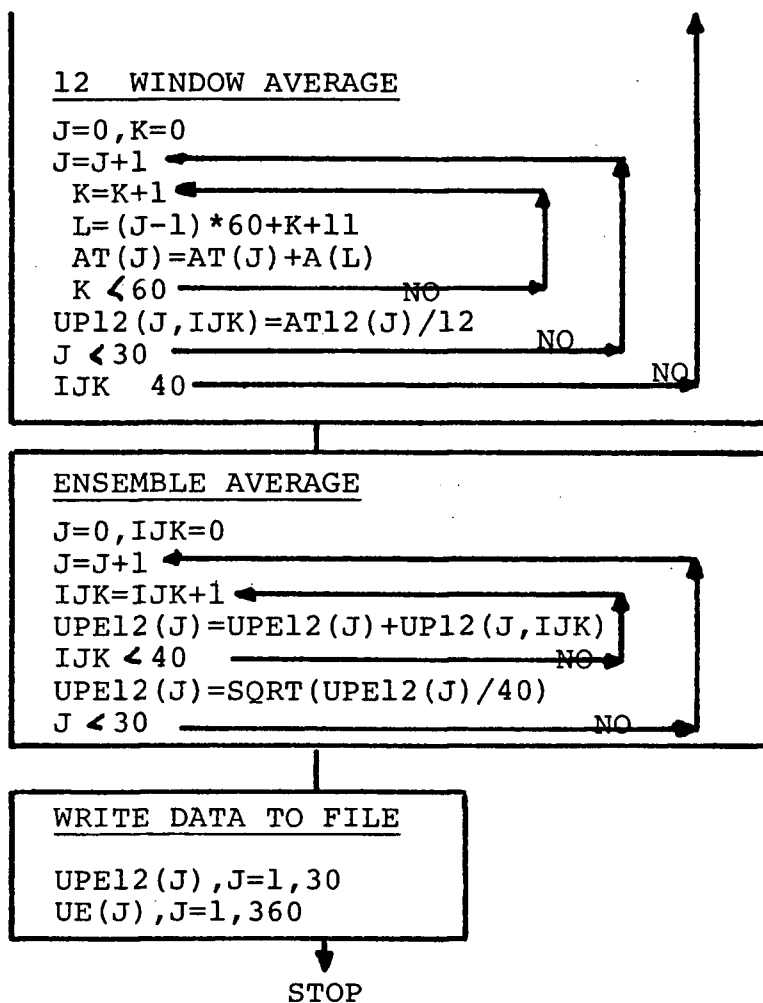
The cyclic dispersion was also evaluated in this program from:

$$U_{\text{RMS}} = \left\{ \frac{1}{40} \sum_{i=1}^{40} [\bar{U}_{\theta}(i) - \bar{U}_{\theta}]^2 \right\}^{1/2} \quad (D.6)$$

A program listing and flow chart follow.

Definition of Program Symbols (TRAP)

A	Trapezoidal Area Under Instantaneous Velocity
AT	Sum of Areas in Averaging Interval for Mean Velocity
AT12	Sum of Areas in Averaging Interval for Intensity
P	Tension Array for Interpolation
SI	Working Array of Interpolation Routine
S	Interpolated Values Returned
S1	First Derivative at End Points
S2	Second Derivative at End Points
T	Crank Angle Degrees for Which Interpolated Velocity Values are Required
U	Instantaneous Velocity
UE	Ensemble Averaged Mean Velocity
UP12	Turbulence Intensity Values
UPE12	Ensemble Averaged RMS Velocity
URMS	Cyclic Variation in Mean Velocity
UT	Interpolated Mean Velocity Values



TRAP at 10:53:05 on JUN 27, 1985 for CCId=CILL Page 1

```

1      REAL UT(357,40),UE(357),U(1801,40),A(1800),AT(180)
2      REAL X(200),Y(200),P(1400),SI(2),S(357),Z1,Z2,URMS(357)
3      REAL UP12(36,40)
4      REAL UPE12(36)
5      REAL AT12(90)
6      REAL S1(357),S2(357),T(357)
7      DO 13 J=1,357
8          URMS(J)=0.
9      13      UE(J)=0.
10         DO 11 J=1,357
11         DO 12 K=1,40
12             UT(J,K)=0.
13         12      CONTINUE
14         11      CONTINUE
15     C READ IN THE INSTANTANEOUS VELOCITY FOR 40 CYCLES
16         DO 10 IJK=1,40
17             READ(5,1) (U(J,IJK),J=1,1801)
18         1      FORMAT(' ',10F7.2)
19             DO 2 J=1,90
20                 AT(J)=0.
21                 AT(J+90)=0.
22                 AT2(J)=0.
23                 AT4(J)=0.
24                 AT8(J)=0.
25                 AT12(J)=0.
26         2      CONTINUE
27     C EVALUATE TRAPAZDIDAL AREAS UNDER VELOCITY TRACE
28         DO 23 J=1,1800
29             A(J)=(U(J,IJK)+U(J+1,IJK))/2/5.
30         23      CONTINUE
31     C
32     C USE A 4 DEGREE INTERVAL FOR MEAN VELOCITY
33     C ADD UP THE AREAS FOR WINDOW OF 4 DEGREES
34         DO 4 J=1,90
35             DO 3 K=1,20
36                 L=(J-1)*20+ K
37                 AT(J)=AT(J)+A(L)
38         3      CONTINUE
39     C TAKE THE AVERAGE IN EACH INTERVAL
40         Y(J)=AT(J)/4.
41         4      CONTINUE
42             SI(1)=-1
43             SI(2)=1
44             DO 40 J=1,1400
45         40         P(J)=0.
46             DO 41 J=1,357
47         41         T(J)=361. + FLOAT(J)
48             DO 42 J=1,180
49         42         X(J)=358. +J*4.
50     C FIT A CUBIC SPLINE TO THE POINTS
51         CALL SMOOTH(X,Y,P,90,SI,1,&99)
52     C GENERATE INTERPOLATION POINTS BETWEEN AVERAGES
53         CALL SMTH(T,S,S1,S2,357,&99)
54     C ADJUST TENSION
55         CALL SMOOTH(X,Y,P,90,SI,0,&99)
56         CALL SMTH(T,S,S1,S2,357,&99)
57         DO 43 J=1,357
58         43         UT(J,IJK)=S(J)

```

TRAP at 10:53:05 on JUN 27, 1985 for CCId=CILL Page 2

```

59      10      CONTINUE
60      C CALC ENSEMBLED CURVE FROM INDIVIDUAL TRACES
61          DO 20 J=1,357
62              DO 19 K=1,38
63                  UE(J)=UE(J)+UT(J,K)
64      19      CONTINUE
65          UE(J)=UE(J)/38.
66      20      CONTINUE
67          WRITE(6,300)
68      300      FORMAT(' ','FINISHED MEAN VELOCITY')
69      C CALCULATE CYCLIC VARIATION IN MEAN
70          DO 800 J=1,357
71              DO 801 K=1,38
72                  URMS(J)=URMS(J)+(UT(J,K)-UE(J))**2
73      801      CONTINUE
74          URMS(J)=SQRT(URMS(J)/38.)
75      800      CONTINUE
76          WRITE(6,802)
77      802      FORMAT(' ','CYCLIC VARIATION COMPLETE')
78      C CALCULATE INTENSITY NOW USE A WINDOW OF 12 DEGREES
79          DO 1000 IJK=1,40
80              IND=1
81              KIND=0
82              DO 100 J=11,1799
83                  KIND=KIND+1
84                  IF (KIND .EQ. 6 ) IND=IND+1
85                  IF (KIND .EQ. 6 )KIND=1
86                  Z1= U(J,IJK)- UT(IND,IJK)
87                  Z2=U(J+1,IJK) -UT(IND,IJK)
88                  A(J)=(Z1**2 +Z2**2)/2./5.
89      100      CONTINUE
90      C 12 DEG WINDOW
91          DO 401 J=1,30
92              DO 402 K=1,60
93                  L=(J-1)*60 +K +11
94                  AT12(J)=AT12(J)+A(L)
95      402      CONTINUE
96          UP12(J,IJK)=(AT12(J)/12.)
97          AT12(J)=0.
98      401      CONTINUE
99      1000      CONTINUE
100         WRITE(6,502)
101     502     FORMAT(' ','INTENSITY CALCS DONE')
102         DO 405 J=1,30
103     405     UPE12(J)=0.
104         DO 407 J=1,30
105         DO 406 IJK=1,40
106     406     UPE12(J)=UPE12(J)+UP12(J,IJK)
107         UPE12(J)=SQRT(UPE12(J)/40.)
108     407     CONTINUE
109         WRITE(6,503)
110     503     FORMAT(' ','ENSEMBLE AVERAGING COMPLETE')
111         DO 21 J=1,357
112             X(J)=361. + FLOAT(J)
113             WRITE(7,22) X(J),UE(J)
114     21      CONTINUE
115         DO 28 J=1,357
116         WRITE(8,22) X(J),URMS(J)

```

ing c TRAP at 10:53:05 on JUN 27, 1985 for CCId=CILL Page 3

```
117      28      CONTINUE
118          DO 410 J=1,30
119              X(J)=370. +(J-1)*12.
120              WRITE(7,22) X(J),UPE12(J)
121      410      CONTINUE
122      22      FORMAT(' ',2F20.2)
123      99      STOP1
124          END
```

3. Nonstationary Analysis (NOTIME)

This program evaluates the turbulence intensity obtained from the type of nonstationary analysis proposed by Lancaster [10]. In this analysis the turbulent fluctuation $u(i,\theta)$ is defined to be the difference between a stationary mean velocity $\bar{U}(i)$, a time varying mean velocity $\bar{U}(\theta)$, and the instantaneous velocity $U(i,\theta)$:

$$u(i,\theta) = U(i,\theta) - \bar{U}(i) - \bar{U}(\theta) \quad (D.7)$$

In this program the instantaneous velocity and ensemble averaged mean velocity from the program ANEM are inputs.

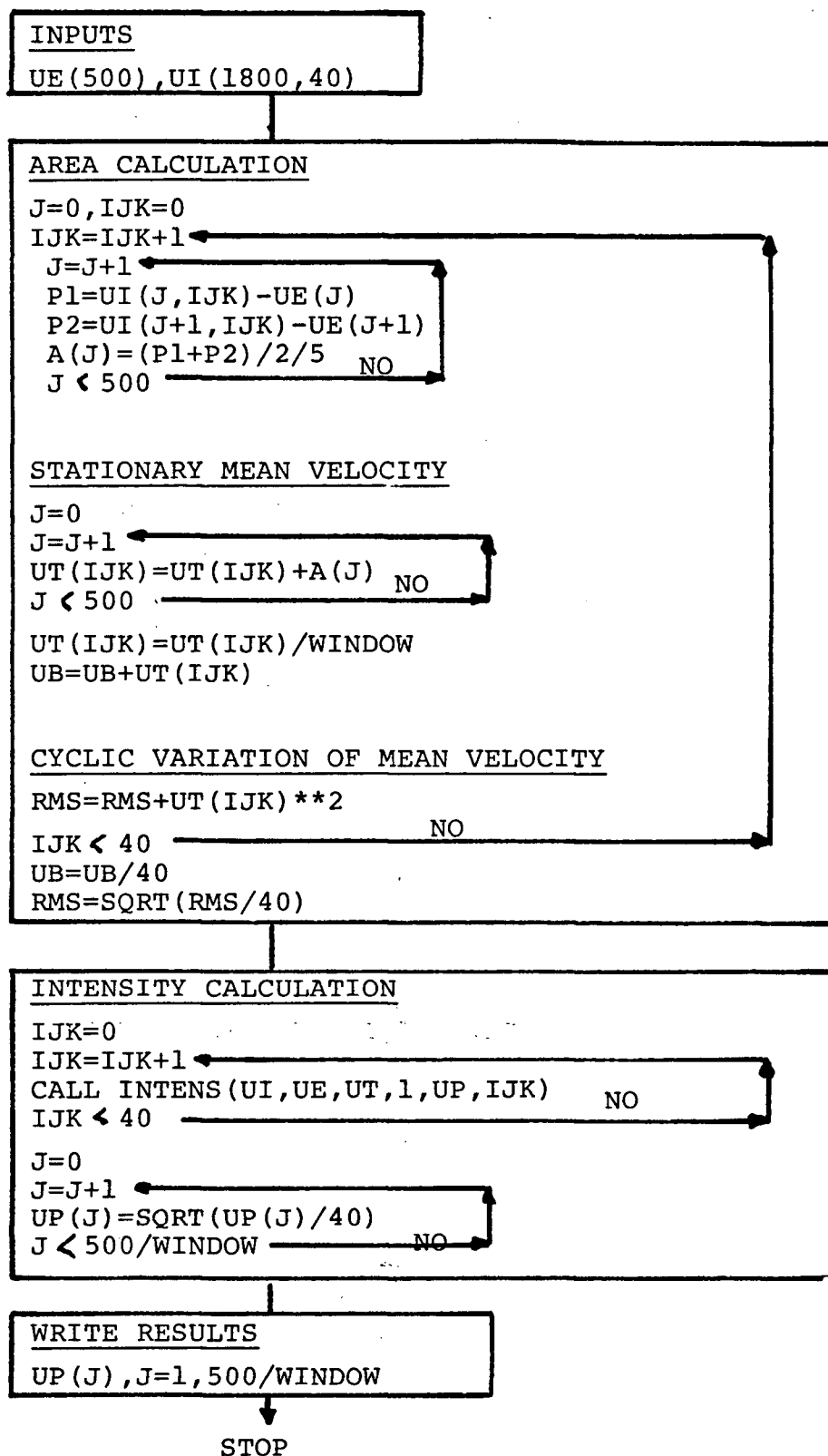
For each engine cycle the stationary mean is calculated from Equation 6.19 using the trapezoidal rule to evaluate the integral. The averaging window was varied from 40 to 100 degrees about TOC. The average turbulence intensity is evaluated for 12 degree intervals from Equation 6.20. The intensity records were then ensembled to give an ensemble averaged turbulence intensity.

A program listing and flow chart follow.

Definition of Program Symbols (NOTIME)

A	Trapezoidal Areas
UE	Ensemble Averaged Mean Velocity
UI	Instantaneous Velocity
UP40	RMS Velocity for Averaging Window of 40°
UP60	RMS Velocity for Averaging Window of 60°
UP80	RMS Velocity for Averaging Window of 80°
UP100	RMS Velocity for Averaging Window of 100°
UT40	Stationary Velocity for Averaging Window of 40°
UT60	Stationary Velocity for Averaging Window of 60°
UT80	Stationary Velocity for Averaging Window of 80°
UT100	Stationary Velocity for Averaging Window of 100°

FLOWCHART FOR PROGRAM NOTIME



* c NOTIME at 10:53:49 on JUN 27, 1985 for CCid=CILL Page 1

```

1      REAL UE(500),UI(1801,40),UT40(40),UT60(40),UT80(40),X(20)
2      REAL UT100(40),A(500),UP40(40),UP60(40),UP80(40),UP100(40)
2.5    C THIS PROGRAM CALCULATES THE STATIONARY MEAN VELOCITY IN A GIVEN
2.7    C WINDOW FROM THE ENSEMBLED MEAN VELOCITY AND THE INSTANEQUA VELOCITY
2.8    C BY THE METHOD OF LANCASTER. THE TURBULENCE INTENSITY IS THEN
2.9    C CALCULATED FROM THE DIFFERENCE OF THE INSTANTANEOUS VELOCITY
2.95   C AND THE TWO MEANS, ENSEMBLED AND STATIONARY
3      DO 1 J=1,40
4          UT40(J)=0.
5          UT60(J)=0.
6          UT80(J)=0.
7          UT100(J)=0.
7.5    UP40(J)=0.
7.7    UP60(J)=0.
7.8    UP80(J)=0.
7.9    UP100(J)=0.
8      1    CONTINUE
9          U40B=0.
10         U60B=0.
11         U80B=0.
12         U100B=0.
13         RMS40=0.
14         RMS60=0.
15         RMS80=0.
16         RMS100=0.
17         DO 3 J=1,500
17.5    C READ IN THE ENSEMBLED MEAN
18         READ(5,2) D,UE(J)
19         2    FORMAT(' ',F5.1,3X,F10.2)
20         3    CONTINUE
20.5    C READ IN 40 CYCLES OF THE INSTANTANEOUS MEAN
21         DO 100 IJK=1,40
22         READ(4,4) (UI(J,IJK),J=1,1801)
23         4    FORMAT(' ',10F7.2)
23.5    C EVALUATE THE INTEGRAL BT THE TRAPAZOIDAL METHOD
24         DO 5 J=1,499
25         P1=UI(J+649,IJK)-UE(J)
26         P2=UI(J+650,IJK)-UE(J+1)
27         A(J)=(P1+P2)/2./5.
28         5    CONTINUE
28.5    C CALCULATE THE STATIONARY MEAN VELOCITY
29         DO 6 J=1,499
30         UT100(IJK)=UT100(IJK)+A(J)
31         IF ((J.LT.50) .OR. (J .GE. 450)) GO TO 6
32         UT80(IJK)=UT80(IJK) + A(J)
33         IF ((J .LT.100) .OR. (J .GE.400)) GO TO 6
34         UT60(IJK)=UT60(IJK) + A(J)
35         IF ((J.LT.150) .OR. (J .GE. 350)) GO TO 6
36         UT40(IJK)=UT40(IJK) + A(J)
37         6    CONTINUE
37.5    UT40(IJK)=UT40(IJK)/40.
37.7    UT60(IJK)=UT60(IJK)/60.
37.8    UT80(IJK)=UT80(IJK)/80.
37.9    UT100(IJK)=UT100(IJK)/100.
38         U40B=U40B+UT40(IJK)
39         U60B=U60B+UT60(IJK)
40         U80B=U80B+UT80(IJK)
41         U100B=U100B+UT100(IJK)

```

NOTIME at 10:53:49 on JUN 27, 1985 for CCId=CILL Page 2

```

41.5 C EVALUATE THE CYCLIC VARIATION OF THE MEAN VELOCITY
42     RMS40=RMS40 + UT40(IJK)**2
43     RMS60=RMS60 + UT60(IJK)**2
44     RMS80=RMS80 + UT80(IJK)**2
45     RMS100=RMS100 + UT100(IJK)**2
46     100 CONTINUE
47     U40B=U40B/40.
48     U60B=U60B/40.
49     U80B=U80B/40.
50     U100B=U100B/40.
51     RMS40=SQRT(RMS40/40.)
52     RMS60=SQRT(RMS60/40.)
53     RMS80=SQRT(RMS80/40.)
54     RMS100=SQRT(RMS100/40.)
55     DO 200 IJK=1,40
55.5 C EVALUATE THE INTENSITY
56     CALL INTENS(UI,UE,UT40,1,UP40,IJK)
57     CALL INTENS(UI,UE,UT60,2,UP60,IJK)
58     CALL INTENS(UI,UE,UT80,3,UP80,IJK)
59     CALL INTENS(UI,UE,UT100,4,UP100,IJK)
60     200 CONTINUE
61     DO 300 J=1,20
62     UP100(J)=SQRT(UP100(J)/40.)
63     IF (J .GT. 16) GO TO 300
64     UP80(J)=SQRT(UP80(J)/40.)
65     IF (J .GT. 12) GO TO 300
66     UP60(J)=SQRT(UP60(J)/40.)
67     IF (J .GT. 8) GO TO 300
68     UP40(J)=SQRT(UP40(J)/40.)
69     300 CONTINUE
70     WRITE(7,400) U40B,U60B,U80B,U100B
71     400 FORMAT(' ',4F10.2)
72     WRITE(7,400) RMS40,RMS60,RMS80,RMS100
73     DO 500 J=1,8
74     X(J)=522.5+(J-1)*5. -360.
75     WRITE(7,600) X(J),UP40(J)
76     500 CONTINUE
77     DO 501 J=1,12
78     X(J)=512.5+(J-1)*5. - 360.
79     WRITE(7,600) X(J),UP60(J)
80     501 CONTINUE
81     DO 502 J=1,16
81.5     X(J)=502.5+(J-1)*5. -360.
81.7     WRITE(7,600) X(J),UP80(J)
81.8     502 CONTINUE
81.9     DO 503 J=1,20
81.95     X(J)=492.5+(J-1)*5. -360.
81.97     WRITE(7,600) X(J),UP100(J)
81.98     503 CONTINUE
81.99     600 FORMAT(' ',2F20.2)
82     STOP
83     END
83.5 C THIS SUBROUTINE EVALUATES THE INTENSITY
84     SUBROUTINE INTENS(UI,UE,UT,IFLG,UP,IJK)
85     REAL UI(1801,40),UE(500),UT(100),UP(100),A(500)
86     INTEGER IFLG,LOW,HI,IJK
87     TEMP=0.
88     NP=(IFLG-1)*20 + 40

```

NOTIME at 10:53:49 on JUN 27, 1985 for CCid=CILL Page 3

```
89      LOW=(4-IFLG)*50 +1
90      HI=(LOW)+NP*5 -2
91      DO 1 J=LOW,HI
91.5    K=J+649
92      P1=UI(K,IJK)-UE(J)-UT(IJK)
93      P2=UI(K+1,IJK)-UE(J+1)-UT(IJK)
94      A(J)=(P1**2 +P2**2)/2./5.
95      1  CONTINUE
96      NP1=NP/5
97      DO 3 J=1,NP1
98      DO 2 K=1,25
99      L=LOW + (J-1)*25 + K -1
100     TEMP=TEMP+A(L)
101     2  CONTINUE
102     UP(J)=(TEMP/5.) + UP(J)
103     TEMP=0.
104     3  CONTINUE
105     RETURN
106     END
```

4. Time Scale Analysis (PEAK)

This program was used to obtain turbulence time scale information from unprocessed anemometer signals. The basic procedure is to scan the signal for peaks. The time separation between peaks is recorded and a relative probability distribution is constructed for this variable. An amplitude threshold is input to the program as a criteria for defining a peak. This amplitude threshold was determined by operating the hot wire probe in quiescent ambient air and forming a distribution of the noise amplitude for this condition. The mean of this distribution was selected as the amplitude threshold.

The program starts by looking at the first two data points. If the second point is less than the first the program begins to search for a valley; otherwise it scans for a peak. The procedure for scanning for a peak or a valley are similar and only one will be described here. The reader should refer to the following flow chart for complete detail.

The data is read to the program in array. The program keeps track of the index and as long as the following data point is greater than or equal to the present one the index is increased by one. When a peak is found the index is saved until the next peak is found. There are many tests to check for the peak validity and the reader is referred to the flow chart for a clear description of these.

Once two peaks have been found with indexes i and j respectively, the difference between the two indexes gives the time separation. This is because the sample rate was set for every $1/5$ of a crank angle degree. Thus the time separation t is obtained from:

$$t = \frac{(j-1)}{5} \frac{1}{\text{RPM}} \quad (\text{D.8})$$

Because the time separation between peaks can only occur in multiples of 1/5 of a crank angle degree the program can easily keep track of the occurrences of a given time separation. The array PDF keeps track of the number of occurrences of a specific separation; for example, Pdf(1) keeps track of the number of occurrences of m/5 of a crank angle degree separation between peaks. The relative probability distribution of the time between peaks can then be easily determined.

A program listing and flow chart follow.

Definition of Program Symbols (PEAK)

AMP	Signal Amplitude Array
D	Digital Anemometer Data Array
DAT	Working Array of Digital Data
KCNT	Keeps Track of Number of Peaks
NOISE	Noise Amplitude Threshold
PDF	Keeps Track of Number of Occurences of Specific Peak Time Separation
PK	Index of Peak
PICIND	Array of Peak Indexes
RDF	Real Probability Distribution Function of Peak Time Separation
VALE	Valley Value
VALE2	Valley Value

FLOWCHART FOR PROGRAM PEAK

INPUTS

DAT(40,300),NOISE

INITIALIZE ALL ARRAYS
READ IN THE INTEGER DATA
INITIALIZE ALL COUNTERS
INITIALIZE ALL FLAGS

NCYC = NCYC + 1
J = 1
KCNT=0
PKIND(J)=0,J=1,200

DAT(NCYC,2) < DAT(NCYC, 1)?

NO

SEARCH FOR A PEAK

FLG=1

DAT(NCYC,J+1) > DAT(NCYC,J)?

NO

J=J+1

DAT(NCYC,J) ≠ DAT(NCYC,J+1)?

NO

PK=J

DAT(NCYC,J) - VALE ≤ NOISE?

NO

DAT(NCYC,J) > VALE?

NO

KCNT = KCNT + 1

PKIND(KCNT)=PK

JP=J

SEARCH FOR A VALLEY

FLG = 0

DAT(NCYC,J+1) < DAT(NCYC,J)?

NO

J = J + 1

DAT(NCYC,J) ≠ DAT(NCYC,J+1)?

NO

DAT(NCYC,J+1) ≥ DAT(NCYC,J)?

NO

VALE2=DAT(NCYC,J)

TEST=DAT(NCYC,JP)

TEST - VALE2 > NOISE?

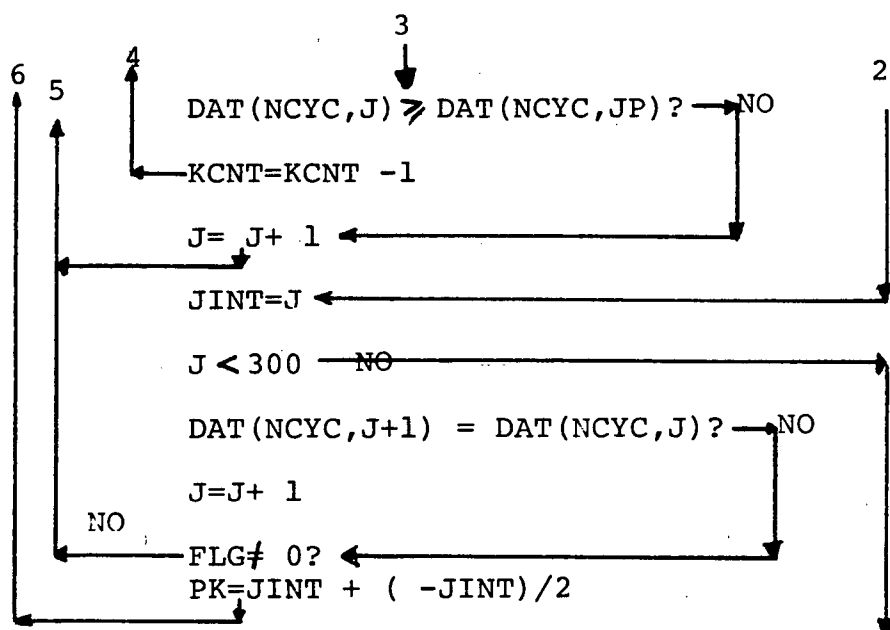
NO

VALE=VALE2

4 6 5

3

2



1 PEAK at 17:47:25 on JUN 26, 1985 for CCId=CILL Page 1

```

1      INTEGER DAT(4,300),VALE,VALE2,NOISE,PKIND(200)
2      INTEGER PK,FLG,PDF(200),D(4,3600),AMP(30)
2.02   C THIS PROGRAM COUNTS THE TIME SEPARATION BETWEEN PEAKS AND
2.03   C FORMS A RELATIVE PROBABILITY DISTRIBUTION OF THIS QUANTITY
2.05   REAL RDF(200)
2.1    DO 103 K=1,200
2.15   RDF(K)=0.
2.2    PKIND(K)=0
2.3    PDF(K)=0
2.4    103 CONTINUE
2.5    DO 98 MM=1,20
2.7    NREC=((MM-1)*502 + 1)*1000
2.8    FIND(5,NREC)
3      READ(5,100)(D(1,M),M=35,3600),((D(M,N),N=1,3600),M=2,4)
4      100 FORMAT(' ',32I5)
5      KCNT=0
6      NOISE=7
7      PK=0
8      JP=0
9      JINT=0
10     VALE=0
11     VALE2=0
12     DO 99 K=1,30
13     AMP(K)=0
14     99 CONTINUE
15     DO 102 K=1,4
16     DO 101 L=1,300
17     M=L + 2549
18     DAT(K,L)=D(K,M)
19     101 CONTINUE
20     102 CONTINUE
25     DO 30 NCYC=1,4
26     J=1
27     KCNT=0
28     DO 104 K=1,200
29     PKIND(K)=0
30     104 CONTINUE
31     IF (DAT(NCYC,2) .GT. DAT(NCYC,1)) GO TO 4
32     1 GO TO 9
33     2 GO TO 4
34     3 IF (J .LE. 300) GO TO 1
35     GO TO 18
36     4 FLG=1
37     C
38     C SEARCH FOR A PEAK
39     C
40     IF (J .GE. 300) GO TO 18
41     5 IF (DAT(NCYC,J+1) .LE. DAT(NCYC,J)) GO TO 6
42     J=J+1
43     GO TO 5
44     6 IF (DAT(NCYC,J) .EQ. DAT(NCYC,J+1)) GO TO 15
45     PK=J
46     IF ((DAT(NCYC,J)-VALE) .GT. NOISE) GO TO 8
47     7 IF (DAT(NCYC,J) .LE. VALE) GO TO 9
48     8 KCNT= KCNT + 1
49     PKIND(KCNT)=PK
50     IAMP=DAT(NCYC,J)-VALE
51     IF (IAMP .GT. 30)IAMP=30

```

PEAK at 17:47:25 on JUN 26, 1985 for CCId=CILL Page 2

```

52      AMP(IAMP)=AMP(IAMP)+1
53      JP=J
54      GO TO 3
55  9      FLG=0
56  C
57  C SEARCH FOR A VALLEY
58  C
59      IF (J .GE. 300) GO TO 18
60  10      IF (DAT(NCYC,J+1) .GE. DAT(NCYC,J)) GO TO 11
61          J=J+1
62          GO TO 10
63  11      IF (DAT(NCYC,J) .EQ. DAT(NCYC,J+1)) GO TO 15
64  12      IF (DAT(NCYC,J+1) .LT. DAT(NCYC,J)) GO TO 10
65          VALE2=DAT(NCYC,J)
66          TEST=DAT(NCYC,JP)
67          IF (JP .EQ. 0) TEST=10000
68          IF ((TEST -VALE2) .LE. NOISE) GO TO 13
69          VALE=VALE2
70          GO TO 2
71  13      IF (DAT(NCYC,J) .LT. DAT(NCYC,JP)) GO TO 14
72          KCNT=KCNT-1
73          GO TO 4
74  14      J=J+1
75          GO TO 10
76  15      JINT=J
77          IF (J .GE. 300) GO TO 18
78  16      IF (DAT(NCYC,J+1) .NE. DAT(NCYC,J)) GO TO 17
79          J=J+1
80          GO TO 16
81  17      IF (FLG.EQ.0) GO TO 12
82          PK=JINT +(J-JINT)/2
83          GO TO 7
84  18      CONTINUE
85          DO 20 K=1,300
86              INDEX=PKIND(K+1)-PKIND(K)
87              IF (INDEX .LE. 0) GO TO 21
88              PDF(INDEX)=PDF(INDEX) + 1
89  20      CONTINUE
90  21      CONTINUE
91  30      CONTINUE
91.5  98      CONTINUE
92          KSUM=0
93          DO 23 K=1,200
94              KSUM=KSUM + PDF(K)
95  C      WRITE(6,22) K,PDF(K),KSUM
96  C22      FORMAT(' ',3I10)
97  23      CONTINUE
101.5      DO 26 L=1,200
101.7          RDF(L)=FLOAT(PDF(L))/FLOAT(KSUM)
101.8          X=L/5.*(60./((1140.*360.))*1000000.
101.9          WRITE(7,27) X,RDF(L)
101.95  27      FORMAT(' ',F10.2,2X,F10.3)
101.97  26      CONTINUE
102      STOP
103      END

```

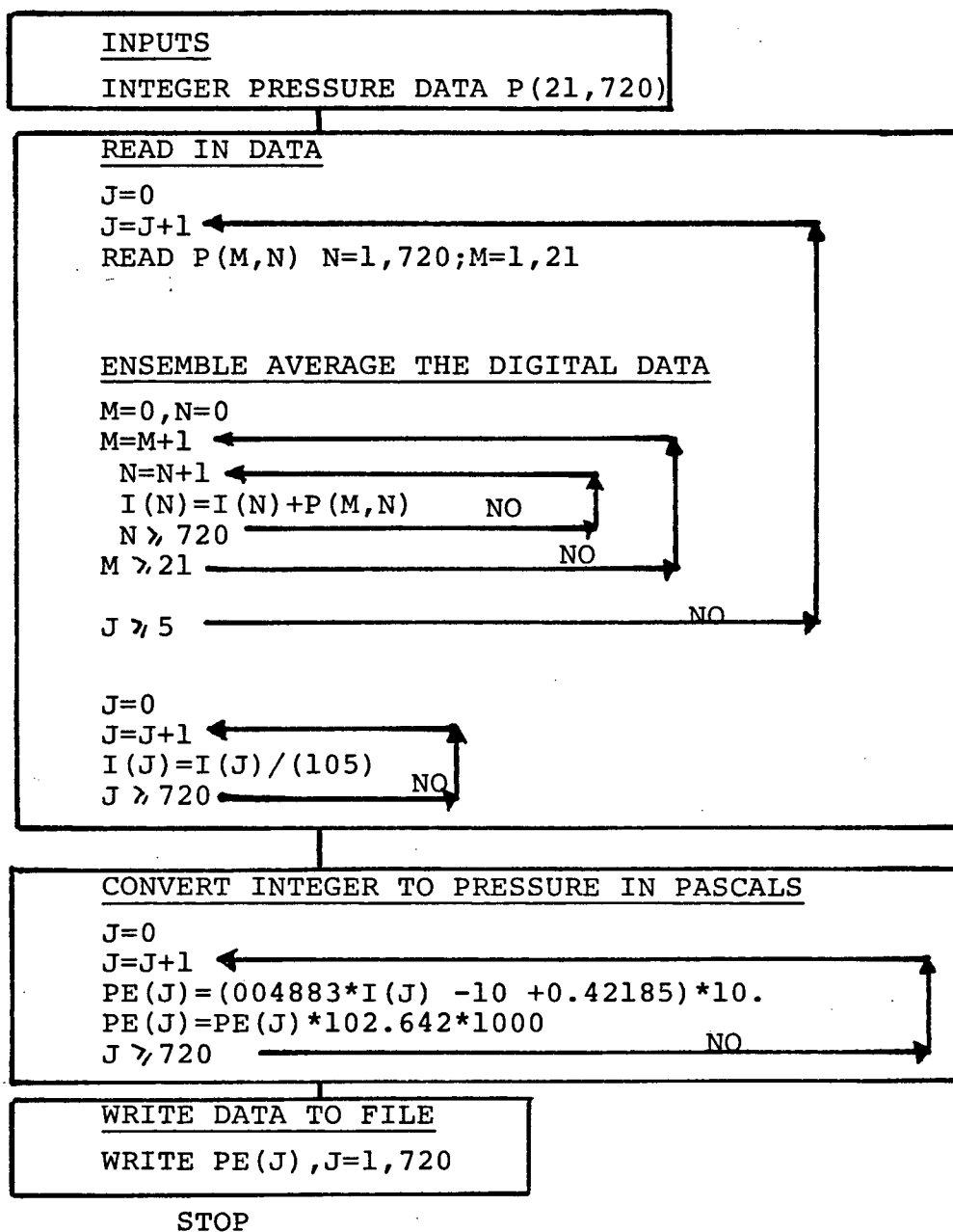
APPENDIX E - COMBUSTION DATA PROCESSING1. Pressure Evaluation and Ensemble Averaging from Digital Data (PENH)

This program was used to read in the digitized pressure data, ensemble average it, convert the integers to a pressure in bars, and then save the data in a file for later use.

A program listing and flow chart follow.

Definition of Program Symbols (PENH)

I	Integer Array Used to Ensemble Digital Pressure Data
KG	Thermal Conductivity of Air
NV	Kinematic Viscosity of Air
P	Digital Pressure Data
PE	Pressure Converted to Bars
RHO	Density of Air
TG	Temperature of Air
V	Voltage Obtained From Digital Data

FLOWCHART FOR PROGRAM PENH

ing of PENH at 10:53:24 on JUN 27, 1985 for CCId=CILL Page 1

```

1      C*****
2      C*
3      C*
4      C*   THIS PROGRAM ENSEMBLES THE DIGITAL DATA FROM THE PRESSURE
5      C*   TRACE. 5-10 GRABS OF 32 K CHUNKS ARE MADE.  THIS CORRESPONDS
6      C*   APPROX 22.75 CYCLES PER GRAB.
7      C*
8      C*   THE INTEGERS ARE READ INTO A MATRIX, 22 CYCLES AT A TIME AND
9      C*   ARE THEN ENSEMBLED THEY ARE THEN CONVERTED TO PRESSURE DATA
10     C*
11     C*   AMBIENT CONDITIONS ARE ASSUMED TO EXIST IN THE CYLINDER FOR
12     C*   THE BDC CRANK POSITION
13     C*
14     C*****
15     INTEGER P(21,720),D(720),I(720)
16     REAL PE(720),TG(720),U(720),KG(720),RHO(720),NU(720)
17     REAL TO,KO,PO,UO
18     PO=101300
19     DO 101 J=1,720
20     I(J)=0
21     101 CONTINUE
22     C READ IN THE DATA
23     DO 1 J=1,5
24     NREC=( 502*(J-1) + 1)*1000
25     FIND(5,NREC)
26     READ(5,99) K
27     READ(5,99)(D(L),L=1,685),((P(M,N),N=1,720),M=1,21)
28     99 FORMAT(' ',32I5)
29     C ENSEMBLE AVERAGE THE DATA
30     DO 2 M=1,21
31     DO 3 N=1,720
32     I(N) = I(N) + P(M,N)
33     3 CONTINUE
34     2 CONTINUE
35     NCNT=J
36     1 CONTINUE
37     DO 4 J=1,720
38     I(J)=I(J)/(NCNT*21)
39     4 CONTINUE
40     C
41     C   THE DATA HAS NOW BEEN READ IN DIGITAL FORM AND ENSEMBLED
42     C   FOR DIGITIZATION, -10 TO +10 VOLTS CORRESPONDS TO 0 TO 4096
43     C   CONVERT INTEGERS BACK INTO A VOLTAGE
44     C   V=(-10 + 0.004883 * I)
45     C   FOR PRESSURE TRANSDUCER, 10 BAR PER VOLT, REF PRESSURE IS AT BDC
46     C   AND CORRESPONDS TO THE INTAKE MAINIFOLD PRESSURE
47     C
48     DO 10 J=1,720
49     V= (.004883*I(J) - 10.)
50     PE(J)= (V+0.42185 )*10.
51     PB=PE(J)
52     C
53     C   CONVERT TO PASCALS
54     C
55     PE(J)= (PE(J)*102.642)*1000.
56     10 CONTINUE
57     DO 5 J=1,180
58     K= 360 +(J-1)*2
59     WRITE(7,6) PE(K)
60     5 CONTINUE
61     6 FORMAT(' ',F12.4)
62     STOP
63     END

```

2. Geometric Analysis of a Spherical Flame Front (DFLAME)

This program was written to produce the flame front geometry figures required by the program MASBRN. The required information was the volume, surface area, and wetted perimeter area for a spherical flame front of radius r in an engine cylinder with the CFR squish geometry under study.

The geometry is shown schematically in Figure E.1. The combustion chamber is a cylinder of radius RC and variable height H . The spark is on the side. The flame is assumed to expand spherically into the chamber from the spark location.

First the equations to solve for a geometry without squish will be developed. Then the procedure to incorporate squish in the calculation will be outlined.

From Figure E.1 it can be seen that the volume of the flame V_F may be expressed as:

$$V_F = \int_0^h [\text{Area of flame section}] dz \quad (\text{E.2})$$

where the area of the flame section AFS1 is given by:

$$\text{AFS1} = R^2\alpha + Rc^2 (\beta - \sin\beta) \quad (\text{E.3})$$

and the flame front area AFF1 is:

$$\text{AFF1} = 2R_F \int_0^H \alpha dz \quad (\text{E.4})$$

Similarly the area of the wetted perimeter AWP1 is expressed by:

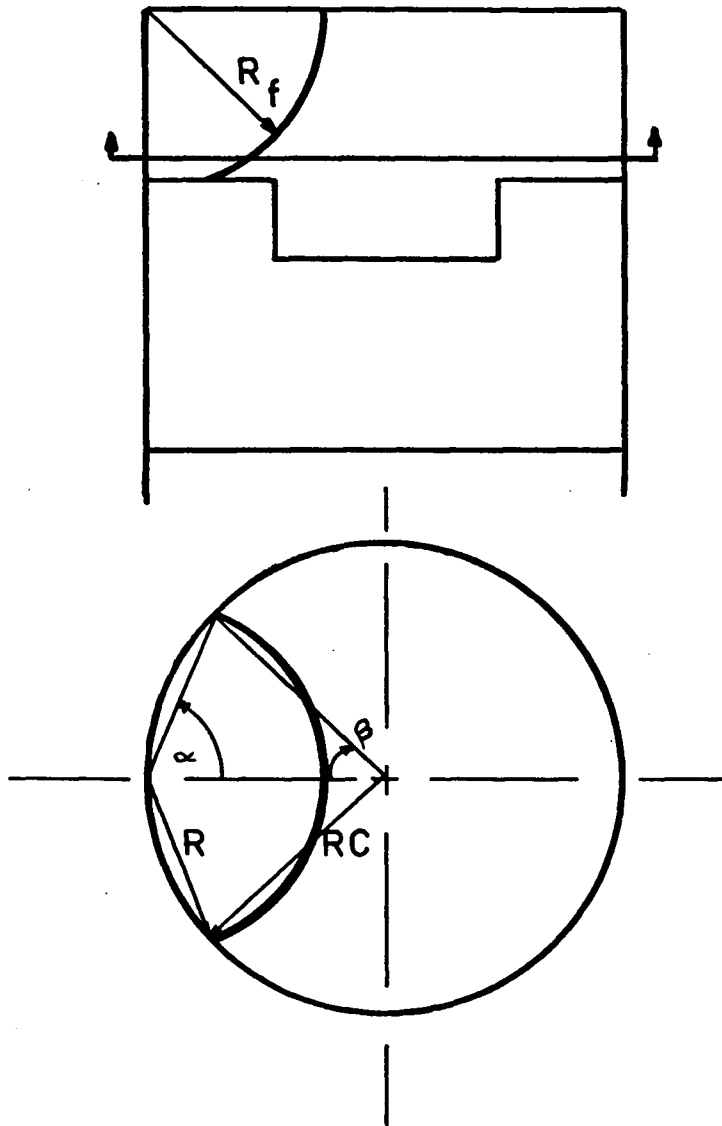


Figure E.1 Flame geometry for a section through a flame above the piston bowl (Flame Section 1).

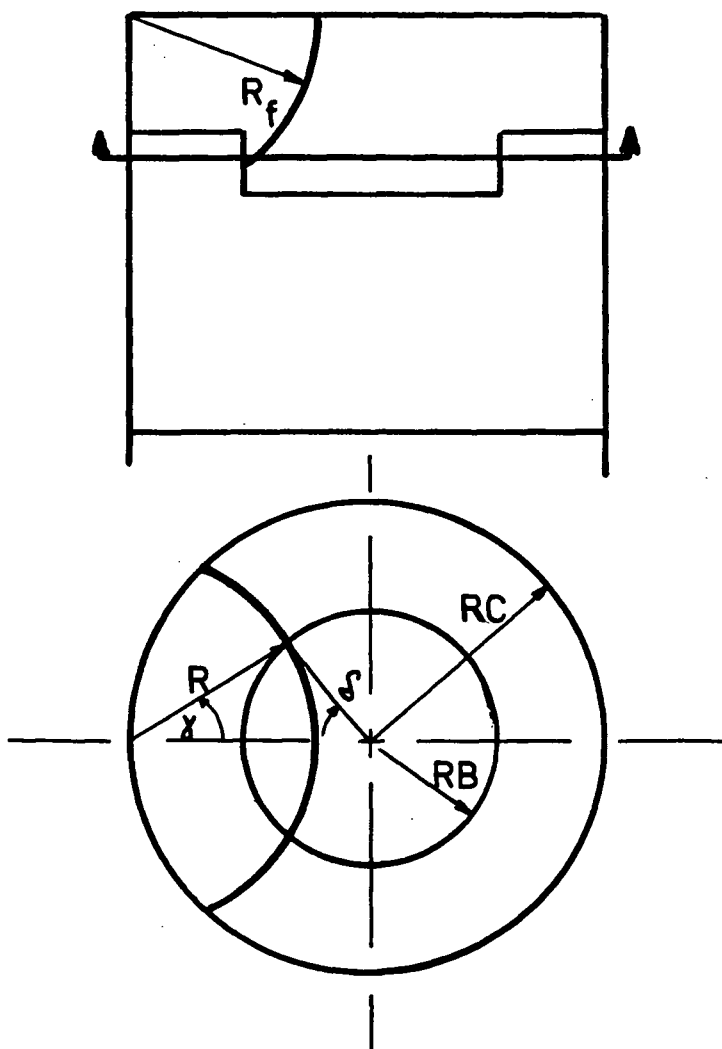


Figure E.2 Flame geometry for a section through a flame in the piston bowl (Flame Section 2).

$$AWP1 = 2RC \int_0^H \beta \, dz + AFS1(z=0) + AFS1(z=H) \quad (E.5)$$

If the flame radius is small enough that the flame does not contact the bowl then the above equations are sufficient. However when the flame enters the bowl the geometry of the flame section shown in Figure E.2, AFS2 becomes important. The area AFS2 is given by:

$$AFS2 = \gamma R^2 + \delta RB^2 - R^2 \sin \gamma - RB^2 \sin \delta \quad (E.6)$$

The expressions for the volume, flame front area, and wetted perimeter are similar to those given previously except that the lower limit of integration is now H and the upper limit H+D (D is the bowl depth).

The program DFLAME generates a table of volumes and areas for combinations of flame radius and cylinder height. All calculations are done in two parts. The first for a cylinder without a squish bowl and the second adds in the effect of the squish bowl if required. The integration is performed with the aid of UBC DCADRE [41].

A program listing and flow chart follow.

Definition of Program Symbols (DFLAME)

AFLAM1	Area of Flame Front 1
AFLAM2	Area of Flame Front 2
AFND	Nondimensional Area of Flame Front
AFS1	Area Function for Section 1
AFS2	Area Function for Section 2
ALF	Function for Angle Alfa
APND	Nondimensional Area of Wetted Perimeter
AWP1	Area of Wetted Perimeter, Section 1
AWP2	Area of Wetted Perimeter, Section 2
BET	Function for Angle Beta
D	Depth of Piston Bowl
DEL	Function for Angle Delta
ERRAF	Error in Flame Area
ERRAP	Error in Wetted Perimeter Area
ERRV	Error in Volume
GAM	Function for Angle Gamma
H	Piston Distance from Head
HND	Nondimensional H
HU1	Upper Integration Limit for Section 1
HU2	Upper Integration Limit for Section 2
RB	Radius of Piston Bowl
RC	Radius of Cylinder
RF	Radius of Flame
RND	Nondimensional Radius
VOLF	Volume of Flame
VND	Nondimensional Flame Volume

FLOWCHART FOR PROGRAM DFLAME

INITIALIZE ALL VARIABLES TO ZERO

K=0
K=K+1
CA=(K-1)*PI/180.

CALC PISTON HEIGHT

B=ARCSIN(R/S * SIN(CA))
H=S + R - S*COS(B) - R*COS(CA) + HC
HND(K)= H/HC

START FLAME GEOMETRY CALC

J=0
J=J+1

SET FLAME RADIUS

RF=J*0.08125/2
RND(J)=RF/RC

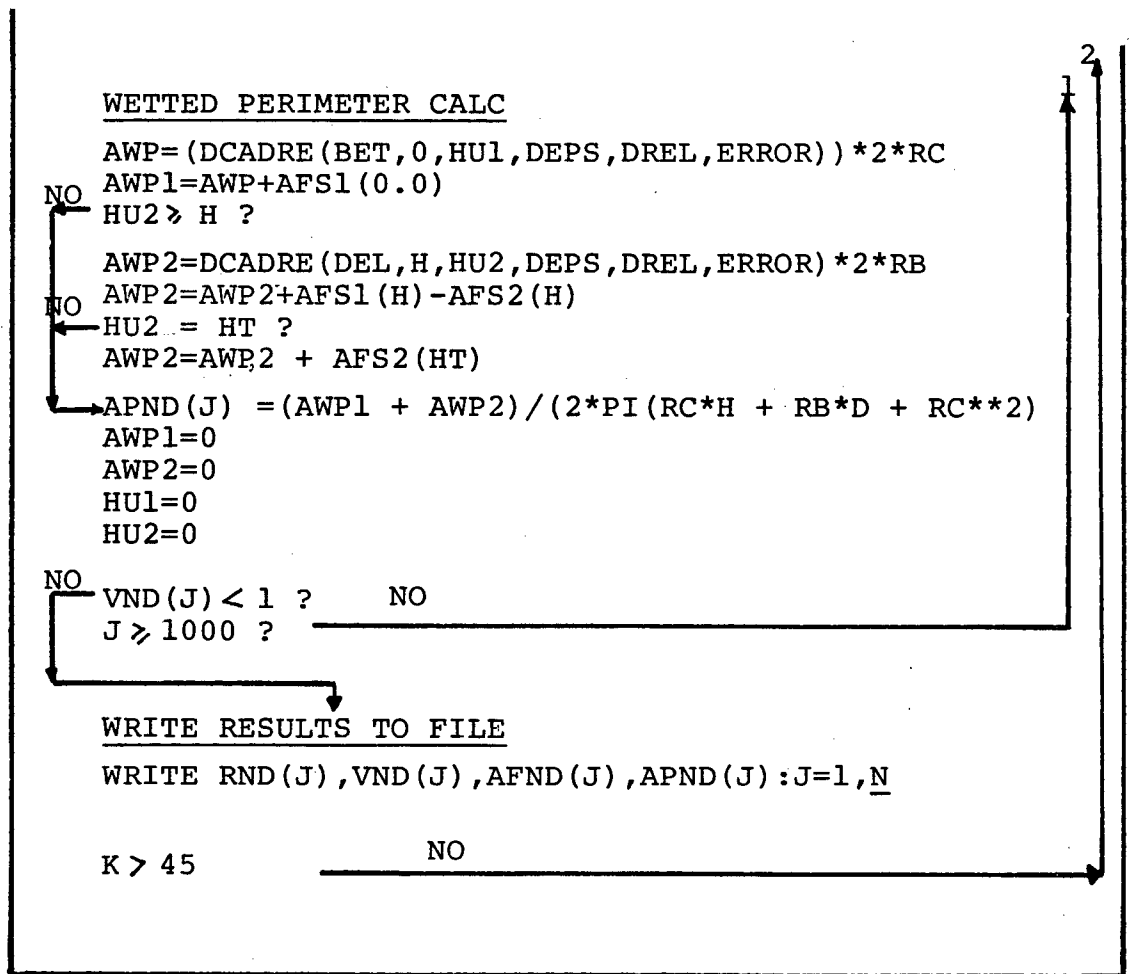
VOLUME CALC

HU1=RF
NO → HU1 > H ?
→ HU1=H
→ VOLF1=DCADRE(AFS1,0,HU1,DEPS,DREL,ERROR)
NO → HU1 > H ?
→ HU1 ≠ RF ?
→ NO
→ HU2=RF
→ NO → RF > H+D?
→ HU2=H+D
→ VOLF2=DCADRE(AFS2,H,HU2,DEPS,DREL,ERROR)
→ VOLF=VOLF1+VOLF2
→ VOLF1=0
→ VOLF2=0
→ VND(J)=VOLF/(PI*(RC**2 *H + RB**2 *D))

AREA OF FLAME FRONT CALC

AFLAM1=DCADRE(ALF,0,HU1,DEPS,DREL,ERROR)
NO → HU2 > H ?
→ AFLAM2=DCADRE(GAM,H,HU2,DEPS,DREL,ERROR)
→ AFLAME=(AFLAM1+AFLAM2)*2*RF
→ AFLAM1=0
→ AFLAM2=0
→ AFND(J)=AFLAME/(2*PI*RC**2)

I 2



STOP

FUNCTION AFS1(Z)

R=SQRT(RF**2 - Z**2)

ALFA=ARCOS(R/(2*RC))

BETA=ARCOS((2*RC**2-R**2)/(2*RC**2))

BETA < PI/2 ?

AFS1=R**2*ALFA + RC**2(BETA-SIN(BETA))

AFS1= R**2 (ALFA- SIN(ALFA)) + BETA*RC**2
+ (R*COS(GAMMA) - RC)*R*SIN(ALFA)

RETURN

FUNCTION AFS2(Z)

R=SQRT(RF**2 - Z**2)

GAMMA=ARCOS(R/(2*RB))

DELTA=ARCOS((2*RB**2-R**2)/(2*RB**2))

DELTA < PI/2 ?

AFS2=R**2*GAMMA + RB**2*DELTA - R**2*SIN(GAMMA)
- RB**2*SIN(DELTA)AFS2=R**2*(GAMMA-SIN(GAMMA)) + DELTA*RB**2
+ (R*COS(GAMMA)-RC)*R*SIN(GAMMA)

RETURN

FUNCTION ALF(Z)

R=SQRT(RF**2 - Z**2)

ALF= ARCOS(R/(2*RC))

RETURN

FUNCTION GAM(Z)

R=SQRT(RF**2-Z**2)

GAM=ARCOS(R/(2*RB))

RETURN

FUNCTION DEL(Z)

R=SQRT(RF**2-Z**2)

DEL=ARCOS((2*RB**2 - R**2)/(2*RB**2))

RETURN

FUNCTION BET(Z)

R=SQRT(RF**2 - Z**2)

BET= ARCOS((2*RC**2 - R**2)/(2*RC**2))

RETURN

ing of DFLAME at 17:47:41 on JUN 26, 1985 for CCId=CILL Page 1

```

1      IMPLICIT REAL*8(A-H,O-Z,$)
2      EXTERNAL AFS1,AFS2,ALF,GAM,BET,DEL
3      REAL*8 RND(100),VND(100),AFND(100),APND(100),HND(100)
3.5    REAL*8 ERRV(100),ERRAF(100),ERRAP(100)
4      C  HU1 IS THE UPPER LIMIT OF INTEGRATION FOR SECTION 1
5      C  HU2 IS THE UPPER LIMIT OF INTEGRATION FOR SECTION 2
6      C  RND IS THE NONDIMENSIONAL RADIUS; RF/RC
7      C  VND IS THE NONDIMENSIONAL VOLUME; VOLF/VC
8      C  AFND IS THE NONDIMENSIONAL FLAME FRONT AREA; AFLAME/AC
9      C  APND IS THE NONDIMENSIONAL WET PERIMETER AREA; AWP/(AC + AB)
10     C  S IS THE CONNECTING ROD LENGTH
11     C  H IS S+HC,(HC IS THE CLEARANCE HEIGHT)
12     C  RF IS THE FLAME RADIUS
13     C  RC IS THE CYLINDER RADIUS
14     C  RB IS THE BOWL RADIUS
15     C  VOLF IS THE VOLUME ENCLOSED BY THE SPHERICAL FLAME FRONT
16     C  D IS THE DEPTH OF THE BOWL
17     COMMON RF,RC,RB
18     PI=3.141593
18.1    VOLF2=0.0
18.2    AWP=0.0
18.3    AWP1=0.0
18.4    AWP2=0.0
18.5    AFLAM1=0.0
18.6    AFLAM2=0.0
19     S=10.0
20     R=2.25
21     DO 2000 K=1,45
22     CA=(K-1)*PI/180.0
23     B=DARSIN(R/S*DSIN(CA))
24     H= S + R - S*DCOS(B) - R*DCOS(CA)
25     DEPS=0.0
25.5    DREL=0.00000001
26     D=1.337
27     RC=3.25/2
28     RB=0.83
29     HC=.059
30     H=H+HC
31     HU2=0.
32     HT=H+D
33     RF=.00
34     HND(K)=H/HC
35     WRITE(6,20) HND(K)
36     20  FORMAT('1',' DIMINSIONLESS HEIGHT OF PISTON H/RC = ',F8.5)
37     DO 1000 J=1,100
38     DEPS=1.00E-11
39.5    N=J
40     RF=J*.08125/2.
41     RND(J)=RF/RC
42     C  FIRST CALC THE VOLUME OF THE FLAME. THE CALC IS DONE IN
43     C  TWO PARTS. PART ONE ASSUMES A DISC CHAMBER OF HEIGHT H
44     C  PART TWO BRINGS IN THE EXTRA VOLUME OF BOWLS OR DEPRESSIONS
45     C  IN THE CYLINDER HEAD OR PISTON
46     HU1=RF
47     C  THE UPPER LIMIT OF INTEGRATION IS SET TO THE FLAME RADIUS
48     IF (HU1 .GT. H) HU1=H
49     VOLF1=DCADRE(AFS1,0.0,DO,HU1,DEPS,DREL,ERROR)
50     ERRV(J)=ERROR
51.2

```

ing of DFLAME at 17:47:41 on JUN 26, 1985 for CCId=CILL Page 2

```

53         IF (HU1 .LT. H) GO TO 98
54         IF (HU1 .EQ. RF) GO TO 98
55     C     THIS MEANS THE SPHERE DOES NOT INTERSECT THE PISTON & THEREFORE
56     C     NO FURTHER VOLUME CALC IS REQUIRED.
57         HU2=RF
58         IF (RF .GT. H+D) HU2=H+D
59         VOLF2=DCADRE(AFS2,H,HU2,DEPS,DREL,ERROR)
59.2       ERRV(J)=ERRV(J)+ERROR
60     98     VOLF=VOLF1 + VOLF2
60.5       ERRV(J)=100.000-(VOLF - ERRV(J))/VOLF *100.
61         VOLF1=0.
62         VOLF2=0.
63         VND(J)=VOLF/(3.14*(RC**2*H + RB**2*D))
64     C     NOW CALCULATE AREA OF FLAME FRONT
65     C     THE CALCULATION IS SIMILAR TO THE VOLUME CALC
66         AFLAM1=DCADRE(ALF,O.,HU1,DEPS,DREL,ERROR)
66.5       ERRAF(J)=ERROR
67         IF (HU2 .LT. H) GO TO 99
68         AFLAM2=DCADRE(GAM,H,HU2,DEPS,DREL,ERROR)
68.5       ERRAF(J)=ERRAF(J)+ERROR
69     99     AFLAME=(AFLAM1 + AFLAM2)*2*RF
69.2       IF ((AFLAM1+AFLAM2).LE. 0.0)GO TO 33
69.5       ERRAF(J)=100.-((AFLAM1+AFLAM2)-ERRAF(J))/(AFLAM1+AFLAM2)*100.
69.7       GO TO 34
69.8     33     ERRAF(J)=100.00- ERRAF(J)*100.0
70     34     AFLAM1=0.
71         AFLAM2=0.
72         AFND(J)=AFLAME/(2*3.14*RC**2)
73     C     NOW CALCULATE AREA OF WETTED PERIMETER
74     C
75         AWP=(DCADRE(BET,O.,HU1,DEPS,DREL,ERROR))*2*RC
75.2       AWP1=AWP+AFS1(O.DO)
75.5       ERRAP(J)=ERROR
76         IF (HU2 .LT. H)GO TO 100
77         AWP2=(DCADRE(DEH,H,HU2,DEPS,DREL,ERROR))*2*RB
77.2       AWP=AWP+AWP2
77.5       ERRAP(J)=ERRAP(J)+ERROR
78         AWP2=AWP2+ AFS1(H)-AFS2(H)
79         IF (HU2 .EQ. HT) AWP2=AWP2+AFS2(HT)
80     100     APND(J)=(AWP1 + AWP2)/(2*3.14*(RC*H + RB*D +RC**2 ))
80.5       ERRAP(J)=100.00-(AWP-ERRAP(J))/(AWP)*100.
80.7       AWP=0.0
81         AWP1=0.
82         AWP2=0.
83         HU1=0.
84         HU2=0.
85         IF (VND(J).GE. 1.) GO TO 2
86     1000    CONTINUE
87     2       CONTINUE
88         WRITE(6,3) N
89     3       FORMAT('-', 'N = ',I3)
90         WRITE(6,30)
91     30     FORMAT('-',4X,'RF/RC',9X,'VF/VT',9X,'ERROR%',7X,'AFF/AFT',
91.5       1 8X,'ERROR%',7X,'AWP/APT',8X,'ERROR%')
92         DO 10 J=1,N
93         WRITE(6,1) RND(J),VND(J),ERRV(J),AFND(J),ERRAF(J),APND(J),
93.5       1 ERRAP(J)
94     1       FORMAT('O',2(F12.10,2X),F12.9,2X,2(F12.10,2X,F12.9,2X))

```

ing of DFLAME at 17:47:41 on JUN 26, 1985 for CCId=CILL Page 3

```

95      10      CONTINUE
96      2000     CONTINUE
97          STOP
98          END
99          DOUBLE PRECISION FUNCTION AFS1(Z)
100         IMPLICIT REAL*8(A-H,O-Z,$)
101         COMMON RF,RC,RB
101.5      PI=3.141593
102         R=DSQRT(RF**2 - Z**2)
103         IF (R .GT. 2*RC) R=2*RC
104         ALFA=DARCOS(R/(2*RC))
105         BETA=DARCOS((2*RC**2 - R**2)/(2*RC**2))
106         IF(BETA .GT. PI/2) GO TO 1
107         AFS1=R**2 * ALFA +RC**2*(BETA-DSIN(BETA))
108         GO TO 2
109         1      AFS1=R**2*(ALFA-DSIN(ALFA)) + BETA*RC**2 +
110         1      (R*DCOS(GAMMA)- RC)*R*DSIN(ALFA)
110.5      2      CONTINUE
111         RETURN
112         END
113         DOUBLE PRECISION FUNCTION AFS2(Z)
114         IMPLICIT REAL*8(A-H,O-Z,$)
115         COMMON RF,RC,RB
115.5      PI=3.141593
116         DIFF= RF**2-Z**2
120         R=DSQRT(RF**2 - Z**2)
121         IF (R .GT. 2*RB) R=2*RB
122         GAMMA=DARCOS(R/(2*RB))
123         DELTA=DARCOS((2*RB**2-R**2)/(2*RB**2))
124         IF (DELTA .GT. PI/2) GO TO 1
125         AFS2=R**2*GAMMA +RB**2*DELTA - R**2*DSIN(GAMMA) -
125.2      1 RB**2*DSIN(DELTA)
126         RETURN
129         1      AFS2=R**2*(GAMMA-DSIN(GAMMA)) + DELTA*RB**2
130         1 + (R*DCOS(GAMMA)-RC)*R*DSIN(GAMMA)
131         RETURN
132         END
133         DOUBLE PRECISION FUNCTION ALF(Z)
134         IMPLICIT REAL*8(A-H,O-Z,$)
135         COMMON RF,RC,RB
136         R=DSQRT(RF**2-Z**2)
137         IF (R .GT. 2*RC) R=2*RC
138         ALF=DARCOS(R/(2*RC))
139         RETURN
140         END
141         DOUBLE PRECISION FUNCTION GAM(Z)
142         IMPLICIT REAL*8(A-H,O-Z,$)
143         COMMON RF,RC,RB
144         R=DSQRT(RF**2-Z**2)
145         IF (R .GT. 2*RB) R=2*RB
146         GAM=DARCOS(R/(2*RB))
147         RETURN
148         END
149         DOUBLE PRECISION FUNCTION DEL(Z)
150         IMPLICIT REAL*8(A-H,O-Z,$)
151         COMMON RF,RC,RB
152         R=DSQRT(RF**2 - Z**2)
153         IF (R .GT. 2*RB) R=2*RB

```

ing of DFLAME at 17:47:41 on JUN 26, 1985 for CCId=CILL Page 4

```
154      DEL=DARCOS((2*RB**2 - R**2)/(2*RB**2))
155      RETURN
156      END
157      DOUBLE PRECISION FUNCTION BET(Z)
158      IMPLICIT REAL*8(A-H,O-Z,$)
159      COMMON RF,RC,RB
160      R=DSQRT(RF**2-Z**2)
161      IF (R .GT. 2*RC)R=2*RC
162      BET=DARCOS((2*RC**2 - R**2)/(2*RC**2))
163      RETURN
164      END
```

3. Burning Rate Analysis (MASBRN)

The program used to perform the mass burn rate analysis was developed by Jones [36] and a complete description and flow chart may be found. Only alterations concerned with the CFR cylinder geometry were made. These occur in statements defining cylinder volume. The other change was in the way the flame front geometry is evaluated. The old geometry was calculated based on a cylindrical chamber with a hemispherical head. The program DFLAME was used to produce a table of values which MASBRN reads in when required. No other changes were made.

MASBRN at 17:46:21 on JUN 26, 1985 for CCid=CILL Page 1

```

1  C  MB  THIS PROGRAM CALCULATES MASS BURNING RATE AND
2  C  === FLAME SPEED FROM MEASURED PRESSURE DATA TAKEN
3  C  FROM THE CFR ENGINE.
4  C
5      IMPLICIT REAL*8(A-H,O-Z)
6      REAL*8 MPV,K,L,M,N,NO,N2,NO2,NCH,KK,NUM,NUM1,NMIX,MOLFL,
7      -NM,NM1,NNM1,NNM2,NN2,NNO2,MEP,LENG,MTOT,MWMIX,MFX1,NNCH,
8      -MFX2,MW(14),MMFX2,NRN2,NRES,NRO2,NRCO2,NRH20,NNFUEL
9      -,MF(5,200),IGNDEL,MWBMIX
10 C
11     COMMON /AREA1/ NCH,NO2,K,L,M,N,KFUEL
12     COMMON /AREA2/ MOLFL,NMIX,HF1,NNO2,NN2,NNFUEL,KOM
13     COMMON /AREA3/ AREAB,HTEXP,MPV,HTFCN,TWALL,VISC,THCOND
14     COMMON /AREA4/ NDISS,IPRINT
15 C
16     DIMENSION X(10),PP(5,200),VV(5,200),VV2(5,200),VVX(20),
17     -DH(20),CPG(20),PP2(5,200),DI(5,200),TIM(5,200),XX(5,200),
18     -CCA(10),DL(5,200),ZZ(5,200),DC(5,200),YY(5,200),POUT(180),
19     -UUU(10),CC(10),PDAT(5,200),CB(5,200),TB(5,200),
20     -FS(5,200),RB(5,200)
21 C
22     INTEGER IPRES(5,200),NREP,NMODE
23 C
24 C  STATEMENT FUNCTION USED THROUGHOUT PROGRAM TO CALCULATE CYLINDER
25 C  VOLUME (DVOL) AT A GIVEN CRANK ANGLE (DALFA). VOLUME OBTAINED MUST
26 C  BE ADDED TO THE CLEARANCE VOLUME TO GIVE TOTAL CYLINDER VOLUME
27 C
28     DVOL(DALFA)=3.14159*((BORE/2.)**2.)*((STROK/2.)*(1.-DCOS(DALFA*
29     -0.0174532))+LENG*(1.-DSQRT(1.-(DSIN(DALFA*0.0174532)*DSIN(DALFA
30     -*0.0174532)*((STROK/2./LENG)**2.))))))
31     PI=3.14159
31.5    NUMBR=1
32     IPRINT=0
33     JFLG=0
33.5    IGRAPH=0
34     DO 222 IL=1,NUMBR
35 C
36 C
37 C  READ TYPE OF FUEL (11=CH4, 12=C8H18, 13=C3H8 );
38 C  TEMP. (T1)(K) AT START OF COMBUSTION;
39 C  ENGINE SPEED (RPM); COMPRESSION RATIO (COMPR); REL. AIR/FUEL
40 C  RATIO, LAMBDA (AF); SPARK ADVANCE (SPKAD)(DEG. B.T.D.C.);
41 C  HEAT TRANSFER MULTIPLIER (HTFCN);
42 C  HEAT TRANSFER EXPONENT (HTEXP);
43 C  RESIDUAL GAS FRACTION (%),(F); PERCENTAGE CONSTITUENTS IN
44 C  RES. FRACTION (PRO2,PRCO2,PRH2O,PRN2);
45 C  WHETHER FULL DISSOCIATION (NDISS=0), OR PARTIAL (NDISS=1);
46 C  CRANK ANGLE ITERATION INCREMENT (PDCA); CYL. WALL TEMP. (TWALL);
47 C
48 C  THERE IS AN OPTION TO ENTER DATA IN THE INTERACTIVE MODE OR
49 C  CONVENTIONALLY THRU A DATA FILE
50 C
51 C
52     WRITE(6,1)
53     1  FORMAT(' ', 'DO YOU WANT TO READ THE DATA FILE (O) OR ENTER DATA
54     1INTERACTIVELY (I) ?')
55     CALL FREAD('GUSER','I:',NMODE)
55.5    JFLG=0
56     IF (NMODE .EQ. 1) GO TO 3

```

MASBRN at 17:46:21 on JUN 26, 1985 for CCId=CILL Page 2

```

57      READ(5,47) KFUEL,T1,SPEED,COMPR,AF,SPKAD,HTFCN,HTEXP
58      47  FORMAT(I3,2F7.1,3F6.2,F6.3,F5.2)
59      READ(5,46) F,PRO2,PRCO2,PRH2O,PRN2,NDISS,PDCA,TWALL
60      46  FORMAT(5F7.3,I3,F6.2,F7.1)
61      READ(5,2) PINLET,AIRFLO,IGNDEL,SCONST,IPRNTS,PAMB
62      READ(5,22) CUPD,CUPH,HC
63      22  FORMAT(3F8.3)
64      2   FORMAT(F6.1,3F6.2,I3,F6.2)
64.5    JFLG=1
64.7    WRITE(6,5)
64.8    5   FORMAT(' ','DO YOU WANT TO CHANGE ANY OF THE INPUTS 1=Y,0=N ?')
64.9    CALL FREAD('GUSER','I:',NREP)
65      IF ( NREP .EQ. 0)GO TO 4
66      3   CALL INPUTS(JFLG,KFUEL,T1,SPEED,COMPR,AF,
67      1 SPKAD,HTFCN,HTEXP,F,PRO2,PRH2O,PRN2,NDISS,PDCA,
68      1 TWALL,PINLET,AIRFLO,IGNDEL,SCONST,IPRNTS,PAMB,CUPD,CUPH,HC)
69      4   CONTINUE
70      C
71      C   READ IN PRESSURE DATA
72      C
73      CALL SMOOTH(POUT,SCONST,IPRNTS)
74      C
75      DO 658 KJ=1,180
76      PDAT(IL,KJ)=POUT(KJ)
77      658 CONTINUE
78      C
79      C   DETERMINE FUEL PROPERTIES: MOL.WEIGHT, LOW HEAT VAL.,
80      C   ENTHAL. OF FORMATION
81      C
82      IF(KFUEL.GT.11) GOTO 10
83      CN=1.0
84      HM=4.0
85      MW(11)=16.04
86      QVS=50050.0
87      HF1=-74873.0
88      WRITE(9,45) CN,HM
89      45  FORMAT(1H,'FUEL TYPE:- METHANE C ',F3.1,' H ',F3.1/)
90      GOTO 30
91      C
92      10  IF(KFUEL.GT.12) GOTO 20
93      CN=8.0
94      HM=18.0
95      MW(12)=114.14
96      QVS=43500.0
97      HF1=-208447.0
98      WRITE(9,43) CN,HM
99      43  FORMAT(1H,'FUEL TYPE:- OCTANE C ',F3.1,' H ',F4.1/)
100     GOTO 30
101     C
102     20  IF(KFUEL.GT.13) STOP
103     CN=3.0
104     HM=8.0
105     MW(13)=44.097
106     QVS=46353.0
107     HF1=-103847.0
108     WRITE(9,44) CN,HM
109     44  FORMAT(1H,'FUEL TYPE:- PROPANE C ',F3.1,' H ',F3.1/)
110     C

```

MASBRN at 17:46:21 on JUN 26, 1985 for CCId=CILL Page 3

```

111 C ENGINE PARAMETERS
112 C
113 30 CONTINUE
114 STROK=4.5*.0254
115 BORE=3.25*.0254
116 LENG=10.0*.0254
117 HTCLRV=HC
118 C CLEARANCE HEIGHT IS SET FOR EACH GEOMETRY
119 CLRV=HTCLRV*3.141593*(BORE**2)/4.0 +CUPD**2/4.*PI*CUPH+0.0000027
120 C
121 C GAS CONSTANT (KJ/KMOL K)
122 C
123 RMOL=8.31434
124 JJ=0
125 C
126 C
127 C CALC STOICH A/F RATIO(STAFR) AND AIR/FUEL RATIO(AFR)
128 C
129 STAFR=((CN+HM/4.)*32.+3.762*(CN+HM/4.)*28.01)/((CN*12)+HM)
130 AFR=STAFR*AF
131 C
132 C CALCULATE VOLUMETRIC EFFICIENCY FROM AIR MASS FLOW(g/sec),
133 C INLET TEMP(K) AND PRES(kpa), RPM, AND DENSITY FACTOR
134 C FOR GASEOUS FUELS
135 C VOLEFF=AIRFLOW/(P/RT)*FACTOR*SPEED*(SWEPT VOL./2)
136 C FACTOR=DENSITY CORRECTION FOR FUEL VAPOUR IN CHARGE
137 C PINLET=PAMB-PLOSS(LOSS THRU VENTURI ELEMENT)
137.5 C PLOSS=1.8
138 C FACTOR=1
139 C IF(KFUEL.EQ.12) GOTO 700
140 C FACTOR=1.0+(1.0/AFR)*(29.0/(MW(KFUEL)))
141 C
142 C INLET PRES REDUCED BY PLOSS
143 C
144 700 VOLEFF=45.858*FACTOR*AIRFLO*T1/(SPEED*(PINLET-PLOSS))
144.5 C
145 C
146 C CONVERT PRESSURE DATA IN BAR TO KPA, AND CORRECT DATA FOR
147 C VOL. EFF.
148 C
149 C P1=VOLEFF*(PINLET-PLOSS)
150 C PVEFF=(101.3)-P1
151 C WRITE(9,701) P1,VOLEFF,FACTOR,PVEFF
152 701 FORMAT(1H , 'P1,VOLEFF,FACTOR,PVEFF ',4F10.3/)
153 C DO 267 I=1,180
154 C PDAT(IL,I)=PDAT(IL,I)/1000.-PVEFF
155 267 CONTINUE
156 C
157 C
158 C CALC. NUMBER OF KMOLS OF REACTANTS AND PRODUCTS BEFORE AND AFTER
159 C COMBUSTION RELATIVE TO ONE KMOL OF FUEL
160 C (NOT INCLUDING DISSOCIATION). NCH=HYDROCARBON
161 C NO2=AVAILABLE OXYGEN, N=NITROGEN, K=CO2, L=H2O, M=UNBURNT OXYGEN
162 C
163 NCH=1
164 NO2=(CN+HM/4)*AF
165 N=3.762*(CN+HM/4)*AF
166 K=CN

```

MASBRN at 17:46:21 on JUN 26, 1985 for CCId=CILL Page 4

```

167      L=HM/2
168      M=(CN+HM/4)*(AF-1)
169      C
170      WRITE(9,655) NCH,NO2,N,K,L,M
171      655 FORMAT(1H,'NCH,NO2,N,K,L,M=',6F9.5/)
172      C
173      C CALC. TOTAL NUMBER OF KMOLS OF REACTANTS...
174      SUMNS=NCH+NO2+N
175      C CALC. NO. OF KMOLS OF RESIDUAL GAS GIVEN THE VOLUME FRACTION OF
176      C RESIDUAL GASES 'F'....
177      NRES=(F/(1-F))*SUMNS
178      C CALC. NO. OF KMOLS IN CYLINDER PER KMOL OF FUEL...
179      NMIX=SUMNS+NRES
180      SUMNS=NMIX
181      C CALC. NO OF KMOLS OF EACH RESIDUAL GAS...
182      NRO2=PRO2*NRES/100.0
183      NRCO2=PRCO2*NRES/100.0
184      NRH2O=PRH2O*NRES/100.0
185      NRN2=PRN2*NRES/100.0
186      C CALC. NEW VALUES FOR THE TOTAL NO. OF KMOLS OF N2, O2, CO2,& H2O...
187      N=N+NRN2
188      NO2=NO2+NRO2
189      K=K+NRCO2
190      L=L+NRH2O
191      M=M+NRO2
192      WRITE(9,655) NCH,NO2,N,K,L,M
193      C
194      C CALC. ENERGY OF REACTANTS AT INLET TEMP; 5=O2, 6=N2, 11=CH4
195      C 12=C8H18, 13=C3H8, 1=CO2, 3=H2O,... (IN KJ/KMOL OF FUEL)
196      DH(1)=((3.096*T1+0.00273*(T1**2))-7.885E-07*(T1**3))
197      1+8.66E-11*(T1**4))-1+45.0)*RMOL
198      DH(3)=((3.743*T1+5.656E-04*(T1**2))+4.952E-08*(T1**3))
199      1-1.818E-11*(T1**4))-1167.0)*RMOL
200      DH(5)=((3.253*T1+6.524E-04*(T1**2))-1.495E-07*(T1**3))
201      1+1.539E-11*(T1**4))-1024.0)*RMOL
202      DH(6)=((3.344*T1+2.943E-04*(T1**2))+1.953E-09*(T1**3))
203      1-6.575E-12*(T1**4))-1023.0)*RMOL
204      DH(11)=((1.935*T1+4.965E-03*(T1**2))-1.244E-06*(T1**3.)
205      1+1.625E-10*(T1**4.))-8.586E-15*(T1**5.))-985.9)*RMOL
206      DH(12)=((-0.72*T1+4.643E-02*(T1**2.))-1.684E-05*(T1**3.))
207      1+2.67E-09*(T1**4.))-3484.0)*RMOL
208      DH(13)=((1.137*T1+1.455E-02*(T1**2.))-2.959E-06*(T1**3.))
209      1)-1552.9)*RMOL
210      UUU(1)=-3.93522E05
211      UUU(3)=-2.41827E05
212      C CALC. TOTAL ENERGY OF MIXTURE (KJ/KMOL FUEL)
213      ERCT=(NCH*(HF1+DH(KFUEL)-RMOL*T1)+NO2*(DH(5)-RMOL*T1)
214      +-N*(DH(6)-RMOL*T1)+NRCO2*(UUU(1)+DH(1)-RMOL*T1)+NRH2O*
215      -(UUU(3)+DH(3)-RMOL*T1))
216      C
217      C CALC. SWEEP VOL.(CYLV),CLEARANCE VOL.(CLRV),TOTAL VOL.(V1),
218      C VOLUME CORRESPONDING TO GIVEN SPARK ADVANCE (DVOLM)...
219      CYLV=3.1415926*((BORE/2.)**2.)*STROK
220      V1=CYLV + CLRV
221      VTOTAL=V1
222      MPV=SPEED*STROK/30.0
223      C SUBT. SPK ADV. ANGLE FROM 360'AND ADD IGNITION DELAY...
224      ANG=(360.0-SPKAD+IGNDEL)

```

MASBRN at 17:46:21 on JUN 26, 1985 for CCId=CILL Page 5

```

225 C INITIALISE CRANK ANGLE COUNTER AT B.D.C. & SET TIME TO ZERO
226 DLF1=180.0
227 TIME=0.0
228 C CALC. VOLUME IN CYLINDER AT SPARK TIME (USED LATER)
229 DVOLM=(CLRV+DVOL(ANG))
230 TIME=0.0
231 C TOTAL NO. OF MOLS IN CYL.=NO. OF MOLS OF FUEL*(1+4.76(CN+HM/4).AF)
232 C WHERE (1+4.76(CN+HM/4).AF)=NMIX.
233 C I.E. NTOT=MOLFL*NMIX
234 C BUT P1.V1=NTOT.RMOL.T1 OR NTOT=P1.V1/RMOL.T1 = MOLFL.NMIX
235 C THEREFORE NO. OF MOLS OF FUEL IN CYL. = P1.V1/NMIX.RMOL.T1 .....
236 MOLFL=(P1*V1)/(NMIX*RMOL*T1)
237 C ENERGY OF CYLINDER CONTENTS IN KJ .....
238 ENGY1=ERCT*MOLFL
239 C CALC. STOICH. A/F RATIO (STAFR),AIR/FUEL RATIO (AFR),PERCENTAGE
240 C OXYGEN (NNO2), NITROGEN (NN2) AND FUEL (NNCH) IN MIXTURE...
241 STAFR=((CN+HM/4.)*32.+3.762*(CN+HM/4.)*28.01)/((CN*12)+HM)
242 AFR=STAFR*AF
243 NNO2=(NO2/NMIX)*100.
244 NN2=(N/NMIX)*100.
245 NNCH=100.-(NNO2+NN2)
246 NNFUEL=NNCH
247 C GIVEN MOLECULAR WEIGHTS OF FUELS, CALC. MOLECULAR WEIGHT OF
248 C MIXTURE (MWMIX); TOTAL MASS OF MIXTURE (MTOT); AND SPECIFIC
249 C VOLUME OF MIXTURE.....
250 MWMIX=(NNO2*32.0/100.)+(NN2*28.0/100.)+(NNCH*MW(KFUEL)/100.)
251 MTOT=(PDAT(IL,1)*V1*MWMIX)/(T1*RMOL)
252 VTOT1=V1
253 VSU1=VTOT1/MTOT
254 ETOT1=ERCT/MWMIX/NMIX
255 C
256 C
257 WRITE(9,735) MPV,TWALL,HTFCN,HTEXP
258 735 FORMAT(1H,'MPV,TWALL,HTFCN,HTEXP',4E12.4/)
259 WRITE(9,734) ERCT,ENGY1,NMIX,MWMIX,MOLFL,MTOT
260 734 FORMAT(1H,'ERCT,EG1,NMIX,MWMX,MOLFL,MTOT;',6E12.4//)
261 C
262 WRITE(9,652) SPEED,SPKAD
263 652 FORMAT(1H,'SPEED (RPM) = ',F7.1,
264 -7X,'SPARK ADVANCE (DEG. BTDC) = ',F7.2,3X/)
265 WRITE(9,813) AFR,STAFR,AF,COMPR
266 813 FORMAT(1H,'15HAIR/FUEL RATIO=',F6.2,3X,18HSTOICH. A/F RATIO=,
267 -F6.2,3X,7HLAMBDA=,F6.2,3X,12HCOMP. RATIO=,F5.1/)
268 WRITE(9,31)
269 31 FORMAT(1H,'1X','STEP',1X,'VOL',3X,'PRESS',3X,'TU',5X,'TB',5X
270 -, 'MFX',4X,'VFRBNT',2X,'CBVEL',3X,'TBVEL',3X,'FLMSPD',2X,
271 -'FSR',3X,'RADF',2X,'AREAF',3X,'C.A.',3X,'ENERGY'/)
272 DO 106 KI=1,10
273 X(KI)=0.0
274 106 CONTINUE
275 NI=1
276 V1=V1*(1E+06)
277 WRITE(9,893) NI,V1,PDAT(IL,NI),T1,(X(I),I=1,9).
278 -DLF1,ENGY1
279 893 FORMAT(1H,'I3,1X,F6.1,3F7.1,F9.4,F7.2,2F8.3,F7.2,F7.2,F7.3,
280 -F7.2,F7.1,F9.5)
281 TU1=T1
282 V1=V1/(1E+06)

```

ASBRN at 17:46:21 on JUN 26, 1985 for CCId=CILL Page 6

```

283      T2=T1
284      PP2(IL,1)=PDAT(IL,1)
285      VV2(IL,1)=V1
286      TIM(IL,1)=TIME
287      MF(IL,1)=0.0
288      CB(IL,1)=0.0
289      TB(IL,1)=0.0
290      FS(IL,1)=0.0
291      RB(IL,1)=0.0
292      JJJ=1
293      NUT=0
294      DCA=PDCA
295      NDCA=(360./DCA)
296      ADCA=0.0
297      C
298      C  START COMPRESSION STROKE
299      C  =====
300      C
301      C  THIS SECTION CALCULATES ADIABATIC PRESSURE RISE AT EACH CRANK
302      C  ANGLE INTERVAL AND COMPARES THE RESULT WITH THE CORRESPONDING
303      C  MEASURED PRESSURE VALUE TO DETERMINE IF COMBUSTION HAS STARTED.
304      C
305      C  DO 40 NI=2,NDCA
306      C  -----
307      C  CALC. VOLUME DIVISION (DIV) FOR GIVEN C.A. DIVISION (DCA)
308      C  DIV=DVOL(DLF1)-DVOL(DLF1+DCA)
309      C  CALC. NEW VOLUME IN CYLINDER & RESET C.A. COUNTER TO NEW VALUE
310      C  V2=V1-DIV
311      C  DLF1=DLF1+DCA
312      C  DTIME=DCA/(6.0*SPEED)
313      C  DIST=(DVOL(DLF1))/(3.14159*((BORE/2.)**2))
314      C
315      C  CALC. NEW MIXTURE TEMPERATURE USING P.V = R.T
316      C  T2=(MWMIX*PDAT(IL,NI)*V2)/(MTOT*RMOL)
317      C  CALL COMP(T2,ENG2,NRCO2,NRH2O)
318      C
319      C  IF NEW C.A. < SPK. ADV., CONTINUE WITH COMP. STROKE CALCS.
320      C  IF(DLF1.GT.ANG) GOTO 610
321      C  IF NEW C.A. > SPK. ADV., CALCULATE ADIABATIC PRESSURE RISE
322      C  AND COMPARE RESULT WITH MEASURED VALUE..
323      C
324      C  IF(IPRINT.EQ.0) GOTO 393
325      C  CALL GAM(T2,T1,GAMU)
326      C  PISEN=((V1/V2)**GAMU)*PDAT(IL,(NI-1))
327      C  WRITE(9,257) PDAT(IL,NI),PISEN,T2,GAMU
328      C 257 FORMAT(1H , 'PDAT,PISEN,T2,GAMU ',4F10.3)
329      C
330      C-----)
331      C  IF(IDELP.EQ.2) GOTO 217 )
332      C  DELP1=(PDAT(IL,NI)-PISEN) )
333      C  IDELP=2 )
334      C  GOTO 51 )
335      C )
336      C217 DELP2=(PDAT(IL,NI)-PISEN) )
337      C  IF((DELP2-DELP1).GT.PTHRES) GOTO 610 )
338      C-----)
339      C
340      C  CALC. CURRENT TIME; AND PRESS. AT GIVEN VOL. & TEMP.

```

MASBRN at 17:46:21 on JUN 26, 1985 for CCId=CILL Page 7

```

341      393 TIME=(DLF1-180.)/(6.0*SPEED)
342      C RECORD PERMANENT VALUES OF PRESS., VOL., TIME, VOL. DIV, AND
343      C C.A. DIV, AT END OF EACH C.A. STEP...
344          PP2(IL,NI)=PDAT(IL,NI)
345          VV2(IL,NI)=V2
346          TIM(IL,NI)=TIME
347          DI(IL,(NI-1))=DABS(DIV)
348          DC(IL,(NI-1))=DCA
349          MF(IL,NI)=0.0
350          CB(IL,NI)=0.0
351          TB(IL,NI)=0.0
352          FS(IL,NI)=0.0
353          RB(IL,NI)=0.0
354      C DELP1=DELP2
355          KTDC=0
356          T1=T2
357          V1=V2
358      C ADJUST MAGNITUDE OF VOLUME FOR WRITE STATEMENT...
359          V2=V2*(1E+06)
360      C-----
361          WRITE(9,893) NI,V2,PDAT(IL,NI),T2,(X(I),I=1,9),
362          -DLF1,ENGY2
363      C-----
364          650 V2=V2/(1E+06)
365          40 CONTINUE
366          610 TU1=T1
367          VSU1=V1/MTOT
368      C CALCULATE ENERGY OF MIXTURE JUST BEFORE START OF COMBUSTION
369      C
370          CALL COMP(T1,ENGY1,NRCO2,NRH2O)
371          KZZ=2
372      C
373      C START OF PROGRESSIVE BURNING
374      C *****
375      C
376      C ITERATION CONTROLS AND INITIALISATION
377          NG=0
378          KOM=0
379          NED=1
380          JJJ=1
381          NDC=1
382          IDTM=1
383          IMX=1
384          MFX1=0.0
385          NNN=1
386          IVOL=1
387          KTDC=0
388          SUMXS=NMIX
389          TB2=1900.0
389.5      MWBMIX=MWMIX
390          THCOND=0.1
391          VISC=0.5E-04
392          VSB2=0.5
393          DQSUM=0.0
394          PDVSUM=0.0
395          ESPARK=ENGY1
396      C
397      C-----

```

MASBRN at 17:46:21 on JUN 26, 1985 for CCid=CILL Page 8

```

398      DO 333 LMN=1,50
399      C      =====
400      C
401      C 1500LC. TIME TAKEN FOR PISTON TO TRAVEL THROUGH 'DCA' DEGREES C.A.
402      C
403      C IF FIRST TIME THROUGH FROM COMPRESSION STROKE, SKIP VOLUME
404      C CALCULATIONS...
405      C
406      C      IF(KZZ.EQ.2) GOTO 727
407      C      NI=NI+1
408      C      508 DTIME=DCA/(6.0*SPEED)
409      C UPDATE TIME AND CRANK ANGLE COUNTER...
410      C      TIME=TIME+DTIME
411      C      DLF1=DLF1+DCA
412      C CALC. DISTANCE FROM PISTON TOP TO T.D.C....
413      C      DIST=DVOL(DLF1)/(3.14159*((BORE/2.)**2))
414      C CALC. CHANGE IN VOLUME DUE TO PISTON MOTION...
415      C      DIV=DVOL(DLF1-DCA)-DVOL(DLF1)
416      C CALC. NEW TOTAL VOLUME....
417      C      V2=V1-DIV
418      C      727 VTOT1=V2
419      C      WRITE(9,461) DTIME,TIME,DLF1,DIST,DIV,V2
420      C 461      FORMAT(1H,'DTIME,TIME,DLF1,DIST,DIV,V2=',6E11.4)
421      C UPDATE ITERATION COUNTER AND FIND NO. OF ITERATION AT T.D.C.
422      C      IF(KTDC.GT.0) GOTO 350
423      C      IF(DLF1.GE.360.0) KTDC=NI
424      C
425      C START BURNING...
426      C *****
427      C
428      C 350 IF(NG.EQ.0) AREAB=0.0
429      C
430      C      PDT1=PDAT(IL,(NI-1))
431      C      PDT2=PDAT(IL,NI)
432      C      CALL ENUFLS(PDT2,PDT1,TU1,VSU1,MWMIX,TU2,VSU2,
433      C      -EU2,TBVEL,AF,T2,NRCO2,NRH20)
434      C      HTCDEF=(THCOND/BORE)*((MPV*BORE/(VSB2*VISC))*HTEXP)/1000.0
435      C      DQ=HTCDEF*AREAB*(TB2-TWALL)*HTFCN*DTIME
435.5      C      IF (DCA .GT. 60.) WRITE(6,7777) AREAB,DQ,DCA
435.7      C 7777      FORMAT(' ',3F20.10)
436      C      NG=1
437      C      PDV=((PDAT(IL,NI)+PDAT(IL,(NI-1)))/2.)*DIV
438      C      ENGY2=ENGY1+PDV-DQ
439      C      PDVSUM=PDVSUM+PDV
440      C      DQSUM=DQSUM+DQ
441      C      TRT=(MWMIX*PDAT(IL,NI)*V2)/(MTOT*RMOL)
442      C-----
443      C      IF(IPRINT.EQ.0) GOTO 971
444      C      WRITE(9,737) ENGY2,ENGY1,PDV,DQ,HTCDEF,TRT
445      C 737      FORMAT(1H,'E2,E1,PDV,DQ,HTCDEF ',5E12.4,F8.1)
446      C-----
447      C 971      ETOT1=ENGY2/MTOT
448      C      CALL TEMP(PDT2,TB2,NNN,CC,MFX2,MTOT,EU2,VSU2,
449      C      -VTOT1,ETOT1,VSB2,MWMIX)
450      C
451      C      IF(MFX2.LT.0.5) GOTO 394
452      C      IF(MFX2.GT.0.98) GOTO 312
453      C      IF((MFX2-MFX1).GT.0.01) GOTO 394

```

MASBRN at 17:46:21 on JUN 26, 1985 for CCId=CILL Page 9

```

454      312 KZZ=2
455      GOTO 365
456      394 CALL CALFLS(MFX1,MFX2,VS2,MTOT,DTIME,VSU2,CBVEL,VSU1,
457      -AREAF1,VOLB2,IVOL,VOLB1,AREAF2,RB1,RB2,DLF1,DIST)
458      KOM=0
459      C
460      970 VOLU2=VTOT1-VOLB2
461      FLMSPD=(RB2-RB1)/(DTIME)
462      VFRBNT=(VOLB2/VTOT1)*100.0
463      FSR=CBVEL/TBVEL
464      V=VTOT1*(1E+06)
465      PRB2=RB2*100.0
466      PAREAF=AREAF2*10000.0
467      C-----
468      WRITE(9,893) NI,V,PDAT(IL,NI),TU2,TB2,MFX2,VFRBNT,CBVEL,
469      -TBVEL,FLMSPD,FSR,PRB2,PAREAF,DLF1,ENGY2
470      C-----
471      PP2(IL,NI)=PDAT(IL,NI)
472      TIM(IL,NI)=TIME
473      VV2(IL,NI)=V2
474      DI(IL,(NI-1))=DABS(DIV)
475      DC(IL,(NI-1))=DCA
476      MF(IL,NI)=MFX2
477      CB(IL,NI)=CBVEL
478      TB(IL,NI)=TBVEL
479      FS(IL,NI)=FLMSPD
480      RB(IL,NI)=PRB2
481      C
482      VOLB1=VOLB2
483      AREAF1=AREAF2
484      RB1=RB2
485      TU1=TU2
486      MFX1=MFX2
487      VSU1=VSU2
488      V1=V2
489      T1=T2
490      ENGY1=ENGY2
491      KZZ=1
492      IVOL=2
493      333 CONTINUE
494      C
495      365 T1=MFX2*TB2+(1-MFX2)*TU2
496      ECEND=ENGY2
497      C WRITE(9,266) MWBMIX,PDAT(IL,NI),V2,MTOT,RMOL
498      C 266 FORMAT(1H,5E12.4/)
499      TRT=(MWBMIX*PDAT(IL,NI)*V2)/(MTOT*RMOL)
500      CALL ENERGY(TRT,PDAT(IL,NI),EPROD,SUMXS,NNN,CC,X,EB2,VS2,
501      -GAMMA,MWBMIX)
502      TENG=EPROD*MOLFL
503      TDQ=(ESPARK-TENG)-PDVSUM
504      WRITE(9,265) ESPARK,ECEND,TENG,PDVSUM,DQSUM,TDQ,T1,TRT
505      265 FORMAT(1H,'ESPARK,ECEND,TENG,PDVS,DQS,T1,TRT',6F10.6,2F7.1/)
506      DO 249 KKI=1,10
507      249 X(KKI)=0.0
508      NUT=0
509      JUJ=1
510      NNN=1
511      IF(KZZ.EQ.2) GOTO 396

```

MASBRN at 17:46:21 on JUN 26, 1985 for CCid=CILL Page 10

```

512
513 C START EXPANSION STROKE
514 C *****
515 C
516 310 DIV=DVOL(DLF1+DCA)-DVOL(DLF1)
517 V2=V1+DIV
518 IF(V2.LT.497.0E-06) GOTO 851
519 DLF1=DLF1+DCA
520 IF(DLF1.GE.538) JJJ=2
521 TIME=(DLF1-180.0)/(6.0*SPEED)
522 NI=NI+1
523 GOTO 718
524 851 DLF1=DLF1+DCA
525 DIST=DVOL(DLF1)/((3.14159*((BORE/2.))**2))
526 DTIME=DCA/(6.0*SPEED)
527 TIME=(DLF1-180.0)/(6.0*SPEED)
528 NI=NI+1
529 NUT=NUT+1
530 IF(NUT.GT.80) STOP
531 396 ATOT=3.14159*(2.*BORE**2/4 +(HC+DIST)*BORE + CUPD*CUPH)
533 CALL EXP(PDAT(IL,(NI-1)),V1,T1,PDAT(IL,NI),V2,T2,NNN,CC,
534 -SUMXS,ENGY1,ENGY2,ATOT,DTIME,MTOT,MWBMIX)
535 718 ENGY1=ENGY2
536 T1=T2
537 V1=V2
538 PP2(IL,NI)=PDAT(IL,NI)
539 VV2(IL,NI)=V2
540 TIM(IL,NI)=TIME
541 DI(IL,(NI-1))=DABS(DIV)
542 DC(IL,(NI-1))=DCA
543 MF(IL,NI)=MFX2
544 CB(IL,NI)=O.O
545 TB(IL,NI)=O.O
546 FS(IL,NI)=O.O
547 RB(IL,NI)=O.O
548 V4=V2
549 T4=T1
550 V4=V4*(1E+06)
551 C 285 IF(JJJ.EQ.2) GOTO 277
552 C IF(NUT.GT.2) GOTO 817
553 C-----
554 277 WRITE(9,893) NI,V4,PDAT(IL,NI),X(1),T4,MFX2,VFRBNT,(X(I),I=1,6),
555 -DLF1,ENGY2
556 C-----
557 817 IF (JJJ.EQ.1) GOTO 310
558 C
559 WRITE(9,818) (CC(I),I=1,8)
560 818 FORMAT(1H ,'%CO2=',F7.3,' %CO=',F7.3,' %H2O=',F7.3,' %H2=',F7.3,
561 -' %O2=',F7.3,' %N2=',F7.3,' %ND=',F7.3,' %OH=',F7.3/)
562 C
563 C
564 C THIS SECTION CALCULATES INTEGRAL OF PDV (PDV),MEAN EFFECTIVE
565 C PRESSURE (MEP),POWER AND THERMAL EFFICIENCY.
566 C *****
567 C
568 304 PDV=O.O
569 SUMDI=O.O
570 AREA1=O.O

```

t . . . MASBRN at 17:46:21 on JUN 26, 1985 for CCId=CILL Page 11

```

571      AREA3=0.0
572      MTDC=KTDC-1
573      DO 300 J=1,MTDC
574      300 AREA1=AREA1+(PP2(IL,J)+PP2(IL,(J+1)))*DI(IL,J)/2.0
575      NTDC=KTDC+1
576      NID=NI-1
577      DO 302 J=NTDC,NID
578      302 AREA3=AREA3+(PP2(IL,J)+PP2(IL,(J+1)))*DI(IL,J)/2.0
579      DO 303 J=1,MTDC
580      303 SUMDI=SUMDI+DI(IL,J)
581      VA1=CYLV-SUMDI
582      VA2=DI(IL,KTDC)-VA1
583      PPTDC=PP2(IL,KTDC)+((VA1/DI(IL,KTDC))*(PP2(IL,NTDC)-
584      -PP2(IL,KTDC)))
585      AREA2=(PPTDC+PP2(IL,KTDC))*VA1/2.0
586      AREA4=(PPTDC+PP2(IL,NTDC))*VA2/2.0
587      IF(IPRINT.EQ.0) GOTO 269
588      WRITE(9,486) AREA1,AREA2,AREA3,AREA4,VA1,VA2,PPTDC,PDV
589      486 FORMAT(1H,'A1,A2,A3,A4,VA1,VA2,PTDC,PDV',8E12.4/)
590      269 PDV=(AREA3+AREA4)-(AREA1+AREA2)
591      MEP=PDV/(CYLV*100.0)
592      POWER=(PDV*SPEED/120.)
593      EFF=(PDV*100.)/(MOLFL*QVS*(12.*CN+HM))
594      C-----
595      WRITE(9,301) POWER,MEP,EFF
596      301 FORMAT(10X,6HPower=,F8.3,5X,9HI.M.E.P.=,F7.3,5X,11HEFFICIENCY=,
597      -F10.5///)
598      C-----
599      C WRITE VALUES OF PRESSURE, MASS FRACTION BURNT, CALC. BURNING
600      C VELOCITY, LAMINAR BURNING VELOCITY, AND FLAME SPEED FOR USE
601      C BY THE PLOTTING PROGRAM 'DP2'....
602      C
603      IJUMP1=0
604      IJUMP2=0
605      IJUMP3=0
606      IJUMP4=1
607      NUMM=1
608      ISPK=IDINT(SPKAD)
609      IF(IL.GT.1) GOTO 799
610      C WRITE(9,933) NUMBR,IJUMP1,IJUMP2,IJUMP3,IJUMP4
611      C933 FORMAT(5I3)
612      799 WRITE(9,934) NUMM,SPEED,ISPK,KFUEL
613      934 FORMAT(I4,F8.1,I4,I3)
614      DO 928 JK=1,180
615      WRITE(9,929) PP2(IL,JK),MF(IL,JK),CB(IL,JK),TB(IL,JK),FS(IL,JK)
616      -,RB(IL,JK)
617      929 FORMAT(6F10.4)
618      928 CONTINUE
619      C
620      C-----
621      C
622      222 CONTINUE
623      C
624      C*****
625      C
626      C
627      C THIS SECTION GENERATES A P-V DIAGRAM AND A
628      C PRESSURE-CRANK ANGLE DIAGRAM.

```

MASBRN at 17:46:21 on JUN 26, 1985 for CCid=CILL Page 12

```

629 C *****
630 C
631 IF(IGRAPH.EQ.O) GOTO 599
632 387 DO 605 IL=1,NUMBR
633 DLF=180.O
634 ZZ(IL,1)=2.O
635 DO 605 J=1,NID
636 VV(IL,J)=VV2(IL,J)*1000.
637 PP(IL,J)=PP2(IL,J)/100.
638 DLF=DLF+DC(IL,J)
639 DL(IL,(J+1))=DLF
640 C XX(IL,J)=(5.*VV(IL,J))+2.O
641 YY(IL,J)=(PP(IL,J)/20.)*2.O
642 ZZ(IL,(J+1))=((DL(IL,(J+1))-180.O)/60.O)+2.O
643 605 CONTINUE
644 C-----
645 C CALL AXIS(2.,2.,'VOLUME (L)',-10,5.,0.,0.,0.2)
646 C CALL AXIS(2.,2.,'PRESSURE (BAR)',14,5.,90.,0.,20.)
647 C DO 607 IL=1,NUMBR
648 C DO 607 I=1,NID
649 C 607 CALL SYMBOL(XX(IL,I),YY(IL,I),0.05,IL,0.,-1)
650 C CALL LINE(XX(1,I),YY(1,I),NID,1)
651 C-----
652 CALL PLOT(10.,0.,-3)
653 CALL AXIS(2.,2.,'CRANK ANGLE',-11,6.0,0.,180.,60.)
654 CALL AXIS(2.,2.,'PRESSURE (BAR)',14,5.,90.,0.,20.)
655 DO 415 IL=1,NUMBR
656 DO 415 I=1,NID
657 415 CALL SYMBOL(ZZ(IL,I),YY(IL,I),0.05,IL,0.,-2)
658 C CALL LINE(ZZ(1,I),YY(1,I),84,1)
659 CALL PLOTND
660 599 STOP
661 END
662 C
663
664 C
665 C SUBROUTINE TEMP CALCULATES TEMP. OF BURNT GAS AND MASS FRACTION
666 C ***** BURNED.
667 C
668 SUBROUTINE TEMP(P1,TB2,NNN,CC,MFX,MTOT,EU2,VSU2,VTOT1,ETOT,VSU2,
669 -MWB MIX)
670 C
671 COMMON /AREA1/ NCH,NO2,K,L,M,N,KFUEL
672 COMMON /AREA2/ MOLFL,NMIX,HF1,NNO2,NN2,NNFUEL,KOM
673 COMMON /AREA4/ NOISS,IPRINT
674 C
675 REAL*8 XF,DX,EPS,Y1,Y2,Y3,XX2,YY2,
676 -X1,X2,X3,X3OLD,P1,P2,P3,CC(10),X(10),K,L,M,N,GAMMA,MFX,MTOT
677 -,EU2,VSU2,VTOT1,VSU2,EB2,TB2,ETOT,VTOTC,NMIX,MFXE,MFXV
678 -,EPROD,SUMXS,NCH,NO2,MOLFL,HF1,NNO2,NN2,NNFUEL,GA,MWB MIX
679 C
680 NNN=1
681 KOM=KOM+1
682 IF(KOM.GT.10) GOTO 93
683 NUT=0
684 JDX=1
685 IDX=1
686 X1=1900.O

```

MASBRN at 17:46:21 on JUN 26, 1985 for CCid=CILL Page 13

```

687      XF=4000.0
688      DX=100.0
689      EPS=0.00010
690      5 CALL ENERGY(X1,P1,EPROD,SUMXS,NNN,CC,X,EB2,VSU2,GA,MWBMIX)
691      MFXE=(ETOT-EU2)/(EB2-EU2)
692      C WRITE(9,777) X1,ETOT,VTOT1,P1,EB2,MFXE
693      C 777 FORMAT(1H,'X1,ETOT,VTOT1,P1,EB2,MFXE',6E12.4)
694      IF(MFXE.GT.0.0) GOTO 10
695      X1=X1+DX
696      IF(X1.GT.XF) GOTO 91
697      JDX=2
698      GOTO 5
699      10 MFXV=(VTOT1/MTOT-VSU2)/(VSU2-VSU2)
700      Y1=MFXV-MFXE
701      IF(JDX.EQ.1) GOTO 30
702      IF(Y1.LT.0.0) GOTO 30
703      DX=-DX/2.
704      IDX=2
705      30 X2=X1+DX
706      IF(X2.GT.XF) GOTO 91
707      20 CALL ENERGY(X2,P1,EPROD,SUMXS,NNN,CC,X,EB2,VSU2,GA,MWBMIX)
708      MFXE=(ETOT-EU2)/(EB2-EU2)
709      C 747 FORMAT(1H,'X2,MFXE,MFXV,VSU2,EB2,EU2;',7E10.3)
710      IF(MFXE.GT.0.0) GOTO 15
711      DX=DX/2.
712      IDX=2
713      X2=X2-DX
714      NUT=NUT+1
715      IF(NUT.GT.30) GOTO 91
716      GOTO 20
717      15 IF(IDX.EQ.1) GOTO 16
718      DX=DX/2.
719      16 MFXV=(VTOT1/MTOT-VSU2)/(VSU2-VSU2)
720      Y2=MFXV-MFXE
721      C WRITE(9,747) X2,MFXE,MFXV,VSU2,EB2,EU2
722      IF(Y1*Y2.LE.0.0) GOTO 25
723      X1=X2
724      Y1=Y2
725      NUT=NUT+1
726      IF(NUT.GT.60) GOTO 91
727      GOTO 30
728      25 IF(Y2.EQ.0.0) GOTO 50
729      IF(X2.GT.X1) GOTO 35
730      XX2=X2
731      YY2=Y2
732      X2=X1
733      Y2=Y1
734      X1=XX2
735      Y1=YY2
736      35 IF(MFXE.LT.10.0) GOTO 36
737      DX=DX/10.0
738      X2=X2-DX
739      GOTO 20
740      36 X3OLD=X2
741      40 X3=(X1*Y2-X2*Y1)/(Y2-Y1)
742      NUT=NUT+1
743      IF(NUT.LT.150) GOTO 80
744      91 IS=2

```

MASBRN at 17:46:21 on JUN 26, 1985 for CCId=CILL Page 14

```

745      RETURN
746      93 WRITE(9,90) KOM
747      90 FORMAT(1H , 'PROGRAM STOP DUE TO TEMP ITERATIONS EXCEEDING',14)
748      STOP
749      80 IF(DABS((X3-X3OLD)/X3).LT.EPS) GOTO 60
750      X3OLD=X3
751      CALL ENERGY(X3,P1,EPROD,SUMXS,NNN,CC,X,EB2,VSB2,GA,MWBMIX)
752      MFXE=(ETOT-EU2)/(EB2-EU2)
753      MFXV=(VTOT1/MTOT-VSU2)/(VSB2-VSU2)
754      Y3=MFXV-MFXE
755      C WRITE(9,767) X3,MFXE,MFXV,Y3
756      C 767 FORMAT(1H , 'X3,MFXE,MFXV,Y3',4E12.4)
757      IF(Y1*Y3.LE.O.) GOTO 45
758      X1=X3
759      Y1=Y3
760      GOTO 40
761      45 X2=X3
762      Y2=Y3
763      GOTO 40
764      50 TB2=X2
765      GOTO 70
766      60 TB2=X3
767      70 MFX=(MFXE+MFXV)/2.0
768      IF(IPRINT.EQ.O) GOTO 225
769      C-----
770      WRITE(9,112) TB2,MFXE,MFXV,EB2,VSB2,GA
771      112 FORMAT(1H , 'TB2,MFXE,MFXV,EB2,VSB2,GA:',6E12.4)
772      C-----
773      225 IS=1
774      RETURN
775      END
776      C
777      C SUBROUTINE ENERGY TO CALCULATE ENERGY (EPROD) OF BURNT GAS
778      C ***** AT A GIVEN TEMP. AND PRESS. ( INCLUDES
779      C DISSOCIATION ).
780      C
781      SUBROUTINE ENERGY(T,P,EPROD,SUMXS,NNN,CC,X,EB2,VSB2,GAMMA,
782      -MWBMIX)
783      C
784      COMMON /AREA1/ NCH,NO2,K,L,M,N,KFUEL
785      COMMON /AREA2/ MOLFL,NMIX,HF1,NNO2,NN2,NNFUEL,KOM
786      COMMON /AREA3/ AREAB,HTEXP,MPV,HTFCN,TWALL,VISC,THCOND
787      COMMON /AREA4/ NDISS,IPRINT
788      C
789      REAL*8 K,L,M,N,X(10),CPG(10),UUU(10),DH(10),KA,KB,KC,KD,
790      -KE,KF,NM,P,T,A1,B1,C1,D1,E1,F1,S,SUMXS,TT,A,B,C,D,E,F,RMOL,
791      -A2,B2,C2,D2,E2,F2,RESA,RESA1,RESB,RESB1,RESC,RESC1,RESD,
792      -RESD1,RESE,RESE1,RESF,RESF1,KK,CC(10),EPROD,GAMMA,MWBMIX
793      -,MW(10),EB2,VSB2,NMIX,NCH,NO2,MOLFL,HF1,NNO2,NN2,NNFUEL
794      -,VCO2,KCO2,VH2O,KH2O,VN2,KN2,VISC,THCOND,AREAB,ATOT,MPV,
795      -HTFCN,TWALL,HTEXP
796      C
797      IF(T.LT.1750.0) GOTO 17
798      IF(NNN.EQ.2) GOTO 15
799      C INITIAL ESTIMATES OF THE NO. OF MOLES OF SPECIES DISSOCIATED
800      C A:- CO2=CO+O.5O2; B:- H2O=OH+O.5H2 C:- H2O=H2+O.5O2
801      C D:- NO2=.5N2+.5O2; E:- H2=2H F:- O2=2O
802      IF(NDISS.EQ.1) GOTO 747

```

MASBRN at 17:46:21 on JUN 26, 1985 for CCid=CILL Page 15

```

803      A=.7
804      B=0.1
805      C=.5
806      D=0.1
807      E=0.0
808      F=0.00
809      GOTO 737
810 747  A=.7
811      B=0.0
812      C=.5
813      D=0.0
814      E=0.0
815      F=0.0
816 737  A2=0
817      B2=0
818      C2=0
819      D2=0
820      E2=0
821      F2=0
822      NNN=2
823 C    CALC. OF EQUILIBRIUM CONSTANTS INCLUDING PRESSURE TERM
824 15  KA=DEXP(DLOG(T)**(-7.4721)*(-65549000)+10.53)
825      1*DSQRT(101.3/P)
826      KB=DEXP(DLOG(T)**(-7.0457)*(-30372100)+10.1590)
827      1*DSQRT(101.3/P)
828      KC=DEXP(DLOG(T)**(-6.8674)*(-18878550)+8.7095)
829      1*DSQRT(101.3/P)
830      KD=DEXP(DLOG(T)**(-7.3355)*(-16592550)+1.80127)
831      KE=DEXP(DLOG(T)**(-6.81208)*(-30743850)+17.8668)
832      1*(101.3/P)
833      KF=DEXP(DLOG(T)**(-6.93319)*(-43428280)+19.3067)
834      1*(101.3/P)
835      RMOL=8.3143
836      NUT=0
837 C    CALC. NO. OF MOLES OF SPECIES DISSOCIATED (A TO F)
838 10  QQ=1
839      NUT=NUT+1
840      IF (NUT.LT.200) GOTO 400
841      WRITE(9,401) NUT
842 401  FORMAT(1H,'PROGRAM STOP DUE TO ENERGY ITERATIONS
843      1EXCEEDING',I4)
844      STOP
845 400  IF (KA.LE.1E-10) GOTO 2
846 1    S=(A+B+C)/2+E+F+K+L+M+N
847      A1=A
848      IF ((M+((A+C-D)/2)-F).LE.0.0) GOTO 2
849      RESA=A/(K-A)*DSQRT((M+((A+C-D)/2)-F)/S)-KA
850      A=A+.001
851      IF ((M+((A+C-D)/2)-F).LT.0) A=2*(F-M)+D-C
852      RESA1=A/(K-A)*DSQRT((M+((A+C-D)/2)-F)/S)-KA
853      A=A+.001*RESA1/(RESA-RESA1)
854      IF (A.GT.K) A=K-.0011
855      IF (A.LT.0) A=1E-12
856      IF (A.EQ.A1) GOTO 2
857      IF (DABS((A-A1)/A1).GT.0.01) GOTO 1
858      IF (DABS((A-A2)/A1).GT.0.010) QQ=0
859 2    IF (NDISS.EQ.1) GOTO 3
860      S=(A+B+C)/2+E+F+K+L+M+N

```

MASBRN at 17:46:21 on JUN 26, 1985 for CCId=CILL Page 16

```

861      IF (KB.LE.1E-10) GOTO 3
862      B1=B
863      IF ((B/2+C-E).LE.O.O) GOTO 3
864      RESB=B/(L-B-C)*DSQRT((B/2+C-E)/S)-KB
865      B=B+.001
866      IF ((B/2+C-E).LT.O) B=2*(E-C)
867      RESB1=B/(L-B-C)*DSQRT((B/2+C-E)/S)-KB
868      B=B+.001*RESB1/(RESB-RESB1)
869      IF (B.GT.(L-C)) B=L-C-.0011
870      IF (B.LT.O) B=1E-12
871      IF (B.EQ.B1)GOTO 3
872      IF (DABS((B-B1)/B1).GT.O.O1) GOTO 2
873      IF (DABS((B-B2)/B1).GT.O.O10) QQ=O
874      3 S=(A+B+C)/2+E+F+K+L+M+N
875      IF (KC.LE.1E-10) GOTO 4
876      C1=C
877      IF ((M+((A+C-D)/2)-F).LE.O.O) GOTO 4
878      RESC=(B/2+C-E)/(L-B-C)*DSQRT((M-F+(A+C-D)/2)/S)-KC
879      C=C+.001
880      IF ((M+((A+C-D)/2)-F).LT.O) C=2*(F-M)+D-A
881      RESC1=(B/2+C-E)/(L-B-C)*DSQRT((M-F+(A+C-D)/2)/S)-KC
882      C=C+.001*RESC1/(RESC-RESC1)
883      IF (C.GT.(L-B)) C=L-B-.0011
884      IF (C.LT.O) C=1E-12
885      IF (C.EQ.C1) GOTO 39
886      IF (DABS((C-C1)/C1).GT.O.O1) GOTO 3
887      IF (DABS((C-C2)/C1).GT.O.O10) QQ=O
888      39 IF(NDISS.EQ.1) GOTO 67
889      IF (N.LT.O.O1) GOTO 5
890      4 S=(A+B+C)/2+E+F+K+L+M+N
891      IF (KD.LE.1E-10) GOTO 5
892      D1=D
893      IF (((N-D/2)*(M-F+(A+C-D)/2)).LE.O.O) GOTO 5
894      RESD=D/DSQRT((N-D/2.)*(M-F+(A+C-D)/2.))-KD
895      D=D+.001
896      IF (((N-D/2)*(M-F+(A+C-D)/2)).LE.O.O) GOTO 5
897      RESD1=D/DSQRT((N-D/2.)*(M-F+(A+C-D)/2.))-KD
898      D=D+.001*RESD1/(RESD-RESD1)
899      IF (D.GT.(2*N)) D=2*N-.0011
900      IF (D.LT.O) D=1E-12
901      IF (D.EQ.D1) GOTO 5
902      IF (DABS((D-D1)/D1).GT.O.O1) GOTO 4
903      IF (DABS((D-D2)/D1).GT.O.O10) QQ=O
904      GOTO 413
905      5 GO TO 67
906      E1=E
907      IF ((B/2+C-E).LE.O.O01) E=B/2+C-.002
908      RESE=((2*E)**2)/S/(B/2+C-E)-KE
909      E=E+.001
910      RESE1=((2*E)**2)/S/(B/2+C-E)-KE
911      E=E+.001*RESE1/(RESE-RESE1)
912      IF (E.GT.(C+B/2)) E=B/2+C
913      IF (E.LT.O) E=1E-12
914      IF (E.EQ.E1) GOTO 6
915      IF (DABS((E-E1)/E1).GT.O.O1) GOTO 5
916      IF (DABS((E-E2)/E1).GT.O.O10) QQ=O
917      6 S=(A+B+C)/2+E+F+K+L+M+N
918      IF (KF.LE.1E-10) GOTO 67
919

```

MASBRN at 17:46:21 on JUN 26, 1985 for CCId=CILL Page 17

```

920      F1=F
921      IF ((M-F+(A+C-D)/2).EQ.O) GOTO 67
922      RESF=((2*F)**2)/S/(M-F+(A+C-D)/2)-KF
923      F=F+.001
924      RESF1=((2*F)**2)/S/(M-F+(A+C-D)/2)-KF
925      F=F+.001*RESF1/(RESF-RESF1)
926      IF (F.GT.(M+(A+C-D)/2)) F=M+(A+C-D)/2-.011*F
927      IF (F.LT.O) F=1E-12
928      IF (F.EQ.F1) GOTO 67
929      IF (DABS((F-F1)/F1).GT.O.O1) GOTO 6
930      IF (DABS((F-F2)/F1).GT.O.O10) QQ=O
931      413 CONTINUE
932      67  A2=A
933          B2=B
934          C2=C
935          D2=D
936      IF(QQ.EQ.O)GOTO 10
937
938 C  CALCULATING CHANGE IN ENTHALPIES FOR SPECIES 1 TO 10 BET. T AND 289K
939 C  CO2=1, CO=2, H2O=3, H2=4, O2=5, N2=6, NO=7, H=10, O=9, OH=8
940      KK=O
941      17  TT=T/100
942          IF (T.GT.3000.O) GOTO 99
943          DH(1)=((3.096*T+O.00273*(T**2)-7.885E-07*(T**3)
944      1+8.66E-11*(T**4))-1145.O)*RMOL
945          DH(2)=((3.317*T+3.77E-04*(T**2)-3.22E-08*(T**3)
946      1-2.195E-12*(T**4))-1022.O)*RMOL
947          DH(3)=((3.743*T+5.656E-04*(T**2)+4.952E-08*(T**3)
948      1-1.818E-11*(T**4))-1167.O)*RMOL
949          DH(4)=((3.433*T-8.18E-06*(T**2)+9.67E-08*(T**3)
950      1-1.444E-11*(T**4))-1025.O)*RMOL
951          DH(5)=((3.253*T+6.524E-04*(T**2)-1.495E-07*(T**3)
952      1+1.539E-11*(T**4))-1024.O)*RMOL
953          DH(6)=((3.344*T+2.943E-04*(T**2)+1.953E-09*(T**3)
954      1-6.575E-12*(T**4))-1023.O)*RMOL
955          DH(7)=((3.502*T+2.994E-04*(T**2)-9.59E-09*(T**3)
956      1-4.904E-12*(T**4))-1070.O)*RMOL
957          DH(10)=((2.5*T)-745.O)*RMOL
958          DH(9)=((2.764*T-2.514E-04*(T**2)+1.002E-07*(T**3)
959      1-1.387E-11*(T**4))-804.O)*RMOL
960          DH(8)=((81.546*TT-47.48*(TT**1.25)+9.902*(TT**1.75)
961      1-2.133*(TT**2.))*100-10510)
962      GOTO 91
963
964      99  DH(1)=((5.208*T+O.00059*(T**2)-5.614E-08*(T**3)
965      1+2.05E-12*(T**4))-1126.O)*RMOL
966          DH(2)=((3.531*T+2.73E-04*(T**2)-3.28E-08*(T**3)
967      1+1.565E-12*(T**4))-1042.O)*RMOL
968          DH(3)=((143.05*TT-146.83*(TT**1.25)+55.17*(TT**1.5)
969      1-1.85*(TT**2.))*100-11945.O)
970          DH(4)=((3.213*T+2.87E-04*(T**2)-2.29E-08*(T**3)
971      1+7.666E-13*(T**4))-1018.O)*RMOL
972          DH(5)=((3.551*T+3.203E-04*(T**2)-2.876E-08*(T**3)
973      1+1.005E-12*(T**4))-1044.O)*RMOL
974          DH(6)=((3.514*T+2.583E-04*(T**2)-2.841E-08*(T**3)
975      1+1.242E-12*(T**4))-1043.O)*RMOL
976          DH(7)=((3.745*T+1.950E-04*(T**2)-1.88E-08*(T**3)
977      1+7.703E-13*(T**4))-1106.O)*RMOL
978          DH(10)=((2.5*T)-745.O)*RMOL
979          DH(9)=((2.594*T-3.843E-05*(T**2)+7.514E-09*(T**3)

```

ting of MASBRN at 17:46:21 on JUN 26, 1985 for CCId=CILL Page 18

```

980      1-3.209E-13*(T**4))-809.0)*RMDL
981      DH(8)=((81.546*TT-47.48*(TT**1.25)+9.902*(TT**1.75)
982      1-2.133*(TT**2.))*100-10560.)
983      C  CALCULATE CP VALUES
984      91  CPG(1)=-3.7357+30.529*(TT*(0.5))-4.1034*TT+0.024198*(TT**2)
985          CPG(2)=69.145-.70463*(TT*(0.75))-200.77*(TT*(-0.5))
986          -+176.76*(TT*(-0.75))
987          CPG(3)=143.05-183.54*(TT*(0.25))+82.751*(TT*(0.5))
988          --3.69889*TT
989          CPG(4)=56.505-702.74*(TT*(-.75))+1165.0/TT-560.7*(TT*(-1.5))
990          CPG(5)=37.432+0.020102*(TT**1.5)-178.57*(TT*(-1.5))
991          -+236.88*(TT*(-2))
992          CPG(6)=39.060-512.79*(TT*(-1.5))+1072.7*(TT*(-2))
993          --820.4*(TT*(-3))
994          CPG(7)=59.283-1.7096*(TT*0.5)-70.613*(TT*(-0.5))
995          -+74.889*(TT*(-1.5))
996          CPG(8)=81.546-59.35*(TT*0.25)+17.329*(TT*0.75)-4.266*TT
997      C  NUMBER OF MOLES OF EACH SPECIES AFTER DISSOCIATION
998          X(1)=K-A
999          X(2)=A
1000          X(3)=L-B-C
1001          X(6)=N-D/2
1002          X(7)=D
1003          X(4)=C+B/2-E
1004          X(5)=M-F+(A+C-D)/2
1005          X(10)=2*E
1006          X(9)=2*F
1007          X(8)=B
1008      C  CALC. VISCOSITY & THERMAL CONDUCTIVITY OF PRODUCTS...
1009          VC02=((0.019*T+24.2)*X(1)*1E-06)/(X(1)+X(3)+X(6))
1010          KC02=((0.041*T+36.1)*X(1)*1E-03)/(X(1)+X(3)+X(6))
1011          VH20=((0.025*T+15.8)*X(3)*1E-06)/(X(1)+X(3)+X(6))
1012          KH20=((0.130*T-0.60)*X(3)*1E-03)/(X(1)+X(3)+X(6))
1013          VN2=((0.019*T+24.1)*X(6)*1E-06)/(X(1)+X(3)+X(6))
1014          KN2=((0.039*T+35.8)*X(6)*1E-03)/(X(1)+X(3)+X(6))
1015          VISC=VC02+VH20+VN2
1016          THCOND=KC02+KH20+KN2
1017      C  HFD FOR EACH SPECIES
1018          UUU(1)=-3.93522E05
1019          UUU(2)=-1.10529E05
1020          UUU(3)=-2.41827E05
1021          UUU(4)=0.00000E00
1022          UUU(5)=0.00000E00
1023          UUU(6)=0.00000E00
1024          UUU(7)=9.05920E04
1025          UUU(10)=2.17986E05
1026          UUU(9)=2.49195E05
1027          UUU(8)=39463.0
1028      C  MOLECULAR WEIGHT FOR EACH SPECIES
1029          MW(1)=44.01
1030          MW(2)=28.01
1031          MW(3)=18.01
1032          MW(4)=2.02
1033          MW(5)=32.00
1034          MW(6)=28.01
1035          MW(7)=30.00
1036          MW(8)=17.00
1037          MW(9)=16.00

```

MASBRN at 17:46:21 on JUN 26, 1985 for CCId=CILL Page 19

```

1038      MW(10)=1.00
1039      C   CALC. ENERGY OF PRODUCTS 1 TO 10
1040      EPROD=0.
1041      DO 109 I=1,10
1042      ECOMP=X(I)*(UUU(I)+DH(I)-RMOL*T)
1043      EPROD=EPROD+ECOMP
1044      109 CONTINUE
1045      C   CALCULATE SUM OF X VALUES
1046      SUMXS=0
1047      DO 231 ILG=1,10
1048      231 SUMXS=SUMXS+X(ILG)
1049      C   CALC PERC. OF PRODUCTS AND MOLECULAR WEIGHT OF MIXTURE
1050      MWBMIX=0.0
1051      DO 232 ILH=1,10
1052      CC(ILH)=(X(ILH)/SUMXS)*100.
1053      232 MWBMIX=MWBMIX+(CC(ILH)*MW(ILH)/100.)
1054      EB2=EPROD/MWBMIX/SUMXS
1055      VSB2=RMOL*T/(MWBMIX*P)
1056      C   CALC CP
1057      CP=0
1058      DO 233 ILF=1,8
1059      233 CP=CP+(CC(ILF)*CPG(ILF))/100.
1060      CV=CP-RMOL
1061      GAMMA=CP/CV
1062      C   WRITE(9,889) MWBMIX,EB2,VSB2,GAMMA,NNN,NDISS
1063      C 889 FORMAT(1H,'MWBMIX,EB2,VSB2,GAMMA,N,NDS',4E12.4,2I3)
1064      RETURN
1065      END
1066      C
1067      C   SUBROUTINE CALFLS THIS IS USED TO OBTAIN THE CALCULATED
1068      C   ===== BURNING VELOCITY
1069      C
1070      SUBROUTINE CALFLS(MFX1,MFX2,VSB2,MTOT,DTIME,VSU2,CBVEL,
1071      -VSU1,AREA1,VOLB2,IVOL,VOLB1,AREA2,RB1,RB2,DLF1,DIST)
1072      C
1073      COMMON /AREA4/ NDISS,IPRINT
1074      COMMON /AREA3/ AREAB,HTEXP,MPV,HTFCN,TWALL,VISC,THCOND
1075      C
1076      INTEGER NREC,CA,NDIM
1077      REAL RCA1
1078      REAL*8 RF,DR,EPS,Y1,Y2,Y3,BORE,D,XDOT,ARAVG,AREA,
1079      -R1,R2,R3,R3OLD,DTIME,RMAX,R,VOLB1,MFX2,AREA1,AREA2,RB1,RB2,
1080      -FFF,MFX,VSB2,VSU2,MTOT,MFX1,VOLB2,VOLB,CBVEL,VSUAVG,VSU1,RADBMB
1081      -,DLF1,RFT(100),VFT(100),AFF(100),AWP(100),DIST,AREAB
1082      C
1083      IF (IVOL .GE. 2) GO TO 546
1084      RB1=0.DO
1085      AREA1=0.DO
1086      546 RCA1=SNGL(DLF1)
1087      CA=IFIX(RCA1)
1088      IF(CA.LE.360) CA=360-CA
1089      IF (CA .GT. 360)CA=CA-360
1090      CALL BLKRD(CA,RFT,VFT,AFF,AWP,NDIM)
1091      VOLB2=MTOT*MFX2*VSB2
1092      CALL GEOM(NDIM,DIST,VOLB2,RFT,VFT,AFF,AWP,RB2,AREA2,AREAB,CA)
1093      ARAVG=(AREA1+AREA2)/2.
1094      VSUAVG=(VSU1+VSU2)/2.
1095      XDOT=(MFX2-MFX1)/DTIME

```

MASBRN at 17:46:21 on JUN 26, 1985 for CCId=CILL Page 20

```

1096      CBVEL=MTOT*XDOT*VSUAVG/ARAVG
1097      RETURN
1098      END
1099      C
1100      C
1101      C SUBROUTINE ENUFLS THIS CALCULATES THE PROPERTIES OF THE UNBURNT
1102      C ***** GAS AT THE GIVEN PRESS. BY FIRST CALCULATING
1103      C GAMMA AND THEN ASSUMING ISENTROPIC COMPRESSION
1104      C THE BURNING VELOCITY IS THEN CALCULATED USING THE UNBURNT GAS
1105      C TEMP. AND PRESS. USING PUBLISHED FORMULAE FOR GIVEN FUEL.
1106      C
1107      SUBROUTINE ENUFLS(P2,P1,T1,VSU1,MWMIX,TU2,VSU2,EU2,TBVEL,AF,
1108      -T2,NRCO2,NRH2O)
1109      C
1110      COMMON /AREA1/ NCH,NO2,K,L,M,N,KFUEL
1111      COMMON /AREA2/ MOLFL,NMIX,HF1,NNO2,NN2,NNFUEL,KOM
1112      COMMON /AREA4/ NDISS,IPRINT
1113      C
1114      REAL*8 P1,T1,NNO2,NN2,NMIX,TU2,VSU2,EU2,TBVEL,TT,NNFUEL,FFF,
1115      -CPG(14),CP,CV,GAMU,DH(14),ENGY,NO2,N,RMOL,VSU1,POW1,POW2,TT2,
1116      -MWMIX,PU,TU,PBAR2,P2,HF1,T,T2,POW3,C4,AF,PBAR1,GGAM,B1,B2,B3,
1117      -NCH,K,L,M,MOLFL,FI,SUO(15),ALPHA(15),BETA(15),NRCO2,NRH2O,UUU(3)
1118      C
1119      RMOL=8.31434
1120      NUT=0
1121      C
1122      C CALC. GAMMA FOR THE UNBURNT ELEMENTS....
1123      C
1124      NNFUEL=100.-(NNO2+NN2)
1125      TT=T1/100.
1126      CPG(5)=37.432+0.020102*(TT**1.5)-178.57*(TT**(-1.5))
1127      -+236.88*(TT**(-2))
1128      CPG(6)=39.060-512.79*(TT**(-1.5))+1072.7*(TT**(-2))
1129      --820.4*(TT**(-3))
1130      CPG(11)=-672.87+439.74*(TT**0.25)-24.875*(TT**0.75)+323.88*
1131      -(TT**(-0.5))
1132      CPG(13)=-4.042+30.46*TT-1.571*(TT**2.)+0.03171*(TT**3.)
1133      CPG(12)=8.3143*(-0.72+0.09285*T1-5.05E-05*(T1**2.))+1.068E-08*
1134      -(T1**3))
1135      CP=(NNO2*CPG(5)+NN2*CPG(6)+NNFUEL*CPG(KFUEL))/100.
1136      CV=CP-RMOL
1137      GAMU=CP/CV
1138      C
1139      POW1=(GAMU-1.)/GAMU
1140      POW2=1./GAMU
1141      TT2=T1*((P2/P1)**POW1)
1142      20 CALL GAM(TT2,T1,GAMU)
1143      POW1=(GAMU-1.0)/GAMU
1144      T2=T1*((P2/P1)**POW1)
1145      IF(DABS(TT2-T2).LE.1.0) GOTO 10
1146      NUT=NUT+1
1147      IF(NUT.GT.20) STOP
1148      TT2=T2
1149      GOTO 20
1150      10 POW2=1.0/GAMU
1151      TU2=T2
1152      VSU2=VSU1*((P1/P2)**POW2)
1153      C

```

run of MASBRN at 17:46:21 on JUN 26, 1985 for CCId=CILL Page 21

```

1154 C CALC. ENTHALPY OF REACTANTS AT GIVEN TEMP.
1155 DH(1)=((3.096*T2+0.00273*(T2**2)-7.885E-07*(T2**3)
1156 1+8.66E-11*(T2**4))-1145.0)*RMOL
1157 DH(3)=((3.743*T2+5.656E-04*(T2**2)+4.952E-08*(T2**3)
1158 1-1.818E-11*(T2**4))-1167.0)*RMOL
1159 DH(5)=((3.253*T2+6.524E-04*(T2**2)-1.495E-07*(T2**3)
1160 1+1.539E-11*(T2**4))-1024.0)*RMOL
1161 DH(6)=((3.344*T2+2.943E-04*(T2**2)+1.953E-09*(T2**3)
1162 1-6.575E-12*(T2**4))-1023.0)*RMOL
1163 DH(11)=((1.935*T2+4.965E-03*(T2**2.)-1.244E-06*(T2**3.)
1164 1+1.625E-10*(T2**4.)-8.586E-15*(T2**5.))-985.9)*RMOL
1165 DH(12)=((-0.72*T2+4.643E-02*(T2**2.)-1.684E-05*(T2**3.)
1166 1+2.67E-09*(T2**4.))-3484.0)*RMOL
1167 DH(13)=((1.137*T2+1.455E-02*(T2**2.)-2.959E-06*(T2**3.)
1168 1)-1552.9)*RMOL
1169 UUU(1)=-3.93522E05
1170 UUU(3)=-2.41827E05
1171 C CALC. TOTAL ENERGY OF MIXTURE (KJ/KMOL FUEL)....
1172 ENGY=(NCH*(HF1+DH(KFUEL)-RMOL*T2)+NO2*(DH(5)-RMOL*T2)
1173 -+N*(DH(6)-RMOL*T2)+NRCO2*(UUU(1)+DH(1)-RMOL*T2)+NRH2O*
1174 -(UUU(3)+DH(3)-RMOL*T2))
1175 C CONVERT TO KJ/KMOL MIXTURE...
1176 ENGY=ENGY/NMIX
1177 C CONVERT TO KJ/KG MIXTURE...
1178 EU2=ENGY/MWMIX
1179 C CALC. AVERAGE UNBURNT TEMP. AND PRESS.
1180 PU=(P1+P2)/2.
1181 TU=(T1+T2)/2.
1182 C
1183 C CALCULATE LAMINAR BURNING VELOCITY:
1184 C
1185 C METGHALCHI & KECK'S EQN.S FOR PROPANE(13), OCTANE(12),
1186 C AND INDOLINE(14).....
1187 C
1188 IF(KFUEL.EQ.11) GOTO 501
1189 FI=1./AF
1190 IF(FI.GT.0.95) GOTO 87
1191 C DATA SUO(13),SUO(12),SUO(14)/23.20DO,19.25DO,19.15DO/
1192 C DATA ALPHA(13),ALPHA(12),ALPHA(14)/2.27DO,2.36DO,2.27DO/
1193 C DATA BETA(13),BETA(12),BETA(14)/-0.23DO,-0.22DO,-0.17DO/
1194 GOTO 89
1195 87 IF(FI.GT.1.05) GOTO 88
1196 DATA SUO(13),SUO(12),SUO(14)/31.90DO,27.00DO,25.21DO/
1197 DATA ALPHA(13),ALPHA(12),ALPHA(14)/2.13DO,2.26DO,2.19DO/
1198 DATA BETA(13),BETA(12),BETA(14)/-0.17DO,-0.18DO,-0.13DO/
1199 GOTO 89
1200 88 CONTINUE
1201 C DATA SUO(13),SUO(12),SUO(14)/33.80DO,27.63DO,28.14DO/
1202 C DATA ALPHA(13),ALPHA(12),ALPHA(14)/2.06DO,2.03DO,2.02DO/
1203 C DATA BETA(13),BETA(12),BETA(14)/-0.17DO,-0.11DO,-0.087DO/
1204 89 TBVEL=SUO(KFUEL)*((TU/298.)**ALPHA(KFUEL))*
1205 -((PU/100.)**BETA(KFUEL))
1206 GOTO 510
1207 C
1208 C ANDREWS AND BRADLEYS EQUATION FOR METHANE(11)...
1209 C
1210 C PBAR1=PU/100.
1211 C TBVEL=(10.0+0.000371*(TU**2.)*(PBAR1**(-0.5)))

```

MASBRN at 17:46:21 on JUN 26, 1985 for CCId=CILL Page 22

```

1212 C
1213 C RYAN AND LESTZ'S EQN. FOR METHANE(11)...
1214 C
1215 C 501 B1=9655.5
1216 C      B2=-0.623
1217 C      B3=-2144.5/TU
1218 C      TBVEL=B1*((PU/100.)**B2)*DEXP(B3)
1219 C      GOTO 510
1220 C
1221 C AGRAWAL AND GUPTAS EQUATION FOR METHANE...
1222 C
1223 C 501 PBAR1=PU/100.O
1224 C      C4=-418.O+1287.O/AF-1196.O/(AF**2)+360.O/(AF**3)-15.O*AF*
1225 C      -DLOG10(PBAR1)
1226 C      POW3=1.68*DSQRT(AF)
1227 C      IF(AF.GT.1.) GOTO 65
1228 C      POW3=1.68/DSQRT(AF)
1229 C      65 TBVEL=C4*((TU/300.O)**POW3)
1230 C
1231 C DIVIDE BY 100 TO CONVERT FROM CM/S TO M/S...
1232 C
1233 C 510 TBVEL=TBVEL/100.
1234 C
1235 C      IF(IPRINT.EQ.O) GOTO 225
1236 C-----
1237 C      WRITE(9,100) TBVEL,VSU2,EU2,PU,TU,P2,T2
1238 C      100 FORMAT(1H,'TBV,VSU2,EU2,PU,TU,P2,T2 =',7E12.4)
1239 C-----
1240 C      225 RETURN
1241 C      END
1242 C
1243 C
1244 C SUBROUTINE GAM THIS CALCULATES THE AVERAGE RATIO OF SPECIFIC
1245 C ***** HEATS (GAMMA) OF AN UNBURNED GAS MIXTURE
1246 C BETWEEN TWO GIVEN TEMPERATURES.
1247 C
1248 C SUBROUTINE GAM(T2,T1,GAMU)
1249 C
1250 C COMMON /AREA1/ NCH,NO2,K,L,M,N,KFUEL
1251 C COMMON /AREA2/ MOLFL,NMIX,HF1,NNO2,NN2,NNFUEL,KOM
1252 C
1253 C REAL*8 T2,T1,NNO2,NN2,NNFUEL,GAMU,TI,CPA(14),A1,A2,R1,R2,S1,S2,
1254 C -C1,C2,D1,D2,E1,E2,RMOL,CPAV,TT,NCH,NO2,K,L,M,N,MOLFL,NMIX,HF1
1255 C
1256 C CALC. VALUES OF CP FOR THE COMBUSTIBLE MIXTURE;
1257 C 5=O2, 6=N2, 11=CH4, 12=C8H18, 13=C3H8, 14=INDOLINE...
1258 C
1259 C RMOL=8.31434
1260 C TT=T2/100.
1261 C TI=T1/100.O
1262 C
1263 C A1=(37.432*TT+8.041E-03*(TT**2.5)+357.14/DSQRT(TT))-236.88/TT)
1264 C A2=(37.432*TI+8.041E-03*(TI**2.5)+357.14/DSQRT(TI))-236.88/TI)
1265 C CPA(5)=(NNO2/(T2-T1))*(A1-A2)
1266 C
1267 C R1=(39.06*TT+1025.58/DSQRT(TT))-1072.7/TT+410.2/(TT**2))
1268 C R2=(39.06*TI+1025.58/DSQRT(TI))-1072.7/TI+410.2/(TI**2))
1269 C CPA(6)=(NN2/(T2-T1))*(R1-R2)

```

MASBRN at 17:46:21 on JUN 26, 1985 for CCId=CILL Page 23

```

1270 C
1271 S1=-672.87*TT+351.8*(TT**1.25)-14.214*(TT**1.75)+647.76
1272 -*DSQRT(TT)
1273 S2=-672.87*TI+351.8*(TI**1.25)-14.214*(TI**1.75)+647.76
1274 -*DSQRT(TI)
1275 CPA(11)=(NNFUEL/(T2-T1))*(S1-S2)
1276 C
1277 C1=(-4.042*TT+15.23*(TT**2)-0.5237*(TT**3)+7.9275E-03*(TT**4))
1278 C2=(-4.042*TI+15.23*(TI**2)-0.5237*(TI**3)+7.9275E-03*(TI**4))
1279 CPA(13)=(NNFUEL/(T2-T1))*(C1-C2)
1280 C
1281 TT=TT*100.
1282 TI=TI*100.
1283 C
1284 D1=RMOL*(-0.72*TT+4.643E-02*(TT**2)-1.684E-05*(TT**3)+2.67E-09*
1285 -(TT**4))
1286 D2=RMOL*(-0.72*TI+4.643E-02*(TI**2)-1.684E-05*(TI**3)+2.67E-09*
1287 -(TI**4))
1288 CPA(12)=(NNFUEL*0.01/(T2-T1))*(D1-D2)
1289 C
1290 E1=RMOL*(-0.72*TT+4.643E-02*(TT**2)-1.684E-05*(TT**3)+2.67E-09*
1291 -(TT**4))
1292 E2=RMOL*(-0.72*TI+4.643E-02*(TI**2)-1.684E-05*(TI**3)+2.67E-09*
1293 -(TI**4))
1294 CPA(14)=(NNFUEL*0.01/(T2-T1))*(E1-E2)
1295 C
1296 C CALC. CP, GAMMA, AND HENCE PRESSURE(P) AT TEMP. T(J) ASSUMING
1297 C ISENTROPIC COMPRESSION.....
1298
1299 CPAV=CPA(5)+CPA(6)+CPA(KFUEL)
1300 GAMU=CPAV/(CPAV-RMOL)
1301 RETURN
1302 END
1303 C
1304 C
1305 C SUBROUTINE COMP THIS CALCULATES THE SPECIFIC ENERGY OF THE
1306 C ***** UNBURNED MIXTURE.
1307 C
1308 SUBROUTINE COMP(T2,ENG2,NRCO2,NRH20)
1309 C
1310 COMMON /AREA1/ NCH,NO2,K,L,M,N,KFUEL
1311 COMMON /AREA2/ MOLFL,NMIX,HF1,NNO2,NN2,NNFUEL,KOM
1312 C
1313 REAL*8 P1,V1,T1,P2,V2,T2,NCH,NO2,N,ENG1,ENG2,DH(14),RMOL,
1314 -REM,REM1,TT1,REM2,TT2,HF1,MOLFL,DLF1,K,L,M,NMIX,NNO2,NN2,NNFUEL
1315 -,UUU(10),T2OLD,NRCO2,NRH20
1316 C
1317 RMOL=8.31434
1318 C
1319 DH(1)=((3.096*T2+0.00273*(T2**2)-7.885E-07*(T2**3)
1320 +8.66E-11*(T2**4))-1145.0)*RMOL
1321 DH(3)=((3.743*T2+5.656E-04*(T2**2)+4.952E-08*(T2**3)
1322 +1.818E-11*(T2**4))-1167.0)*RMOL
1323 DH(5)=((3.253*T2+6.524E-04*(T2**2)-1.495E-07*(T2**3)
1324 +1.539E-11*(T2**4))-1024.0)*RMOL
1325 DH(6)=((3.344*T2+2.943E-04*(T2**2)+1.953E-09*(T2**3)
1326 +1.6575E-12*(T2**4))-1023.0)*RMOL
1327 DH(11)=((1.935*T2+4.965E-03*(T2**2.))-1.244E-06*(T2**3.))

```

MASBRN at 17:46:21 on JUN 26, 1985 for CCId=CILL Page 24

```

1328      1+1.625E-10*(T2**4.)-8.586E-15*(T2**5.))-985.9)*RMOL
1329      DH(12)=[(-0.72*T2+4.643E-02*(T2**2.))-1.684E-05*(T2**3.)
1330      1+2.67E-09*(T2**4.))-3484.0)*RMOL
1331      DH(13)=[(1.137*T2+1.455E-02*(T2**2.))-2.959E-06*(T2**3.)
1332      1)-1552.9)*RMOL
1333      UUU(1)=-3.93522E05
1334      UUU(3)=-2.41827E05
1335      C  CALC. TOTAL ENERGY OF MIXTURE (KJ)....
1336      ENGY2=MOLFL*(NCH*(HF1+DH(KFUEL)-RMOL*T2)+NO2*(DH(5)-RMOL*T2)
1337      +N*(DH(6)-RMOL*T2)+NRCO2*(UUU(1)+DH(1)-RMOL*T2)+NRH2O*
1338      -(UUU(3)+DH(3)-RMOL*T2))
1339      C
1340      RETURN
1341      END
1342      C
1343      C
1344      C  SUBROUTINE EXP  THIS CALCULATES THE TEMP. AND CONCENTRATION OF
1345      C  ***** THE PRODUCTS OF COMBUSTION DURING THE EXPANSION
1346      C  STROKE.
1347      C
1348      SUBROUTINE EXP(P1,V1,T1,P2,V2,T2,NNN,CC,SUMXS,ENGY1,ENGY2,
1349      -ATOT,DTIME,MTOT,MWBMIX)
1350      C
1351      COMMON /AREA1/ NCH,NO2,K,L,M,N,KFUEL
1352      COMMON /AREA2/ MOLFL,NMIX,HF1,NNO2,NN2,NNFUEL,KOM
1353      COMMON /AREA3/ AREAB,HTEXP,MPV,HTFCN,TWALL,VISC,THCOND
1354      COMMON /AREA4/ NDISS,IPRINT
1355      C
1356      REAL*8 P1,V1,T1,P2,V2,T2,SUMXS,K,L,N,M,NMIX,NM1,TT1,P,EPROD,
1357      -CC(10),X(10),ENGY1,ENGY2,MOLFL,REM1,REM2,TT2,TT3,TT3OLD,NNM1,
1358      -NNM3,REM3,NCH,NO2,HF1,NNO2,NN2,NNFUEL,NNM2,EB2,VSB2,BORE
1359      -,AREAB,ATOT,MPV,HTFCN,TWALL,PDV,DQ,HTCOEF,VISC,THCOND,HTEXP
1360      -,DQMEAS,DTIME,GAMMA,MWBMIX,MTOT
1361      C
1362      BORE=3.25*0.0254
1363      NUT=0
1364      NN=0
1365      C
1366      T2=(MWBMIX*P2*V2)/(MTOT*8.31434)
1367      C
1368      CALL ENERGY(T2,P2,EPROD,SUMXS,NNN,CC,X,EB2,VSB2,GAMMA,MWBMIX)
1369      C
1370      ENGY2=EPROD*MOLFL
1371      HTCOEF=(THCOND/BORE)*((MPV*BORE/(VSB2*VISC))*HTEXP)/1000.0
1372      DQ=HTCOEF*ATOT*(T2-TWALL)*HTFCN*DTIME
1373      PDV=((P1+P2)/2.0)*(V2-V1)
1374      DQMEAS=ENGY2-ENGY1+PDV
1375      C
1376      PISEN=((V1/V2)**GAMMA)*P1
1377      C
1378      IF(IPRINT.EQ.0) GOTO 4
1379      C-----
1380      WRITE(9,409) ENGY1,ENGY2,PDV,DQ,DQMEAS,PISEN
1381      409 FORMAT(1H,'ENGY1,ENGY2,PDV,DQ,DQMEAS',6E12.4)
1382      C-----
1383      4  CONTINUE
1384      C
1385      RETURN

```

MASBRN at 17:46:21 on JUN 26, 1985 for CCId=CILL Page 25

```

1386         END
1387     C
1388     C SUBROUTINE SMOOTH THIS READS IN THE ENSEMBLED PRESSURE VALUES
1389     C ***** AND SMOOTHS THEM USING MTS LIBRARY ROUTINES
1390     C
1391         SUBROUTINE SMOOTH(POUT,SCONST,IPRNTS)
1392     C
1393         IMPLICIT REAL*8(A-H,O-W)
1394     C
1395         DIMENSION PIN(180), DPDTH(180), TOL(180), ANGLE(180), PD1(180)
1396         DIMENSION PD2(180), W(2000), XIPIN(200), POUT(180), D2PDTH(180)
1397     C
1398     C
1399         SVAL=5.0
1400         CONST1=SCONST
1401         CONST2=SCONST
1402         IBEG=60
1403         IEND=120
1404     C
1405     C READ IN PRESSURE DATA...
1406     C
1407         READ(4,20)(PIN(K),K=1,180)
1408     20  FORMAT(F12.4)
1409     C
1410         DO 600 IJ=1,190
1411     C     WRITE(9,601) IPIN(IJ)
1412     C 601 FORMAT(1H ,I10)
1413     C 600 CONTINUE
1414     C
1415         DO 12 IJ=1,180
1416         ANGLE(IJ)=DFLOAT(IJ)
1417     12  CONTINUE
1418     C
1419     C CALCULATE dP/dTHETA AT EACH DATA POINT...
1420     C
1421     490 DO 5 J=2,179
1422     5  DPDTH(J)=(PIN(J+1)-PIN(J-1))/2.0D0
1423         DPDTH(1)=0.0
1424         DPDTH(180)=DPDTH(179)
1425     C
1426     C
1427     C CALCULATE d2P/d(THETA)**2 AT EACH DATA POINT...
1428     C
1429     491 DO 6 J=2,179
1430     6  D2PDTH(J)=(DPDTH(J+1)-DPDTH(J-1))/2.0D0
1431         D2PDTH(1)=0.0
1432         D2PDTH(180)=D2PDTH(179)
1433     C
1434     C
1435     C CALCULATE STANDARD DEVIATION OF THE SLOPE AT EACH CRANK ANGLE
1436     C BASED ON VARIATION OVER RANGE OF 3 DEGREES EITHER SIDE...
1437     C
1438     492 DO 15 IT=4,177
1439         JS=IT-3
1440         JF=IT+3
1441         AV=0.0
1442         DO 16 J=JS,JF
1443         16 AV=AV+D2PDTH(J)

```

MASBRN at 17:46:21 on JUN 26, 1985 for CCId=CILL Page 26

```

1444 C
1445     AV=AV/7.0
1446 C
1447     SA=0.0
1448     DO 17 J=JS,JF
1449     17 SA=SA+DABS(D2PDTH(J)-AV)**2
1450     SD=DSORT(SA/6)
1451     IF(IT.LT.IBEG.OR.IT.GT.IEND) GOTO 431
1452     TOL(IT)=SD*CONST2+0.0001
1453     GOTO 15
1454     431 TOL(IT)=SD*CONST1+0.0001
1455     15 CONTINUE
1456 C
1457     DO 18 IT=1,3
1458     18 TOL(IT)=TOL(4)
1459 C
1460     DO 19 IT=178,180
1461     19 TOL(IT)=TOL(177)
1462     CCCCCCCCCCCCCCCCCCCCCCCCCCCCCC
1463     C DO 88 IT=1,180
1464     C WRITE(9,87) TOL(IT)
1465     C 87 FORMAT(1H ,F12.5)
1466     C 88 CONTINUE
1467     CCCCCCCCCCCCCCCCCCCCCCCCCCCCCC
1468     C
1469     C CALL LIBRARY CURVE FITTING ROUTINES...
1470     C
1471     493 CALL DSPLFT(ANGLE,PIN,TOL,SVAL,180,W,&100)
1472     CALL DSPLN(ANGLE,POUT,PD1,PD2,180,&100)
1473     C
1474     GOTO 92
1475     100 WRITE(9,101)
1476     101 FORMAT(1H , 'ERROR IN CURVE FITTING ROUTINE')
1477     STOP1
1478     C
1479     92 IF(IPRNTS.EQ.0) GOTO 933
1480     DO 45 JK=1,180
1481     WRITE(9,602) PIN(JK),POUT(JK)
1482     602 FORMAT(1H ,2F12.5)
1483     45 CONTINUE
1484     C
1485     933 RETURN
1486     END
1487     SUBROUTINE BLKRD(CA,RF,VF,AFF,AWP,NDIM)
1488     REAL*8 RF(100),VF(100),AFF(100),AWP(100),D1,D2,D3
1489     INTEGER NREC,CA,NDIM
1490     NREC=4 + CA*82
1491     NDIM=79
1492     IF (CA .GE. 3) NDIM=80
1493     IF (CA .GE. 3) NREC=4+246+(CA-3)*83
1493.5 IF (CA .GE. 34) NDIM=81
1493.7 IF (CA .GE. 34) NREC=4+(CA-34)*84 + 246 +2573
1493.8 IF (CA .EQ. 45) NDIM=82
1493.9 IF (CA .EQ. 45) NREC=3663
1496     NREC=NREC*1000
1497     FIND(7,NREC)
1498     DO 2 J=1,NDIM
1499     READ(7,1) RF(J),VF(J),D1,AFF(J),D2,AWP(J),D3

```

MASBRN at 17:46:21 on JUN 26, 1985 for CCId=CILL Page 27

```

1500      1      FORMAT(2(F12.10,2X),F12.9,2X,2(F12.10,2X,F12.9,2X))
1501      2      CONTINUE
1502      RETURN
1503      END
1504      SUBROUTINE GEOM(NDIM,H,VOLB,RF,VF,AFF,AWP,RAD,AFRNT,APER,CA)
1505      REAL*8 RF(100),VF(100),AFF(100),AWP(100),RAD,AFRNT,APER,VOLB
1506      REAL*8 H,VINT,V1,V2,NONDIM
1507      INTEGER CA,NDIM
1508      J=0
1508.5     H=H+0.059
1509      V1=0.
1509.5     V2=0.
1510      J=2
1510.5     FIX=3.14*(.041**2*H+.021**2*.0339)
1511      1      IF (VOLB.LE. VF(J)*FIX) GO TO 2
1512      J=J+1
1513      GO TO 1
1514      2      V1=VF(J-1)*FIX
1514.5     V2=VF(J)*FIX
1515      VINT=(VOLB-V1)/(V2-V1)
1516      L=J-1
1519      RAD=(RF(L)+VINT*(RF(J)-RF(L)))*3.25/2*.0254
1520      AFRNT=(AFF(L)+VINT*(AFF(J)-AFF(L)))*2*3.141593*1.625**2
1521      AFRNT=AFRNT*(.0254**2)
1522      NONDIM=2*3.141593*(1.625*H+.083*1.337+1.625**2)
1523      APER=(AWP(L)+VINT*(AWP(J)-AWP(L)))*NONDIM*0.0254**2
1524      RETURN
1525      END
1526      SUBROUTINE INPUTS(JFLG,KFUEL,T1,SPEED,COMPR,AF,
1527      1 SPKAD,HTFCN,HTEXP,F,PRQ2,PRH2O,PRN2,NOISS,PDCA,
1528      1 TWALL,PINLET,AIRFLO,IGNDEL,SCONST,IPRNTS,PAMB,CUPD,CUPH,HC)
1529      IMPLICIT REAL*8(A-H,O-Z)
1530      INTEGER NCODE,JFLG,NAN,NREP
1530.5     REAL*8 IGNDEL
1531      IF (JFLG.NE. 0) GO TO 99
1532      1      WRITE(6,2)
1533      2      FORMAT(' ','TYPE OF FUEL: 11=CH4 , 12=C8H18 , 13=C3H8')
1534      CALL FREAD('GUSER','I:',KFUEL)
1535      IF (JFLG.NE. 0) GO TO 99
1536      3      WRITE(6,4)
1537      4      FORMAT(' ','TEMPERATURE AT START OF COMBUSTION= ?')
1538      CALL FREAD('GUSER','R:',T1)
1539      IF (JFLG.NE.0) GO TO 99
1540      5      WRITE(6,6)
1541      6      FORMAT(' ','ENGINE SPEED = ?')
1542      CALL FREAD('GUSER','R:',RPM)
1543      IF (JFLG.NE. 0) GO TO 99
1544      7      WRITE(6,8)
1545      8      FORMAT(' ','COMPRESSION RATIO = ?')
1546      CALL FREAD('GUSER','R:',COMPR)
1547      IF (JFLG.NE. 0) GO TO 99
1548      9      WRITE(6,10)
1549      10     FORMAT(' ','AIR TO FUEL RATIO = ?')
1550      CALL FREAD('GUSER','R:',AF)
1551      IF (JFLG.NE. 0) GO TO 99
1552      11     WRITE(6,12)
1553      12     FORMAT(' ','SPARK ADVANCE (DEG. BTDC) = ?')
1554      CALL FREAD('GUSER','R:',SPKAD)

```

MASBRN at 17:46:21 on JUN 26, 1985 for CCid=CILL Page 28

```

35      IF (JFLG .NE. 0) GO TO 99
36      13      WRITE(6,14)
37      14      FORMAT(' ', 'HEAT TRANSFER MULTIPLIER = ?')
38      CALL FREAD('GUSER', 'R:', HTFCN)
39      IF (JFLG .NE. 0) GO TO 99
40      15      WRITE(6,16)
41      16      FORMAT(' ', 'HEAT TRANSFER EXPONENT = ?')
42      CALL FREAD('GUSER', 'R:', HTEXP)
43      IF (JFLG .NE. 0) GO TO 99
44      57      WRITE(6,58)
45      58      FORMAT(' ', 'RESIDUAL GAS FRACTION = ?')
46      CALL FREAD('GUSER', 'R:', F)
47      IF (JFLG .NE. 0) GO TO 99
48      59      WRITE(6,60)
49      60      FORMAT(' ', 'RESIDUAL FRACTION CO2 (%) = ?')
50      CALL FREAD('GUSER', 'R:', PRCD2)
51      IF (JFLG .NE. 0) GO TO 99
52      17      WRITE(6,18)
53      18      FORMAT(' ', 'RESIDUAL FRACTION O2 (%) = ?')
54      CALL FREAD('GUSER', 'R:', PRO2)
55      IF (JFLG .NE. 0) GO TO 99
56      19      WRITE(6,20)
57      20      FORMAT(' ', 'RESIDUAL FRACTION H2O (%) = ?')
58      CALL FREAD('GUSER', 'R:', PRH2O)
59      IF (JFLG .NE. 0) GO TO 99
60      21      WRITE(6,22)
61      22      FORMAT(' ', 'REDISUAL FRACTION N2 (%) = ?')
62      CALL FREAD('GUSER', 'R:', PRN2)
63      IF (JFLG .NE. 0) GO TO 99
64      23      WRITE(6,24)
65      24      FORMAT(' ', 'FULL DISSOCIATION (O), OR PARTIAL ?')
66      CALL FREAD('GUSER', 'I:', NDISS)
67      IF (JFLG .NE. 0) GO TO 99
68      25      WRITE(6,26)
69      26      FORMAT(' ', 'CRANK ANGLE ITERATION INCREMENT = ?')
70      CALL FREAD('GUSER', 'R:', PDCA)
71      IF (JFLG .NE. 0) GO TO 99
72      27      WRITE(6,28)
73      28      FORMAT(' ', 'CYLINDER WALL TEMPERATURE = ?')
74      CALL FREAD('GUSER', 'R:', TWALL)
75      IF (JFLG .NE. 0) GO TO 99
76      29      WRITE(6,30)
77      30      FORMAT(' ', 'INLET PRESSURE (PASCALS) = ?')
78      CALL FREAD('GUSER', 'R:', PINLET)
79      IF (JFLG .NE. 0) GO TO 99
80      31      WRITE(6,32)
81      32      FORMAT(' ', 'AIR MASS FLOW RATE (G/S) = ?')
82      CALL FREAD('GUSER', 'R:', AIRFLO)
83      IF (JFLG .NE. 0) GO TO 99
84      33      WRITE(6,34)
85      34      FORMAT(' ', 'IGNITION DELAY TIME (CA DEG) = ?')
86      CALL FREAD('GUSER', 'I:', IGNDEL)
87      IF (JFLG .NE. 0) GO TO 99
88      35      WRITE(6,36)
89      36      FORMAT(' ', 'SMOOTHING ROUTINE CONST, SCONST = ?')
90      CALL FREAD('GUSER', 'R:', SCONST)
91      IF (JFLG .NE. 0) GO TO 99
92      37      WRITE(6,38)

```

MASBRN at 17:46:21 on JUN 26, 1985 for CCId=CILL Page 29

```

38      FORMAT(' ','DO YOU WANT INTERMEDIATE RESULTS  Y=1, N=0?')
      CALL FREAD('GUSER','I:',IPRNTS)
      IF (JFLG.NE.O) GO TO 99
39      WRITE(6,40)
40      FORMAT(' ','AMBIENT PRESSURE (KPA) ?')
      CALL FREAD('GUSER','R:',PAMB)
      IF (JFLG.NE.O) GO TO 99
41      WRITE(6,42)
42      FORMAT(' ','PISTON CUP DIAMETER (M) ?')
      CALL FREAD('GUSER','R:',CUPD)
      IF (JFLG.NE.O) GO TO 99
43      WRITE(6,44)
44      FORMAT(' ','PISTON CUP DEPTH (M)?')
      CALL FREAD('GUSER','R:',CUPH)
      IF (JFLG.NE.O) GO TO 99
45      WRITE(6,46)
46      FORMAT(' ','CLEARANCE HEIGHT (M) ?')
      CALL FREAD('GUSER','R:',HC)
99      WRITE(6,100)
100     FORMAT(' ','DO YOU WISH TO CHANGE ANY INPUTS (1=YES,0=NO) ?')
      CALL FREAD('GUSER','I:',JFLG)
      IF (JFLG.EQ.O) GO TO 104
101     WRITE(6,102)
102     FORMAT(' ','ENTER THE NUMBER CODE OF THE INPUT (1,2,3,...)')
      CALL FREAD('GUSER','I:',NCODE)
      GO TO (1,3,5,7,9,11,13,15,17,19,21,23,25,27,29,31,33,35,
5       137,39,41,43,45,57,59),NCODE
7       104     WRITE(6,103)
8       103     FORMAT(' ','DO YOU WANT TO SAVE THIS DATA (0=YES,1=NO) ?')
85      CALL FREAD('GUSER','I:',NREP)
9       IF (NREP.EQ.1) RETURN
92      CALL OUTPUT(JFLG,KFUEL,T1,RPM,COMPR,AF,
94      1 SPKAD,HTFCN,HTEXP,F,PRCO2,PRO2,PRH20,PRN2,NDISS,PDCA,
96      1 TWALL,PINLET,AIRFLO,IGNDEL,SCONST,IPRNTS,PAMB,CUPD,CUPH,HC)
      RETURN
      END
      SUBROUTINE OUTPUT(JFLG,KFUEL,T1,RPM,COMPR,AF,
1       1 SPKAD,HTFCN,HTEXP,F,PRCO2,PRO2,PRH20,PRN2,NDISS,PDCA,
1       1 TWALL,PINLET,AIRFLO,IGNDEL,SCONST,IPRNTS,PAMB,CUPD,CUPH,HC)
5       IMPLICIT REAL*8(A-H,O-Z)
7       REAL*8 IGNDEL
      WRITE(8,47) KFUEL,T1,RPM,COMPR,AF,SPKAD,HTFCN,HTEXP
47      FORMAT(I3,2F7.1,3F6.2,F6.3,F5.2)
      WRITE(8,46) F,PRO2,PRCO2,PRH20,PRN2,NDISS,PDCA,TWALL
46      FORMAT(5F7.3,I3,F6.2,F7.1)
      WRITE(8,2) PINLET,AIRFLO,IGNDEL,SCONST,IPRNTS,PAMB
      WRITE(8,22) CUPD,CUPH,HC
22      FORMAT(3F8.3)
2       FORMAT(F6.1,3F6.2,I3,F6.2)
      RETURN
      END

```

APPENDIX F - PROPERTIES OF B.C. NATURAL GASComposition (Volume %)

Methane	94.00
Ethane	3.30
Propane	1.00
Iso-butane	0.15
N-butane	0.20
Iso-pentane	0.02
N-pentane	0.02
Nitrogen	1.00
Carbon Dioxide	0.30
Hexane	0.01

Water Content: 3 to lbs/million cubic feet

This composition may be conveniently approximated by the following composition:

	% Volume	Volume Fraction		Molecular Weight		Mass kg/kmol
Methane CH ₄	94.00	0.940	*	16.040	=	15.078
Ethane C ₂ H ₆	3.30	0.033	*	30.070	=	0.992
Propane C ₃ H ₈	1.00	0.010	*	44.097	=	0.441
Butane C ₄ H ₁₀	0.40	0.004	*	58.124	=	0.232
Nitrogen	1.00	0.010	*	28.013	=	0.280
Carbon Dioxide	0.30	0.003	*	44.010	=	0.132
	<u>100.00</u>	<u>1.000</u>			M=	<u>17.156</u>

It therefore follows that the average molecular weight is 17.156 and the gas constant = $\frac{R}{M} = \frac{8.3143}{17.156} = 0.4846$.

Hence, density = $P/(Z \cdot R \cdot T) = 21.1^\circ\text{C}$ at 1 atm (101.3 kPa). Generally, density at 1 atm = $209/T(^{\circ}\text{K})$ kg/m.

Viscosity

The viscosity of the natural gas at 0°C may be obtained from the following:

$$\mu_{\text{mix}} = \frac{\sum y_i * \mu_i * (M_i)^{1/2}}{\sum y_i * (M_i)^{1/2}} \quad \text{where } y_i = \text{molecule fraction} \\ M_i = \text{molecule weight}$$

given:

$$\begin{aligned} \mu_{\text{CH}_4} &= 102.6 \text{ micropoise at } 0^\circ\text{C.} \\ \mu_{\text{C}_2\text{H}_6} &= 84.8 \text{ micropoise at } 0^\circ\text{C.} \\ \mu_{\text{C}_3\text{H}_8} &= 75.0 \text{ micropoise at } 0^\circ\text{C.} \\ \mu_{\text{CO}_2} &= 139.0 \text{ micropoise at } 0^\circ\text{C.} \\ \mu_{\text{N}_2} &= 166.0 \text{ micropoise at } 0^\circ\text{C.} \end{aligned}$$

Estimating μ as 75.0 for C₄H₁₀ as well as C₃H₈ and including the mole fraction of the former with the latter, the calculation becomes:

	Viscosity	y_i	m_i	$(m_i)^{1/2}$	$y_i * (m_i)^{1/2}$	$y_i \mu_i (m_i)^{1/2}$
CH ₄	102.6	0.940	16.040	4.005	3.765	386.29
C ₂ H ₆	84.8	0.033	30.070	5.484	0.181	15.35
C ₃ H ₈	75.0	0.014	48.105	6.936	0.097	7.28
CO ₂	139.0	0.003	44.010	6.634	0.020	2.78
N ₂	166.0	0.010	28.013	5.293	0.053	8.80
					<u>4.116</u>	<u>420.50</u>

with the result

$$\mu_{\text{mix}} = \frac{420.5}{4.116} = 102.16 \text{ uoise at } 0^\circ\text{C.}$$

The viscosity of natural gas at other temperatures can be obtained from,

$$\text{N.G.} \mu = 9.879 * T^{3/2} / (T + 163.17)$$

Therefore viscosity of N.G. at 70°F (21.1°C) = 108.96 uoise.

Higher and Lower Heating Values

	mass kg/kmol	mass (%)	HHV (kJ/kg)		
CH ₄	15.078	0.879	*	55496	= 48781
C ₂ H ₆	0.992	0.058	*	51875	= 3008
C ₃ H ₈	0.441	0.026	*	50343	= 1309
C ₄ H ₁₀	0.232	0.013	*	49500	= 644
CO ₂ +N ₂	0.412	0.024	*	0	= 0
	<u>17.156</u>	<u>1.000</u>			<u>53742</u>

Therefore the Higher Heating Value of B.C. Natural Gas is 53,742 kJ/kg at 25°C.

The Lower Heating Value is given by,

	mass (%)	LHV		
CH ₄	0.879	*	50010	= 43959
C ₂ H ₆	0.058	*	47484	= 2754
C ₃ H ₈	0.026	*	46353	= 1205
C ₄ H ₁₀	0.013	*	45714	= 640
CO ₂ +N ₂	0.024	*	0	= 0
	<u>1.000</u>			<u>48558</u>

Therefore the Lower Heating Value of B.C. Natural Gas is 48,558 kJ/kg at 25°C.

TABLE I

Engine Specifications

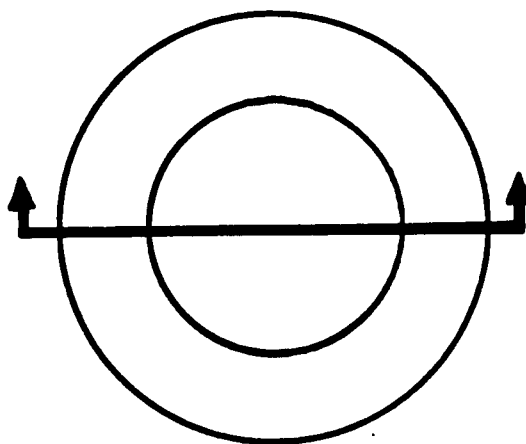
Engine	C.F.R.
Displacement	611.7 C.C.
Bore	82.55 mm
Stroke	114.30 mm
Compression Ratio	11.3
Con-rod Length	254.00 mm
Intake Valves	Diam. 35 mm Opening Angle 10 A.T.D.C. Closing Angle 34 A.B.D.C.
Exhaust Valve	Diam. Opening Angle 40 B.B.D.C. Closing Angle 15 A.T.D.C.
Spark Plug	Champion W18

TABLE II

Hot Wire Probe and Anemometer Specifications

Probe	TSI Model 1226
Wire Material	Platinum-Iridium
Wire Diameter	6.3 μm
Wire Length	1.25 mm
Wire Temperature Coefficient of Resistance	0.0009 / $^{\circ}\text{C}$
Anemometer	Disa Model 55M
Top Resistance	50 Ω
Cable Resistance	0.214 Ω

TOP



SECTION

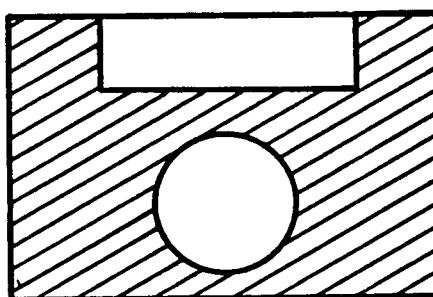
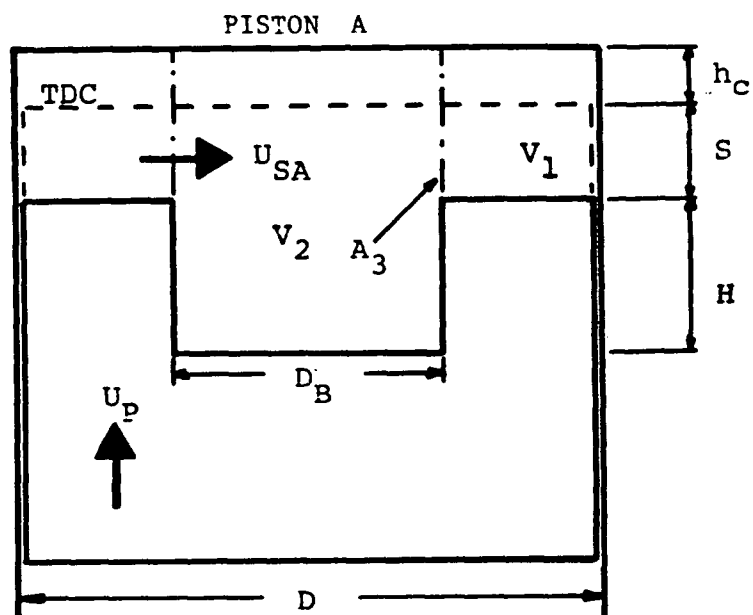
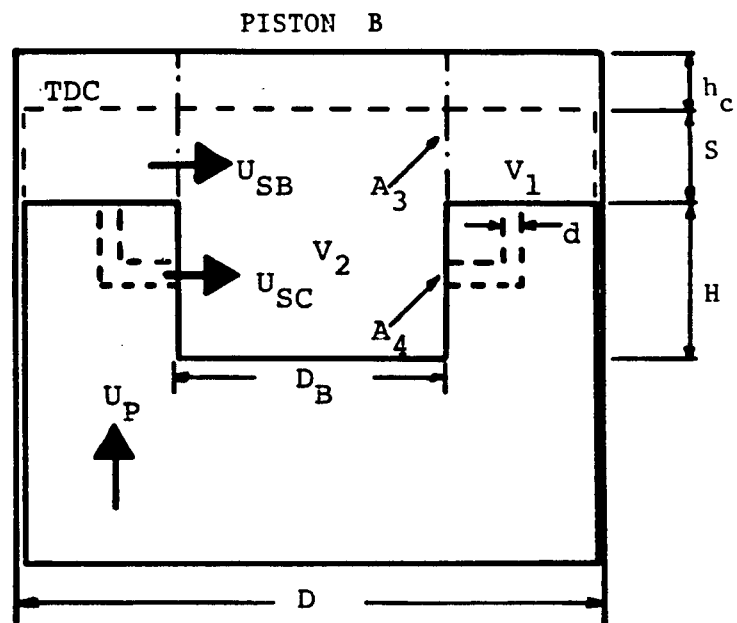


Fig. 1.1 The squish combustion chamber



$$\begin{aligned}
 A_1 &= \pi/4 (D^2 - D_B^2) \\
 A_2 &= \pi/4 D_B^2 \\
 A_3 &= \pi D_B (h_c + S) \\
 \%SQUISH &= A_1 / (A_1 + A_2) \\
 V_1 &= A_1 (h_c + S) \\
 V_2 &= A_2 (h_c + S + H)
 \end{aligned}$$

Fig. 3.1 The standard squish chamber



$$\begin{aligned}
 A_1 &= \pi/4 (D^2 - D_B^2) \\
 A_2 &= \pi/4 D_B^2 \\
 A_3 &= \pi D_B (h_c + S) \\
 A_4 &= \pi/4 d^2 \\
 \%SQUISH &= A_1 / (A_1 + A_2) \\
 V_1 &= A_1 (h_c + S) \\
 V_2 &= A_2 (h_c + S + H)
 \end{aligned}$$

Fig. 3.2 The squish-jet chamber

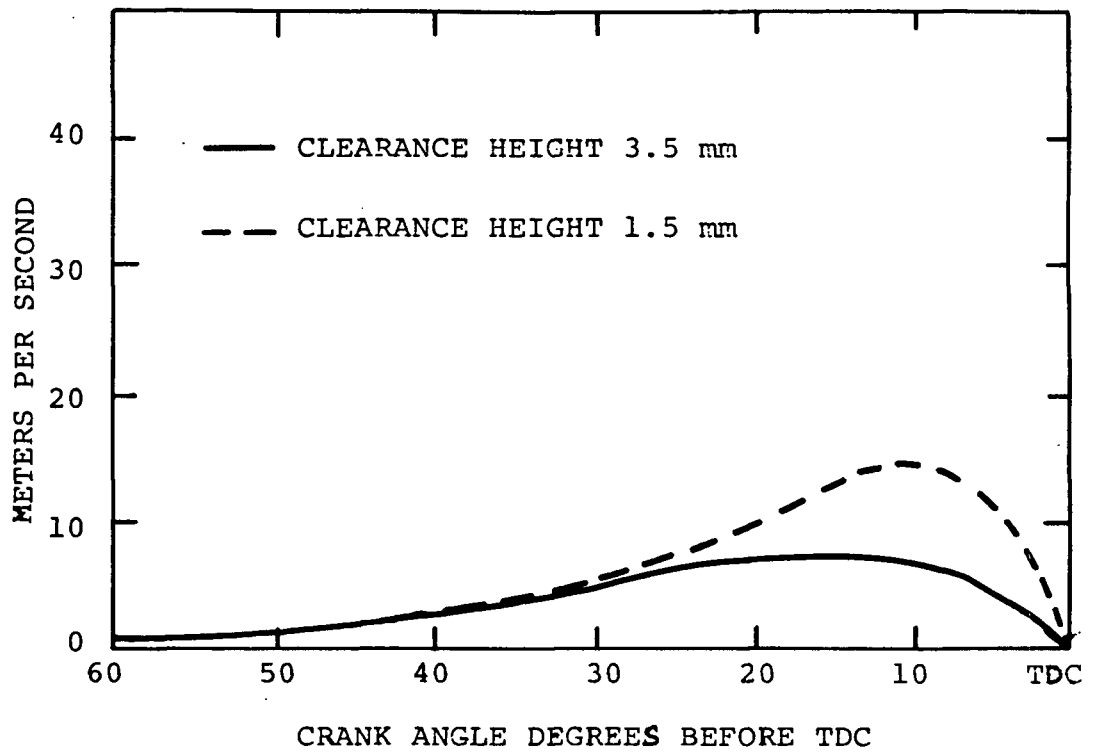


Fig. 3.3 The effect of clearance height on squish velocity

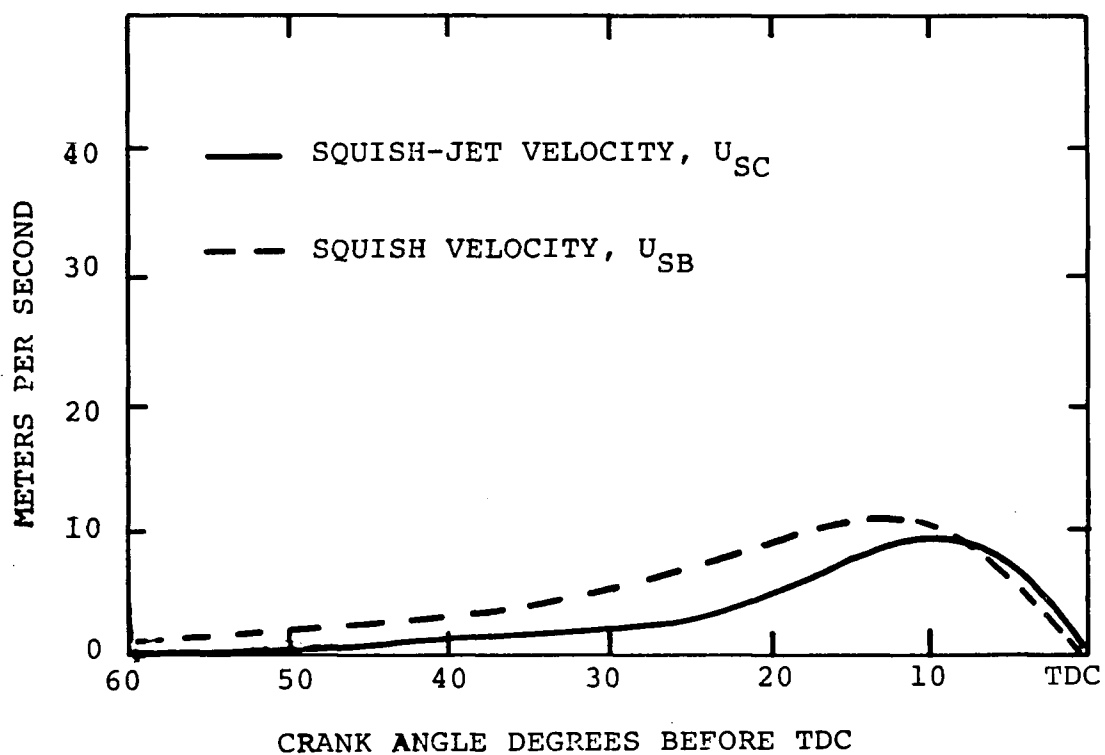


Fig. 3.4 The effect of the squish-jet design on squish velocity

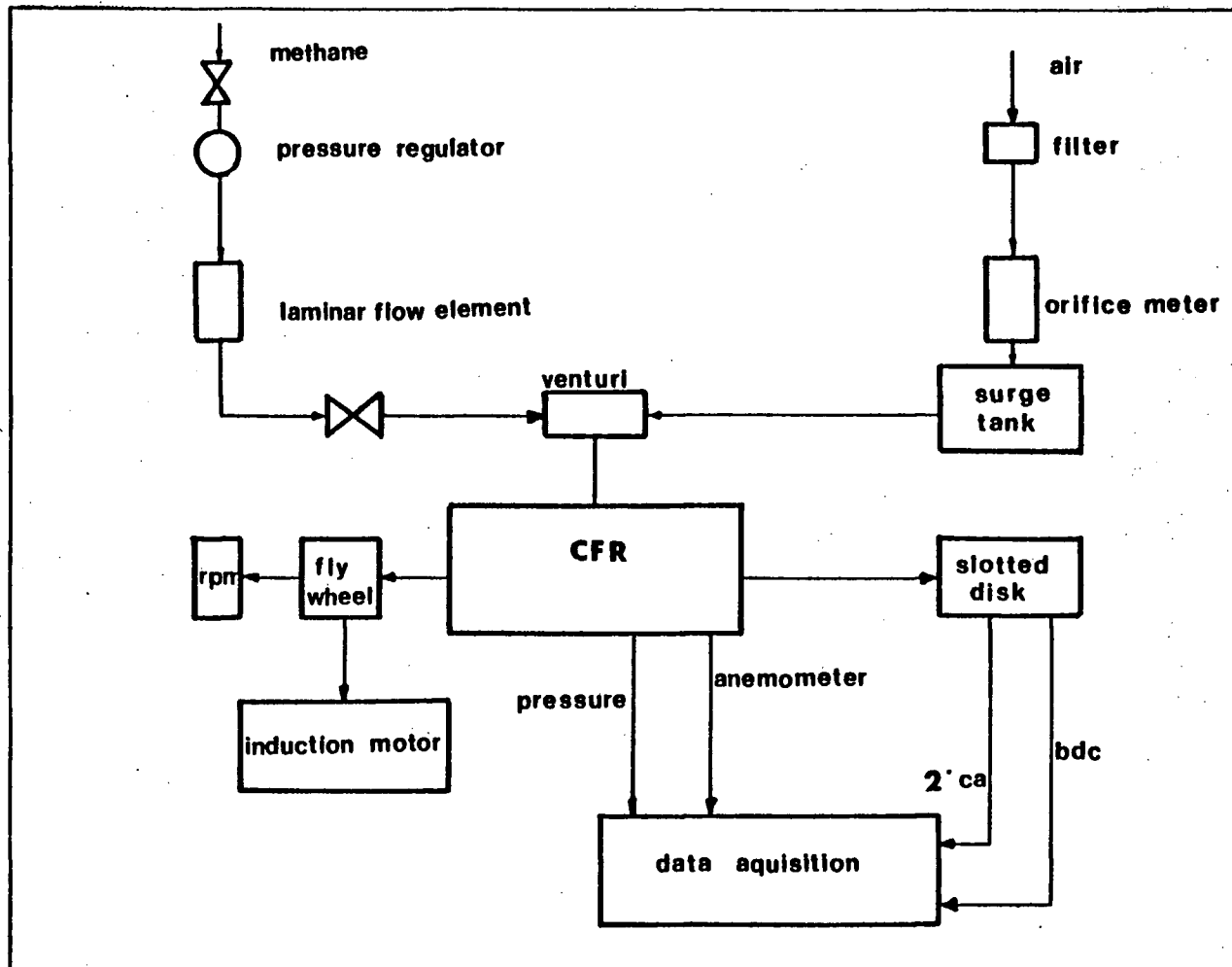


Fig. 4.1 Schematic of experimental setup and instrumentation

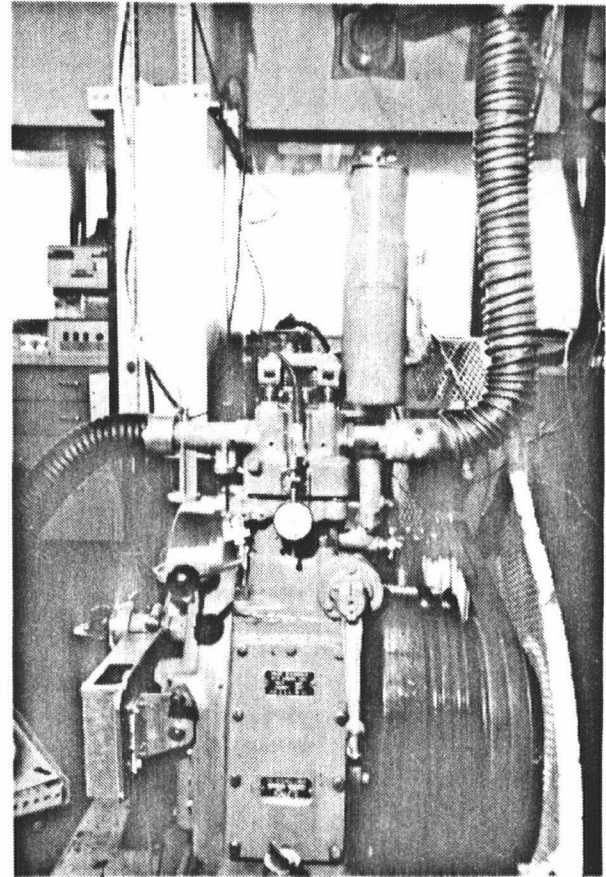
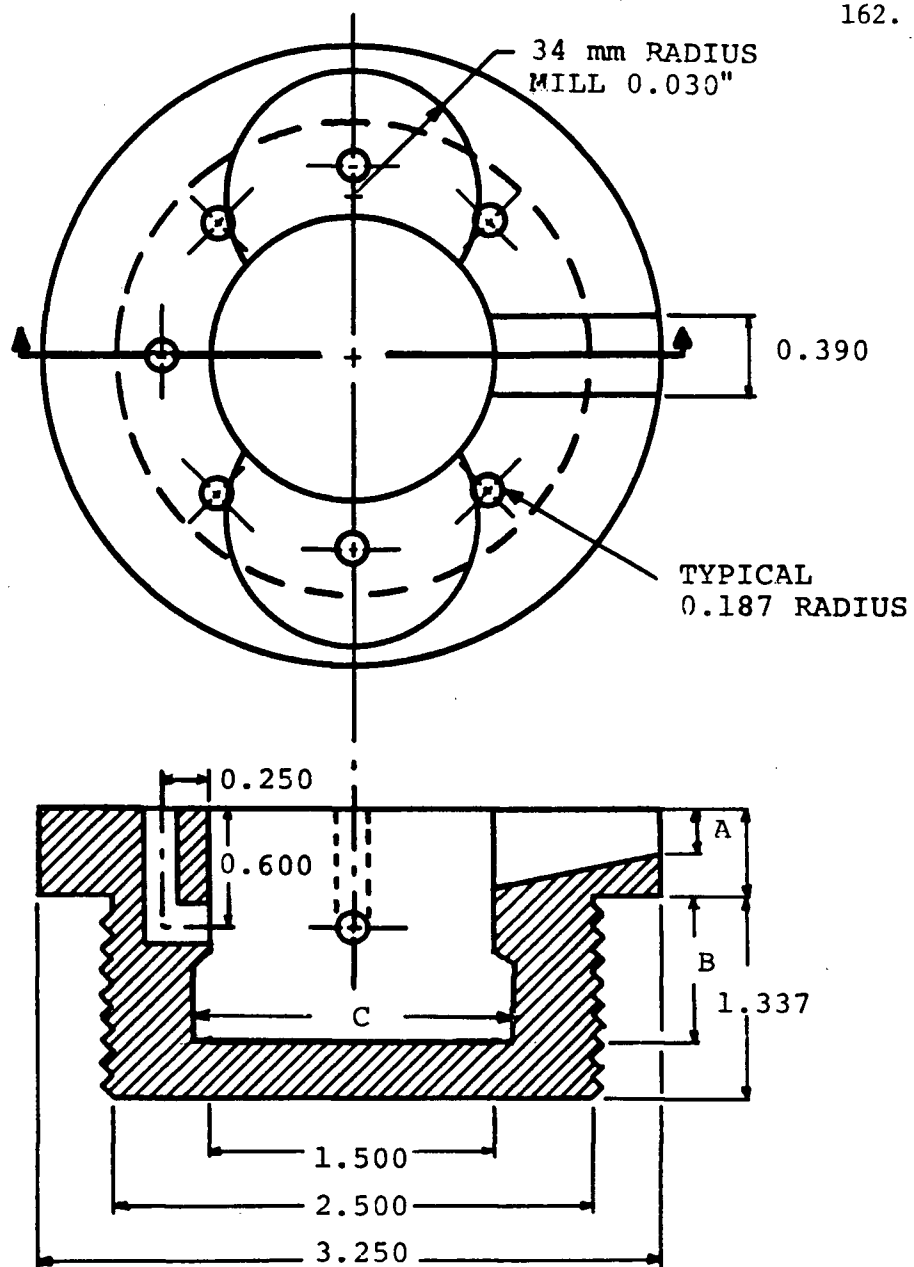


Fig. 4.2 The C.F.R. engine



Piston A, Case 1	A=0.354	B=0.947	C=1.819
Piston B, Case 1	A=0.354	B=0.947	C=1.739
Piston A, Case 2	A=0.354	B=0.931	C=1.500
Piston B, Case 2	A=0.354	B=0.889	C=1.500

Piston A - exclude the 7 holes
 Case 2 - do not mill recess for valves

Fig. 4.3 The squish piston inserts

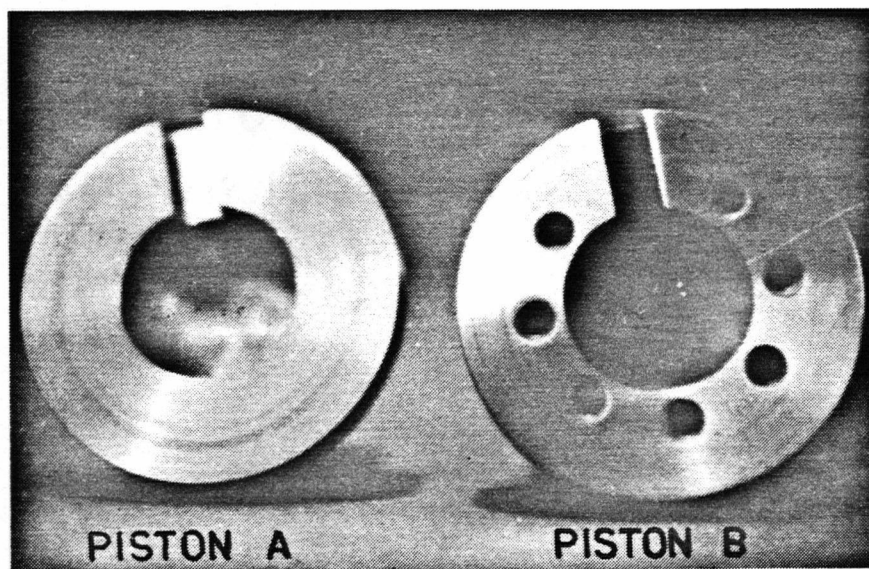


Fig. 4.4 Photograph of squish piston inserts

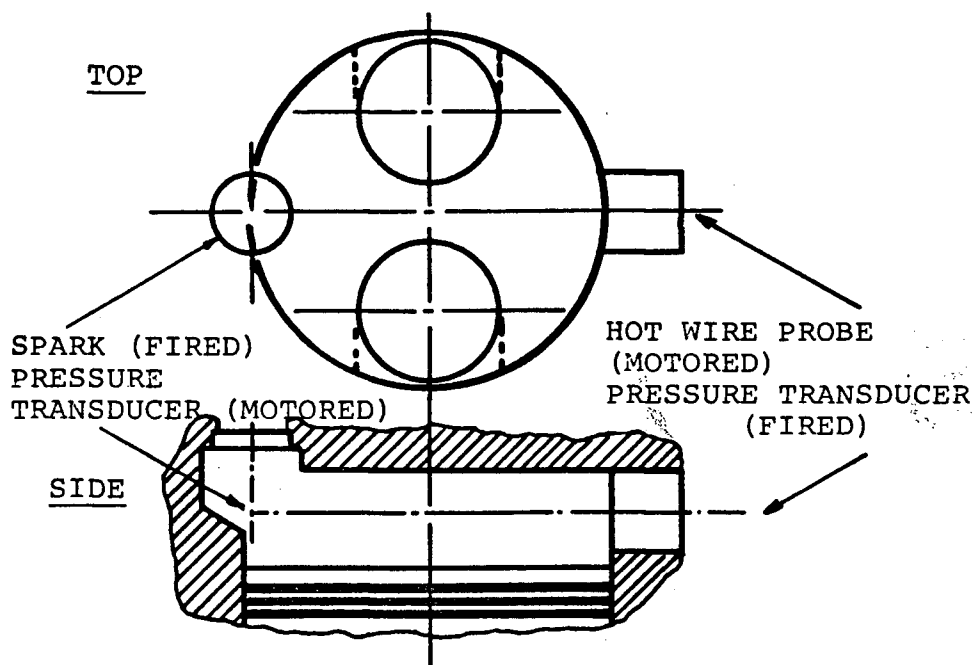


Fig. 4.5 Top and side view of C.F.R. combustion chamber

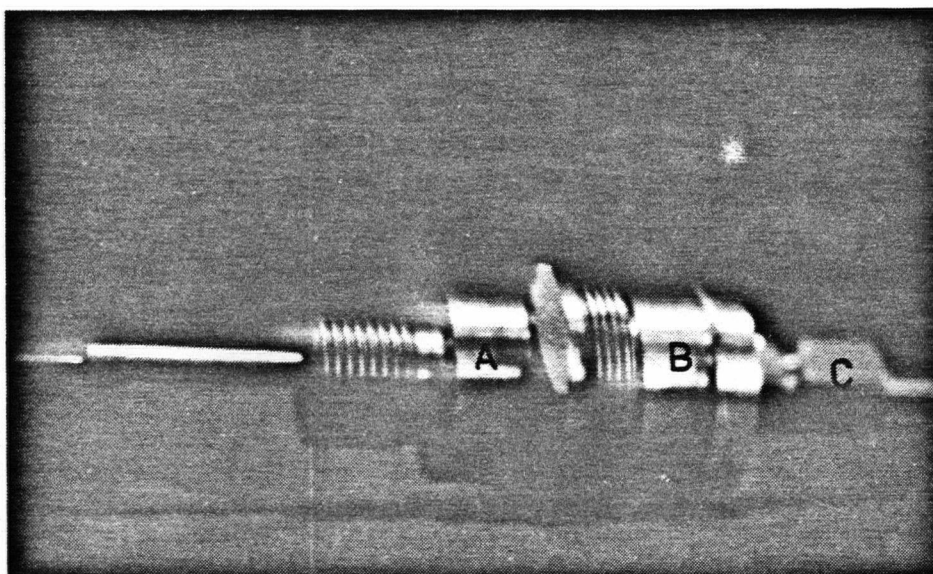


Fig. 4.6 Fitting for hot wire probe

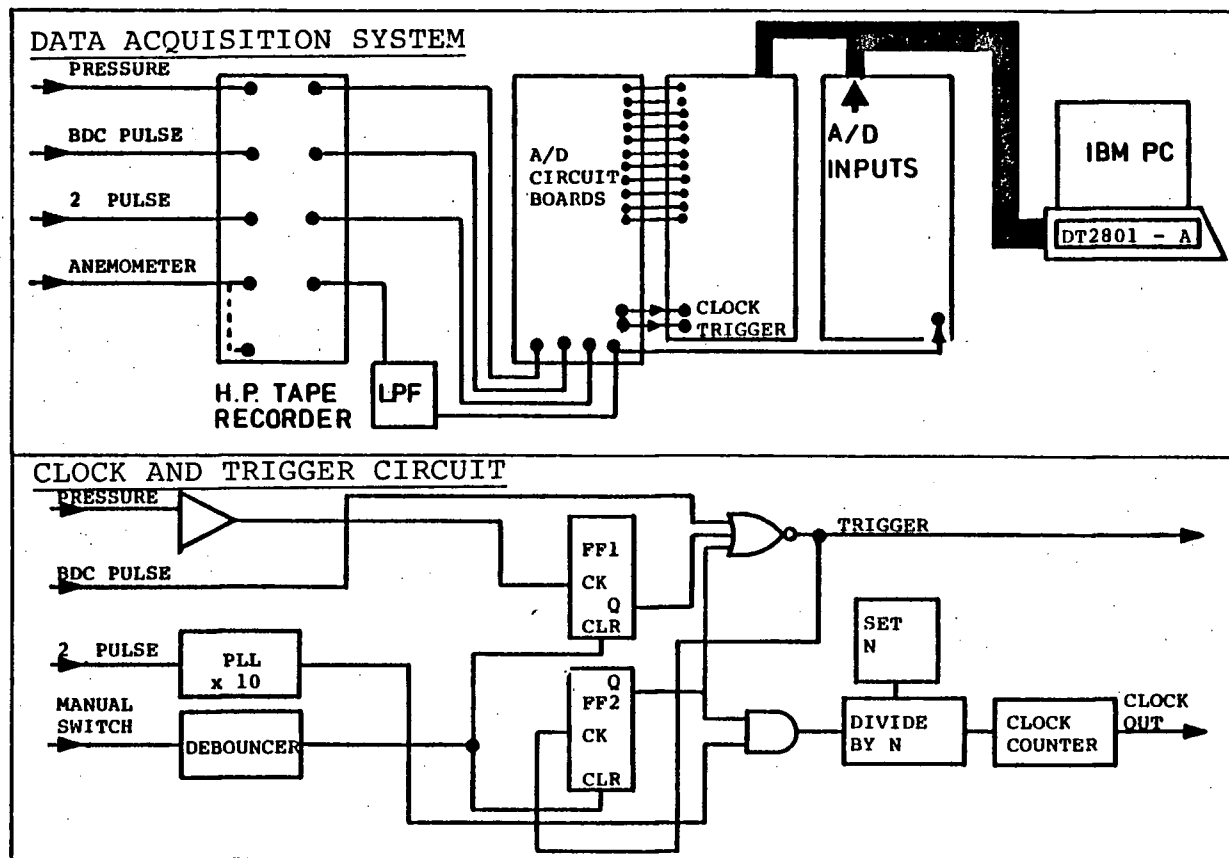
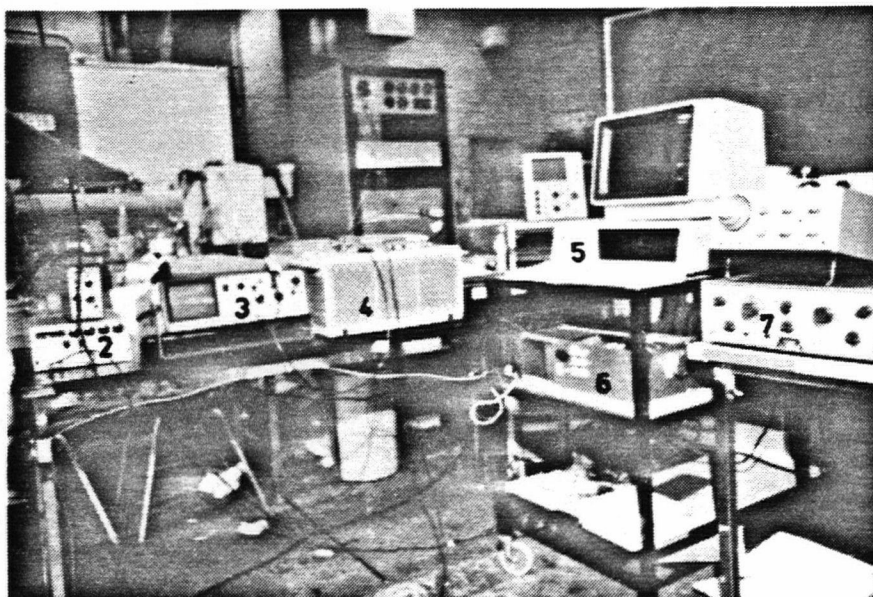
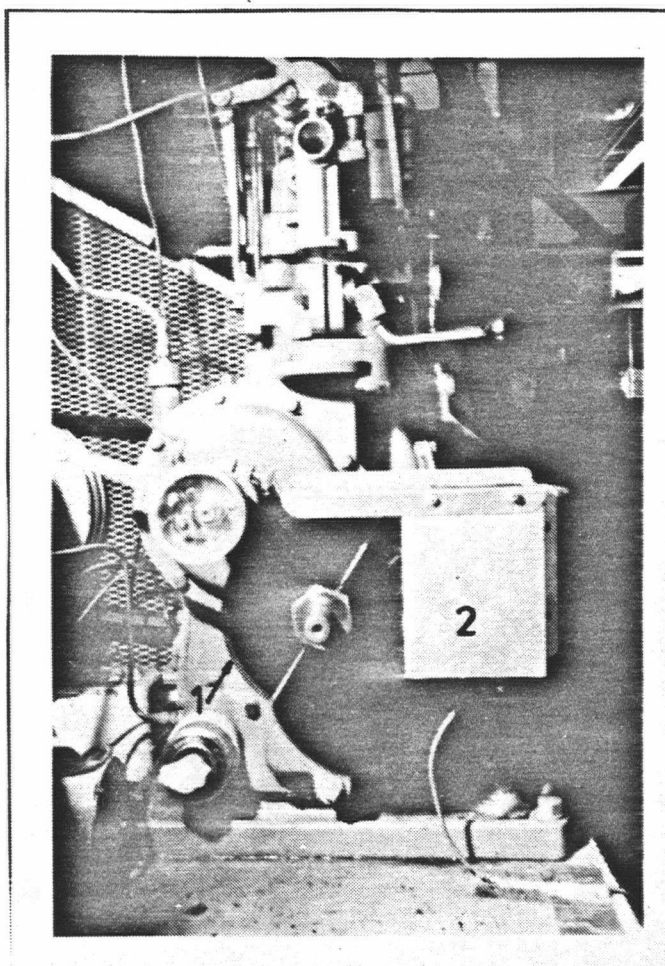


Fig. 4.7 Schematic of data acquisition



- 1 - Charge Amplifier for Pressure Signal
- 2 - Anemometer Bridge Unit
- 3 - Digital Oscilloscope
- 4 - Hewlett Packard Tape Recorder
- 5 - I.B.M. Microcomputer
- 6 - Data Acquisition Circuitry
- 7 - Bandpass Filter

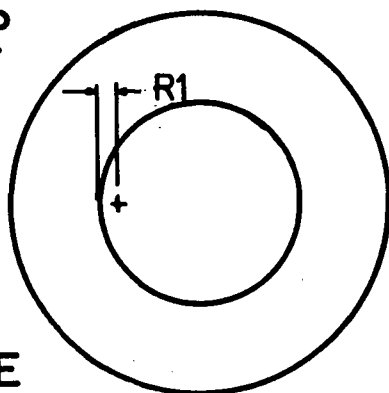
Fig. 4.8 Photograph of data acquisition system



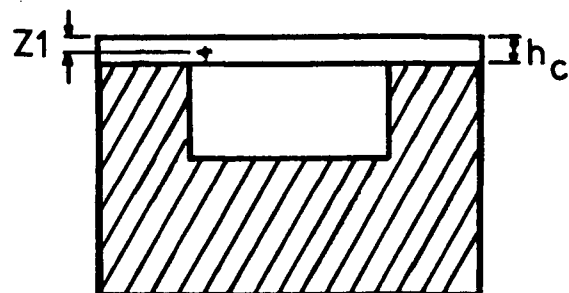
- 1 - Slotted Wheel
- 2 - Optical Pickup and Trigger Circuitry

Fig. 4.9 Photograph of optical trigger system

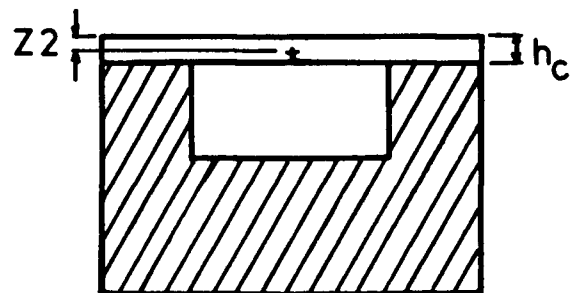
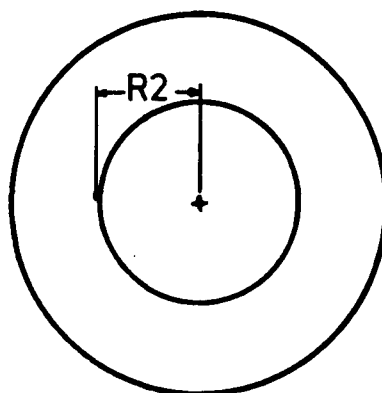
TOP



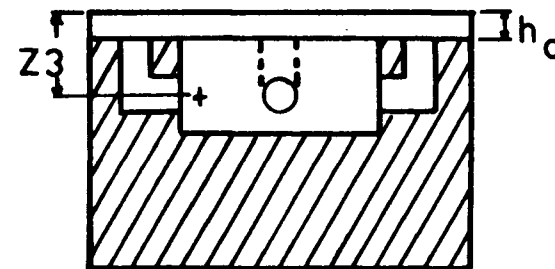
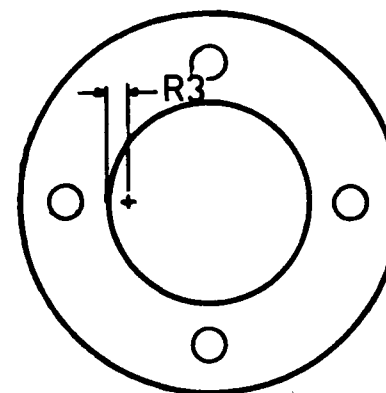
SIDE



Piston	h_c	Z_1	R_1
A,B	3.5	2.0	10.0
A,B	1.5	2.0	10.0
A	2.5	2.0	10.0
FLAT	10.7	2.0	10.0



Piston	h_c	Z_2	R_2
A,B	3.5	2.0	23.0
A,B	1.5	2.0	23.0
A	2.5	2.0	23.0
FLAT	10.7	2.0	23.0



Piston	h_c	Z_3	R_3
B	1.5	16.0	5.0

All dimensions in millimeters

Fig. 5.1 Hot wire probe locations

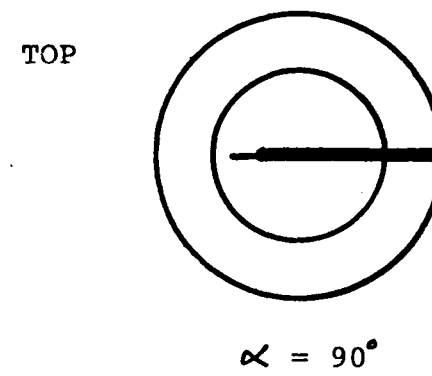
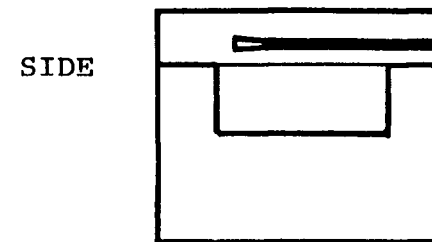
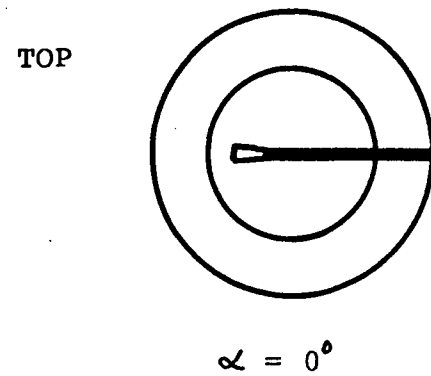
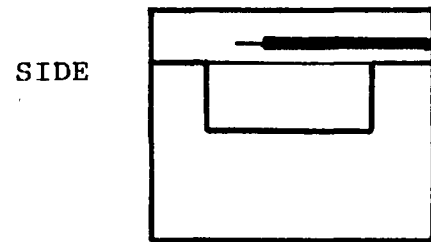


Fig. 5.2 Hot wire probe orientation

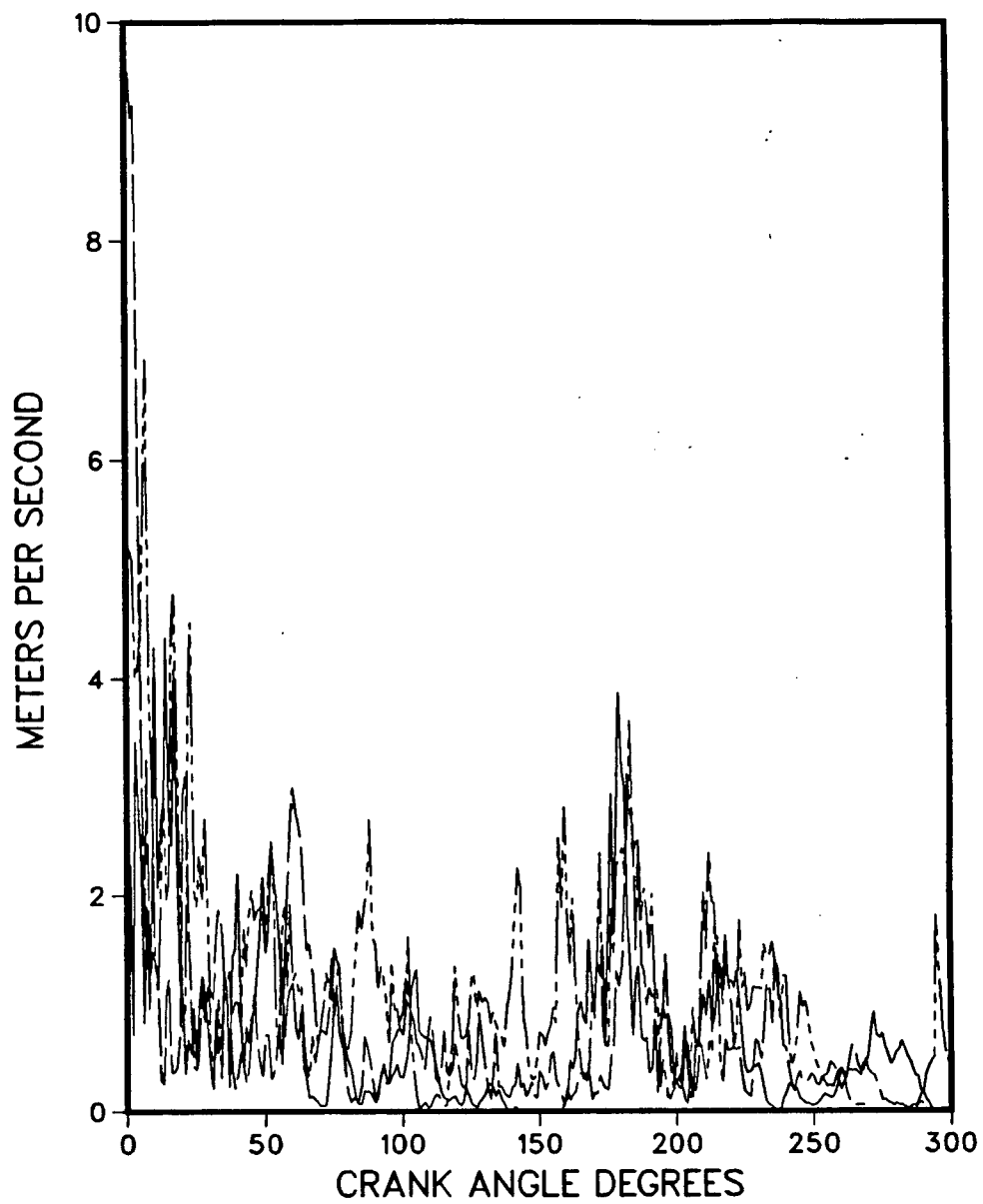


Fig. 7.1 Three consecutive instantaneous velocity records

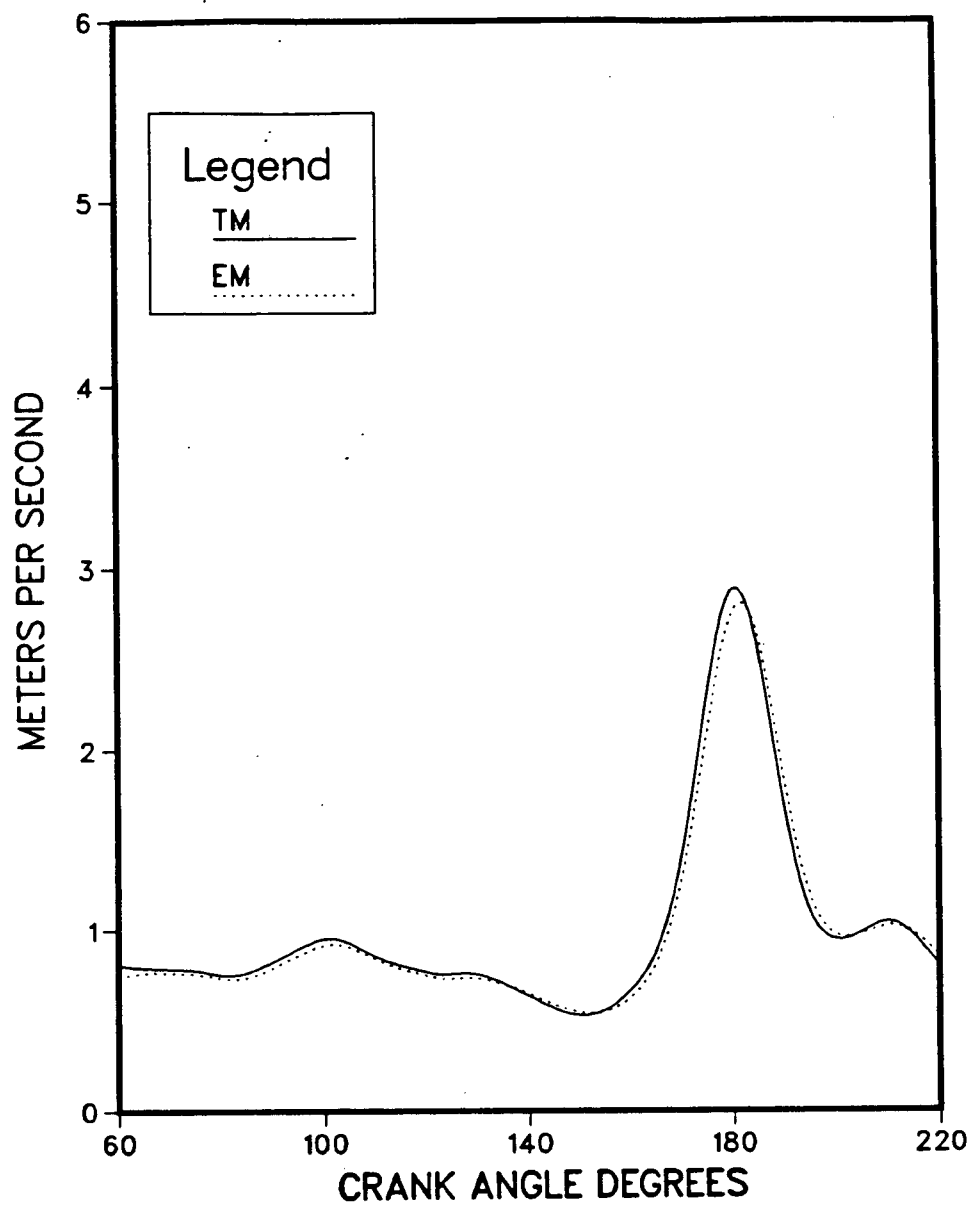


Fig. 7.2 Comparison of time averaged and ensemble averaged mean velocity

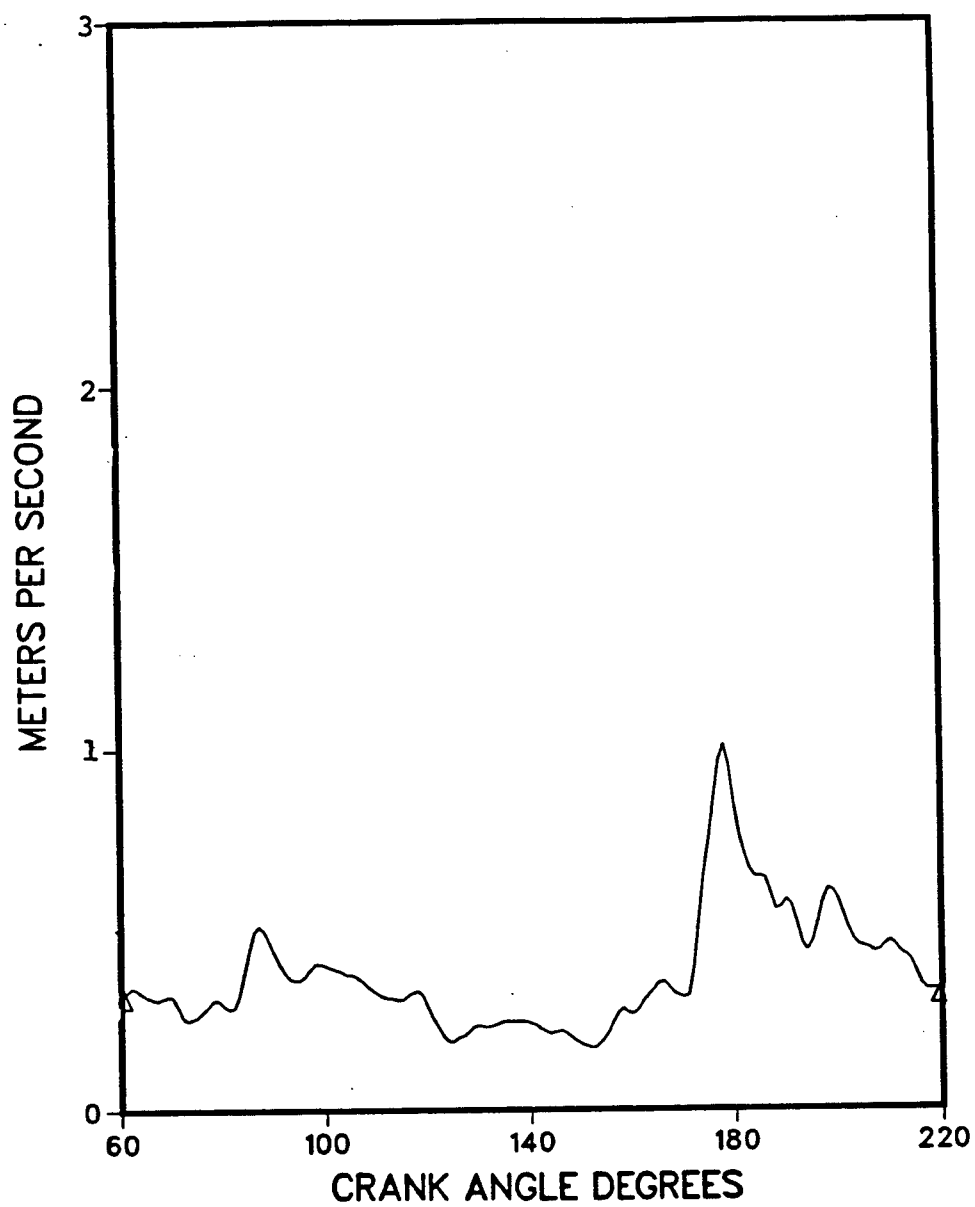


Fig. 7.3 Cyclic variation of the mean velocity

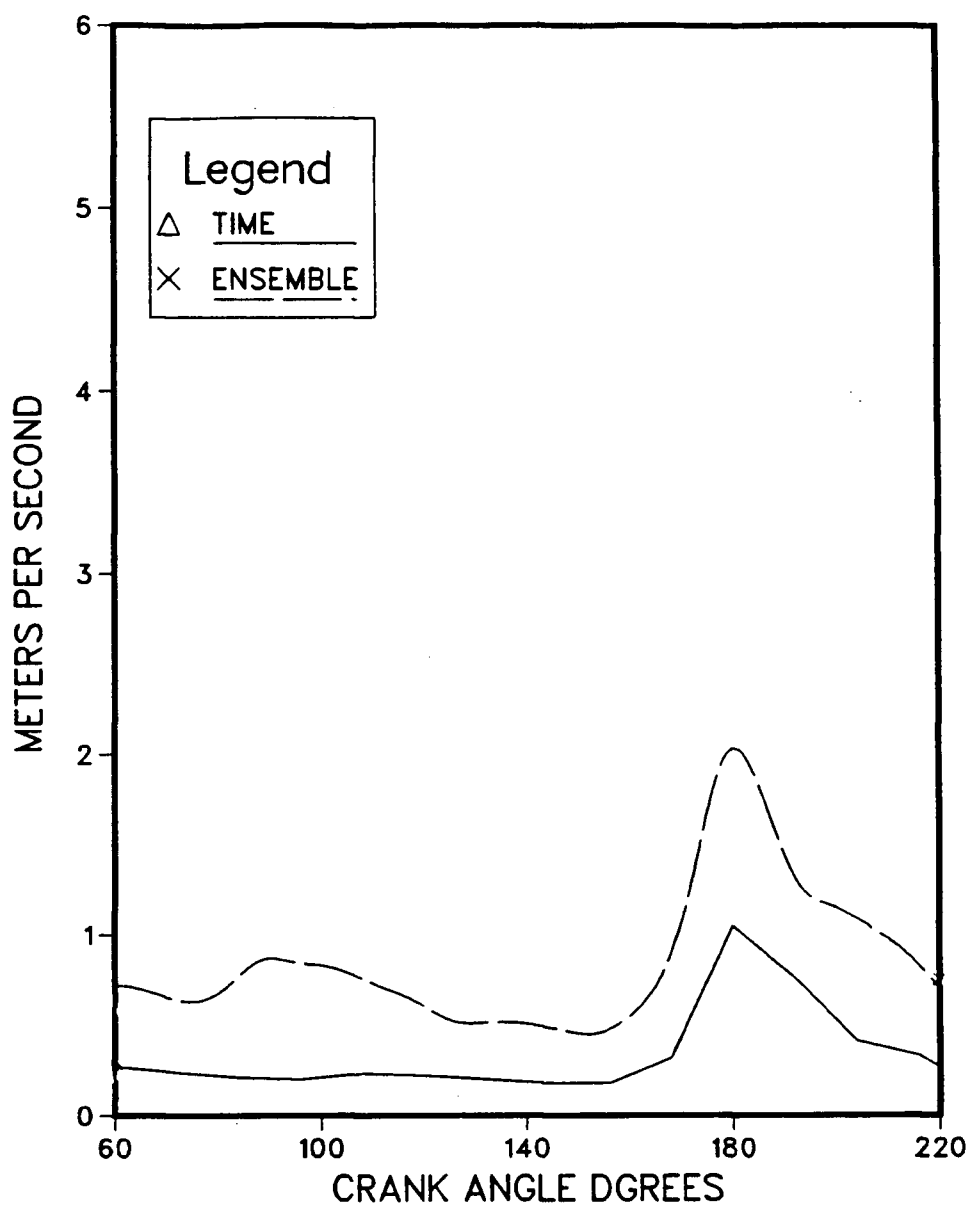


Fig. 7.4 Comparison of time and ensemble averaging techniques for the evaluation of turbulence intensity

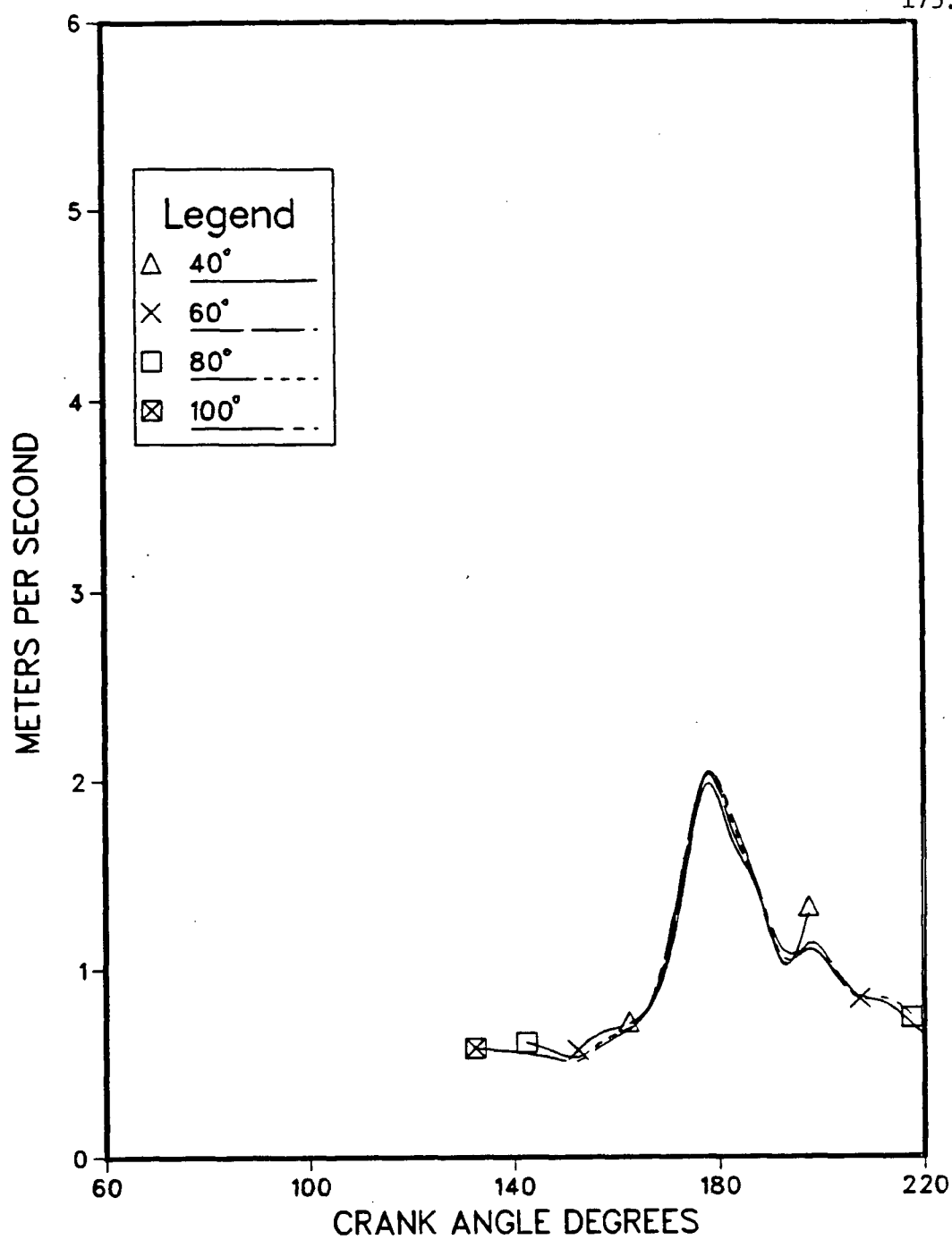


Fig. 7.5 Turbulence intensity evaluated with Lancaster's nonstationary technique

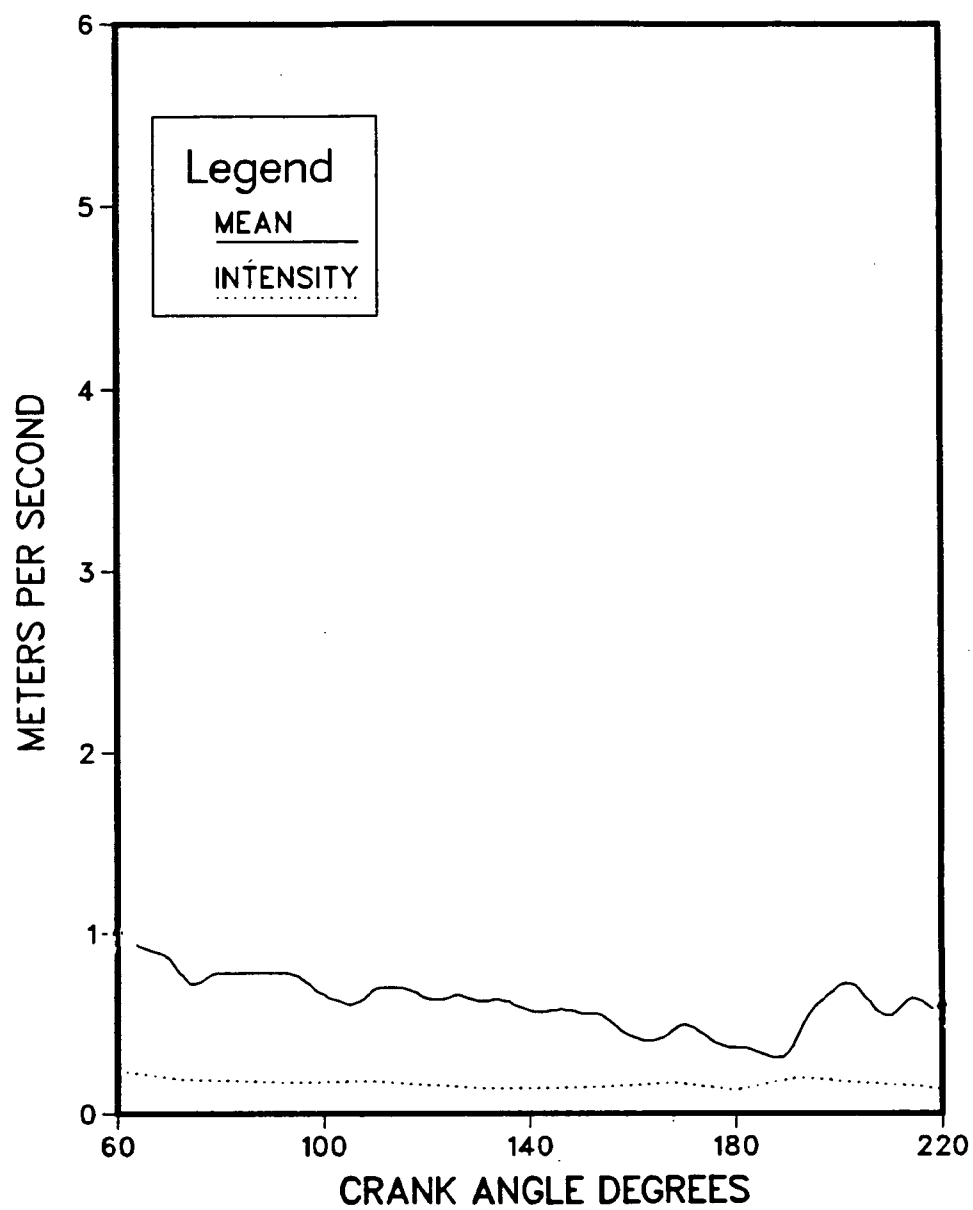


Fig. 7.6 Mean velocity and turbulence intensity for Piston A;
 $h_c = 3.5$ mm; probe at cup edge

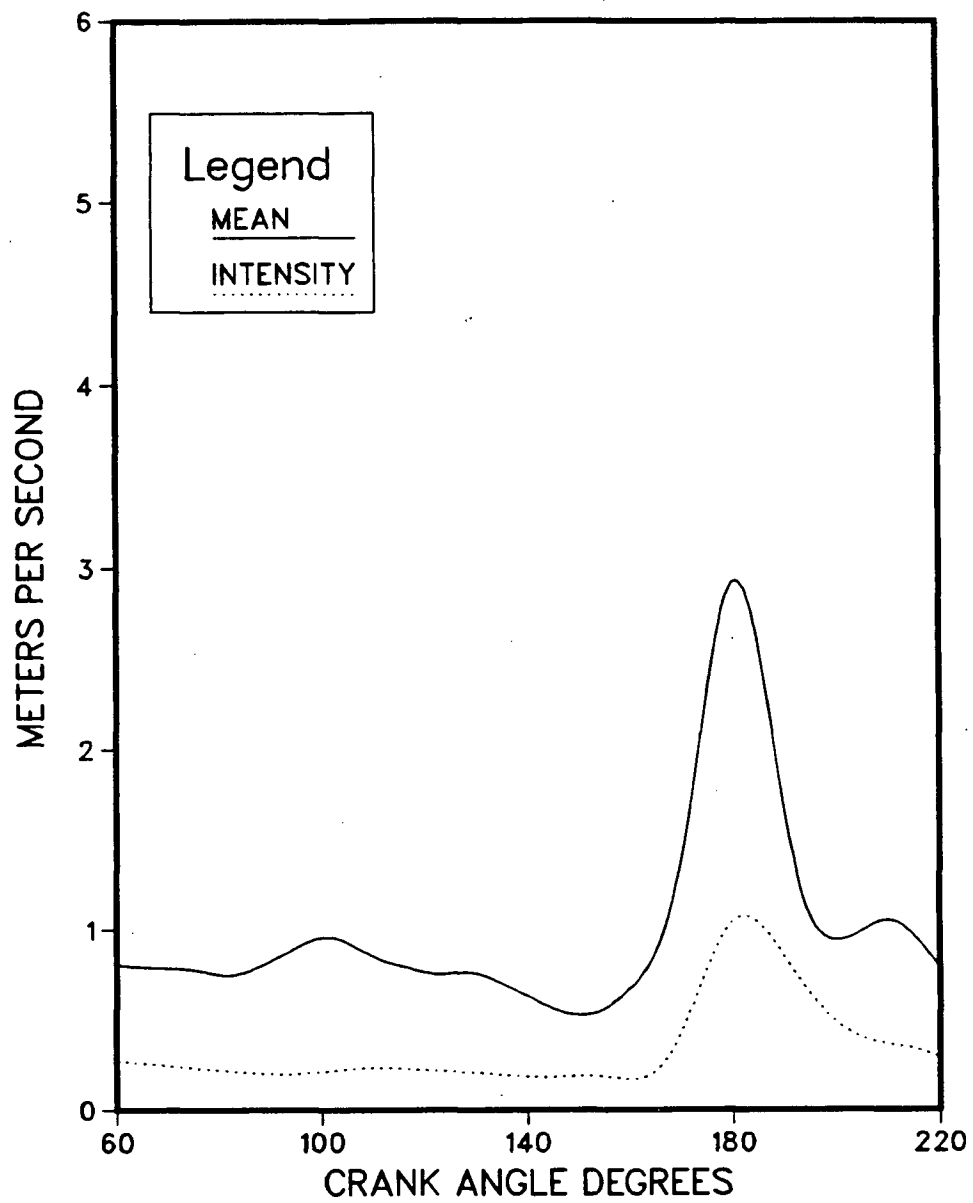


Fig. 7.7 Mean velocity and turbulence intensity for Piston A;
 $h_c = 1.5$ mm; probe at cup edge

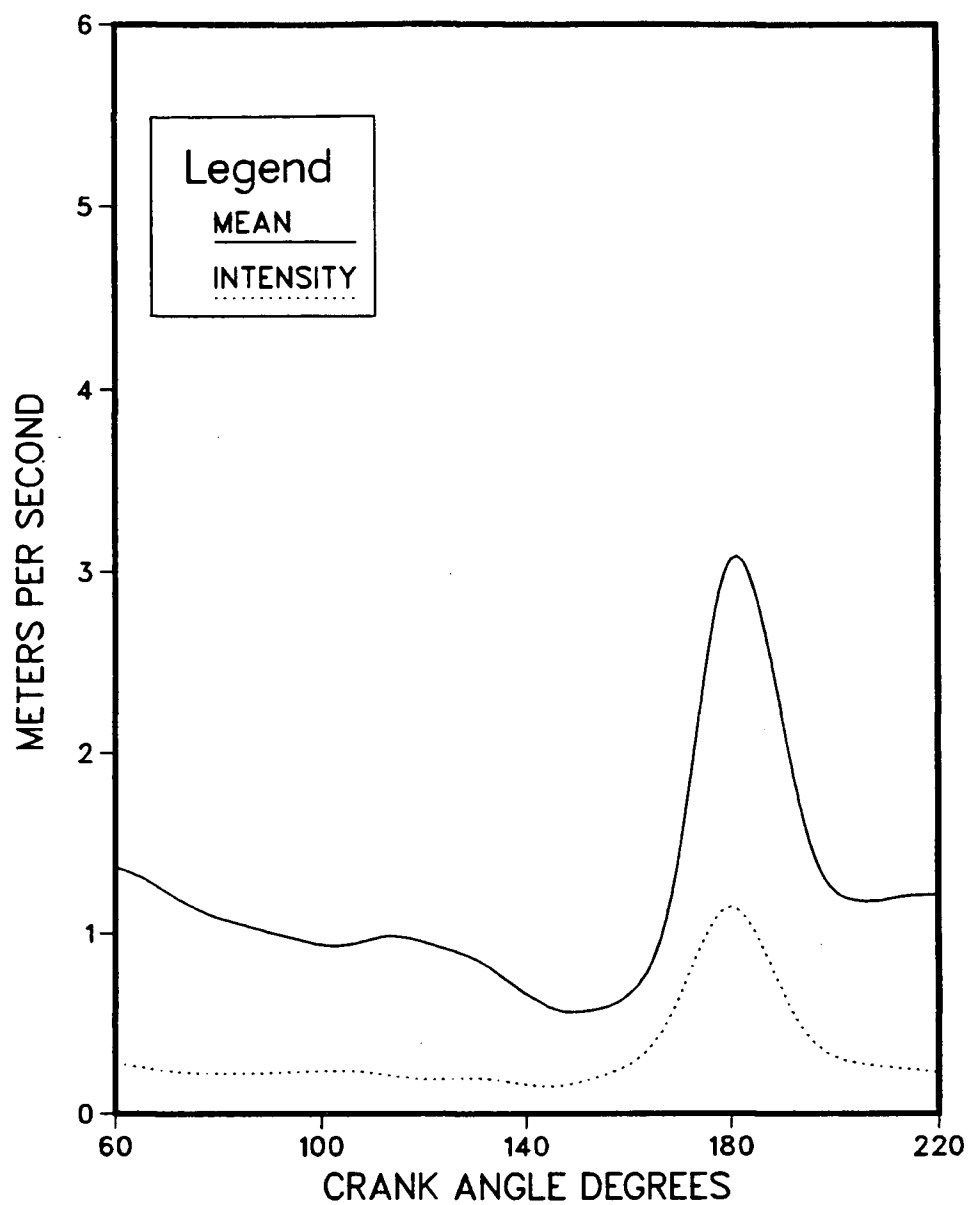


Fig. 7.8 Mean velocity and turbulence intensity for Piston A;
 $h_c = 1.5$ mm; probe at chamber center

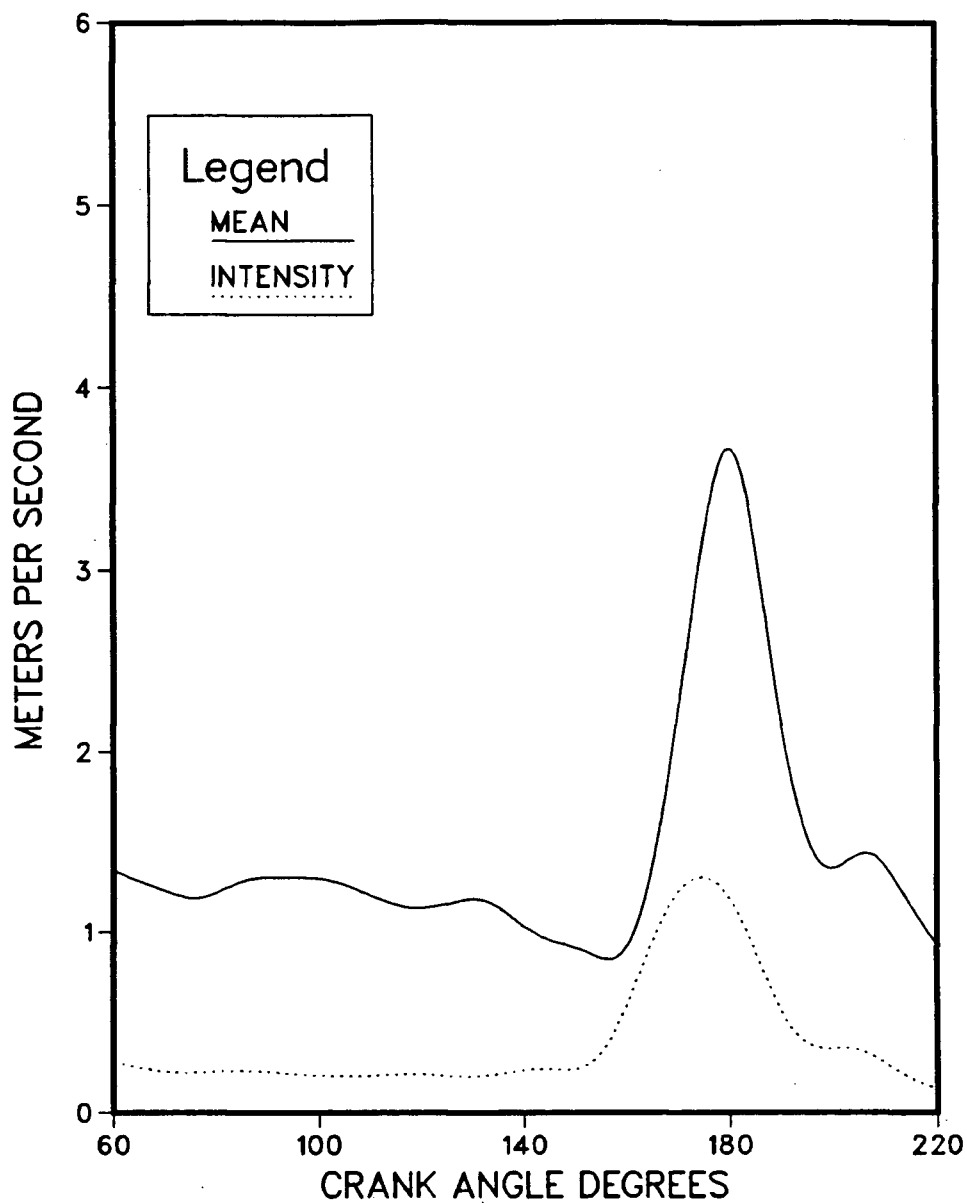


Fig. 7.9 Mean velocity and turbulence intensity for Piston A;
 $h_c = 1.5$ mm; probe at cup edge; $\theta = 90^\circ$

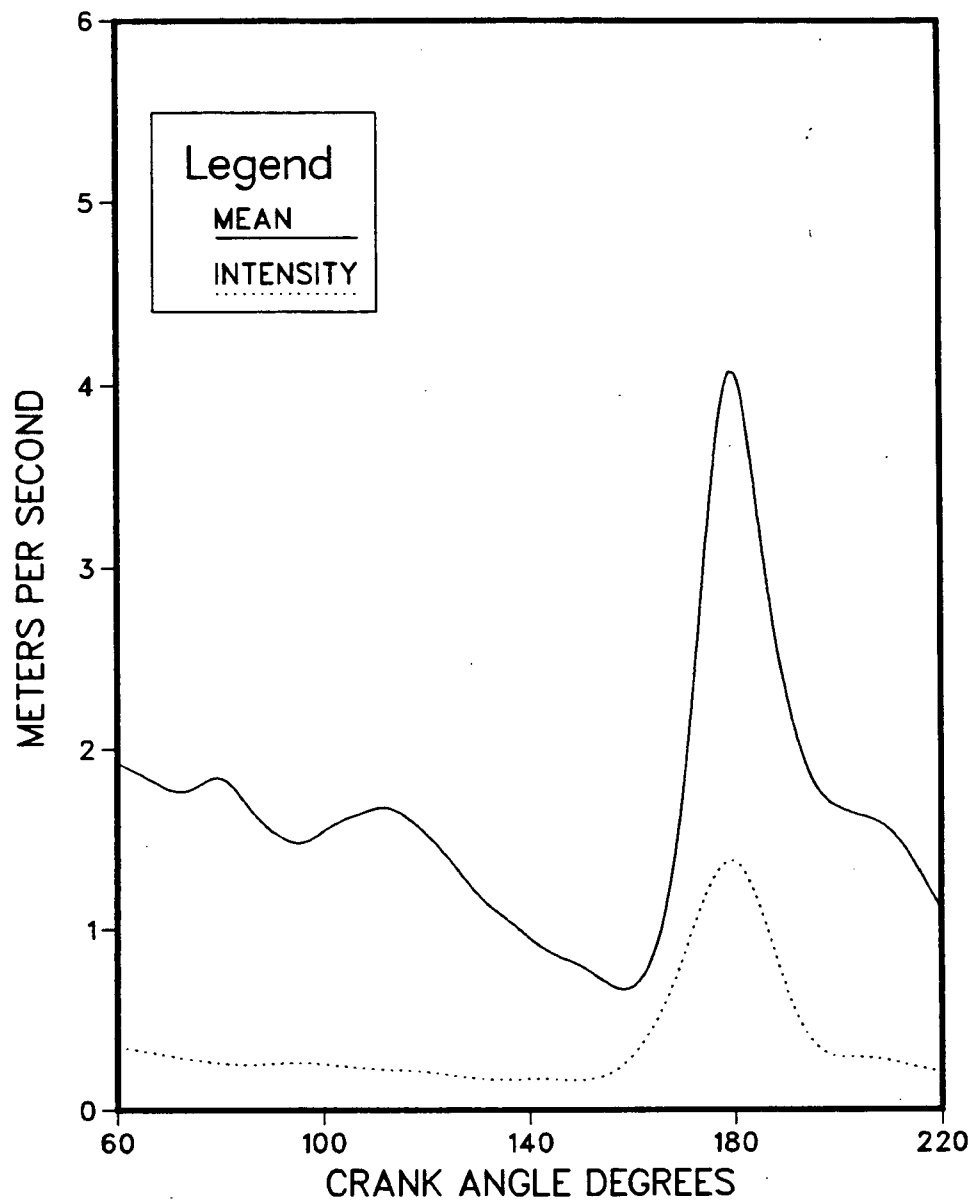


Fig. 7.10 Mean velocity and turbulence intensity for Piston A;
 $h_c = 1.5$ mm; probe at chamber center; $\theta = 90^\circ$

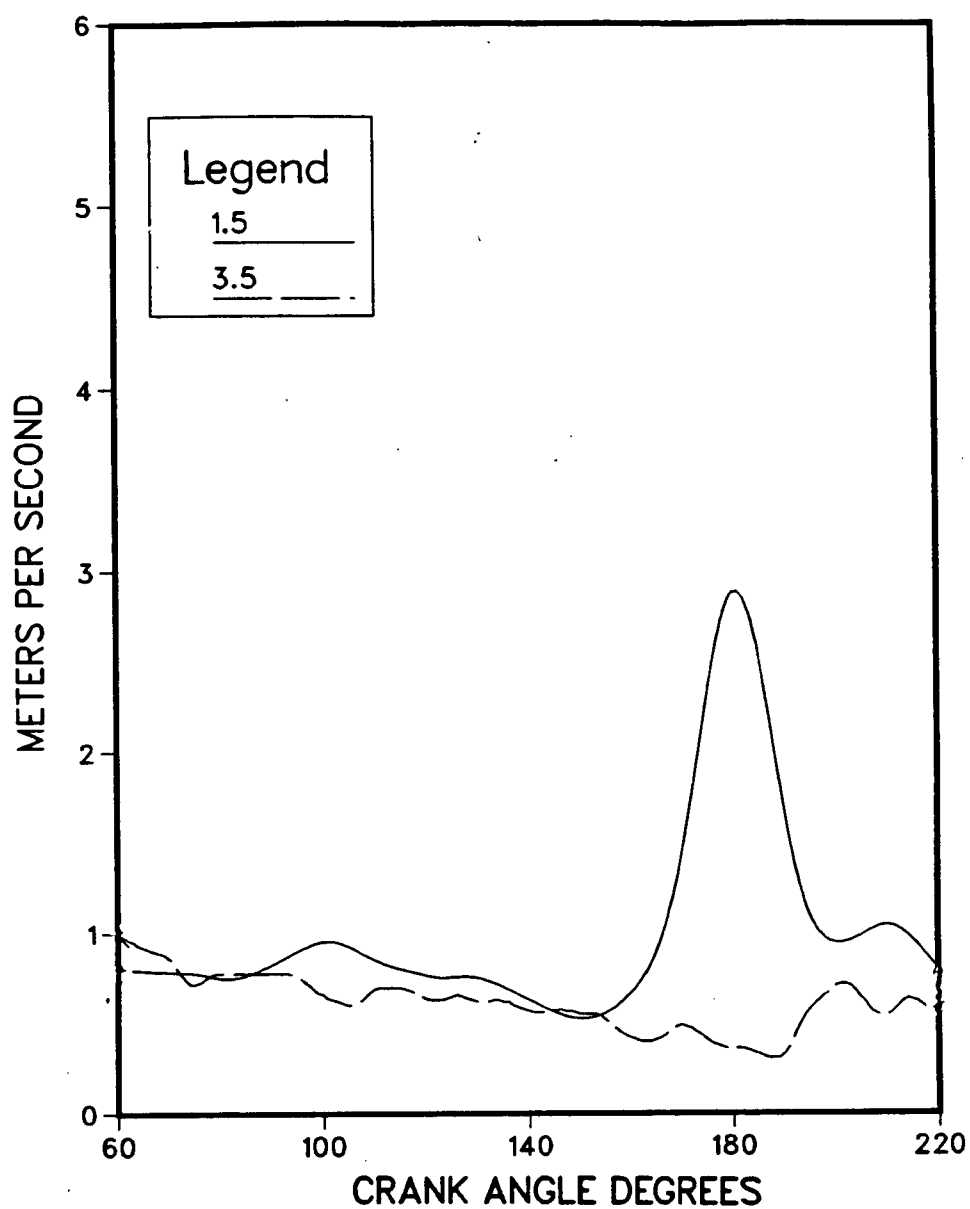


Fig. 7.11 Comparison of mean velocity traces for Piston A;
 $h_c = 3.5$ and 1.5 mm; probe at cup edge

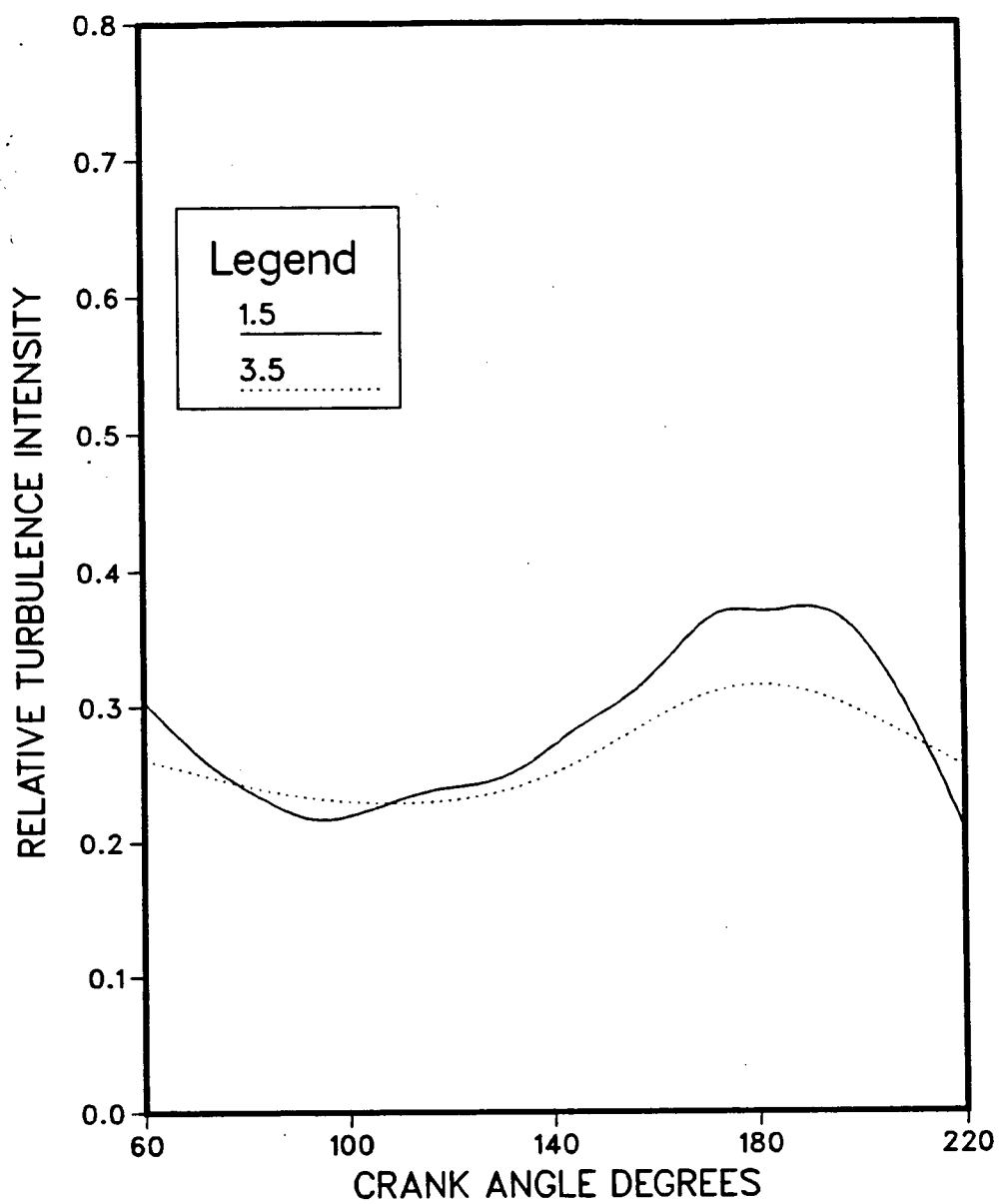


Fig. 7.12 Comparison of relative turbulence intensities for Piston A; $h_c = 3.5$ and 1.5 mm; probe at cup edge

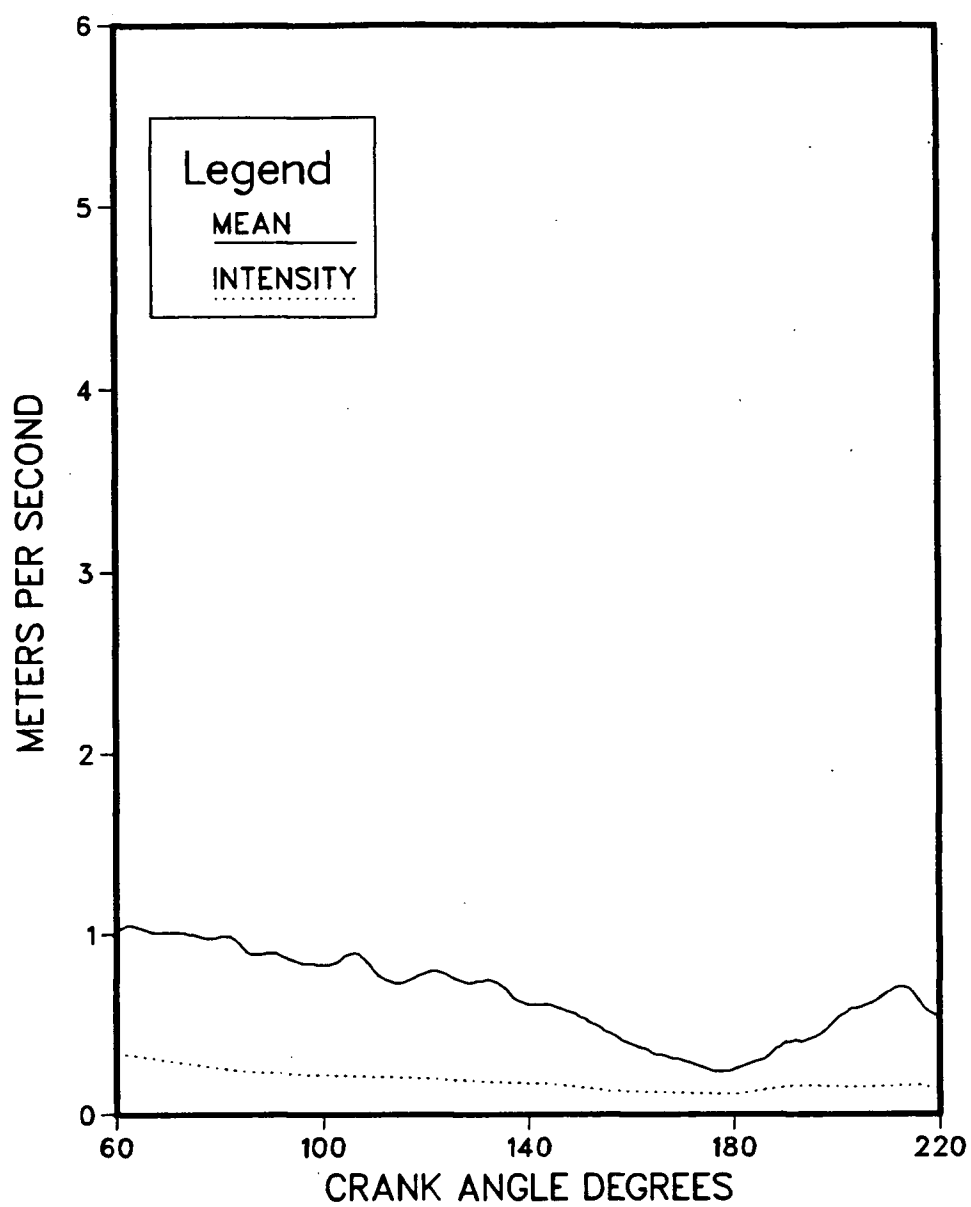


Fig. 7.13 Mean velocity and turbulence intensity for Piston B;
 $h_c = 3.5$ mm; probe at cup edge

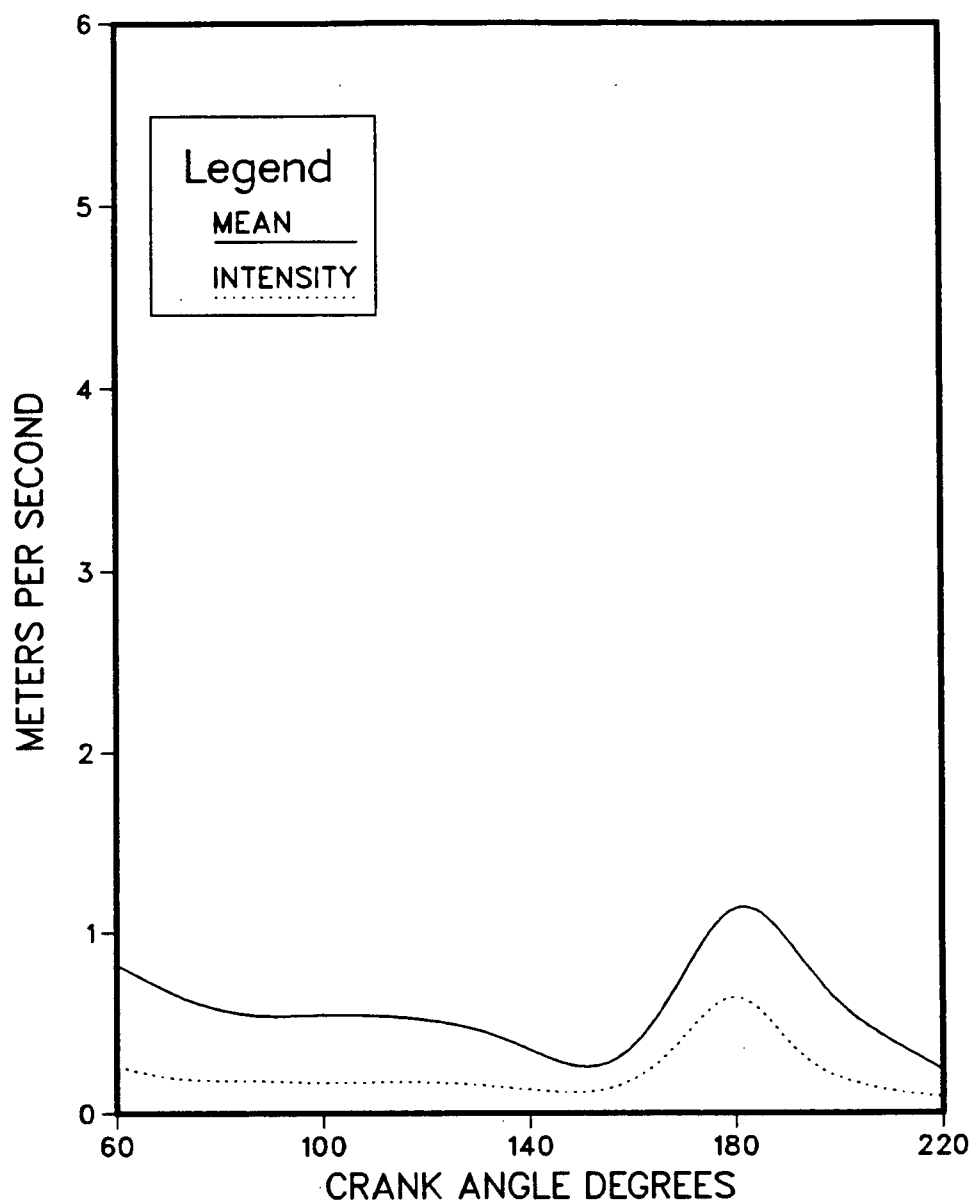


Fig. 7.14 Mean velocity and turbulence intensity for Piston B;
 $h_c = 1.5$ mm; probe at cup edge

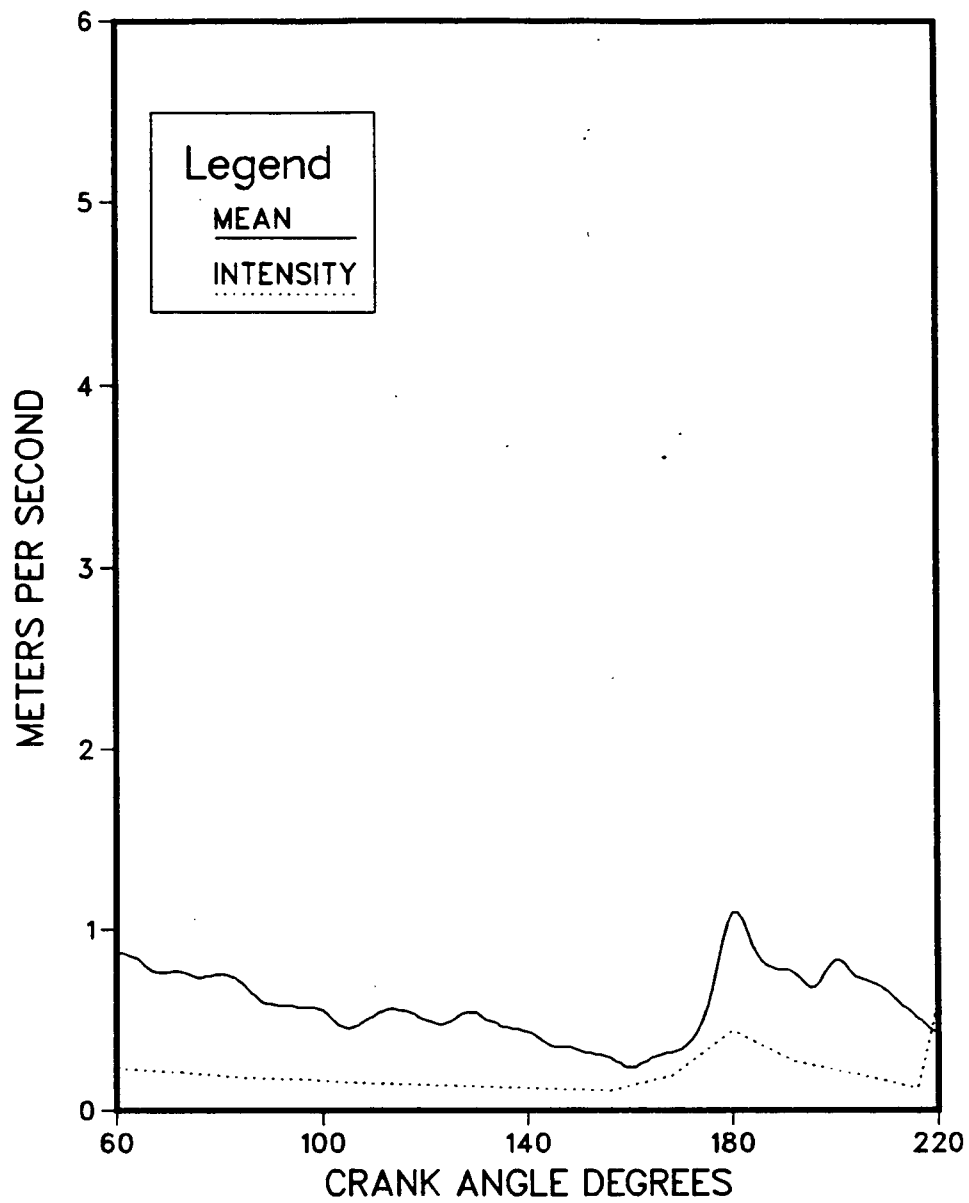


Fig. 7.15 Mean velocity and turbulence intensity for Piston B;
 $h_c = 1.5$ mm; probe at chamber center

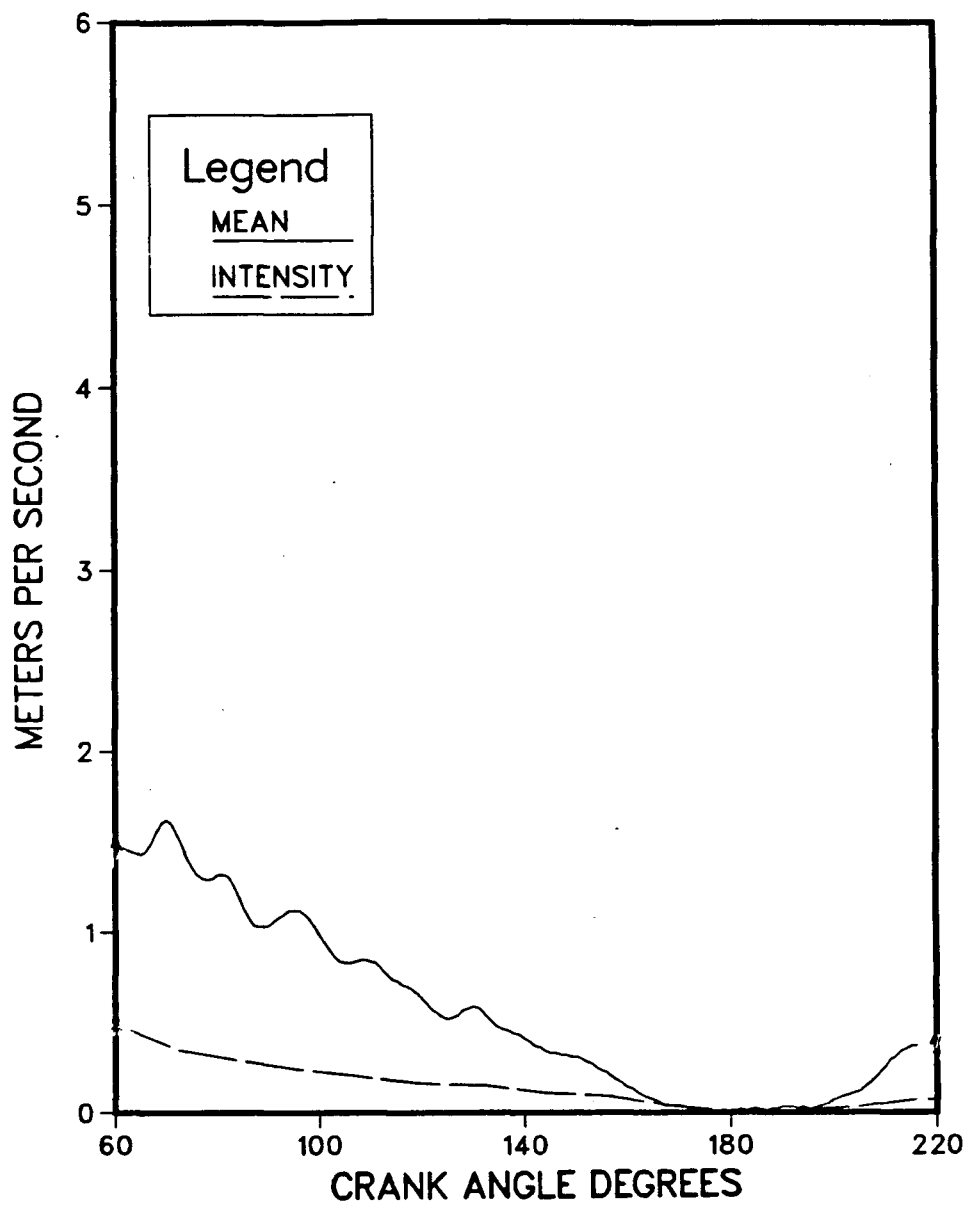


Fig. 7.16 Mean velocity and turbulence intensity for Piston B;
 $h_c = 1.5$ mm; probe inside cup

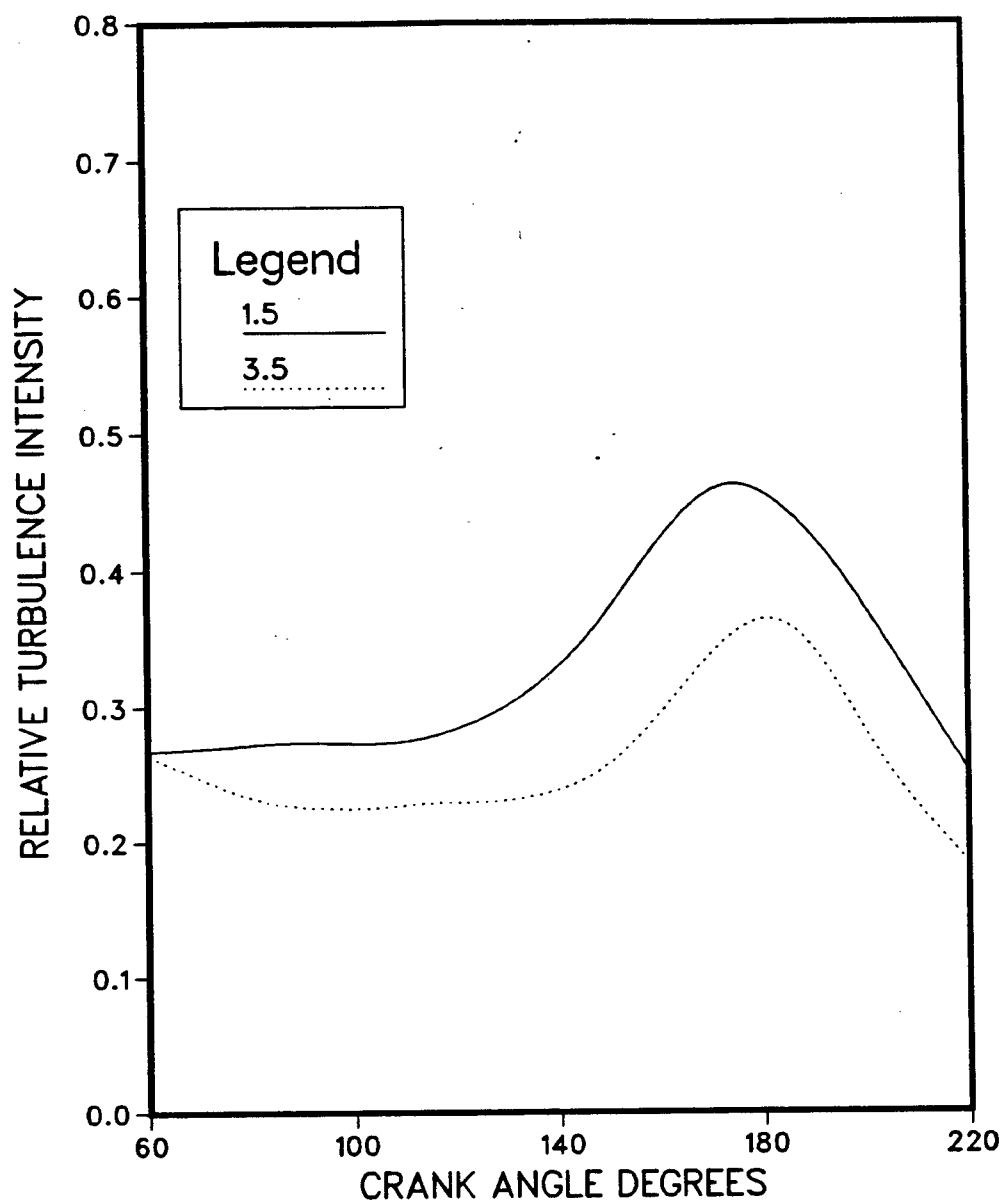


Fig. 7.17 Comparison of relative turbulence intensities for Piston B; $h_c = 3.5$ and 1.5 mm; probe at cup edge

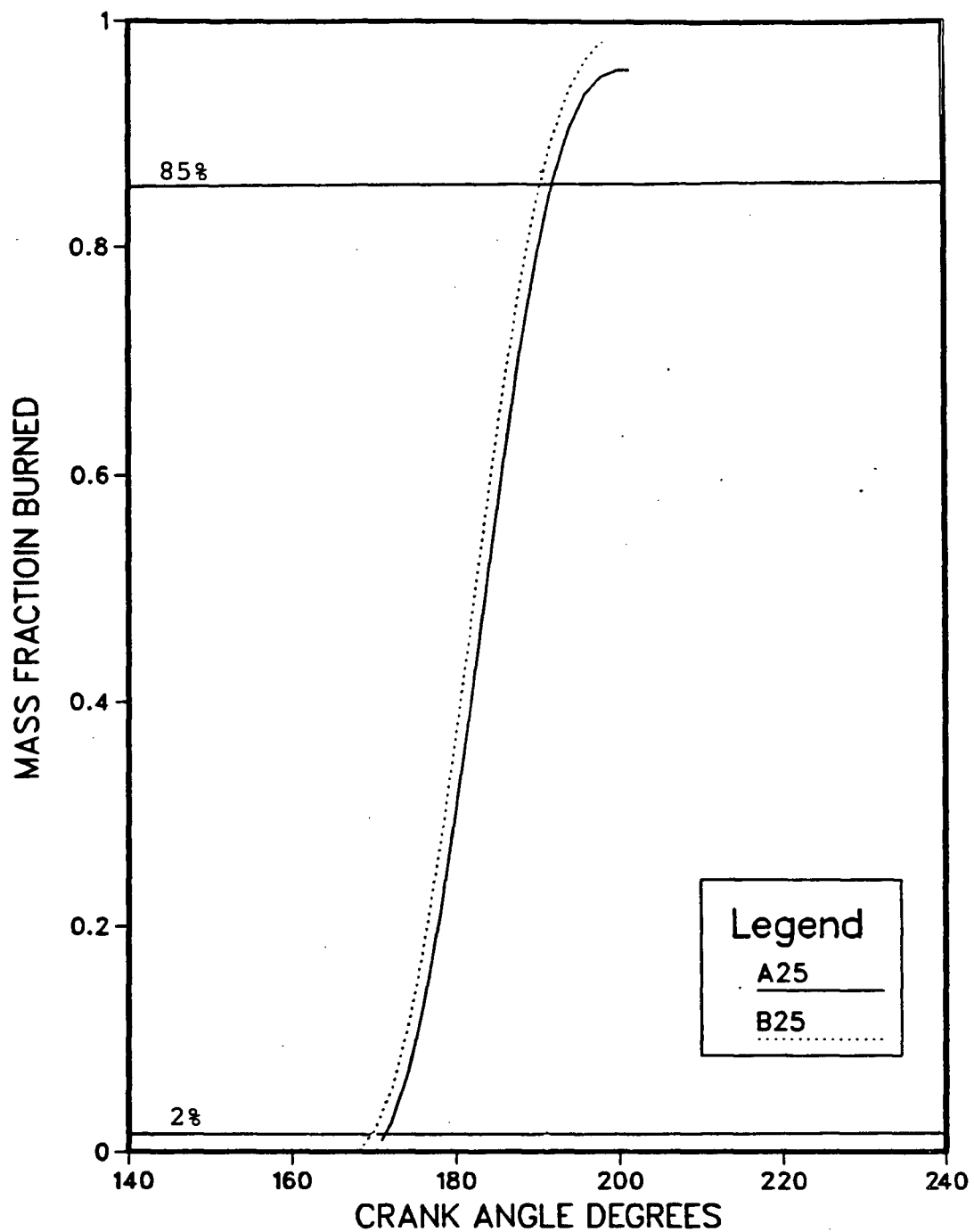


Fig. 7.28 Comparison of mass fraction burn curves for Pistons A and B at a spark timing of 25° BTDC

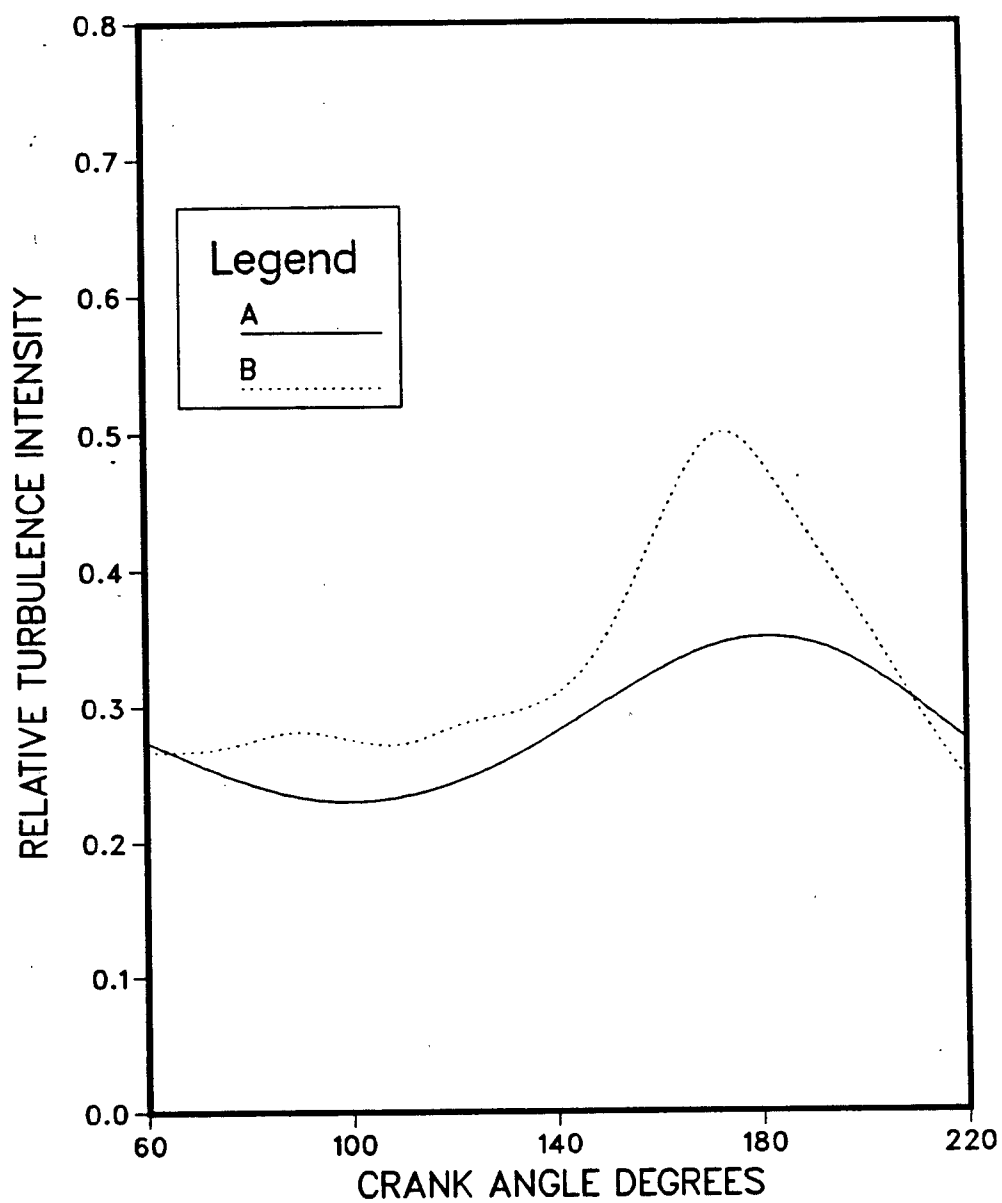


Fig. 7.19 Comparison of relative turbulence intensities for Pistons A and B; $h_c = 1.5$ mm; probe at cup edge

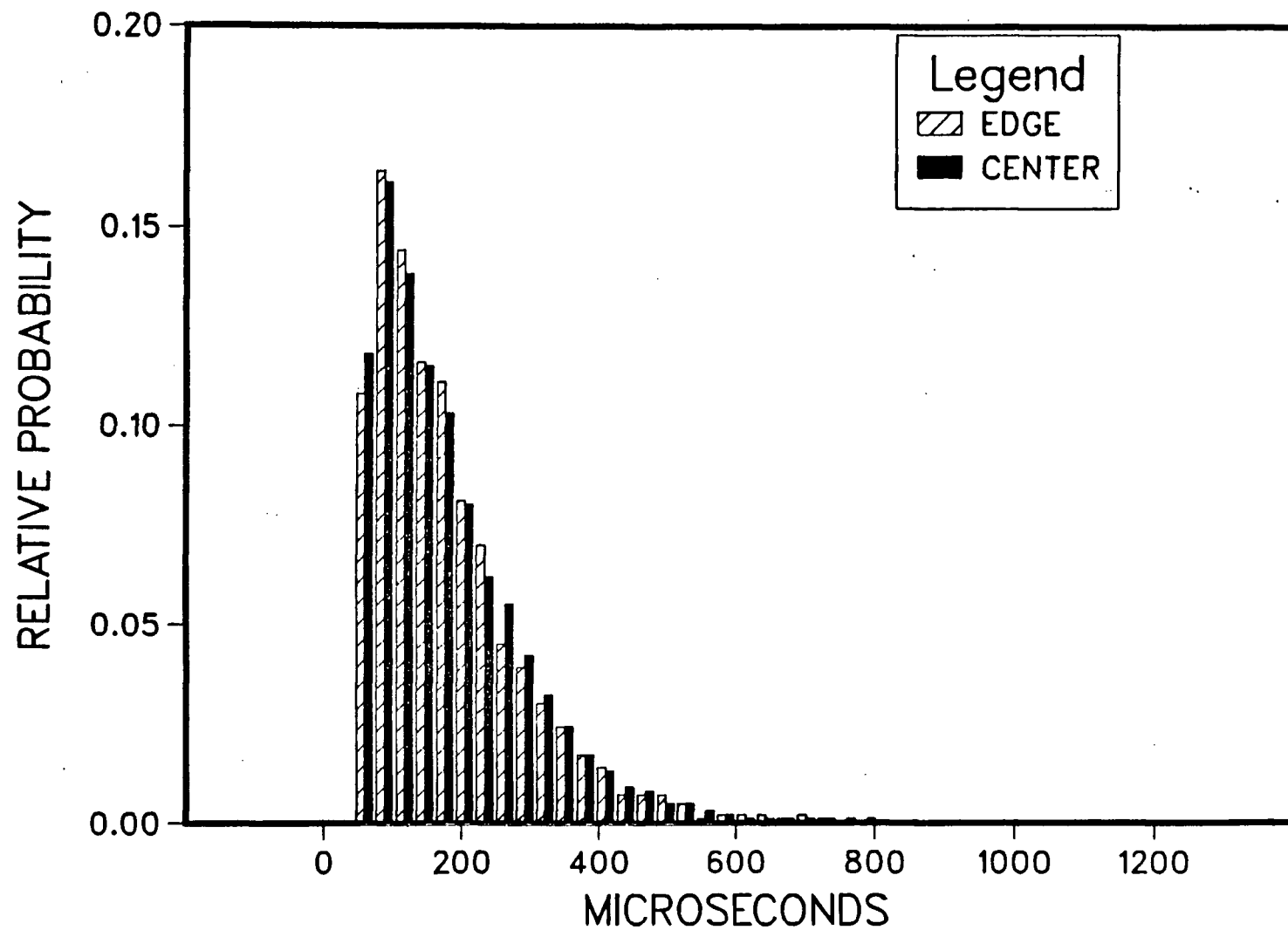


Fig. 7.20 Comparison of the relative probability distributions of small scale turbulence structure for Piston A at the chamber center and at the cup edge

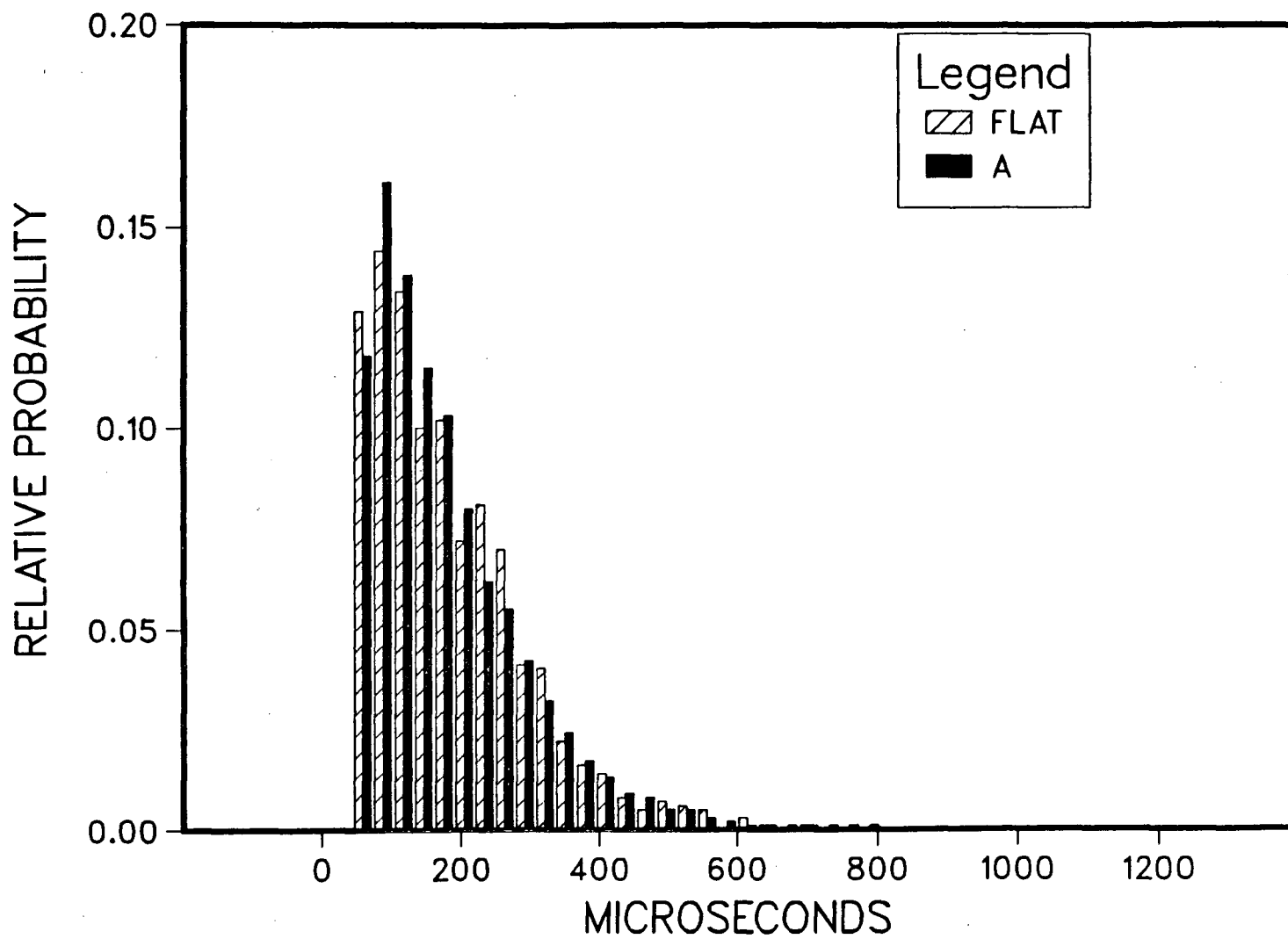


Fig. 7.21 Comparison of relative probability distributions of small scale turbulence structure at the chamber center for Piston A and the flat piston

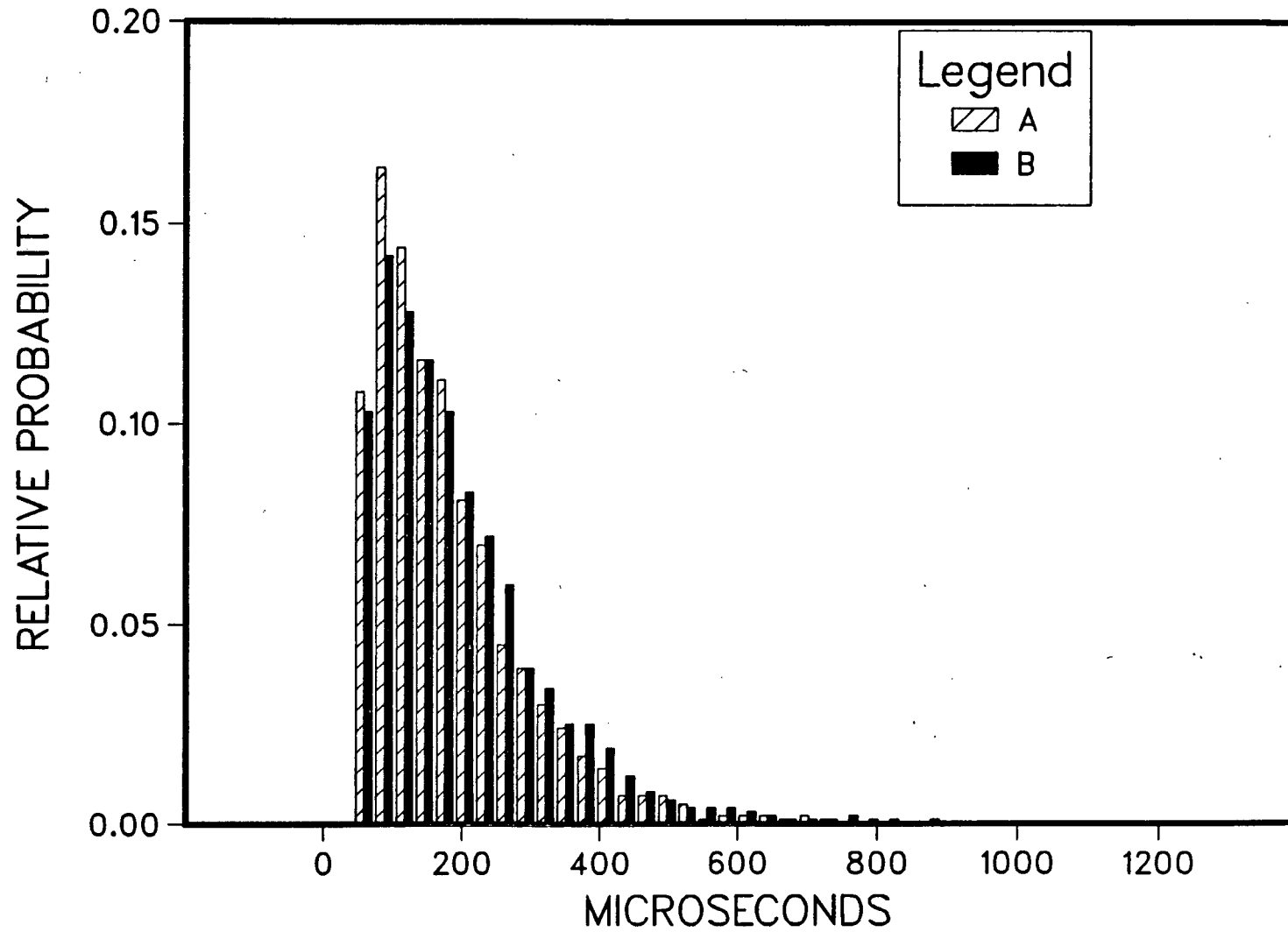


Fig. 7.22 Comparison of relative probability distributions of small scale turbulence structure at the cup edge for Pistons A and B

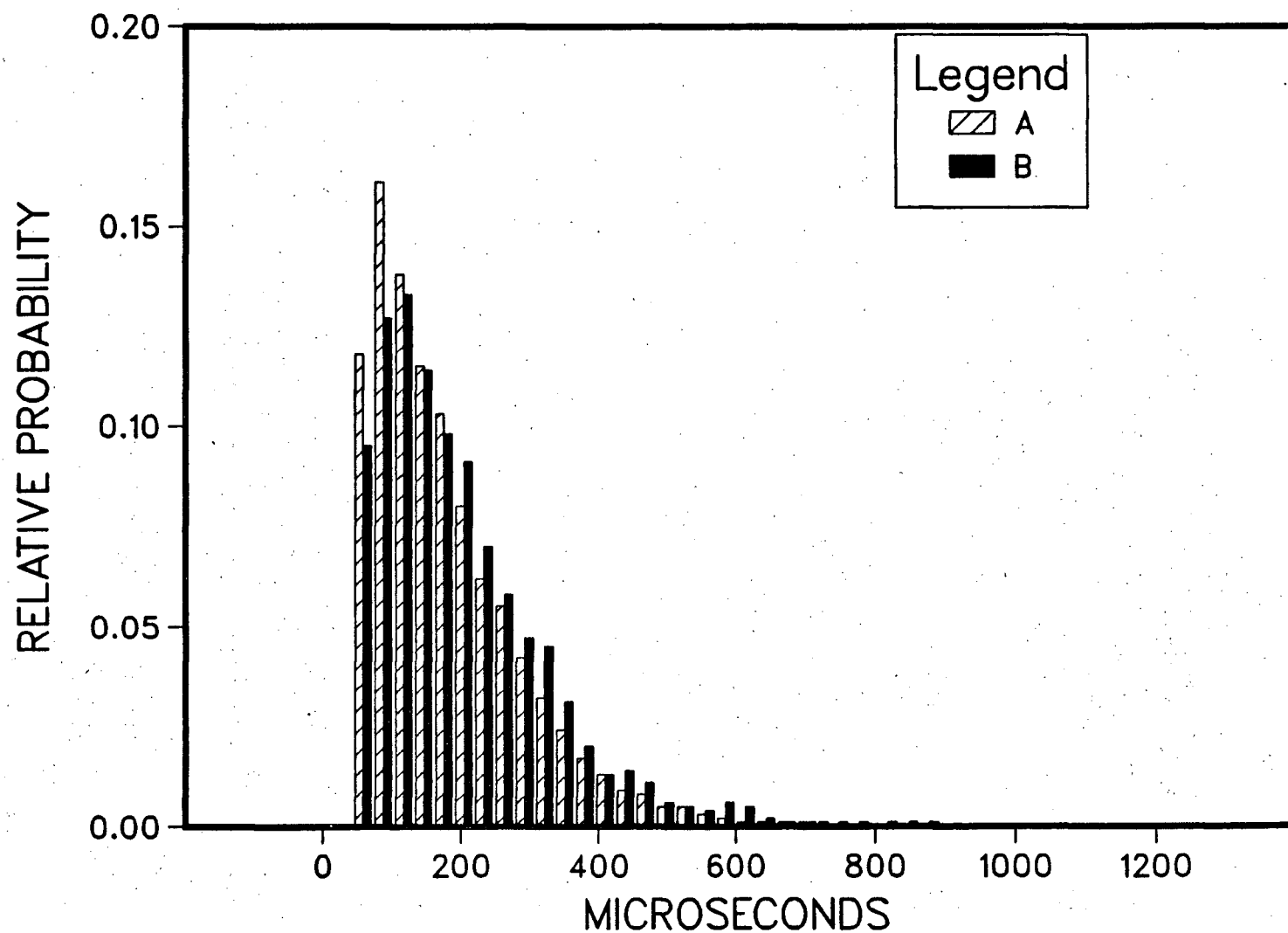


Fig. 7.23 Comparison of relative probability distributions of small scale turbulence structure at the chamber center for Pistons A and B

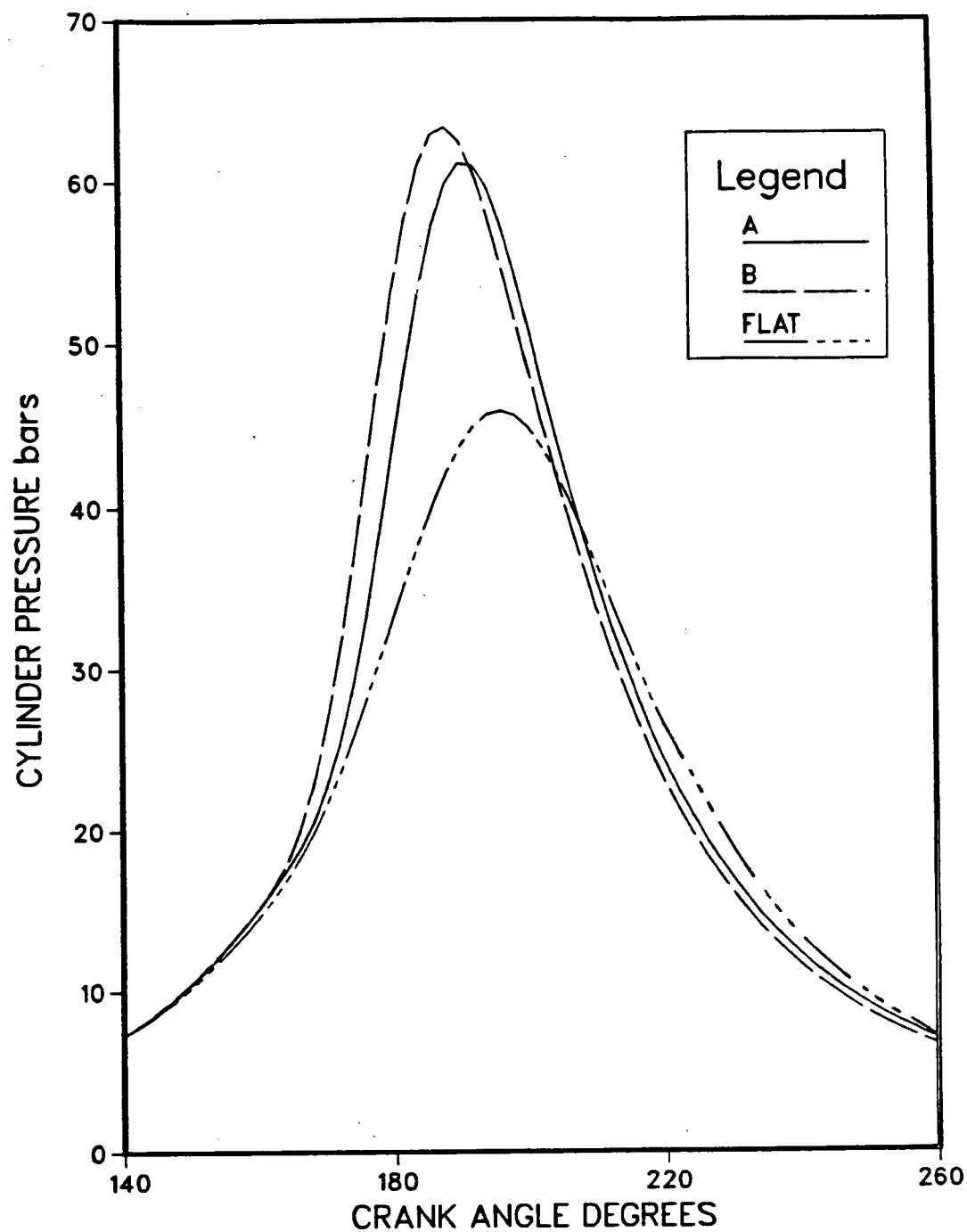


Fig. 7.24 Comparison of pressure history for Pistons A and B and the flat piston for a spark timing of 30° BTDC

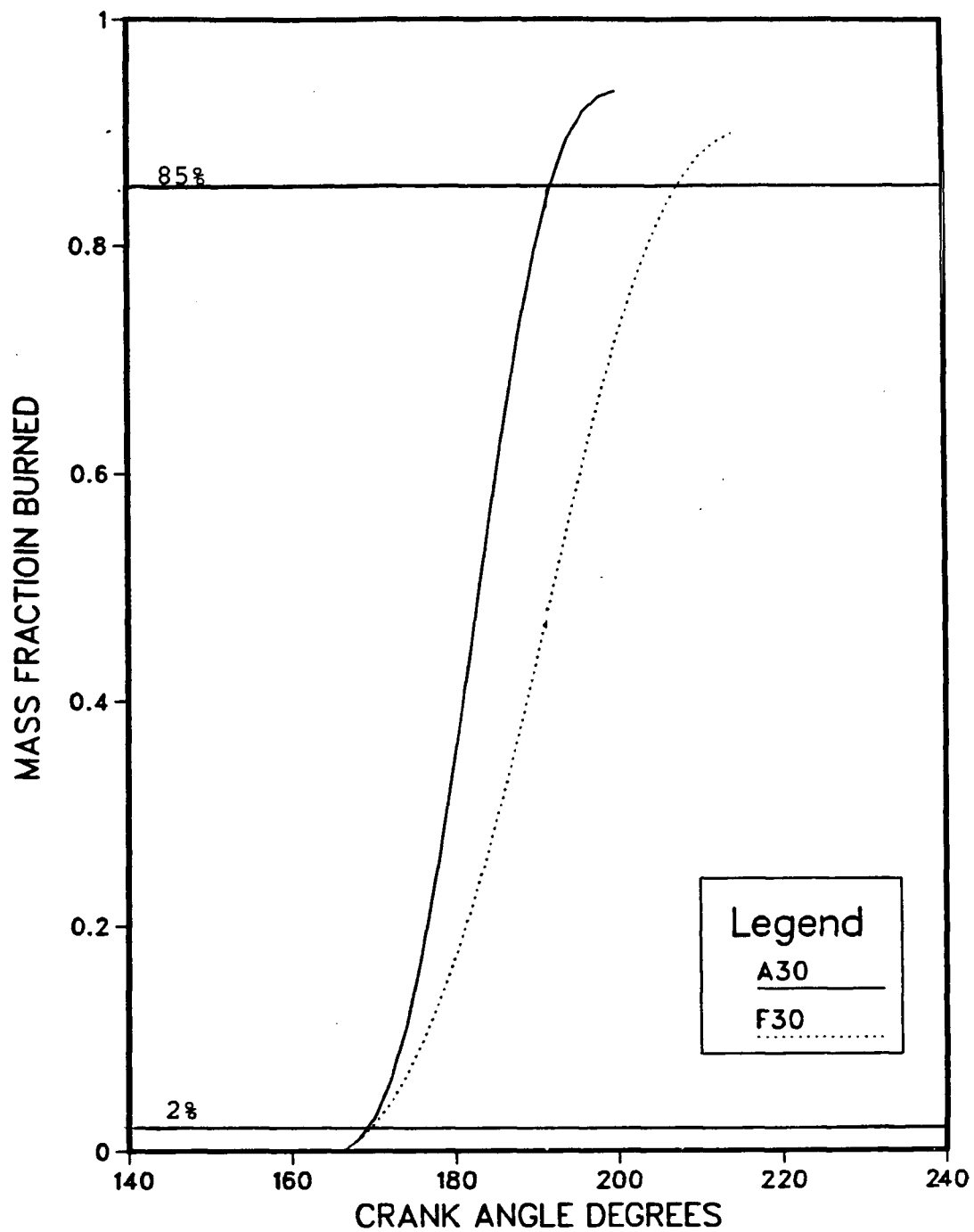


Fig. 7.25 Comparison of mass fraction burn curves for the flat piston and for Piston A at a spark timing of 30° BTDC

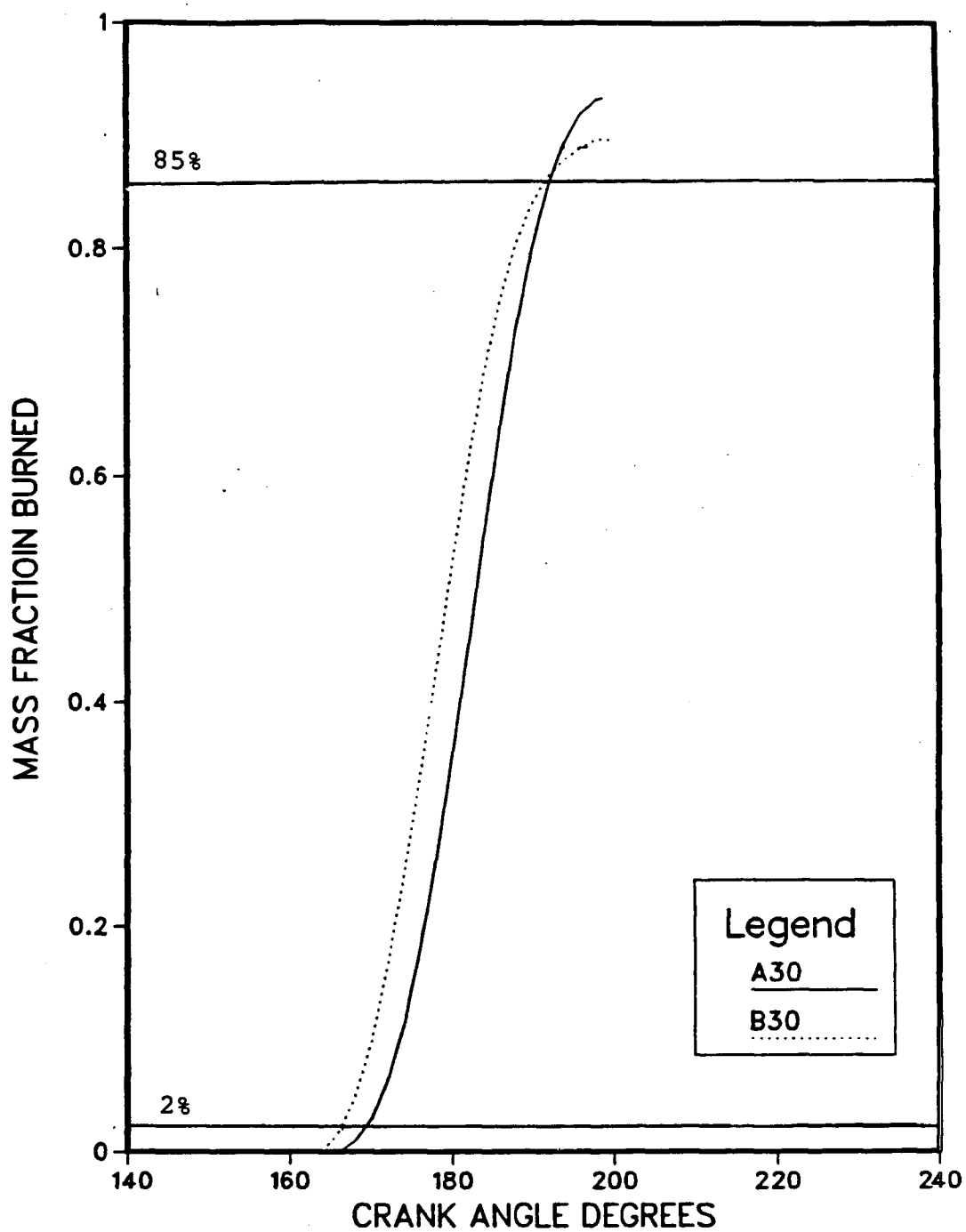


Fig. 7.26 Comparison of mass friction burn curves for Pistons A and B at a spark timing of 30° BTDC

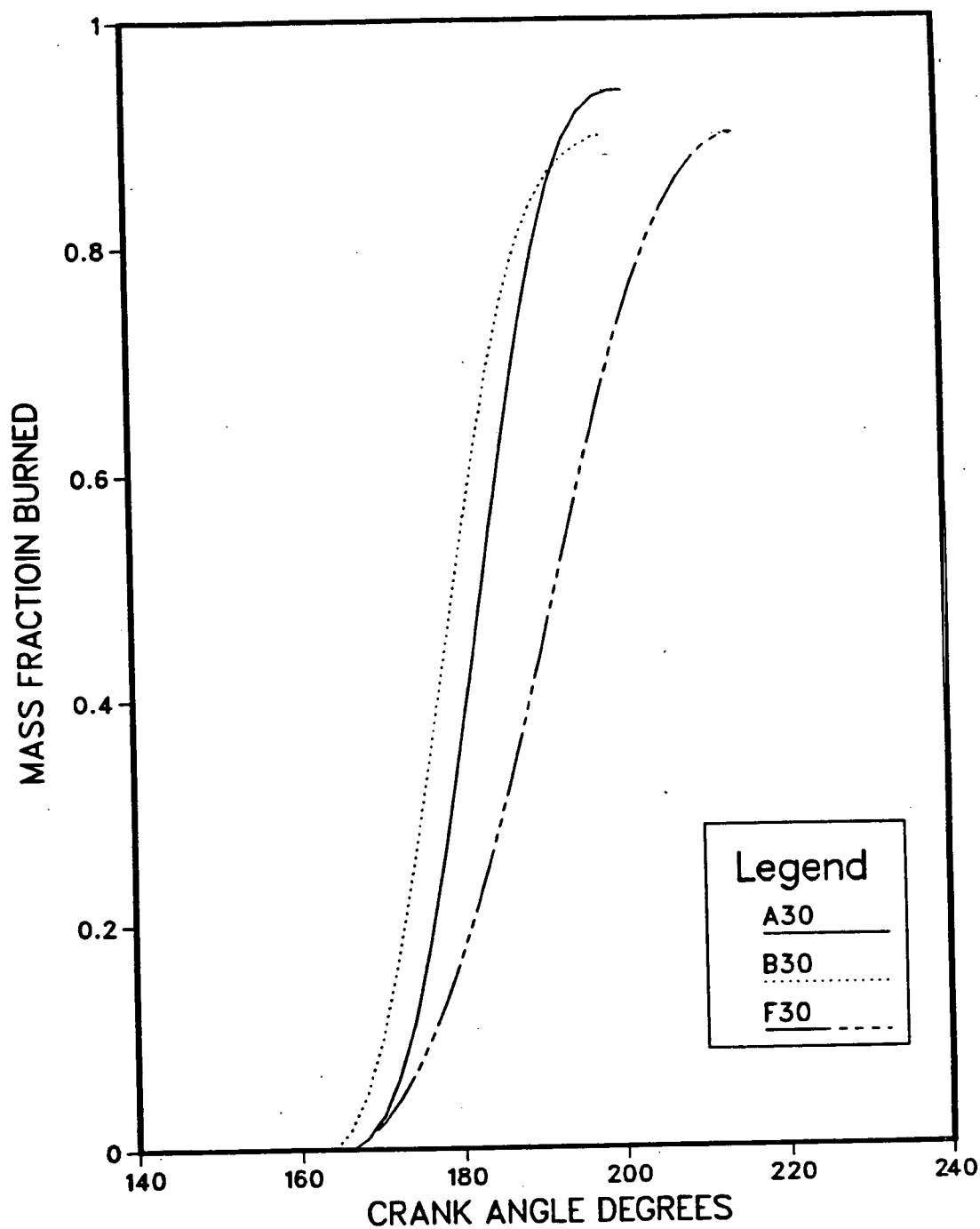


Fig. 7.27 Comparison of mass fraction burn curves for all three pistons at a spark timing of 30° BTDC

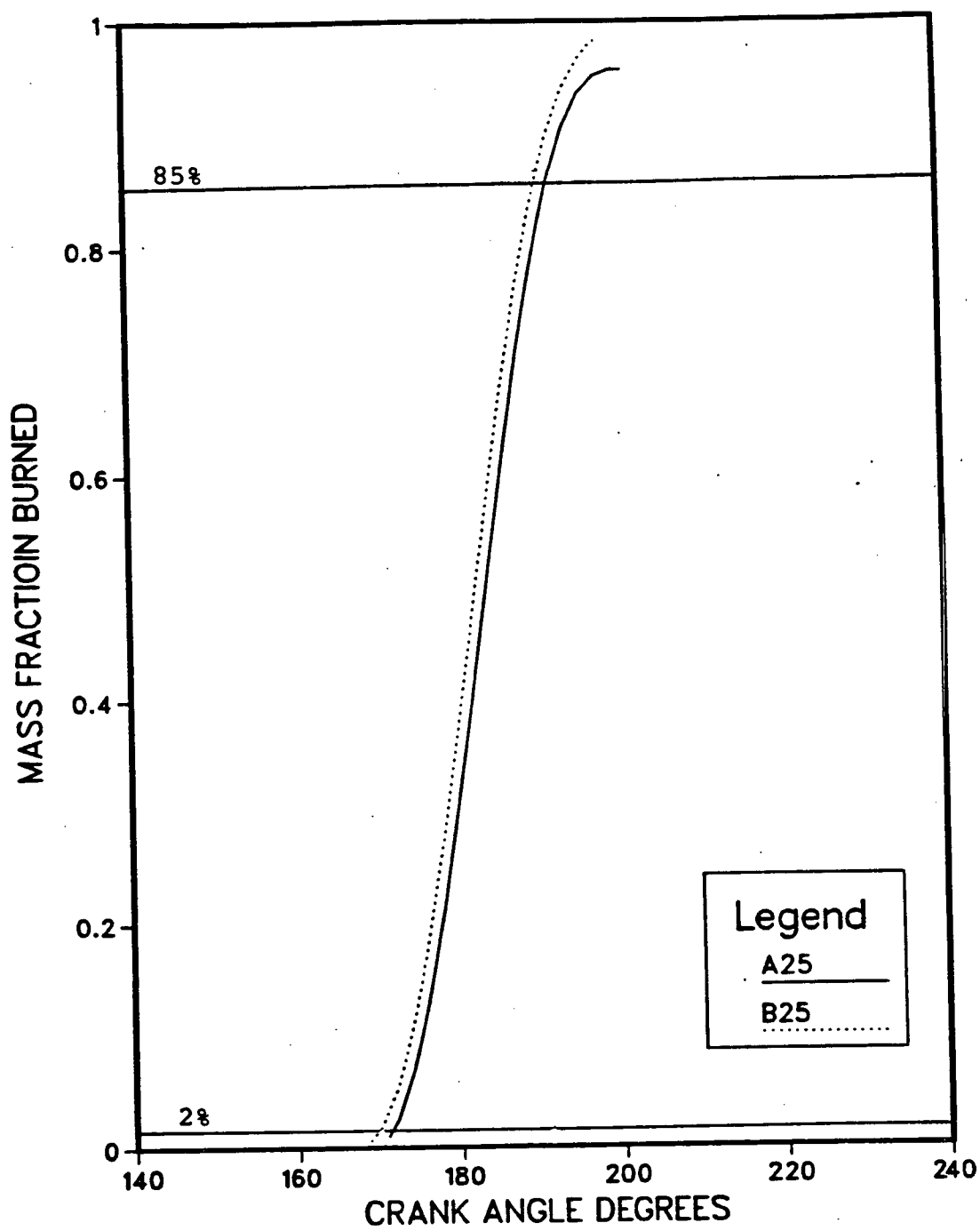


Fig. 7.28 Comparison of mass fraction burn curves for Pistons A and B at a spark timing of 25° BTDC